MINERALOGICAL, GEOCHEMICAL AND STABLE ISOTOPE STUDIES OF CLAY DEPOSITS IN THE LOWER BENUE TROUGH, NIGERIA

BY

SUNDAY OJOCHOGWU IDAKWO
MATRIC. No: 147646
B.Sc (Kogi), M.Sc (Ibadan).

A thesis in the Department of GEOLOGY
Submitted to the Faculty of Science in partial fulfillment of
the requirements for the Degree of
DOCTOR OF PHILOSOPHY
of the
UNIVERSITY OF IBADAN

FEBRUARY, 2020

ABSTRACT

The Lower Benue Trough (LBT) is a clay-shale rich basin with lots of industrial clay deposits with considerable economic value. Previous studies focused mainly on the geochemistry and mineralogy of the clay deposits for industrial applications, while detailed information on the geochemical characterisation, genetic delineation and tectonic setting of the clay deposits are generally lacking. Therefore, the aim of this study was to undertake detailed mineralogical, chemical and stable isotope composition of the clay deposits in part of the LBT.

Clay samples were collected in the LBT purposively on the basis of the lithologic character at Aloji (10), Agbenema (5), Udane-Biomi (5), Ofejiji (10), Okpokwu (5), Otukpa (5) and Enugu (10) areas. Mineralogy and morphology of the samples were determined using X-ray diffractometry and scanning electron microscopy. Fourier Transform Infrared (FTIR), differential thermal and thermogravimetric analyses were used to determine the structure and the thermal conditions of the clays. Major elements composition was determined by inductively coupled plasma- atomic emission spectroscopy, while trace and rare-earth elements were by inductively coupled plasma-mass spectrometry. The Chemical Index of Alteration (CIA), Plagioclase Index of Alteration (PIA) and Chemical Index of Weathering (CIW) of the clay samples were calculated. Hydrogen and oxygen isotopic compositions were measured by Delta Plus XP isotope ratio mass spectrometer (IRMS) and Thermo Scientific MAT 253 mass-spectrometer, respectively. Descriptive statistics was used to analyse the data obtained, while geochemical discrimination diagrams were used to interprete the geochemical data.

Kaolinite (40-49%), quartz (37-55%), vermiculite (1-4%), muscovite (1-8%) and microcline (2-5%), were the minerals in the clay samples. The book-like morphology of the kaolinite and the characteristic FTIR bands at 3694.6-3660.1 cm^{-1} confirmed that it has not undergone diagenesis but rather suffered weight loss at temperature range of 499 to 504 °C. The SiO_2 (66.8-90.3%), Al_2O_3 (6.7-22.7%), Fe_2O_3 (0.3-3.9%) and LOI (3.3-11.1%) were characteristic of quartz-rich kaolinitic clay mineral assemblage. The concentrations (in ppm) of Co (0.6-7.6), Ni (0.1-1.1), and V (42.0-90.0) indicated a felsic source comparable to the upper continental crust, while the calculated CIA (83.1-99.8), PIA (98.5-99.9) and CIW (99.2-99.9) values suggested derivation of the clay from intense chemical weathering of the source rocks. The La/Sc (3.7-9.3), Th/Sc (0.6-3.1), and Th/Co (2.0-21.0); the light rare-earth enrichment and depleted heavy rare-earth with negative Eu anomaly confirmed a felsic crustal origin. The La-Th-Sc discrimination diagram showed typical granitic gneiss source. The log of (K_2O/Na_2O) vs SiO_2, La-Co-Zr/10 and Th-Sc-Zr/10 indicated a passive margin tectonic setting, while the Eu/Eu* vs $(Gd/Yb)_N$ diagram suggested a Proterozoic age for the granitic gneiss source. The oxygen and hydrogen isotope values of +15.4 to +21.2‰ and -66.4 to -50.8‰ were consistent with chemically weathered residual material deposited under an oxic environmental condition at high temperature of formation (54-91°C), which revealed formation of the kaolinitic clay under a hot and humid paleo-climatic condition.

The quartz-rich kaolinitic clay deposits in the Lower Benue Trough were derived from the chemical weathering of Proterozoic granitic gneiss. The clay was deposited in a passive margin tectonic setting, under a tropical climatic condition.

Keywords: Kaolinitic clay, Isotopic composition, Paleo-climatic condition, Tectonic setting

Word count: 500

CERTIFICATION

I hereby certified that this work was carried out by Sunday Ojochogwu Idakwo in the Department of Geology, Faculty of Science, University of Ibadan, Ibadan, Nigeria.

---------- ----------

Dr. A. T. Bolarinwa, **Date**
B.Sc. (Ilorin), M.Sc., Ph.D. PGDTHE (Ibadan)
Associate Professor, Economic Geology
Department of Geology.

DEDICATION

I dedicate this work first and foremost to God Almighty for giving me the wisdom to crave for knowledge, and my late elder brother, Obaje Idakwo, who has contributed in his own way to my success in life before death took him away on the 6th of October, 2003.

ACKNOWLEDGEMENTS

I acknowledge my supervisor, Dr. A.T. Bolarinwa, who contributed meaningfully to this research work through his very intelligent constructive criticisms and suggestions.
In addition to my research supervisor, I acknowledge, Prof. David L. Bish, a professor of clay mineralogy, Geological Sciences Department, Indiana University, Bloomington, U.S.A for inviting me to his clay mineralogy laboratory and allowing me to make use of all the available facilities for this research work.

I am grateful to the Department of Geology's academic staff, namely Prof. O.A. Ehinola (H.O.D), Profs. A.I. Olayinka, G.O. Adeyemi, M.N. Tijani, O.A. Okunlola, M.E. Nton Drs. A.A. Omitogun, O.A. Boboye, A.S. Olatunji, M.A. Oladunjoye, C.O. Adeigbe, A.M. Adeleye, I.A. Oyediran , O.O. Oshinowo, F. Ajayi, Mr. A.A. Jayeoba and Mr. J.A. Aladejana for the knowledge gained from them while on my studies and to the non-academics; Mr. J.A. Mofoluku, Mr. S.O. Akhihiero-Ata, Mr. M.A. Uwaje, Mr. F. Oladapo, Mrs O. Ariori Kudirat, Mrs.Bademosi Mercy Aderemi (Retired), Mr, R.K. Adelakun, Mr. N. Oyeyebi, Mrs. R.O Fakunle, Mr. O.A. Oyekunle. God bless you all for your assistance rendered during my studies.

I thank the management of Kogi State University for granting me leave with pay and sponsoring my trip to the U.S.A to carry out all my research, person worth of mention is Prof. S.D. Musa (Former, Deputy Vice Chancellor (Administration) K.S.U) who expedite the release of my travelling grant from Tertiary Education Trust Fund and members of staff of the Earth Sciences Department, K.S.U, Anyigba most especially Prof. Joseph Omada (Former Dean, Faculty of natural Sciences), Dr. E.G. Ameh (Former, Head of Department of Earth Sciences), Dr. M. Onimisi, Dr. A.O. Omali, Dr. F.A. Akpah, Dr. S.M. Kolawole and Mr. R. Ayuba. I am particularly appreciative of Prof. K.O. Adebowale (Former Dean, Faculty of Sciences, U.I. and current Deputy Vice Chancellor (Administration, U.I) for the encouragement, financial and moral support. May the good Lord reward you all abundantly.

I am most grateful to Prof. and Dr (Mrs.) S.E. Atawodi for the encouragement and inspiration. I pray that God will uphold and bless you. I commend and thank my brothers and sisters; Mr. and Mrs O. Idakwo, Mr. and Mrs. E. Idakwo, Mrs U. Idakwo, Mr. and Mrs A. Idakwo, Mr. and Mrs S. Idakwo, Mr. and Mrs. D. Idakwo, Mrs. Ojochide, Mr. Gabriel Idakwo and Mr. Patrick Idakwo for their encouragement and payers and also I use this opportunity to thank my Dad and Mum for their support always. God's blessings, joy and satisfaction shall never depart from you in Jesus Name. Amen.

I must not forget to mention the moral and spiritual support I received from the members of Redeemed Christian postgraduate Fellowship, U.I and Redeemed Christian Church of God, Power Sanctuary, Anyigba, Kogi State, most especially, Pastor John Odeyemi, Pastor Mattew Nkenchor, Pastor Baba Tunde Alli, Dr and Dr.(Mrs). M. Onimisi, Mr and Mrs. Taiwo Saraye, Mr and Mrs Aduloju, Mr and Mrs. Alo. May God Almighty uphold you all.

This acknowledgement cannot be complete without appreciating my kind-hearted and wonderful loving wife, Mrs. Victoria Ojochogwu Idakwo, for her multifaceted support.

Above all, I thank God Almighty for sparing my life to start and complete the programme.

TABLE OF CONTENTS

CHAPTER FOUR: RESULTS AND DISCUSSION

LIST OF FIGURE

LIST OF TABLES

CHAPTER ONE

INTRODUCTION

1.1 General Statement

The Benue Trough situated on the African continent is a rift that is distinctive because it occupies an intracontinental place with a dense, folded supracrustal filling of the Cretaceous (Olade, 1975; Binks and Fairhead, 1992). This wide depression is about 1050 km long, 250 km wide in the south and decreases to a width of approximately 120 km in the north. According to Burke *et al*. (1971), it is an intracratonic, linear, graben basin that trends in NE-SW direction with origin associated with African and South American plates during the Early Cretaceous.

The trough is characterised by an uplifted basement block, flanked by the separation of African and South American deep basin containing about 6000 m of sediments (Burke and Whiteman, 1973, Ofoegbu, 1985). The intracontinental Benue Trough was initiated during the Lower Cretaceous following the opening of the Atlantic Ocean (Burke and Whiteman, 1973). Non-uniformity in tectonic evolution and sedimentation along the Benue Trough led to the conventional sub-division of the trough into three parts (Fig. 1. 1). The Lower Benue Trough is the southern portion of the Benue Trough, believed to have originated as a failed arm of an aulacogen at the time of the opening of the South Atlantic Ocean during the separation of the African plate from the South American plate (Burke *et al*, 1971). The Lower Benue Trough is made up of the Anambra Basin, the Afikpo Syncline and the Abakaliki Anticlinorium (Nwachukwu, 1972). The Lower Benue Trough, like other sedimentary basins in Nigeria is endowed with mineral resources such as coal, lead-zinc, barytes, limestone and clay (Simpson, 1954, Obaje *et al*, 1999)

In many studies, the Benue Trough's geotectonic setting and metallogeny was reported (Etim *et al.,* 1988 Akande *et al.,* 1989 and Oha *et al*., 2017), mainly because of the numerous occurrences of Pb-Zn-Ba-F deposits within the Trough, with little or no interest on the clay deposits in Aloji, Ofejiji, Agbenema, Udane-Biomi, Oturkpa, Okpokwu and Enugu areas, which is the focus of the present investigation.

Clay minerals are particularly sensitive to environments so that the composition of clay minerals in sequence can provide valuable indications for the depositional environment of such sediments (Ágnes *et al.,* 2011). The contributions of post-depositional diagenetic processes in the determination of clay mineral species in sedimentary basin had been investigated and found to be generally significant (Blatt *et al.,* 1972 and Bessong *et al.,* 2011). However, in the geological assessment of these clay deposits in the Lower Benue Trough, there had been little information on mineralogy and geochemistry and no published data on the isotope (hydrogen and oxygen) geochemistry of these clay deposits.

The need to determine the origin of the clay deposits and whether they are genetically associated with magmatic-hydrothermal, low temperature hydrothermal or meteoric water types could be resolved with stable isotope studies. Stable isotope techniques have shown to be reliable and particularly valuable in determining the nature of the clay deposit and source as well as determining the possible mechanism of mineral transport (Sheppard and Gilg, 1996; Savin and Hsieh, 1998; Nicholas and Neil, 2013).

This research aims at unravelling the paleo-climatic conditions during the weathering of the parent rock to form clay in Aloji, Ofejiji, Agbenema, Udane-Biomi, Oturkpa, Okpokwu of Mamu/Ajali Formation and Enugu of Enugu/Nkporo Formation within the Lower Benue Trough. The hydrogen/oxygen equilibration in clay-water systems, age of the precursor, as well as, the basin’s tectonic setting, in which the clay body was deposited and its economic potential would be investigated.

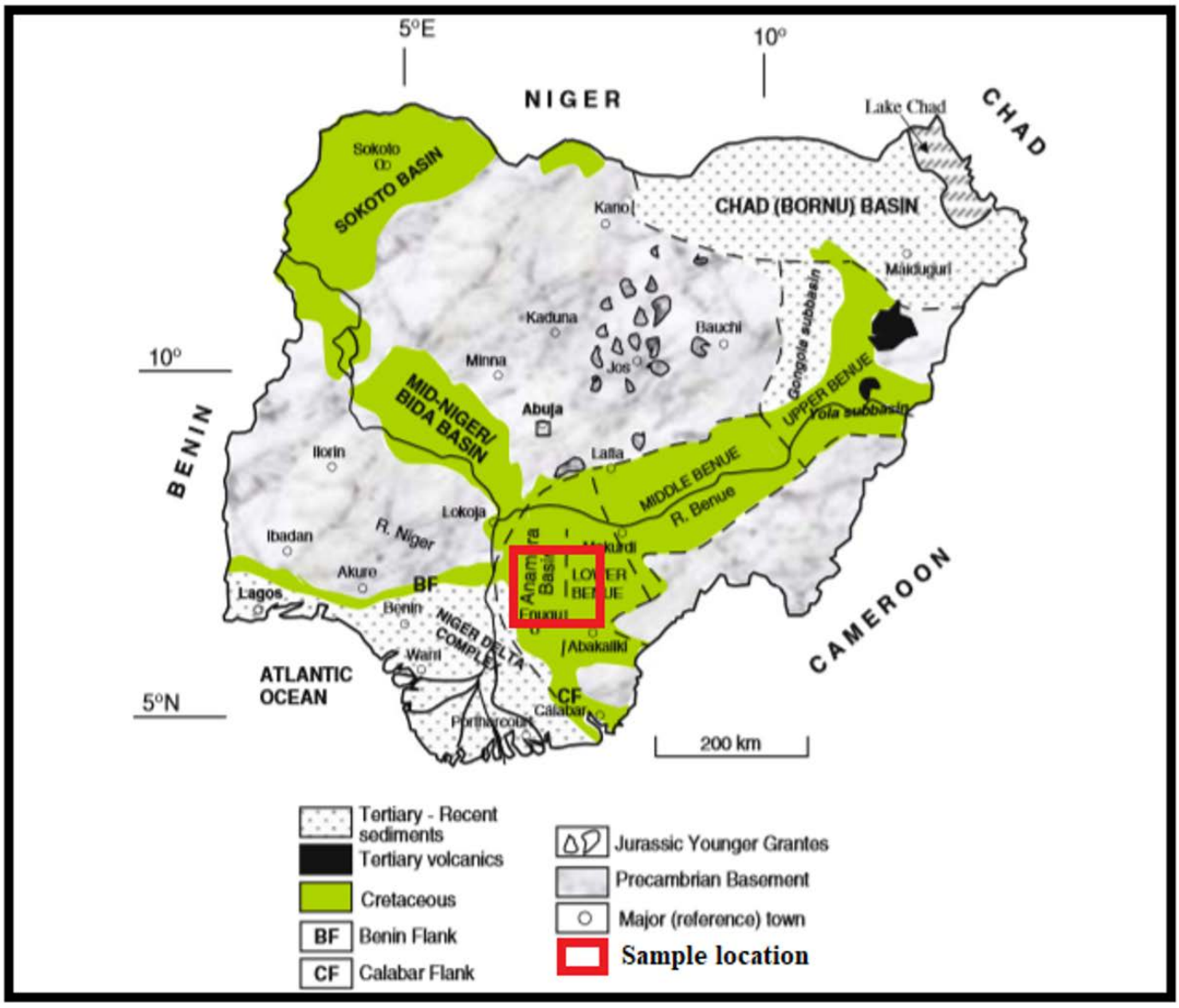

Fig. 1.1. Simplified Nigeria Geological map showing Lower Benue Trough's location (After Obaje, 2009).

1.2 Justification for the research

The clay deposits in the Lower Benue Trough within the Mamu/Ajali and Enugu/Nkporo Formations, which are available from Aloji, Ofejiji, Agbenema,Udane-Biomi, Oturkpa, Okpokwu and Enugu areas were commonly investigated because of the Pb-Zn-Ba-Fl deposits in them. However, mineralogical and chemical investigations in relation to the paleo-climatic condition during the weathering of the parent rocks, hydrogen and oxygen isotope fractionation factors, paleo-temperature when the sediments were deposited, the nature and origin of the deposits of clay, as well as, the age of the precursor were rarely discussed by early researchers.

1.3 Objectives of the Study

The objective of this research is to determine the mineralogical, geochemical and stable isotope composition of deposits of clay in Lower Benue Trough, Nigeria. The specific study's objectives are to:

1. to identify the field occurrences, morphology and mineralogy of clay deposits within Mamu/Ajali and Enugu/Nkporo Formations in the Lower Benue Trough, to deduce the possibility of diagenesis.

2. determine the clay's major, trace and rare earth elemental compositions as an indicator to their provenance, depositional conditions and environments, tectonic setting, paleoclimatic conditions, and age of source rocks.

3. to determine temperature of formation, altitude of deposition and paleoclimatic conditions of deposition of the clays from their oxygen and hydrogen isotopic compositions and ratios.

4. to evaluate the functional applications of the clay body based on their physical, mineralogical and chemical data.

1.4 Scope of the research

The research's scope includes geological mapping of the area for lithology and stratigraphy determination. Mineralogical analysis of the clay samples involving the dried whole rock, oriented and glycolated samples was carried-out. The morphology

of the clay was also determined with the chemical constituents. The hydrogen and oxygen isotopic composition of the clay were measured. Grain size separation of the silt from clay fraction and centrifuging at 800 revolution for 45 minutes to obtain the <2µm fine fraction of clay were achieved. Physical properties of the clay was also evaluated.

1.5 Location and Accessibility

The study area is situated between latitude 6°00' - 8°00' N and longitude 6°50' - 8°00' E (Fig. 1.2). The area is connected by tarred road, which leads from Aloji to Ofejiji, Udane-Biomi, Abocho, Agbenema, Eke-efe, Otukpa, Okpokwu and Enugu (Fig. 1.2). The roads are motorable all the year round.

1.6 Physiography and Drainage

The research area is characterised by undulating topography, which is evident from the variations in elevation from different locations within the Lower Benue Trough. Aloji (7º24'45″ N and 6º56'17 E) (7º24'44″ N and 6º56'14″ E) has an elevation of 225m and 209m, Ofejiji (7º45'57″ N and 7º26'32″ E) at 263m and 277m, Udane-Biomi (7º34'55″ N and 6º56'29 E) at 323m, Agbenema (7º48'00″ N and 7º27'14″ E) (7º47'47″ N and 7º27'07″ E) at 220m, 225m and 226m. Oturkpa (7º09'04" N and 7º44'50" E) at 170m, Okpokwu (7º09'00" N and 7º56'40" E) at 163m, 223m and 264m, while Enugu (6º28'20" N and 7º26'57" E) at 227m, 237m, 242m, 269m and 258m (Fig. 1.2). Okura, Okpokwu and Atavu Rivers with characteristic dentritic pattern were present in the study area.

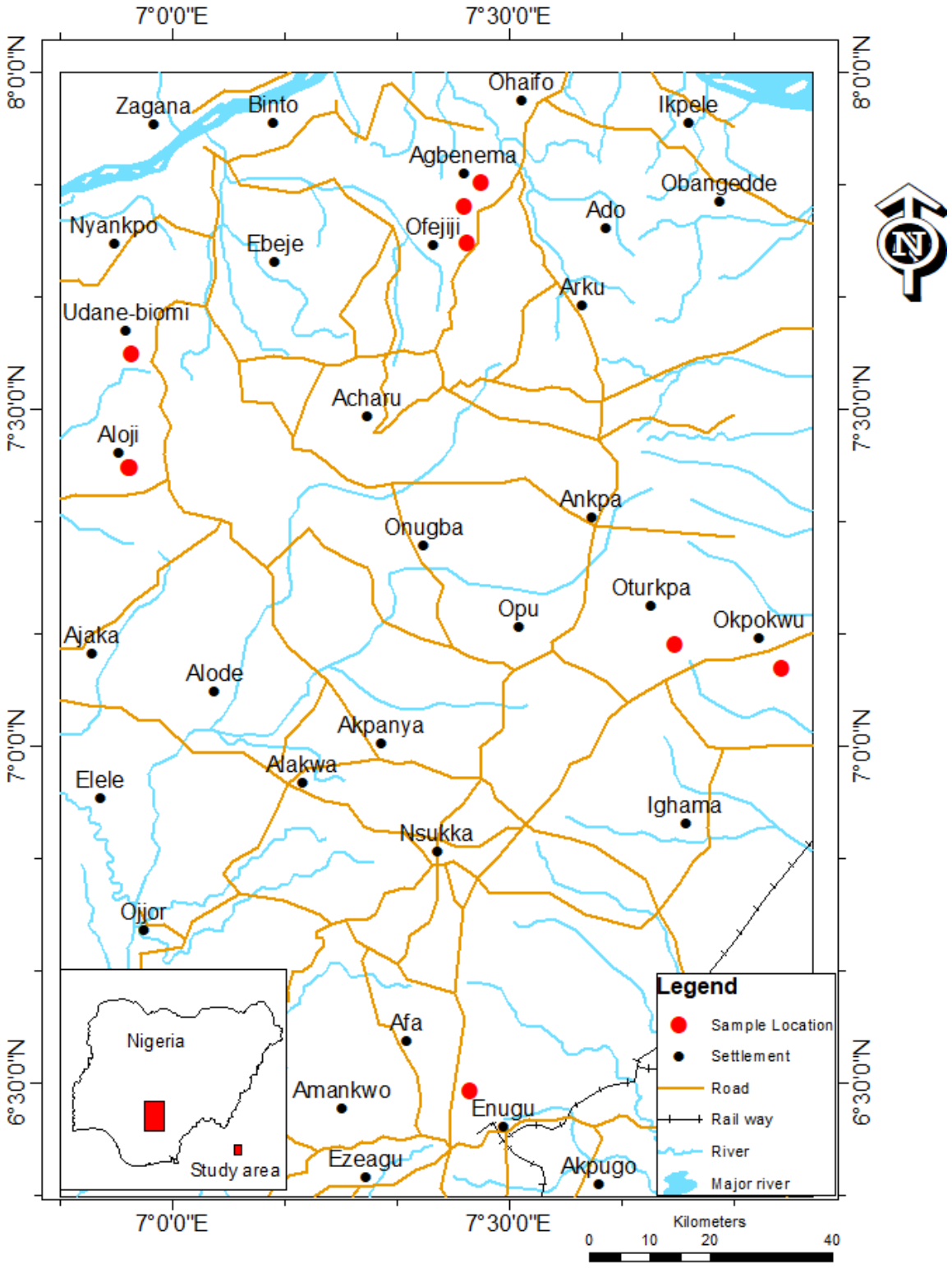

Fig. 1.2. Map of the study area showing sample locations for clay deposits of Ajali/Mamu and Enugu/Nkporo Formations within the Lower Benue Trough, Nigeria.

1.7 Climate and Vegetation

The research area is characterized by dry and wet season tropical climate with the rainy season lasting between April and October when the southwesterly moisture wind prevails over the north easterlies. The dry season is between November and March of the following year when the northeast trade wind, commonly refered to as harmattan prevails over the south westerlies (Ishaku and Majid, 2010).

The study area has an average annual rainfall of 1016 - 1270 mm. Figs. 1.3 and 1.4 are maps of Nigeria showing the distribution of annual rainfall and vegetational cover. Long-term fluctuation in rainfall trend may result in some extreme wet or dry years. During extreme wet years, it may result in flooding, high erosion and deposition rate (Ishaku and Majid, 2010).

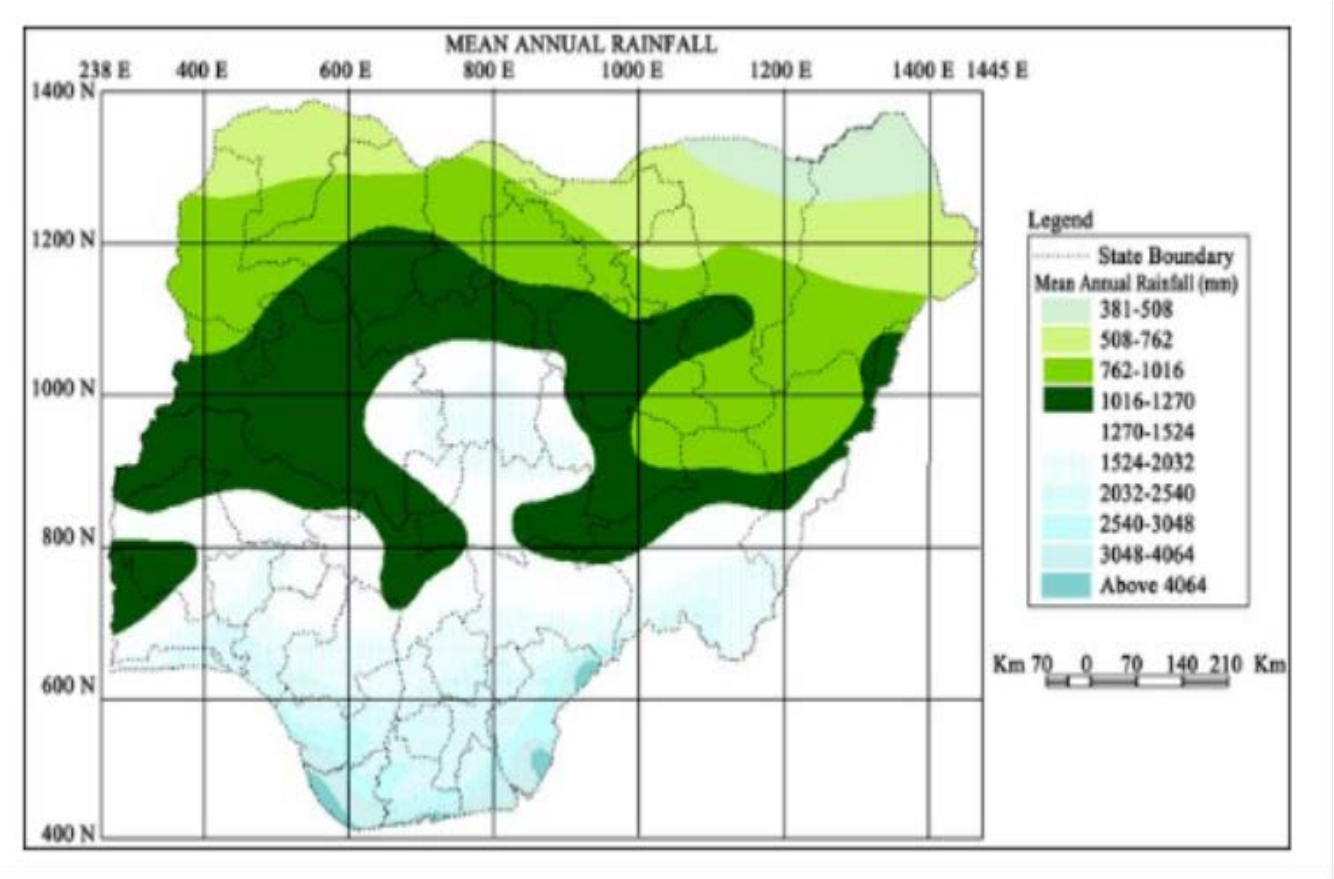

Fig. 1.3. Nigeria's annual rainfall distribution map
(After Ishaku and Majid, 2010).

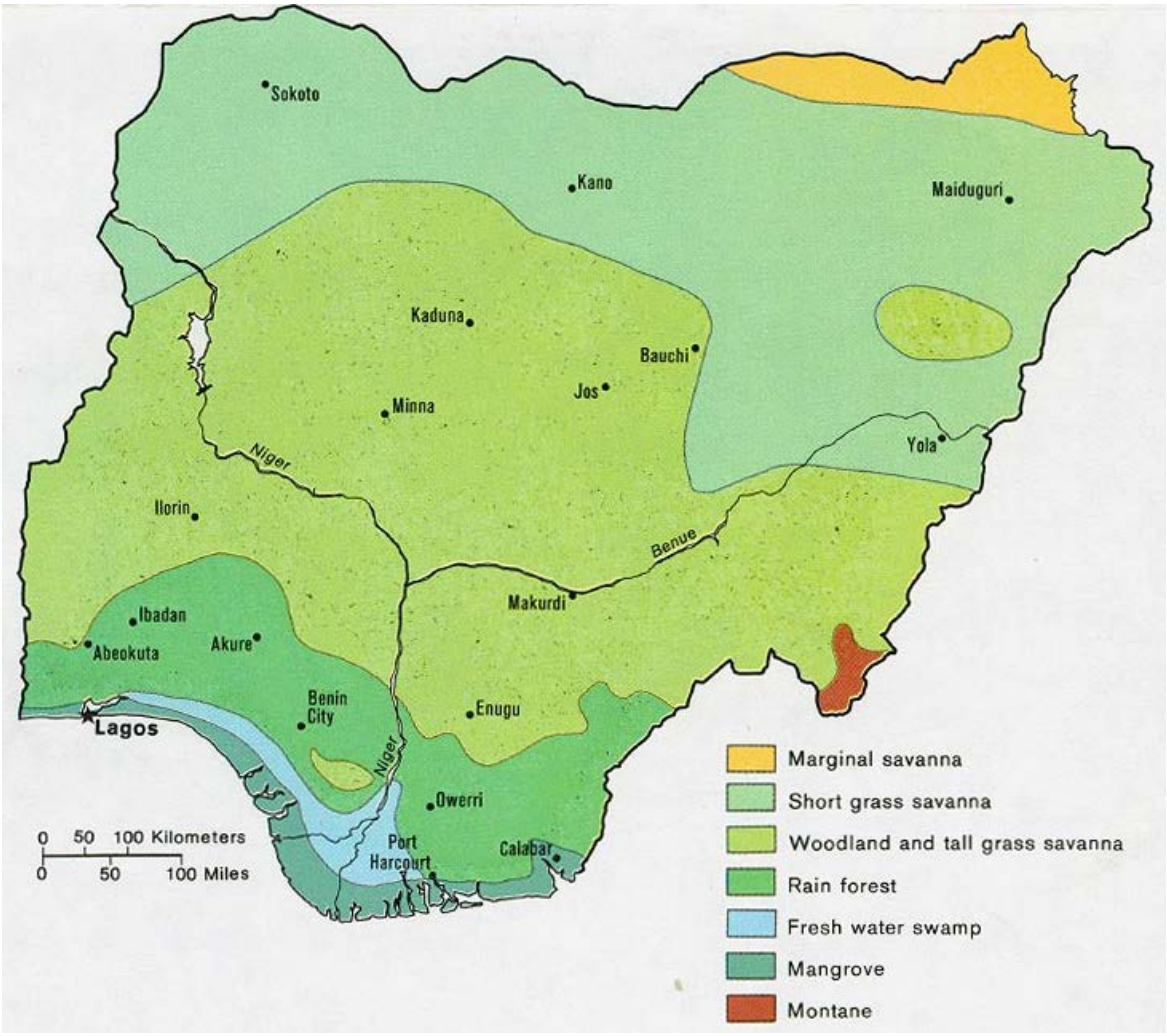

Fig. 1.4. Vegetational distribution of Nigeria. (Perry-Castañeda, 2006).

CHAPTER TWO

LITERATURE REVIEW

2.1 Regional Geology

The Benue Trough is a component of the rift complex known as the West and Central African Rift System during the Early Cretaceous period. Based on structures and sedimentary evidence from gravity measurements, three sections were known: Lower, Middle and Upper Benue Trough (Rebelle, 1990 and Obaje, 2009).

Grant (1969), Burke *et al.* (1970) and Coulon *et al.,* (1996) define Benue Trough as a sediment-filled basin resulting from continental drift and the opening of the Atlantic Ocean during the early Cretaceous period. During the Lower Cretaceous (Albian) according to Burke *et al., (*1970), marine sediments including shales, carbonates, argillites and sandstones was deposited in the basin. Thus, the Lower Benue Trough contains about 6000 m thick of marine to fluvio-deltaic sediments, which span Albian to Maastrichtian in age. These sediments experienced folding, mostly in the northeast to southwest area. Other notable geological activities including faulting, mineralization and igneous activities have been reported (Ezepue, 1984 and Nkwonta and Kene, 2005).

Offodile (1976) defined the Benue valley as a NE-SW trend in the inland Cretaceous basin of approximately 1000 km in length.

During the Santonian period, however, there was a closing period of the Atlantic and African plates that resulted in the folding that could be observed along the valley by their distinctive parallel and sub-parrallel structures Burke *et al.* (1970), Offodile (1976) and Coulon *et al.,* (1996).

Eustatic rise in sea level during the Albian transgression accompanied by subsidence and drawing of continental margins controlled deposition of sediments in three cycles that were interrupted by unconformities marked by three events (Cratchley and Jones 1965; Fig. 2.1). The first depositional cycle was during the Albian, which lasted until

early Cenomanian. The cycle was characterised by the deposition of marine formations. The Benue Trough experienced a non-depositional period during Middle Cenomanian, particularly in the Lower Benue Trough (LBT) (Fig. 2.1).

From Late Cenomanian to Coniacian, the second depositional cycle occurred, which was characterised by renewed transgression of marine sediments discernible by chains of long narrow folds trending ENE-WSW. These folds, are associated with the southeastern folds of the Abakaliki sedimentary region due to the intrusion of alkaline basalts, dolerites and syenites. (Murat, 1972). Santonian was a period of non-deposition.

The third depositional cycle, marked by the presence of a thin belt of lead-zinc mineralisation in anticlinorium of Abakaliki took place in LBT during Campanian to Maastrichitian periods. This belt is flanked by the synclines of Anambra and Afikpo (Akande *et al.,* 1992). The trend in NE-SW of the anticline was flanked by the Kadarko and Wukari Basins in the Middle Benue Trough (MBT). The Kaltungo in the Upper Benue Trough (UBT) distinguishes the Yola Basins from the Gongola Basins (Obaje, 2009; Fig. 2.1).

2.2 Stratigraphy of the Benue Trough

The Benue Trough is split into lower, middle and upper parts (Figs. 2.1, 2.2). The depocenters of the LBT consist mainly of the areas surrounding Nkalagu and Abakaliki. Between Makurdi and Yandev, Lafia, Obi, Jangwa to Wukari is the MBT. Pindiga, Gombe, Nafada, Ashaka (in the Gongola arm) and Bambam, Tula, Jessu, Lakun and Numan in the Yola Arm are the depocenters in the UBT (Idowu and Ekweozor, 1993; Obaje, 2009).

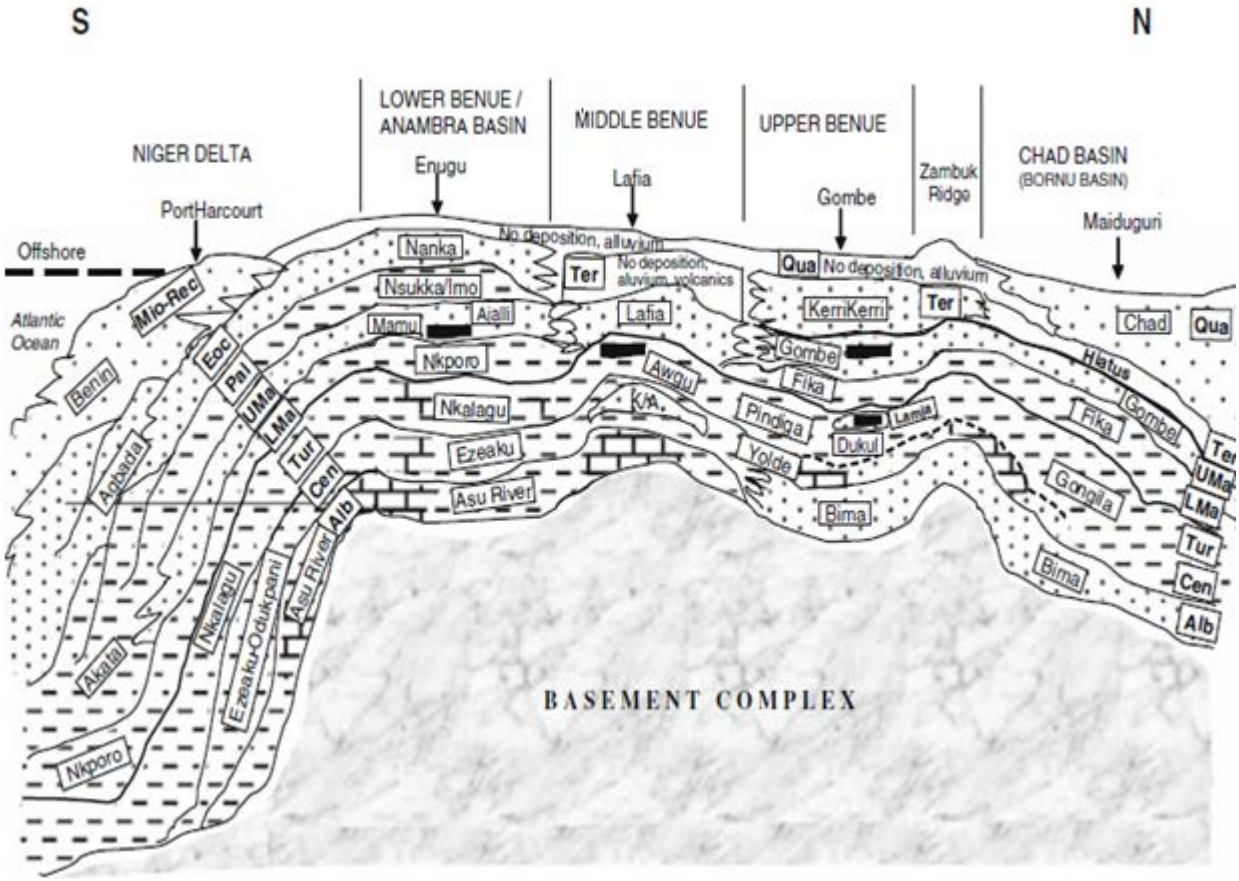

Fig. 2.1. Stratigraphic sections across the Benue Trough in N-S direction (After Obaje, 2009).

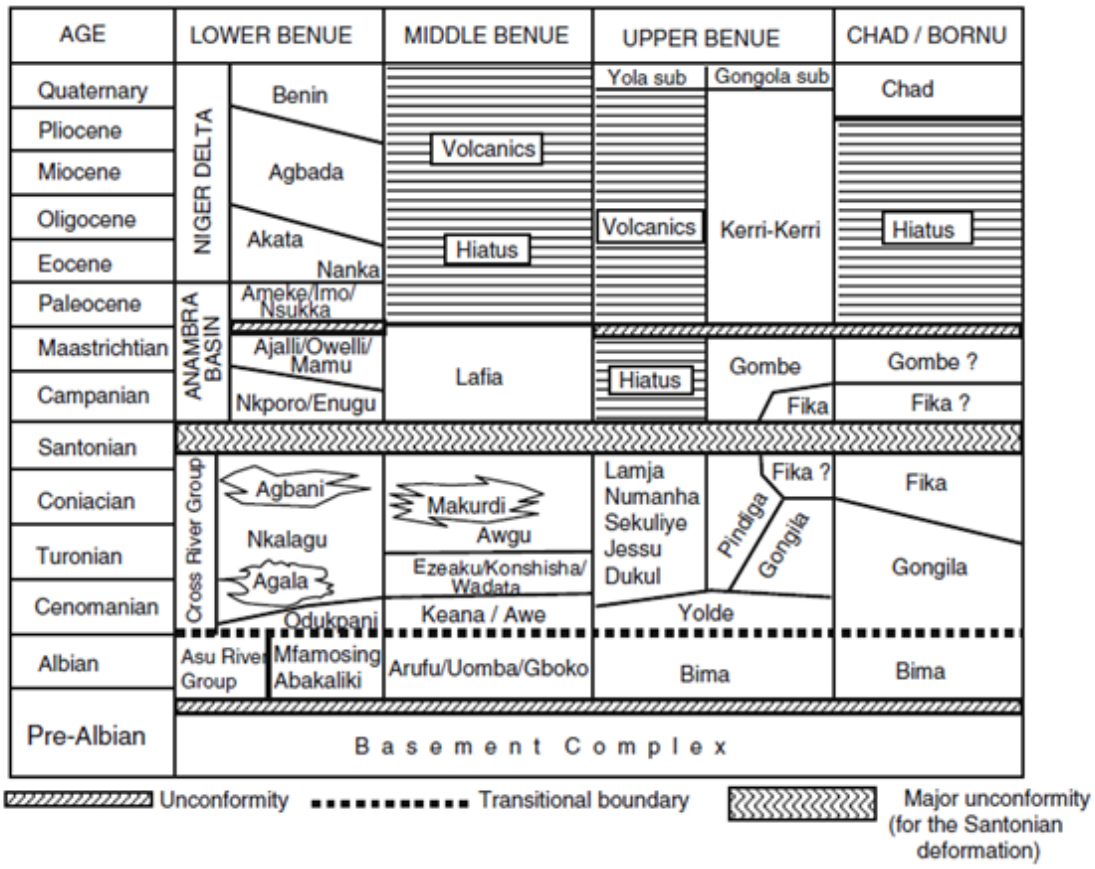

Fig. 2.2. Stratigraphic successions within the Nigeria Benue Trough, (After Simpson, 1954, Reyment, 1965, Petters and Ekweozor, 1982).

2.3 The Geology and Stratigraphy of the Lower Benue Trough

The stratigraphic sequence from the oldest to the youngest of the Lower Benue Troughs includes Asu River Group, Ezeaku Formation, Nkalagu Formation, Enugu and Nkporo Formations, Mamu Formation, Ajali and Owelli Formations, Imo and Nsukka Formations and Nanka Sandstones.

2.3.1 Asu River Group

The Asu River Group comprises shales of Abakaliki Formation, calcareous and sandstone lenses in the Abakaliki region and calcareous lenses of Mfamosing in the Calabar Flank (Petters and Ekweozor, 1982 and Ojoh, 1992; Fig. 2.1 and 2.2).

2.3.2 Ezeaku Formation

Following the Asu River Groups is the Ezeaku shales and the Makurdi Formation of Turonian age (Fig. 2.1 and 2.3). The Ezeaku shales are characterized by thick (calcareous and non-calcareous) flagged shales with sandy or shelly calcareous and calcareous sandstones. An outcrop of this formation is located in the southern area of Oturkpo division at Egedde-Oju area. It is about 300 to 600 m thick in this region (Obaje, 1999).

2.3.3 Nkalagu Formation

The Nkalagu Formation is a marine Cenomanian–Turonian black shales, calcareous, siltstones and the interfingering regressive Agala and Agbani sandstones that rest on the Ezeaku Formation (Fig. 2.1 and 2.2). Mid-Santonian deformation moved the major depositional axis westward in the Benue Trough, leading to the Anambra Basin being created. Therefore, the Anambra Basin is formed in the Lower Benue Trough as a post-deformation sedimentation. Sedimentation in Anambra Basin thus began with marine sediments in Campanian-Maastrichtian (Obaje, 1999; Fig. 2.2).

2.3.4 Enugu and Nkporo Formations

These formations consist of the brackish and fossil facies of the late Campanian-Early Maastrichtian depositional cycle (Ojoh, 1992; Fig. 2.1 and 2.2). The deposition of the sediments of Nkporo / Enugu Formations represents a funnel-shaped shallow marine

environment graded channeled marshes with low energy. The Nkporo shale outcrop on the Enugu-Port Harcourt in the village of Leru, 72 km south of Enugu, whereas the Enugu shale outcrop is in Enugu, close to the Onitsha-Road Flyover. (Obaje, 1999).

2.3.5 Mamu Formation

The Mamu Formation is a coal-bearing formation that accumulated with Ajali Sandstone during the Nkporo phase's overall regression. The Mamu Formation occcurs as a thin strip north–south of the Calabar Flank, swinging south around the Ankpa plateau and ending in Idah near the River Niger (Obaje, 1999; Fig.2.1 and 2.2).

2.3.6 Ajali and Owelli Formations

The fluviodeltaic sandstones of the Ajali and Owelli Formations lie on the Mamu Formation and constitute its lateral equivalents in most places (Fig. 2.1 and 2.2). The Ajali sandstone marks the altitude of the regression at a time when the coastline was still concave. The Ajali sandstone is characterised by tidal sand waves governed by converging littoral drift cells during the sedimentation (Obaje, 1999).

2.3.7 Imo and Nsukka Formations

During the Paleocene, the Imo and Nsukka marine shales were deposited (Fig. 2.1 and 2.2). These formations mark the start of another transgression in the Anambra Basin during the Paleocene. The shales contain significant organic matter and can be a prospective cause of hydrocarbons in the Niger Delta's southern portion (Ojoh, 1992 and Obaje, 1999).

2.3.8 Nanka Sandstone

The Eocene Nanka Sands mark the return of regression conditions (Fig. 2.1 and 2.2). Well-exposed, highly assymetric sandwaves indicate the flood-tidal currents predominance. The Umunya segment, 18 km from the Niger Bridge at Onitsha on the Enugu-Onitsha Expressway, is a good outcrop of the Nanka Formation (Obaje, 1999) .

2.4 Review of the structure, genesis, geology and occurrence of clays

2.4.1 Structure

Clay minerals are layered phyllosilicates (Meunier and Velde, 2004). The fundamental structural characteristic of all clay minerals is the mixture of layers in octahedral coordination involving pseudohexagonal network between SiO_4 tetrahedra and cations. Octahedral layers include gibbsite and brucite. Gibbsite layers are characterised by dioctahedral arrangement, while brucite layers are characterised by trioctahedral pattern, for each layer. Composite arrangement of each of the octahedral and tetrahedral layers result in a 1:1 structure as in kaolinite; or an octahedral layer sandwiched by two tetrahedral layers (2:1), a three-layer structure comprising montmorillonite and illite (Nesse, 2000; Meunier and Velde, 2004; Fig. 2.3). The phyllosilicates are cathegorized on the basis and character of octahedral-tetrahedral layers (Brindley and Brown, 1980). Kaolin minerals are the geochemically and industrially most ubiquitous and abundant species of the phyllosilicate family (Churchman, 2000).

2.4.2 Genesis and geology of clay minerals

Clay mineral comes from a multitute of settings such as crystallization in rock cavities, substitution of other minerals, modification of water-laid clastic silicate parent material, *in situ* variation of 'primary' silicate crystalline rock.. Others are kaolinization with hydrothermal modification, *in situ* modification of clay parent rock, sedimentary deposition of kaolin mineral, diagenesis and formation under complex geological situations (Churchman, 2000). Weathering and hydrothermal alteration are the two natural actions responsible for the creation of aluminosilicate rocks (Churchman, 2000). Formation and stability of clay depend on the changes within its depositional environment. Under distinct climatic conditions, clay minerals build up preferentially with accessible source rocks and minerals in the presence of water and favourable temperature, which makes them more chemically stable phyllosilicate (Weaver, 1985, Churchman, 2000).

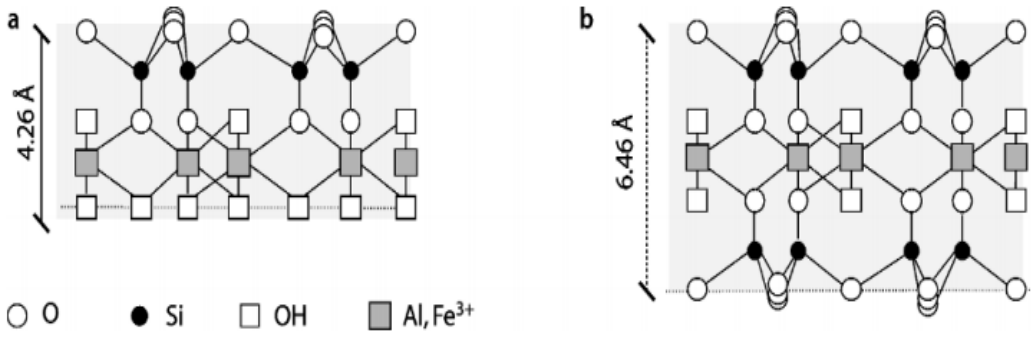

Fig. 2.3. The two crystal structure types of dioctahedral phyllosilicates; a. 1:1 layer; b. 2:1 layer (After Velde and Meunier, 2008).

The influx of groundwater has a major influence on the type of clay mineral formed from a specific main silicate. When a main silicate hydrolyses in an environment of high activity of H^+, alkali and alkaline earth metals are substituted, then the resultant product is a 1:1 layered phyllosilicate. If, on the other hand, the activity of metal ions remains relatively high, minerals of 2:1 clay form. Such an environment typically represents low intensity leaching, either in semi-arid weathering or alternatively in water-logged environment, where the metal ions remain in solution at high activity. For example, the reaction involved during the hydrolysis and subsequent leaching of albite under three different rates of groundwater flow is as shown below (Weaver, 1985):

$$H^+ + NaAlSi_3O_8 + 7H_2O \rightarrow Al(OH)_3 + Na^+ + 3H_4SiO_4\ (aq)$$

(Gibbsite)

(High flow rate)

$$2H^+ + 2NaAlSi_3O_8 + 9H_2O \rightarrow Al_2Si_2(OH)_4 + 2Na^+ + 4H_4SiO_4\ (aq)$$

(Kaolinite)

(Moderate flow rate)

$$Mg^{2+} + 3NaAlSi_3O_8 + 4H_2O \rightarrow 2Na_{0.05} + Al_{1.5}Mg_{0.5}Si4O_{10}(OH)_2 + 2Na^+ + H_4SiO_4\ (aq)$$

(Montmorillonite)

(Stagnant)

Apart from the above variables, the topography of the region also plays an important role in the formation of clay. A high water flow over a long period of time is essential for the formation of dense kaolinite deposits. For that, the terrain should be smooth with quiet tectonic conditions, so that the chemical weathering can be more effective than erosion. Both high relief and high elevation tend to cause a decrease in clay formation (Taylor and Eggleton, 2001).The type of clay formed can be determined by the structure of the parent materials during the previous weathering phases. In addition, their texture, porosity, density, composition, fabric and the degree of consolidation influence the formation of clay relative to the mineralogy of the precursor (Taylor and Eggleton, 2001).

Aluminosilicates are common constituents of bedrock and surrounding soil. With gradual weathering, primary silicates change into secondary clay minerals showing sequential changes in texture, chemistry and mineralogy. Depending on the local weathering environment, different alteration sequences were reported. The most abundant aluminosilicates resulting in clay formation are feldspars and mica group minerals (Cox *et al.*, 2000).

2.4.3 Clay occurrence

Clays are the minerals most prevalent in clay rocks, recent marine sediments and most soils. Clays, apart from kaolinites, generally occur in earthy masses of microscopic crystals. Clays are formed by altering alumino-silicates in weathering and hydrothermal processes at low temperature (Grim, 1968, Taylor and Eggleton, 2001).

The following chemical equations demonstrate K-feldspar's chemical weathering to kaolinite (Thomas, 1992).

$$3KAlSi_3O_8 + 2H^+ \leftrightarrow KAl_3Si_3O_{10}(OH)_2 + 6SiO_2 + 2K^+$$

K-feldspar Mica quartz

$$2KAl_3SiO_{10}(OH)_2 + 2H^+ + 3H_2O \leftrightarrow 3Al_2SiO_5(OH)_4 + 2K^+$$

Mica Kaolinite

By the action of water at a temperature of a few hundred degrees, clay minerals form alumino-silicates. Kaolinite is the weathering end-product under pH 4 to 6 of acid soil solutions. Kaolinite is often the principal mineral on well-drained slopes in humid climate soils, where abundant vegetation makes soil solutions acidic with cation leaching. Montmorillonite is the end product of an alkaline solution with pH 8 to 9; montmorillonite is characteristic of less humid soils. Illite is the most common marine sedimentary rock clay mineral suggesting that montmorillonite is transformed into illite by a slow reaction with abundant K^+ in the sea water. Clay minerals are characteristic of specific weathering settings and a research of clays could enable the paleoenvironment of formation or deposition to be reconstructed (Thomas, 1992).

2.5 Review of isotope geochemistry of clay minerals

Isotope geochemical studies of clay minerals from diverse environments, such as, continental soils and weathering profiles, continental and marine deposits, buried sediments, hydrothermal and metamorphic altered sediments, have shed light on when and how clay minerals form or alter, its temperature during formation and stable isotope (H and O_2) fractionation factor in a system (e.g clay-water) (Savin and Epstein, 1970 a and b, Savin and Hsieh, 1998, Nicholas and Neil, 2013).

Savin and Epstein (1970 a and b) studied $^{2}H/^{1}H$ and $^{18}O/^{16}O$ isotope system of clay minerals from different environments (continental and oceanic) at surface temperatures. Their studies from laboratory experiments and natural samples have shown stable geochemistry of clay minerals to be of great importance in geothermometry, clay provenance, diagenetic processes, origin and development of upper crustal fluids, hydrothermal systems, mineral-water interaction and palaeoclimates. This relies directly or indirectly on the understanding in clay-water processes of H- and O- isotope fractionation variables and the temperature when isotope exchange ceased in the medium. The aqueous fluid composition may influence the H- and O-isotope fractionation variables, but this is usually a secondary impact unless salinities are large and temperatures are low (Kakiuchi, 1994). The kinetic effect of isotopes are more complex and depend on several parameters including temperature, pressure, particle size and shape, mineral and fluid / solid ratio structure and exchange time. (Fallick *et al.*, 1993).

The isotopic composition of the clay can only provide data on a geological process if the mineral retains the isotopic composition that it obtained during the process. This means that the quality of interpretations depends on several variables, including the degree of understanding of the variables of clay-water fractionation and the rates and processes of isotopic exchange for both oxygen and hydrogen in clays; tetrahedral and interlayer water (Savin and Hsieh, 1998, Nicholas and Neil, 2013).

It is often hard to have a monomineral clay sample by separating the grain size. Other phases of fine grain, such as hydroxides, oxides, carbonates, other phyllosillicates or organic matter, must be eliminated in the clay fraction (Jackson, 1979). Organic

matter in the fine size fractions of clay could affect isotope concentrations. It is either absorbed on the surfaces/edges or accommodated within layered spaces, this is mostly not detected during mineralogical analysis, with it's own D/H ratio, it can add certain quantities of hydrogen to many isotopic analyses (Hoefs, 2004). Technique of step-heating extraction can sometimes be useful in the separation of organic hydrogen and carbon. They are conventionally present as H_2O^+ content after heating the mineral at temperatures below 120 to 200 ºC to remove adsorbed and interlayer water. Part of this water (H_2O^+) may be released from the organic constituents as hydrogen or methane gas. Some of the H^2O^+ values may be higher than the theoretical value of the mineral (Hoefs, 2004).

Surfaces of clay are usually connected with 1- or 2-layer dense adsorbed water, Particularly, the expandable ones such as smectites. Moum and Rosenqvist (1958) proved that adsorbed and interlayer water isotopically exchange in hours with vapour of atmospheric water. It is therefore necessary to separate oxygen and hydrogen from the framework (SiO_4) and (OH). Preheating the sample under vacuum at temperatures of up to 200^{o}C removes this water without major isotope exchange and appropriate isotope data can be obtained (Savin and Epstein, 1970a).

2.5.1 Application of isotope geochemistry (oxygen and hydrogen) in clay study

Isotopes are atoms of the same element with the same number of protons but different numbers of neutrons in their nuclei. Stable isotope are those that do not decay (Hoefs, 2004). During weathering, diagenetic processes or hydrothermal changes, clay minerals form in a wide range near the surface of the earth. Hydrogen (H^2/H^1) and O ($^{18}O/^{16}O$) isotope studies of clays are particularly useful to understand their genesis, low-temperature fluid-rock interactions, sedimentary procedures and paleoclimates (Sheppard and Gilg, 1996, Savin and Hsieh, 1998).

Oxygen, which exists in gaseous, liquid and solid states over large temperature ranges, is one of the most abundant elements on earth. These features make oxygen one of the most valuable in geochemical isotope studies. Naturally, O_2 isotopes occur as, ^{16}O (99.763 %), ^{17}O (0.037 %) and ^{18}O (0.199 %) (Rosman and Taylor 1998). Stable isotope abundance determination for oxygen is usually restricted to ^{16}O and ^{18}O

because of their higher average abundances and greater mass differences (Hoefs, 2004).

Oxygen isotope analysis provides a powerful tool for studying water / rock interaction. The geochemical influence of such an interaction between water and rock or mineral is a change in the rock and/or water composition of the oxygen isotope from its original values, as its composition is not in equilibrium. Detailed studies of the processes and kinetics of oxygen exchange between minerals and liquids show that there are three feasible mechanisms for exchange (Giletti, 1985).

Solution-precipitation: Larger grains develop during a solution-precipitation process at the expense of smaller grains. Smaller grains dissolve and recrystallize on larger grain surfaces, reducing the overall surface area and reducing total free energy of the system. Isotopic exchange of fluids occurs while the material is in solution.

Chemical reaction: The chemical activity of both fluid and solid in one substance is so distinct in two phases that a chemical reaction occurs. It involves breaking down a finite portion of the initial crystal and creating new crystals. The new crystals with the fluid would form in or near isotopic equilibrium.

Diffusion: Isotopic exchange takes place at the crystal-fluid interface during a diffusion process with little or no change in reactant grain morphology. In a concentartion or activity gradient, the random thermal motion of the atoms is the driving force. It is known that combined dissolution-reprecipitation is a much more efficient method than diffusion with a fluid phase. This was first experimentally proved by O'Neil and Taylor (1967). Fig. 2.4 Reviews oxygen isotopes naturally observed in major geological reservoirs. Hydrogen occurs in ^{1}H (proton) at 99,985% and ^{2}H (deuterium) at 0,015% respectively (Hoefs, 2004). There are two reasons why hydrogen isotopes are interesting: hydrogen is omnipresent in terrestrial settings, occurring in distinct oxidation states of H_2O, H_3O^+, OH^-, H_2 and CH_4, even at great depths in earth. Hydrogen therefore plays a major role, directly or indirectly, in a wide variety of natural geological processes. Some geologically important reservoirs with their ranges of compositions of hydrogen isotopes are given in Fig. 2.5. (Hoefs, 2004).

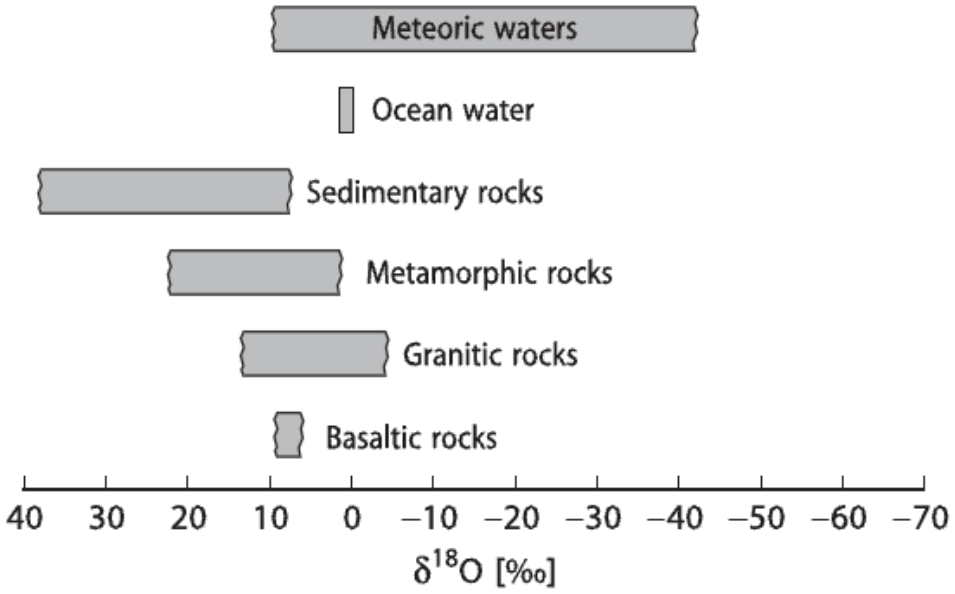

Fig. 2.4. Ranges of δO for some important geological reservoirs within the earth (After, Hoefs, 2004).

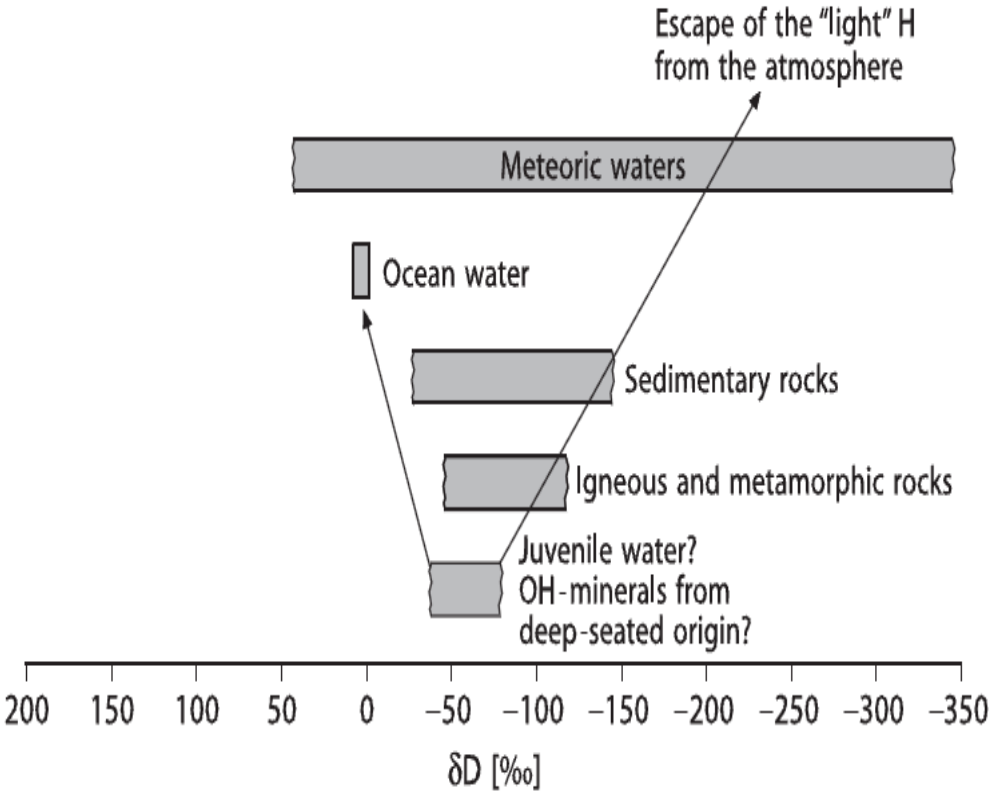

Fig. 2.5. Ranges of δD for some important geological reservoirs within the earth (After Hoefs, 2004).

2.6 Review of previous work

Occurrence of clay deposits in different parts of Nigeria were reported by different workers as early as the inception of the Geological Survey of Nigeria in 1905. Most of these reports are unpublished and commonly describe the geology of the areas of occurrences. Preliminary assessment of clay mineral species in various parts of southern Nigeria were carried out by Adeleye and Parker (1975), Ajayi and Agagu (1981) in order to ascertain the pattern of sedimentation in the entire basin. Agagu (1978) evaluated the extent of clay dewatering at depths in the Lower Benue Trough, to fashion out a model on the relationship between the expulsion of diagenetic water and petroleum migration.

The geology and stratigraphy of the Middle Cretaceous sequences, northeastern part of Afikpo Basin, Lower Benue Trough were reported to contain probably sediments obtained from proximal basement granites in shallow to deep marine settings under fluctuating energy levels, with two significant breaks in the Cenomanian and Turonian periods (Ukaegbu and Akpabio, 2009). Najime (2011) described the depositional framework and Cretaceous stratigraphy of the Gboko Area, Lower Benue Trough, Nigeria. He reported that the Gboko area presents a setting along the eastern margin of the Benue Trough where tectonic effects associated with tectonic evolution of the trough are preserved. Ikoro *et al.* (2012) It was reported that the combination of kaolinite and smecitite / illite indicates warm, humid, tropical weather during the Cretaceous in Southern Benue Trough. Acra *et al*. (2013) found that the Ogwashi-Asaba stratigraphic architecture in Anambra Basin shows various facies associations such as the tidally influenced channels, braided fluvial channels, flood plains and fluvial channel. Also, a new model of a tide dominated depositional system was thus proposed in their study based on integrated ichnological and sedimentological data. Adeigbe and Yusuf (2013) suggested that Cretaceous clastic sediments of Asu River Group and Cross River Group of the Lower Benue Trough Nigeria have diverse Upper Continental Crust (UCC) provenances, underwent moderate to high weathering conditions and were deposited within an oxidizing and shallow marine setting. Idakwo *et al*. (2013) during their studies on the distribution of clay minerals in the Northern Anambra Basin, Nigeria showed that the large quantity

of kaolinite in the Mamu Formation is suggestive of climatic changes from dry to wet. Alege *et al*., (2014) concluded that the clay deposits within the northern Anambra basin, Nigeria are derived from a felsic source, matured and underwent a high intensity of weathering. Adeigbe and Ayoola (2014) interpreted cerium anomalies (Ce/Ce*) in Asu River Group and Cross River Group as an indication of an oxidizing and shallow marine environment for the clastic sediments of southeasthern Nigeria. Odoma *et al*. (2015) revealed that the clay-rich sediments of southeasthern, Nigeria, probably granitic basement derivatives, the Oban massif. They emphasized that Th and Sc remained immobile despite the intense weathering of rare earth elements. Alege *et al.* (2015) reported on the compositional characteristics and industrial assessment of the Cretaceous clay deposits in the northern Anambra Basin and suggested that the clay deposits could be used in the manufacturing of ceramic, pottery and refractory materials. Uzoegbu and Agbo (2019) revealed that the shales from Afikpo Graben, S.E Nigeria comprises of quartz, clay minerals, carbonates and iron rich minerals, while the dominant clay mineral is kaolinite with minor amounts of illite and smectite as typical composition of tropical sediment.

CHAPTER THREE

METHODOLOGY

3.1 Geological field mapping and sample collection

Geological field mapping of the study area was carried out using a topographic map on a scale of 1:875, 300. Reconnaissance surveys of the study area to select areas with clay outcrops were done. The study area consists of the Late Cretaceous (Campanian-Maastrichtian) sedimentary rocks of the Ajali/Mamu and Enugu/Nkporo Formations. Thick deposits of sedimentary clay sequences were observed at Aloji, ~25 kilometres northwest of Anyigba town constitute a thickness of about 11.5 m with 0.5 m lateritised sandstone at the top of the deposit and Ofejij, 20 kilometres NNE of Iyale General Hospital in Kogi State, the clay deposit is about 15 m thick with intercalation of sandstone of 1.0 - 2.3 m thick. The Ofejiji clay deposit overlies a shaly layer. Agbenema clay deposit, 0.5 and 1.5 km from Iyale General Hospital, Kogi State outcrop along road cuts, which alternates with sandstone has an overall thickness of about 7.5m thick. The clay deposits under the bridge near Oyeama mine, Enugu-Onitsha and Abakaliki-Onitsha expressways in Enugu varied from 17 m to about 23 m thick with intercalation of sandstones and lamination of coal seems. Okpokwu and Oturkpo clay deposits are located along Oturkpo – Gbokolo road. The clay is yellowish brown in colour and about 5m thick with intercalation of sandstone. These clay deposits are limited within the Cretaceous sedimentary basin of the Lower Benue Trough of Nigeria.

Fifty samples of clay were collected from Aloji, Ofejiji, Agbenema, Udane-Biomi, Oturkpa, Okpokwu and Enugu for mineralogical and chemical analyses. With the aid of a Global Positioning System, Sample locations including Latitude, Longitude and Elevation were determined and recorded. One to 2 kg representative sample of clays were collected from exposed road cuts with the aid of jigger and shovel at the different locations and stored in pre-labelled polythene bags. The sample colour, grain size, hardness, constituent minerals and level of weathering were determined with the aid of a hand lens for all the sampled clays from Aloji, Ofejiji, Agbenema, Udane-Biomi,

Oturkpa, Okpokwu of Ajali/Mamu Formation and Enugu of Enugu/Nkporo Formation in the Lower Benue Trough.

3.2 Sample Preparation

The fine fraction of the raw clay was separated from the bulk clay based on Stokes' law (Gaspe *et al.*, 1994).

$$V = \frac{2/9\ g.r^2\ (Gs - \gamma w)}{\mu}$$

where V = particle settling velocity, Gs = particle specific gravity,
γw = specific gravity of the liquid medium, g = force of gravity,
μ = viscosity, and r = radius of the particles.

The method of separation involved soaking the sample in water in a blender that is three quarter full and blending for 10 minutes to disaggregate the material. This blending process generated a suspension of the material disaggregated into individual grains. The suspension was then placed in a plastic beaker and ultrasonically disaggregated, vigorously, with an ultrasonic probe for 10 minutes to produce a disaggregated suspension suitable for further size separation via settling and centrifuging. The appropriate time for settling the > 2 μm clay fraction was calculated using the above principle and the suspended slurry comprising the < 2 μm clay fraction was centrifuged and air-dried. Some of the clays that flocculated were washed with deionized water to bring them into suspension. This process was repeated several times. Bottles of 250-mL capacity were used to extract the remaining clay minerals from suspension. Due to the chemical composition of the clay, sodium hexametaphosphate was not used as a dispersing agent in the clay slurry. The fine < 2 μm clay fraction was used for the oriented clay mount (XRD) , H and O_2 stable isotope analyses.

The raw clay samples were pulverised and packaged for XRD (random powder mount and oriented), scanning electron microscope (SEM), differential thermal/thermogravimetric analysis (DTA/TGA), Fourier transform infra-red analysis

(FTIR) and stable isotope (hydrogen and oxygen) analyses at the Geological Sciences Department, Indiana University, Bloomington, Indiana, U.S.A. Major oxides, trace and rare earth elemental analysis were carried out using inductively coupled plasma – emission spectrometry (ICP-ES) and inductively coupled plasma – mass spectrometry (ICPMS) at ACME Laboratory, Canada.

3.3 Mineralogical analyses

The mineralogy of the raw and fine (< 2 μm) clay samples were determined using a combination of analytical methods including XRD, SEM, DTA/TGA and FTIR.

3.3.1 X-ray diffraction (XRD) analysis

The clay (32 raw and 28 fine (< 2 μm) samples were analyzed using a Bruker D8 Advance X-ray diffractometer scanned from 2^{o} to 70^{o} with Cu Kα radiation (45 kV, 35 mA) and counting of 2 sec for 0.02^{o} step. Using the Bruker AXS EVA software and International Centre for Diffraction Data (ICDD) powder diffraction file, clay and non-clay minerals were identified. Rietveld refinement using Bruker AXS Topas was used for quantitative analysis of mineral compositions of the raw samples. Both randomly and oriented mounts were analysed.

3.3.1.1 Randomly oriented mounts

A random sample preparation is essential to determine the clay and non-clay (whole rock) mineralogy and mineral abundance for a sample. Such analyses ideally require a near-perfect random orientation of all the crystals in a sample, which is often very difficult to achieve. Various methods for the random orientation have been suggested by Brindley and Brown (1980) and Moore and Reynolds (1997). In the present work, random orientation of the clay sample was achieved by allowing the free fall of the powdered samples into a 1 mm deep cavity in a titanium sample mount, thereby minimising preferential orientation of clay crystals.

3.3.1.2 Oriented mounts

Preferential orientation of clay minerals involves either placing a clay suspension on a flat surface, usually glass, suction of the suspended material onto a flat unglazed ceramic tile, membrane filters or porous metal surface, smearing a clay paste onto a

glass slide, or application of pressure to a dry powder (Brindley and Brown, 1980, Moore and Reynolds, 1997). Following dispersion of the clay sample in distilled water, oriented mounts were prepared in the present work by extruding the clay slurry onto a zero-background quartz plate. The sample was dried on the quartz plate at room temperature prior to XRD analysis. Analysis was performed on air-dried samples and subjected to ethylene glycol vapour for at least 24 hours to help detect and characterise expandable clays and then re-analysed.

3.4 Thermal analysis

The thermo-analytical methods complement the X-ray diffraction analysis (XRD).

In thermal analysis, the physical property of a substance or its reaction products is measured as a function of temperature, whereas the substance is subject to temperature control (Paterson and Swaffiels, 1987). Thermal analysis was carried out using a SDT 2960 Simultaneous DSC/TGA analyzer at a heating rate of 10 °C/min in the ambient range up to 900°C with alumina as standard. A schematic representation of the thermal analyser having the multichannel system analysis is given in Fig. 3.1. Nine (9) fine (< 2 μm) clay samples were used.

3.4.1 Differential thermal analysis

Differential thermal analysis is a method for studying the behaviour of a material during heating and cooling. The name is derived from the differential struture of the thermocouple, composed of two thermocouple wires (Michael, 1998). The first thermocouple is positioned in a sample of substance to be analysed and the second one in an inert reference substance (Fig. 3.1), which has been selected so that it will experience no thermal change over the temperature array being considered. When the temperature of the sample equals the temperature of the reference substance, the two thermocouples generate indistinguishable voltages and the net output is zero. When sample and reference temperatures vary, the ensuing net voltage disparity mirror the disparity in temperature between sample and reference at any point in time. The μV yield from the differential thermocouple pair is then amplified and recorded. Differential thermal results are recorded as the DTA curves, in which, by convention, ΔμV is plotted on the ordinate with downward pointing endothermic peaks, and

exothermic reactions as upward deflections from the horizontal base line, while on the abscissa, the sample temperature, increases from left to right. The quatity of divergence of the baseline curve represents the temperature difference between the sample and the furnace at any specified temperature and is therefore, a measure of the intensity of thermal reactions (Michael, 1998).

3.4.2 Thermogravimetry (TG)

The heating phenomenon at a regulated pace or above ambient temperature involves a weight loss owing to dehydration, desorption, decomposition and oxidation. In essence, thermogravimetric analysis is a means of observing the sample weight as a function of temperature (dynamic heating) or time (isothermal heating) (Michael, 1998).

The parameter measured in TG includes the measurement of the mass of a substance as a function of temperature while the substance is subject to a controlled temperature program. In reporting the curves, the mass of the sample should deccrease in the ordinate, while in the abscissa, the temperature or time should increase from left to right. Fine (< 2μm) clay samples were used for the thermal analysis.

3.4.3 Infrared spectral analysis

The infrared spectrum of clay minerals provides fundamental information not only on the mineral identification, but also on the surface properties and reactions of the minerals with the chemicals in their environment (Russel, 1987 and Tan, 1998). In the proportion (1:200), The < 2 m clay samples were dispersed in KBr, and are pressed into discs. The sample was scanned and the spectrum over the range of 4000 to 400 cm^{-1} was recorded. The Transmittance (T %) Vs Wavenumber (cm^{-1}) plots are presented. Ten (10) fine (< 2 μm) clay samples were used.

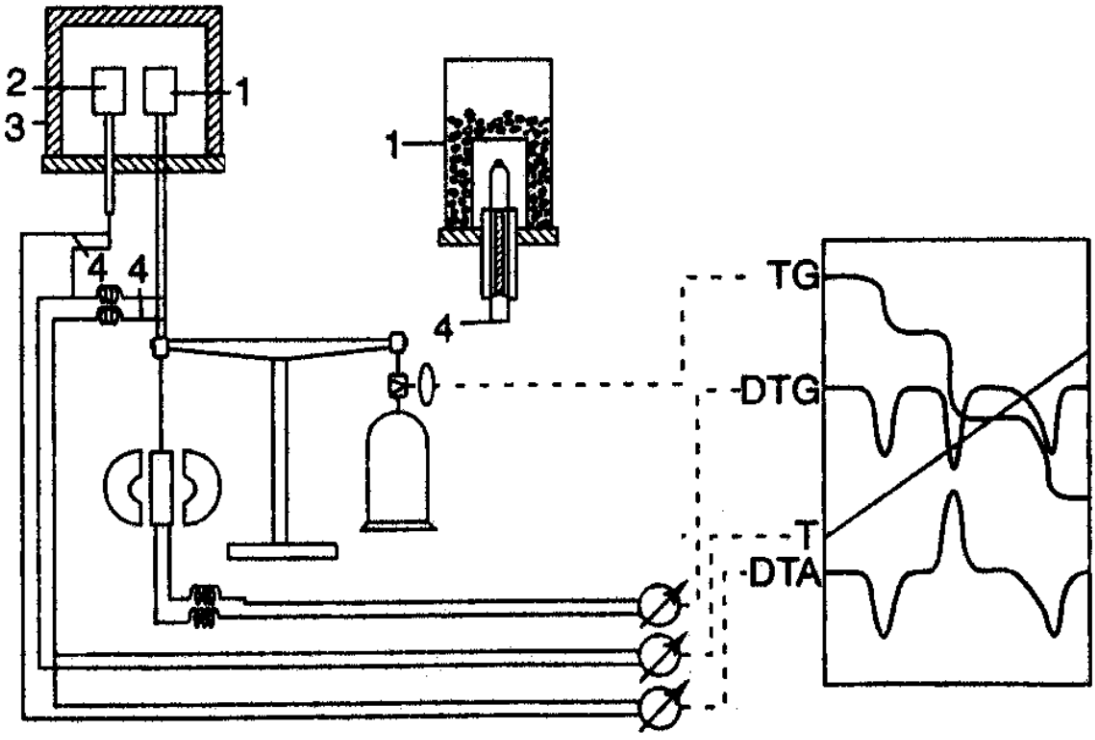

Fig. 3.1. Schematic representation of TG/DTA analyser (After Michael, 1998).
1 = sample, 2 = reference, 3 = furnace and 4 = thermocouple

3.4.4 Scanning Electron Microscope (SEM) Analysis

SEM reveals the fine structure of even the smallest of the clay mineral particle thereby aiding the evaluation of the mineral (Bentabol *et al.* 2006). Preparation for SEM analysis involved sprinkling of clay powder samples onto an adhesive tape on the surface of the brass stud of the microscope. The morphology of the major and the associated minerals on the adhesive tape were analysed. An environmental Scanning Electron Microscope (FEI Quanta 400 FEG), which requires no coating was used for the analyses. Eight fine (< 2 µm) clay samples were used.

3.5 Chemical analysis

The chemical composition of eighteen (18) raw and Fourteen (14) fine (<2µm) clay samples were determined using Inductively Coupled Plasma-Mass Spectrometry (ICP-MS) and Inductively Coupled -Atomic Emission Spectrometry (ICP-AES) at Acme Laboratory, Canada.

3.5.1 Major oxides, trace and rare-earth elements analyses

Thirty-one clay samples, including 15 raw and 16 fine (<2µm) clay samples, were analysed using an ICP-MS (Model: Perkin-Elmer Elan 6000) on a powdered 3-5 g clay samples at the Acme Lab. Ltd., Canada for major, trace and rare-earth elemental compositions. It was digested in a graphite crucible blended with 1.5 g Lithium metaborate/tetraborate ($LiBO_2$/$LiB4O_7$) flux by weighing 0.2 g aliquot. Placed in an oven, the crucibles were heated for 30 minutes at 980 ^oC. The cooled bead was dissolved in 5% HNO_3 (nitric acid grade ACS diluted in demineralized water). Sample sequences were supplemented with calibration norms and reagent blanks. The basic set of 34 components including Ba, Co, Cs, Ga, Hf, Nb, Rb, Sn, Sr, Ta, Th, U, V, Y, Zr, La, Ce Pr, Nd, Sm, Eu, Gd and Lu was established for the clay samples. Digested in Aqua Regia, a second 0.5 g sample was analysed by ICP-MS to determine Au, Ag, As, Bi, Cd, Cu, Hg, Mo, Ni, Pb, Sb, Se and Zn. The ICP-AES (Spectro Ciros Vision) was used to determine major oxides and certain trace elements, such as SiO_2, Al_2O_3, Fe_2O_3, CaO, MgO, TiO_2, P_2O_5, Cr_2O_5, Ba, Nb, Ni, Sr, Sc, Y and Zr. For both packages, loss on ignition (LOI) was determined by measuring the weight loss following 90 minutes of heating a 1.0 g split sample at 95 ^oC.

3.5.2 Stable Hydrogen (H^2/H^1) and oxygen ($^{18}O/^{16}O$) isotope analyses

Stable isotope studies of clays are particularly useful in understanding their genesis, low-temperature fluid-rock interactions, sedimentary processes and paleoclimates (Mizota and Longstaffe, 1996; Sheppard and Gilg, 1996; Savin and Hsieh, 1998).

3.5.2.1 Hydrogen (H^2/H^1) isotopic analysis

For isotopic analysis, the principle of Bigeleisen et al. (1952) was used to extract H. For the removal of adsorbed moisture, Nineteen (19) fine (<2μm) clay samples were degassed at 50°C in an oven. By heating up to 1404 °C in Mo crucible with an induction furnace, water (H_2O) was removed from the clays. Through reduction over hot U, the H_2O was changed to H_2 gas. The yields were calculated manometrically. An isotope ratio mass spectrometer (IRMS) with TCEA inlet spectrometer with model Delta Plus XP was used to measure the hydrogen isotope composition. The instrument was calibrated using Vienna Standard Mean Ocean Water (VSMOW) (Gofiantini, 1984).

3.5.2.2 Oxygen isotopic analysis

According to Clayton and Mayeda (1963), the oxidizing reagent used in this present work is bromine pentafluoride (BrF_5). in the laboratory, copper and nickel metal vaccum systems are used to handle it. It reacts at room temperature easily with glass. Its reactivity to oxides and silicates is approximately equal to that of fluorine. Nickel is the only material suitable to contain bromine pentafluoride at elevated temperatures of 500 – 600 ºC. Bromine pentafluoride's typical reaction with a silicate is:

$$KAlSi_3O_8 + 8BrF_5 \rightarrow KF + AlF_3 + 3SiF_4 + 4O_2 + 8BrF_3$$

Eleven (11) fine (<2μm) clays were used and ranged from 2.9 – 4.2 in mg weight, there were oven dried for 12 hours at 200 ºC. After pretreatment, the reaction tubes are evacuated and each tube is charged with BrF5. By immersing the tube in liquid nitrogen, this reagent, 1/400 mole of BrF_5 was condensed into all the sample tubes. The weight of the material was chosen (2.9 – 4.2mg) to give an approximate 100 –

400 µmol of oxygen, on this basis the quantity of the reagent was such that its five times stoichiometric requirement.

The reaction tubes are then closed and heated at 450°C by a furnace with electrical resistance. After reaction, the furnaces are removed and the tubes allowed to cool to room temperature and the oxygen sample is removed from each tube by opening the valve on the reaction tube to allow the gas mixture to flow into the metal vacuum line up to the V1 and V2 valves (Fig. 3.3 and 34). Valve V2 was slightly opened to allow the gas slowly, cooled with liquid nitrogen to flow through the glass trap. Only oxygen passes through the cold traps of all possible products, namely O_2, BrF_5, BrF_3, Br_2, SiF_4 and HF. An automatic toepler pumped oxygen into a calibrated dimension to determine the quantity of oxygen. It takes about 20 minutes to obtain the whole sample of oxygen (Fig. 3.2 and 3.3).

The gas was passed over hot carbon after oxygen collection and measurement to convert it to carbon dioxide by:

$$C + O_2 \rightarrow CO_2.$$

Inside a water jacketed glass tube, the carbon was suspended and heated by radio frequency induction. The temperature is approximately 550-600 ° C, this low enough to avoid carbon monoxide formation. In a liquid nitrogen-cooled U-tube, oxygen was circulated over the hot carbon, and the carbon dioxide is frozen outThe conversion from oxygen to carbon requires about 15 minutes and is accomplished while the nickel response pipe collects the oxygen from the next sample. The carbon dioxide was transferred to a manometer for measuring the reaction yield and then to a sample tube for transportation to the mass spectrometer. Extracting a set of 5 oxygen samples and one blank (usually less than 1 µmol) requires 3-5 hours. The oxygen appears to be at the walls of the reaction tubes, the quantity of oxygen in the reagent is totally negeligible. You can finish one set of samples everyday by operating the BrF_5 reactions overnight, and extracting oxygen in the morning.

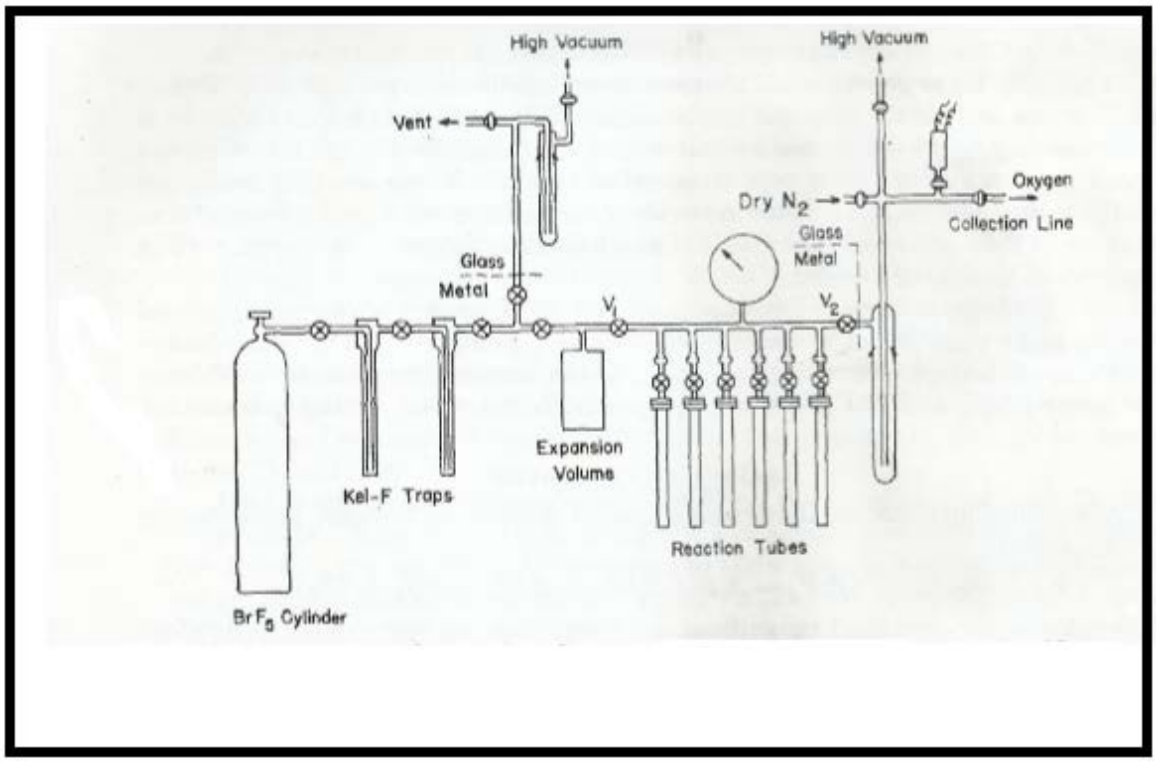

Fig. 3.2. Apparatus for reaction of oxygen with bromine pentafluoride (After Clayton and Mayeda, 1963).

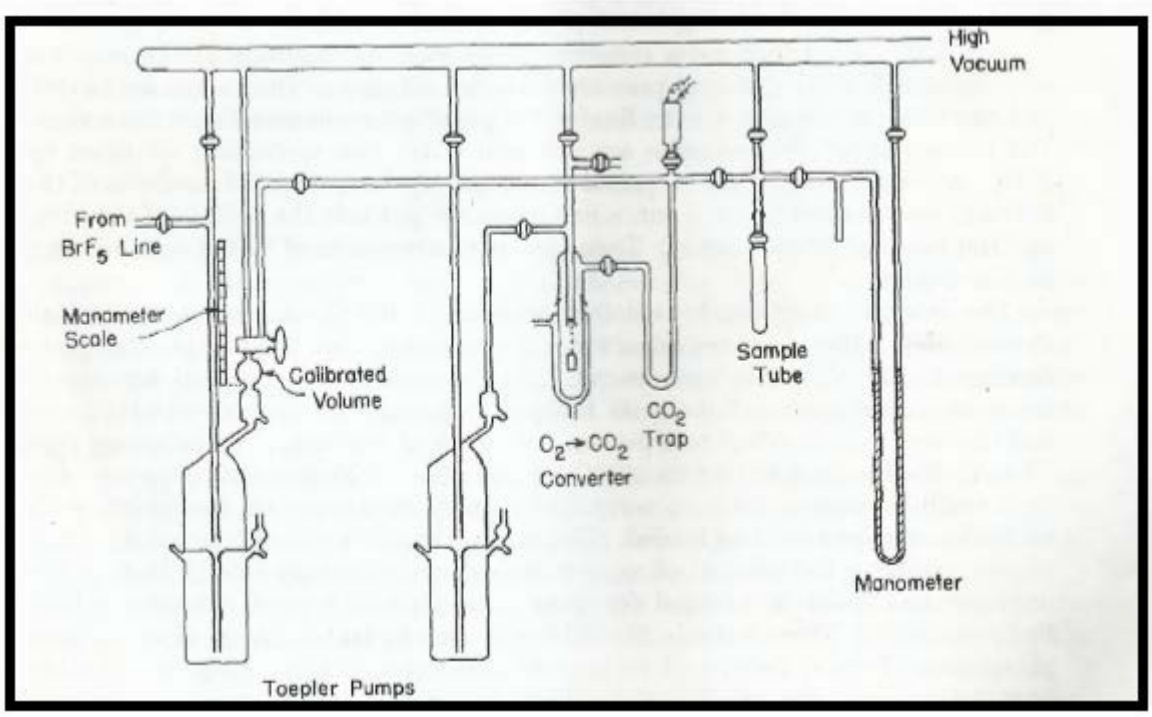

Fig. 3.3. Oxygen collection and carbon dioxide conversion apparatus (After Clayton and Mayeda, 1963).

3.6 Physical and Industrial Tests

Physical tests carried-out include: Atterberg Limits (Liquid Limits, Plastic Limits and Indices of Plasticity). Others are: specific gravity and moisture content. These laboratory analyses were conducted using two standard techniques; British Standard (BS 1377:1990) and American Society for Testing and Materials Standard (D1557:1992) at Earth Sciences Laboratory, KSU, Anyigba, Kogi State, Nigeria. Fifteen (15) raw clay samples were selected for this analysis.

The flowchart for the research methodology is presented in Fig 3.4.

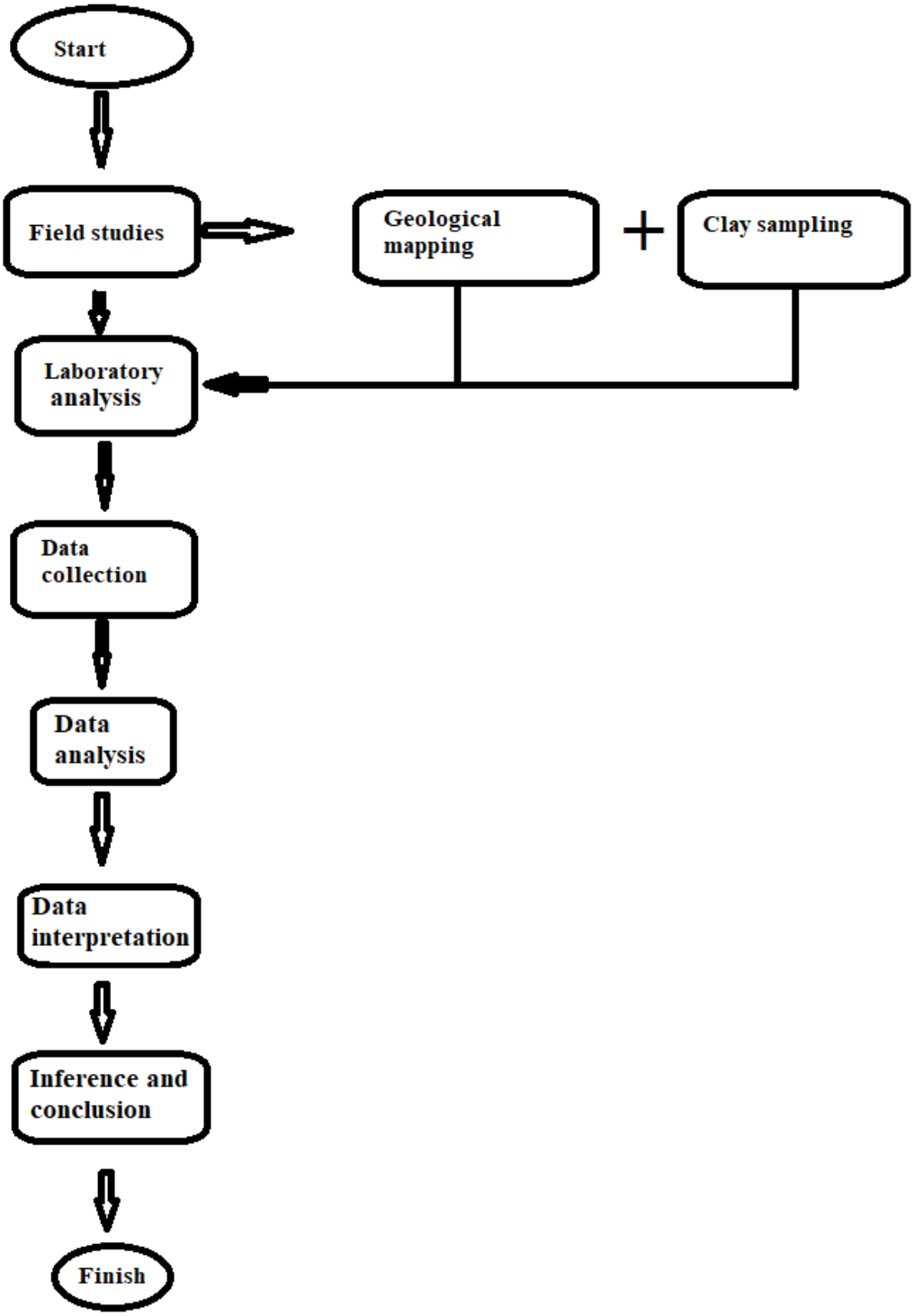

Fig. 3.4. Flow chart for the research methodology

CHAPTER FOUR

RESULTS AND DISCUSSION

4.1 Geology of the study area

Mapping and sampling of the Cretaceous sedimentary rock exposures within the Enugu/Nkporo and Mamu/Ajali Formations of the Lower Benue Trough (Fig. 4.1), showed from bottom to top the presence of shale with intercalation of coal overlained by clay and lateritised sandstone. The shales are thick, fissile and carbonaceous with carbonaceous concretions embedded along lamination planes. The thickness of the shale ranged between 0.8 and 2m.

Clay samples were collected from Aloji (7º24'45″ N and 6º56'17″ E), Udane-Biomi (7º34'55"N and 6º56'29" E), Ofejiji (7º45'57" N and 7º26'32" E), and Agbenema (7º47’60"N and E007º27’14"E) areas. Others were collected from the Pottery mine at Iva-Valley (6º27'55" N and 7º27'17" E) along Enugu-Onitsha expressway. Also sampling of clay on a road cut under the bridge near Oyeama mine (6º28'10" N and 7º27'22" E) and at Abakaliki-Onitsha expressway (6º28'20" N and 7º26'57" E) around Enugu and Okpokwu and Oturkpa (7º09'04" N and 7º44'50" E), were undertaken. The thickness of the clay ranged from 5-23m. Detail descriptions of the profiles are provided in section 4.1.

In the study area, the lateritised sandstone is the topmost rock unit. It is coarse to fine grained and light yellow to reddish brown and indurated with certain feldspathic minerals. The lateritised sandstone overlies the clay. The sandstone's thickness ranges between 0.6 and 2.0 m (Figs. 4.2 to 4.8).

The overall stratigraphy of the study area reveals that Enugu/Nkporo Formation is overlaid by Mamu/Ajali Formation (Fig. 4.1). The specific field occurrences of the clay bodies, location by location, as well as the sampling points are given in the following section.

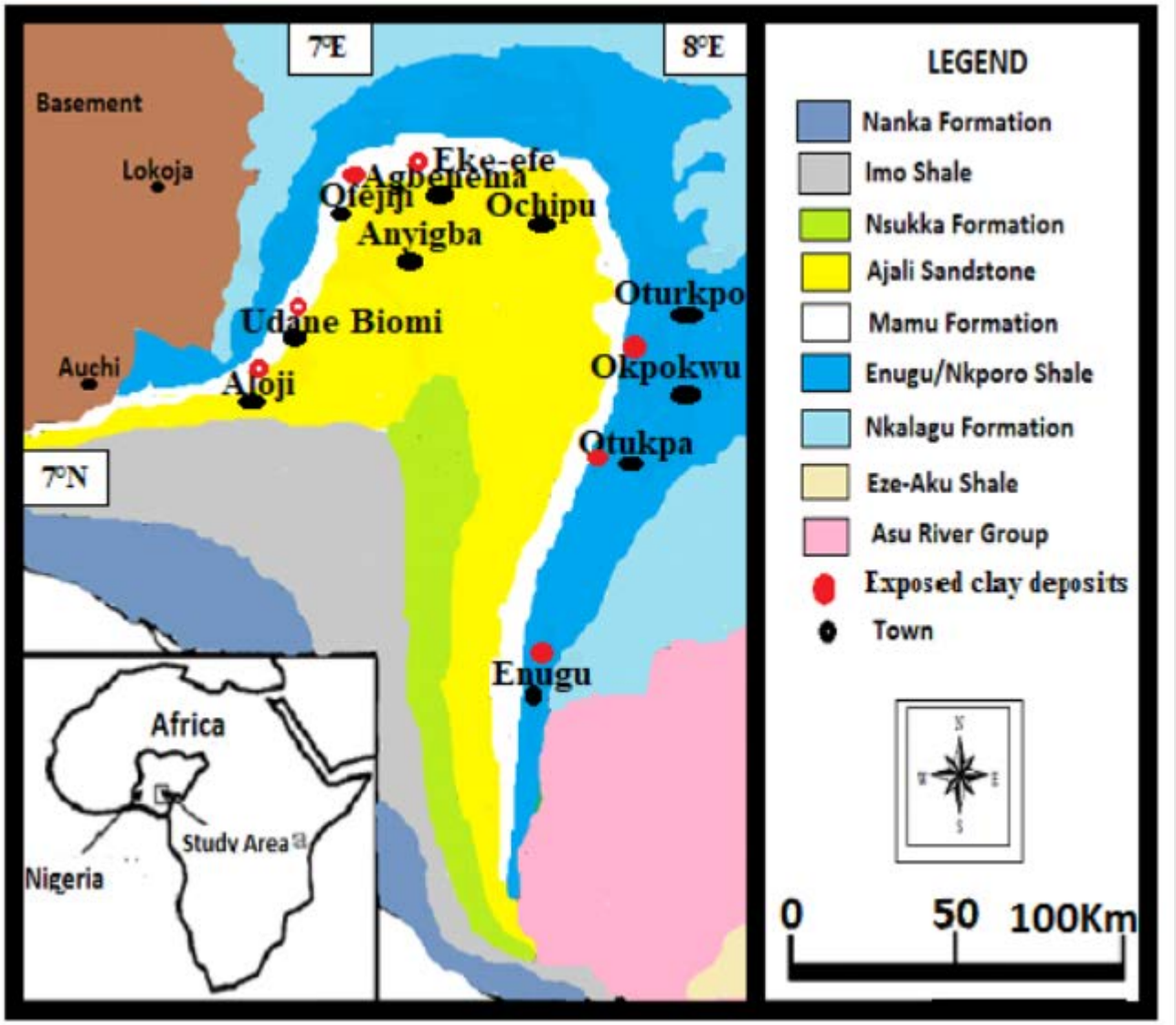

Fig. 4.1. Geological map of the Lower Benue Trough showing clay sample locations (Modified after Murat, 1972).

4.2 Field occurrences and sampling locations of the clay deposits within the Lower Benue Trough

Aloji clay

The clay deposit at Aloji is ~25 kilometres northwest of Anyigba town, where Kogi State University is located. Samples AL1.1, AL1.2 and AL1.3 were collected from location 1 (07º24'45″ N and 006º56'17″ E) in a mine pit revealing an approximately 9.90 m thick dirty white clay layer, brown and grey clay layer of 0.75 m, brown clay layer of 1.55 m, and lateritised sandstone layer of 0.50 m (Fig. 4.2). The clay, a variable thickness unit of the Mamu Formation, increases southwards. It's fine-grained but gradually changes upwards to slightly gritty sandy clay. At a second location within Aloji, (N 07º24'44″ and 006º56'14″ E), the clay deposit is highly weathered with an alternation of dirty white, dark grey and light bands, with each band being approximately 1cm thick (Fig. 4.3).

Ofejiji clay

The Ofejiji clay (07º45'57″ N and 07º26'32″E, Fig. 4.4) is exposed at a road cut about 20 kilometres NNE of Iyale General Hospital in Kogi State. The location's topography is distinctly rugged with an elevation of approximately 277 m above sea level. The clay deposit is massive and extensive with thickness of about 15 m. Intercalation of sandstone of 1.0-2.3 m thick and clay lenses of > 15 m overlies a shaly layer. The clay deposit is mostly dirty white with reddish and brownish stains which is attributable to oxidation of the lateritised sandstone over burden (Fig. 4.4).

Agbenema clay

The Agbenema clay samples were collected at locations 07º48'00″ N; 007º27'14″E and 07º47'47″N; 007º27'07″E, which are at about 0.5 and 1.5 km from Iyale General Hospital, Kogi State, respectively (Fig. 4.1). The clays outcrop along road cuts, extensive and low-lying. The clay layer, which alternate with sandstone is about 7.5m thick.

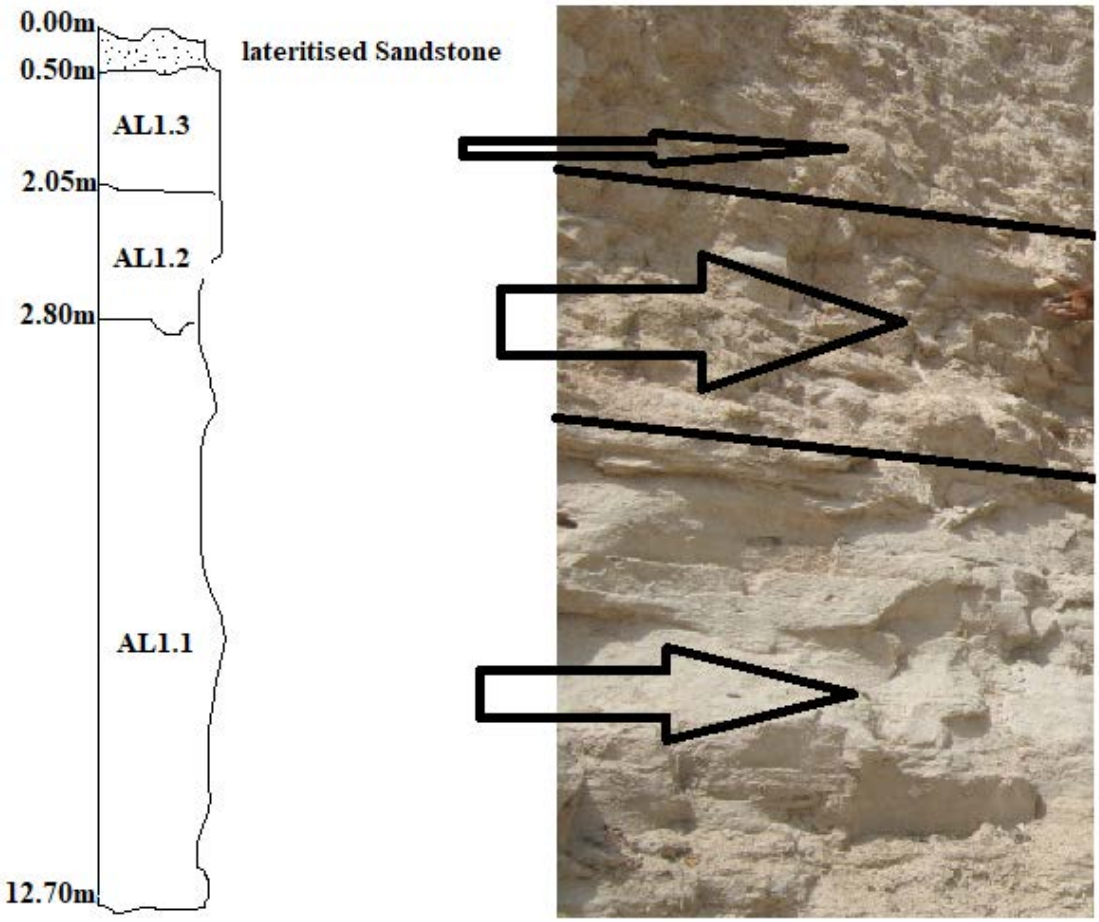

Fig. 4.2. Exposed Aloji clay deposit along Ayingba-Itobe road, Mamu/Ajali Formation, Lower Benue Trough showing sample locations.

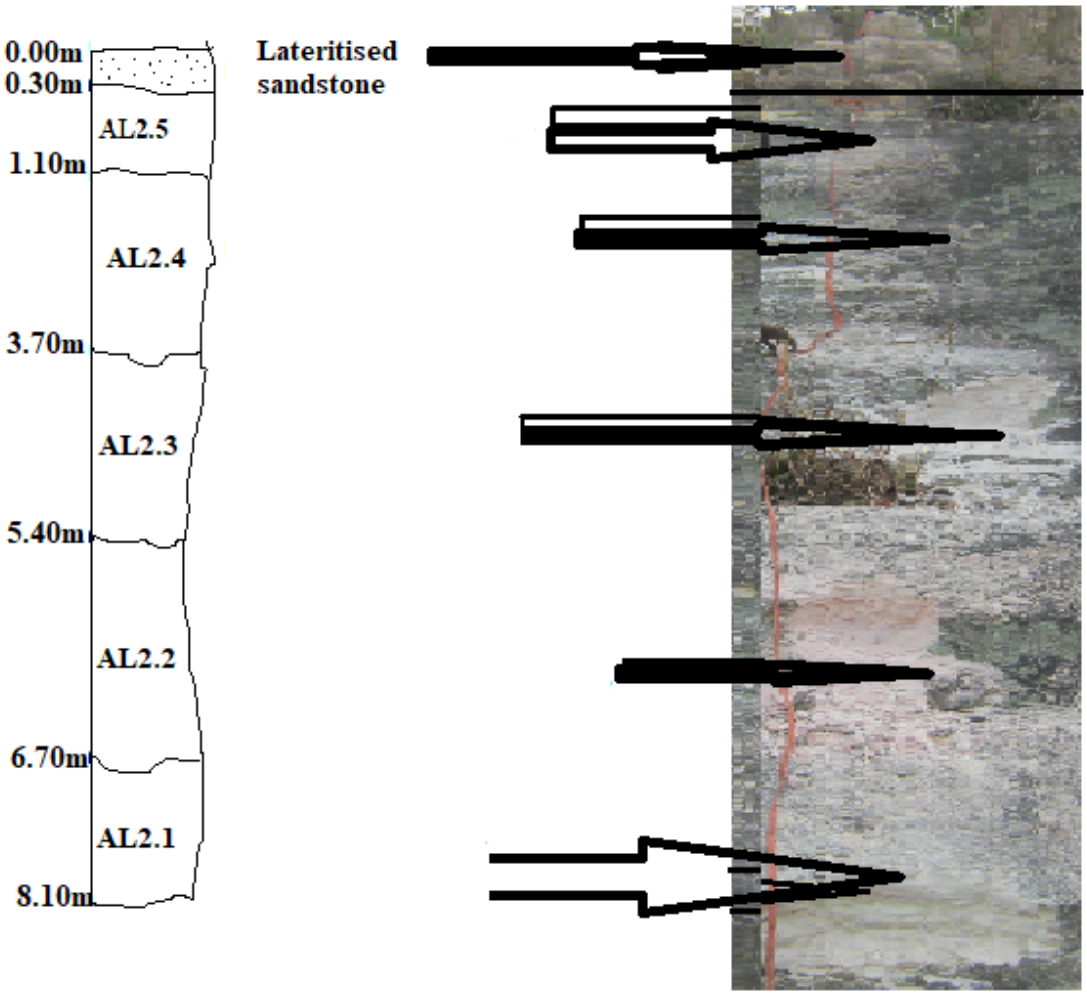

Fig. 4.3. Exposed Aloji clay deposit along the Ayingba-Itobe road, Mamu/Ajali Formation, Lower Benue Trough showing sample locations.

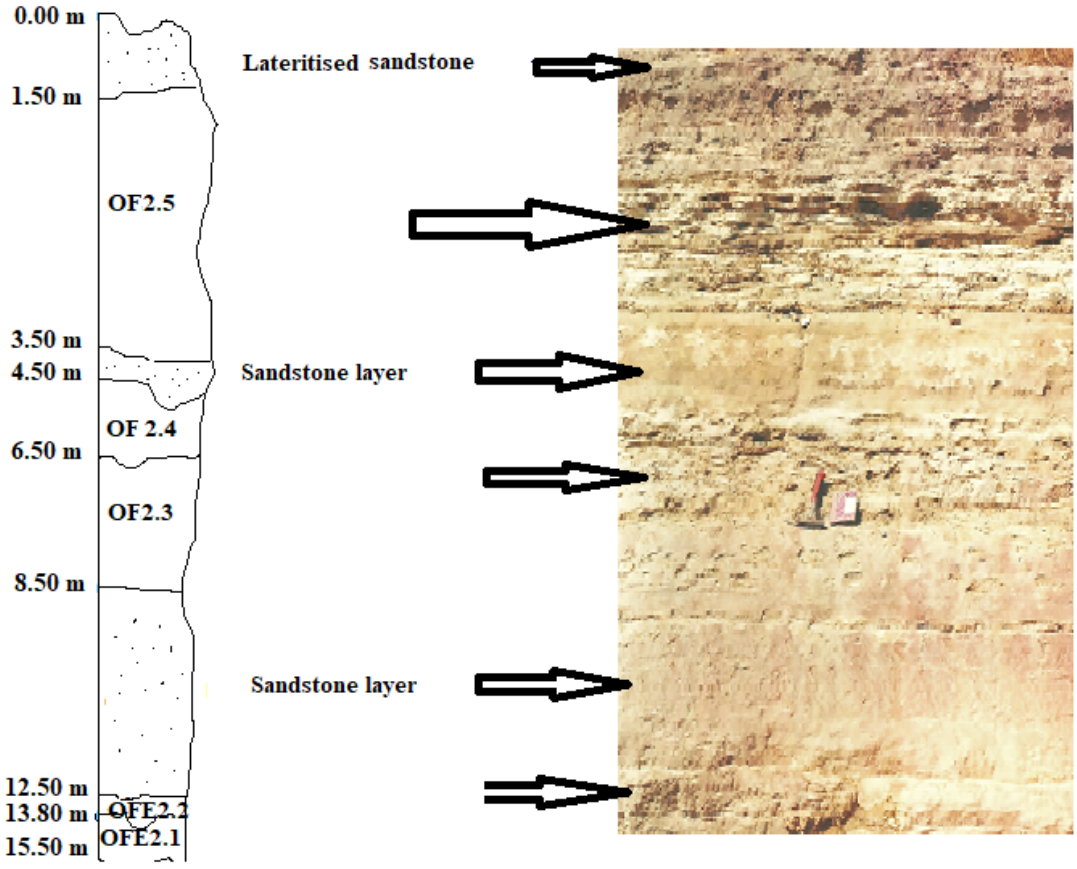

Fig. 4.4. Exposed Ofejiji clay deposit of Mamu/Ajali Formation, Lower Benue Trough showing sample locations.

Udane-Biomi clay

The Udane-Biomi clay samples (UD1.1, UD 1.2 and UD1.3), were collected from a road cut mine face at a location (07º34'55″N and 006º56'29″E), which is 45 kilometres from Abocho town in Kogi State (Figs. 4.1 and 4.5). The clay deposit is situated in a hilly terrain at an altitude of 323 metres. The 5 metre clay is has its top capped with lateritised sandstone of about 0.3 metre (Fig. 4.5).

Oturkpa and Okpokwu clays

The Okpokwu and Oturkpa clays outcrop along Oturkpo – Gbokolo road. The clay is about 5m thick (Figs. 4.1 and 4.6).

Enugu clay

The Enugu Clay (06º28'20''N and 007º26'57''E), part of the Enugu/Nkporo Formation is exposed at the Miliken Hills, River Ekulu near the Onyeama mine bridge and around Pottery in Iva Valley and Enugu-Port Harcourt road in Enugu. The clay is massive and approiatelyt 17 metres thick with 2 m lateritised sandstone capping it (Fig. 4.7 and 4.8).

Fig. 4.5. Exposed Udane-Biomi clay deposit of Mamu/Ajali Formation, Lower Benue Trough showing sample locations.

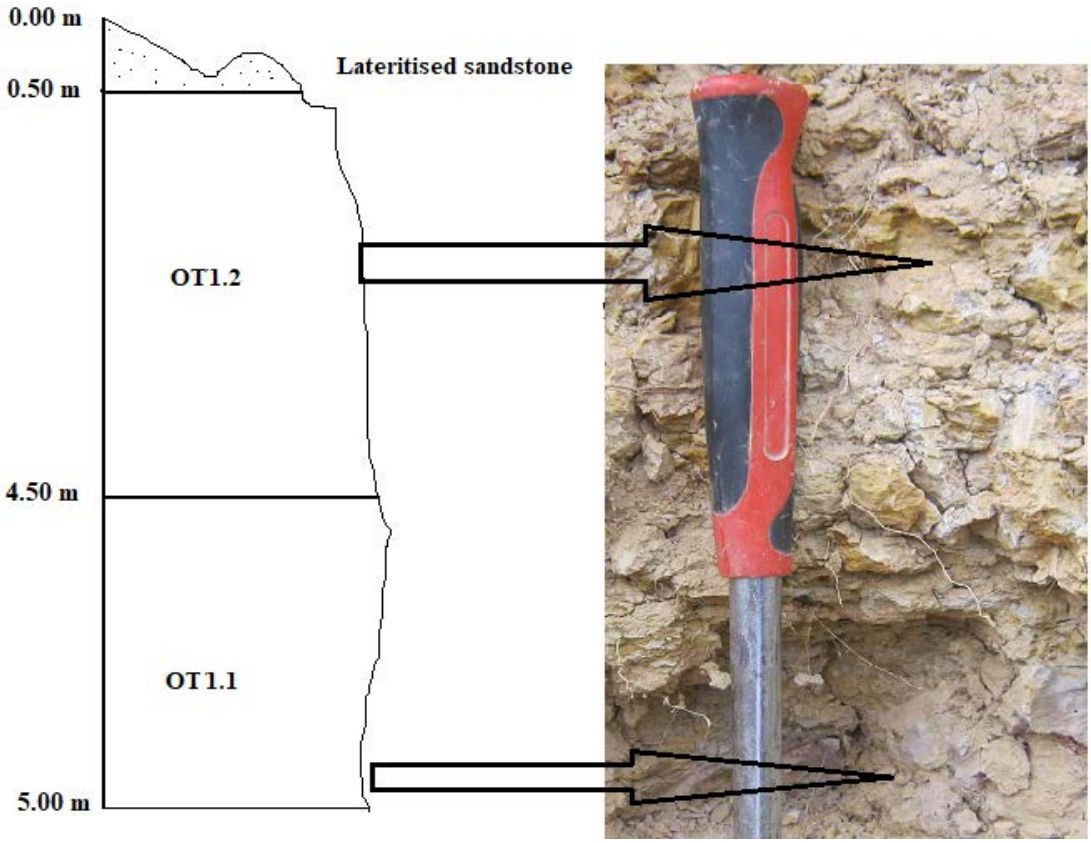

Fig. 4.6. Exposed clay deposit at Otukpa along the Otukpo – Gbokolo road, Enugu/Nkporo Formation, Lower Benue Trough showing sample locations.

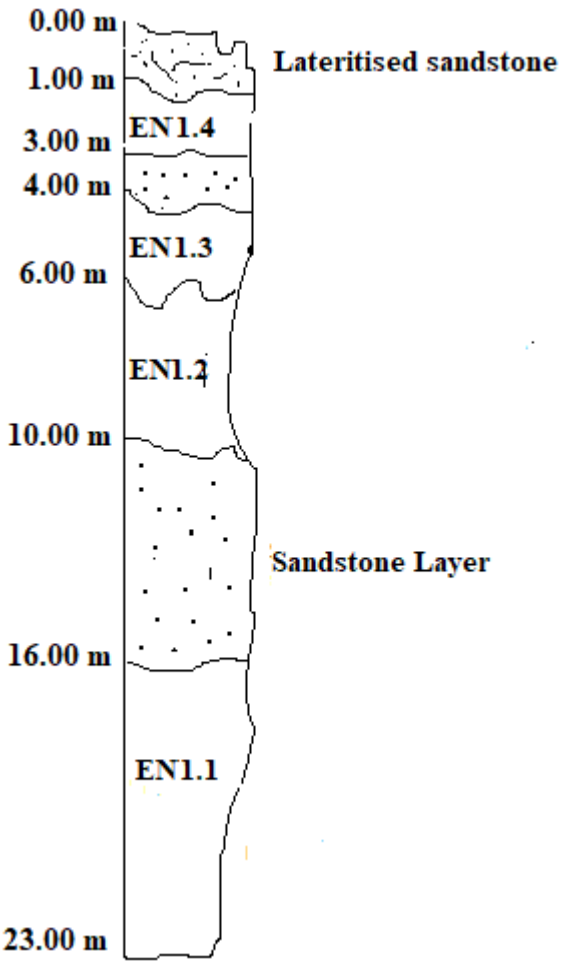

Fig. 4.7. Exposed Enugu clay deposit within Iva Valley along the Abakaliki - Onitsha road, Enugu/Nkporo Formation, Lower Benue Trough showing sample locations.

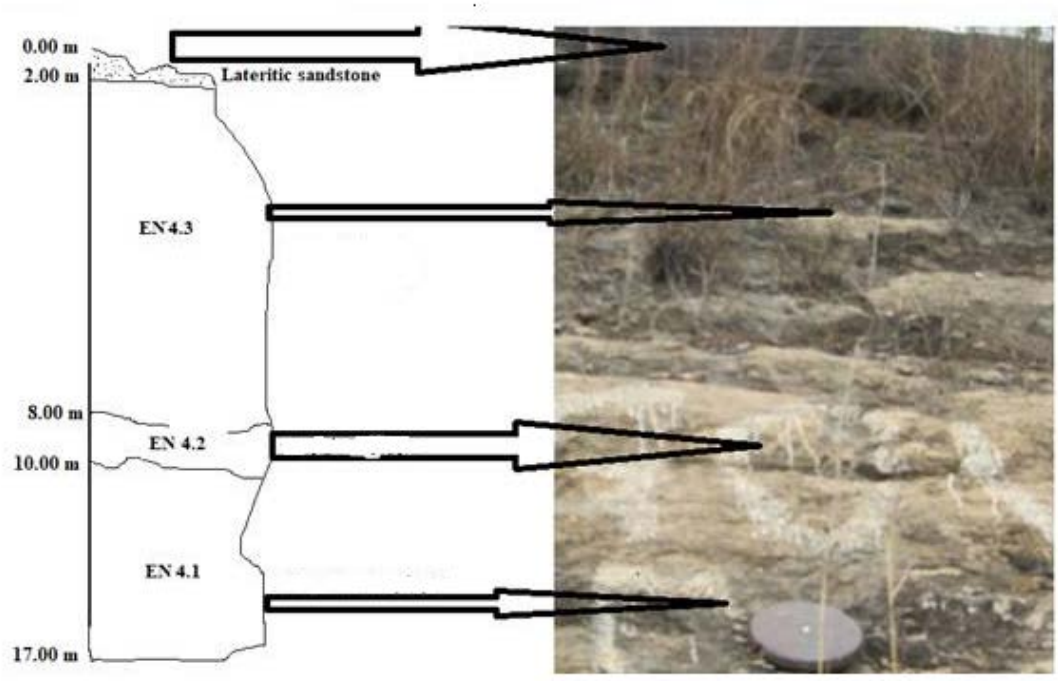

Fig. 4.8. Exposed Enugu clay deposit along the Abakaliki - Onitsha road, Enugu/Nkporo Formation, Lower Benue Trough showing sample locations.

4.3 Mineralogy

4.3.1 X-Ray-Diffraction studies of the raw clay samples

XRD data showed kaolinite as the dominant clay mineral followed by traces of vermiculite with an observed peak at 6.1º 2θ value and non-clay minerals, notably quartz with subordinate microcline, muscovite and ilmenite. Prominent peaks of kaolinite were recorded at 12.4º, 25º and 38º 2θ values (Figs. 4.9 – 4.11). Quartz peaks are mostly at 21º, 27º, 37º, 44º, 50º and 60º 2θ values while muscovite peaks occur at 8.9º and 17º, microcline at 27º and 30º and ilmenite at 32.3º and 47.3º 2θ values correspondingly (Figs. 4.9 – 4.11).

The clay samples are very similar in composition. All the investigated clay samples were characterised by the presence of kaolinite, which constitute between 40-55 % of all the clay. Kaolinite in the samples from Aloji, Ofejiji, Agbenema, Oturkpa and Okpokwu in Mamu/Ajali Formation ranged from 40 – 50 % while those of samples from Enugu in Enugu/Nkporo Formation vary from 46 – 55 %. This revealed a continental to marginal environment as against an essentially marine type where illite and smectites are the dominant clays (Parham, 1966). The presence of kaolinite could be attributed to weathering of K-feldspars, notably microcline, and muscovite in the source rocks (Table 4.1).

The clay samples are gritty due to the presence of very high amounts of quartz (37-55 %; Table 4.1). The quartz composition of samples from Aloji, Ofejiji, Agbenema, Oturkpa and Okpokwu in Mamu/Ajali Formation ranges from 44 to 55 %, while samples from Enugu in Enugu/Nkporo Formation ranged from 37 to 47 %. This suggests that the clay samples from Mamu/Ajali Formation are more silty and gritty than the clay samples from Enugu/Nkporo Formation, which are more clayey (Table 4.1). The presence of negligible peaks of microcline and muscovite in the raw clay samples (Figs. 4.10 – 4.12, Table 4.1) suggests intense weathering of the parent rock to form the clay deposits.

The raw clay samples, although, consist mainly kaolinite and quartz minerals; contain an appreciable amount of muscovite (1 - 8 %) (Figs. 4.9 – 4.11). Muscovite is relatively more in Okpokwu (OK1.1) and Enugu (EN2.1) samples (Table 4.1). Their absence in Aloji (AL1.2 and AL2.5), Ofejiji (OF2.4), Oturkpa (OT2.1), Okpokwu (OK1.2) and Enugu (EN4.3) (Table 4.1; Fig. 4.11) is attributed to its complete conversion to kaolinite. This is supported by research of Heckroodt *et al*. (1987), which indicate that muscovite may form pyrophyllite in the early stages of weathering and subsequently alters to kaolinite as demostrated by the reaction below:

$$2KAl_3Si_3O_{10}(OH)_2 + 6H_4SiO_4 \rightarrow 3Al_2Si_4O_{10}(OH)_2 + 2K^+ + 2(OH)^- + 10H_2O$$
(Muscovite) (Pyrophyllite)

$$Al_2Si_4O_{10}(OH)_2 + 5H_2O \rightarrow Al_2Si_2(OH)_4 + 2H_4SiO_4$$
(Pyrophyllite) (Kaolinite)

Data obtained from the raw clay samples of Aloji, Ofejiji, Agbenema, Oturkpa, Okpokwu and Enugu of Mamu/Ajali and Enugu/Nkporo Formations shows that the clay deposits are kaolinitic with appreciable amounts of microcline and muscovite and very high quartz content. The presence of kaolinite, quartz and muscovite suggests derivation of the clays from felsic rocks in a continental environment.

The presence of traces of vermiculite indicates alteration of biotite in the felsic protoliths to vermiculite. This intense alteration results from high precipitation, which favoured chemical weathering, transportation of the detritus, sorting and post-depositional alterations of the deposited sediments. The types of clay mineral and their quantitative estimates showed that the clay minerals in the basin, climatic conditions and depositional environments of the clay deposits in both the Mamu/Ajali and Enugu/Nkporo Formations are similar. This also provide a basis for suggesting a common parent rock despite both Formations are in different stratigraphic positions and slightly different lithostratigraphic units.

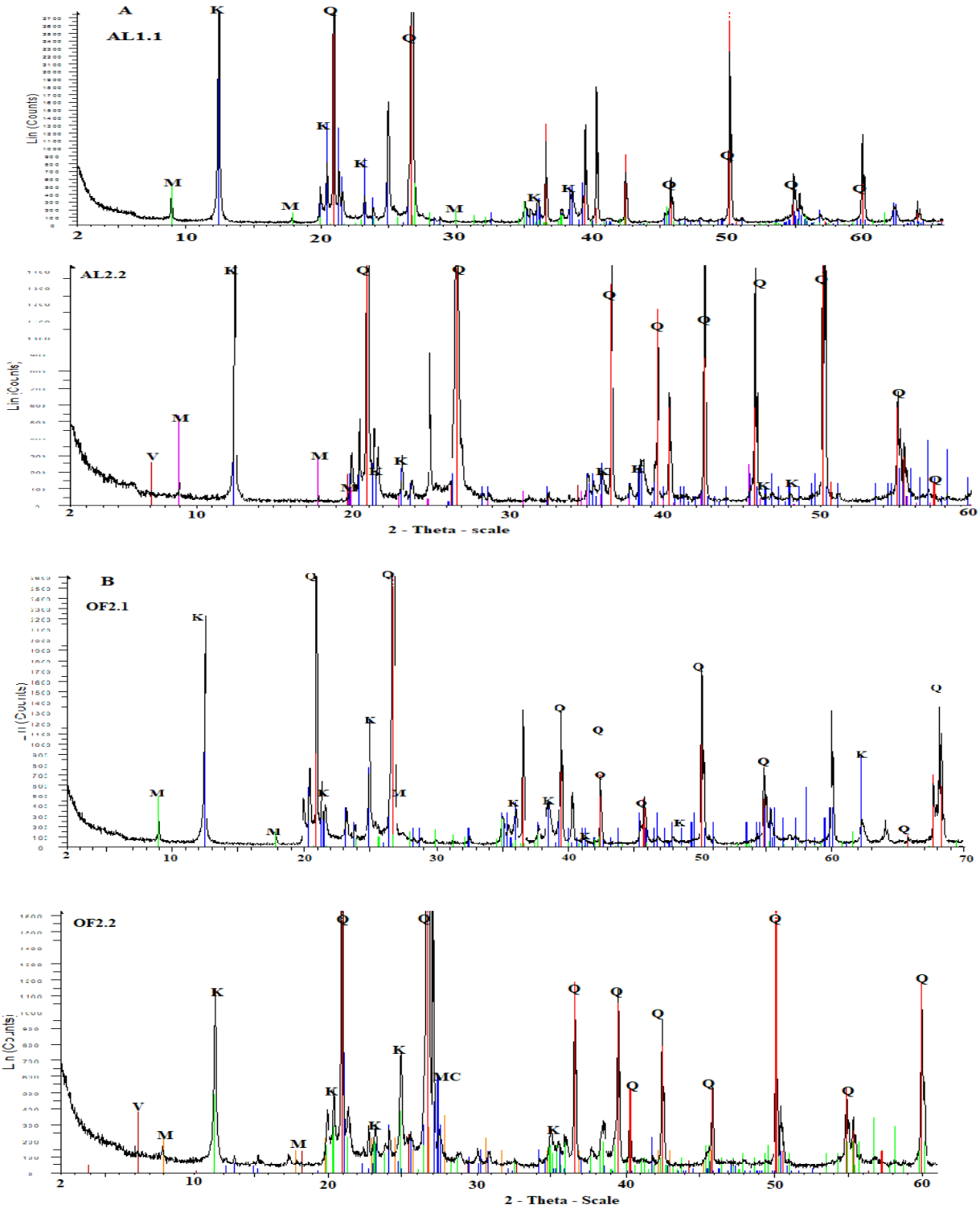

Fig. 4.9. Diffractogram of raw clay samples from (A) Aloji and (B) Ofejiji Mamu/Ajali of Mamu/Ajali Formation, Lower Benue Trough, Nigeria.
K - Kaolinite, Q - Quartz, M – Muscovite, Mc – Microcline.

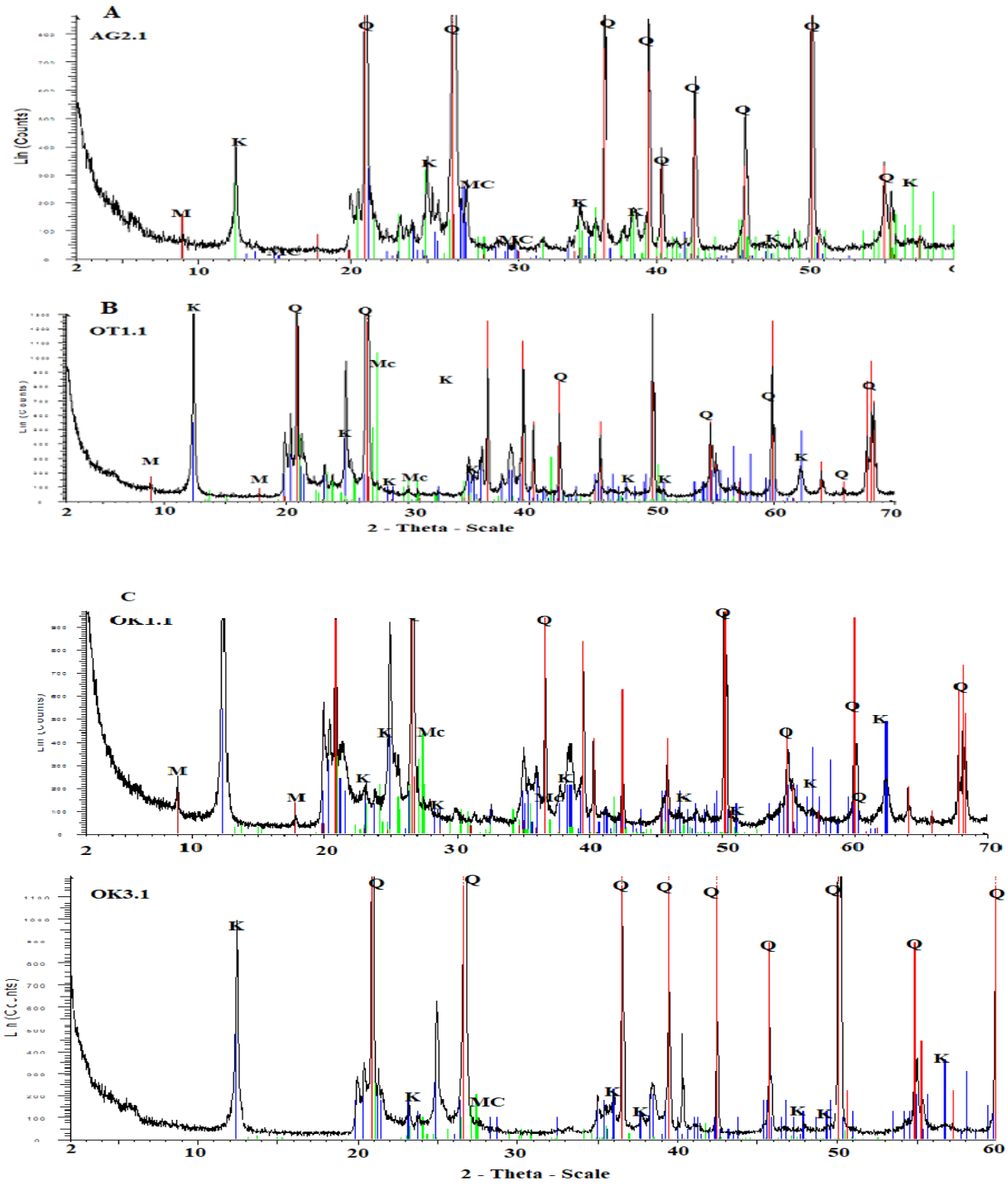

Fig. 4.10. Diffractogram of raw clay samples from (A) Agbenema, (B) Oturkpa and (C) Okpokwu in the Mamu/Ajali Formation, Lower Benue Trough, Nigeria.
K - Kaolinite, Q - Quartz, M - Muscovite, Mc - Microcline

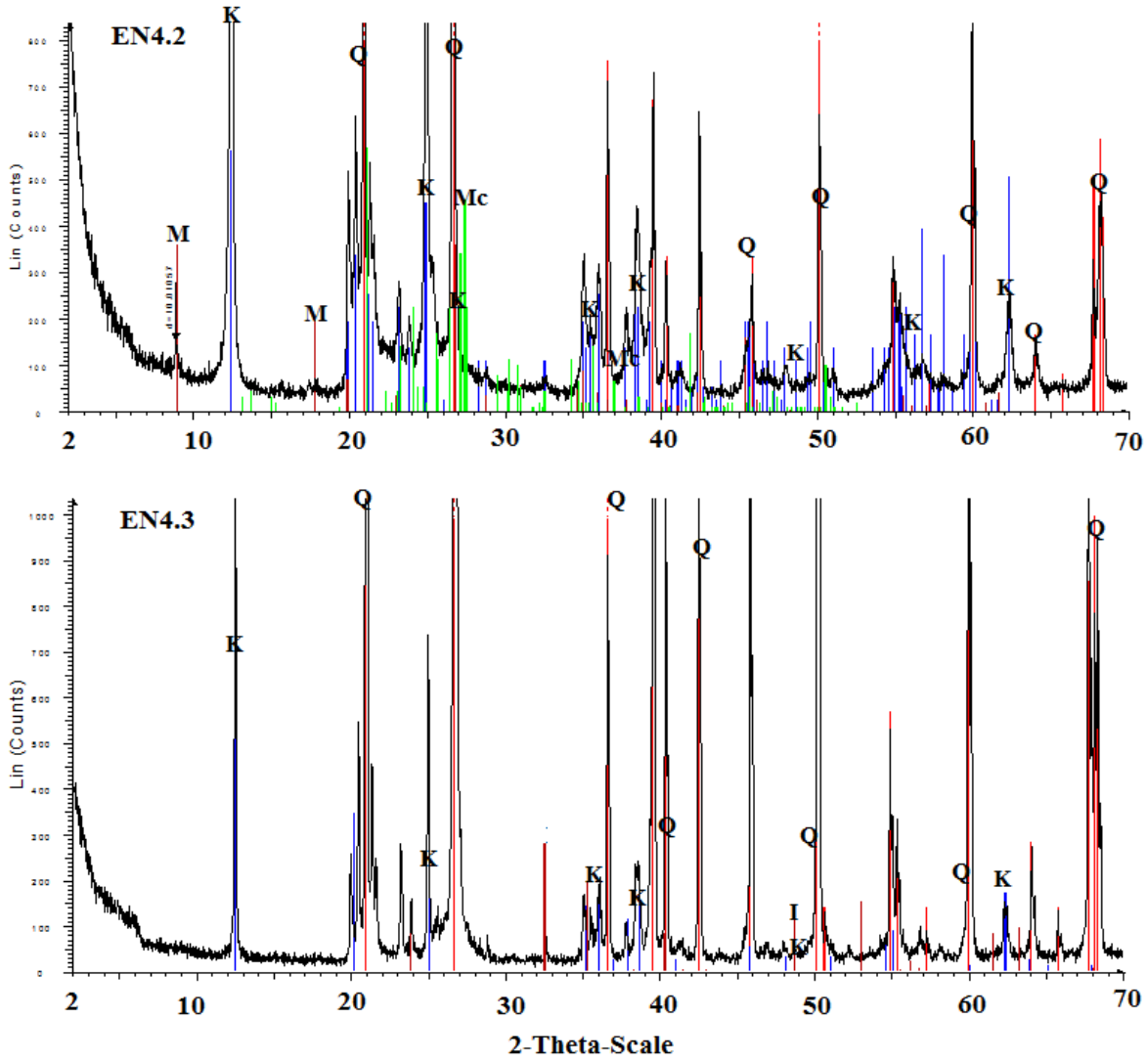

Fig. 4.11. Diffractogram of raw clay samples from Enugu in the Enugu/Nkporo Formation, Lower Benue Trough, Nigeria.
K - Kaolinite, Mc - Microcline, Q - Quartz, I - Ilmenite

Table 4.1. Mineralogical composition (vol. %) of the raw clay samples

Sample No.→ Minerals↓	AL1.1	AL1.2	AL1.3	AL2.1	AL2.2	AL2.4	AL2.5	OF1.3	OF2.1	OF2.2
Quartz	46	50	48	54	52	53	55	50	50	49
Microcline	3	5	3	---	---	2	3	2	2	4
Kaolinite	46	45	46	42	44	45	40	44	46	44
Vermiculite	---	---	--	---	---	---	---	---	---	---
Muscovite	5	---	3	4	4	---	2	4	2	3
Total	100	100	100	100	100	100	100	100	100	100

SampleNo → Minerals ↓	OF 2.3	OF 2.4	OF 2.5	AG 1.1	AG 1.2	AG 2.2	AG 2.1	OT 1.1	OT 1.2	OT 2.1	OT 2.2
Quartz	50	57	53	50	48	52	49	49	50	48	45
Microcline	3	---	---	5		3	3	--	--	---	---
Kaolinite	43	41	44	43	49	40	42	46	45	50	48
Vermiculite	---	---	---	2	1	2	3	3	2	2	4
Muscovite	4	---	3	---	2	3	4	2	1	---	3
Total	100	100	100	100	100	100	100	100	100	100	100

Mamu/Ajali Formation clay

Aloji samples
AL1.1, AL1.2, AL1.3, AL2.1, AL2.2, AL. 2.4 and AL2.5.

Ofejiji samples
OF1.1, OF1.3, OF2.1, OF2.2, OF2.3, OF2.4 and OF2.5.

Agbenema samples
AG1.1, AG1.2, AG2.1 and AG2.2.

Oturkpa samples
OT1.1 and OT1.2, OT2.1, OT2.2.

Table 4.1. Cont.

Sample No → Minerals ↓	OK 1.1	OK 1.2	OK 3.1	OK 3.2	EN 2.1	EN 2.2	EN 3.1	EN 3.2	EN 4.1	EN 4.2	EN 4.3
Quartz	44	47	49	47	47	44	43	45	37	39	43
Microcline	---	4	3	3	---	---	4	---	---	4	3
Kaolinite	45	47	46	47	46	49	47	48	55	50	47
Vermiculite	---	2	---	---	---	3	2	3	4	---	3
Muscovite	8	---	2	1	6	3	3	2	2	5	---
Ilmenite	---	---	---	---	---	---	---	---	---	---	3
Total	97	100	100	100	100	100	100	100	100	100	100

Mamu/Ajali Formation clay samples:

Okpokwu - OK 1.1, OK1.2, OK. 3.1and OK3.2.

Enugu/Nkporo Formation clay samples:

Enugu - EN2.1, EN2.2, EN3.1, EN3.2, EN4.1, EN4.2 and EN4.3.

4.3.1.1 X-Ray-Diffraction studies of the fine (<2μm) clay samples

The XRD data of the oriented clay aggregates were also determined over a 2θ range of 2 - 70^{o} 2θ after the samples were air dried. Sample data showed the existence of kaolinite at 12.4º, 25º and 38º 2θ and traces of vermiculite at 2θ value of 6.1º (Figs. 4.12 – 4.15, Table 4.2). Quartz peaks are mostly at 21º, 27º, 37º, 44º, 50º and 60º 2θ values while muscovite occur at 8.9º and 17º, microcline at 27º and 30º 2θ values.

All the investigated air-dried samples contained abundant kaolinite (39 - 79 %) but poor in quartz (17 – 48 %) compared to the raw clay samples with kaolinite of 40 – 49 %, quartz 37 - 55 %. Kaolinite varied from 39-69 % in the samples from Aloji, Ofejiji, Agbenema, Oturkpa and Okpokwu in the Mamu/Ajali Formation while samples from Enugu in the Enugu/Nkporo Formation varied from 62 – 79 % (Table 4.2).

Vermiculite traces occur in the Aloji (AL1.1, AL1.2, AL1.3, AL2.2, AL2.3), Ofejiji (OF2.1 and 2.2), Oturkpa (OT1.1, OT1.2, OT2.1 and OT2.2), Okpokwu (OK1.2 and OK3.2) and Enugu (EN2.2 and EN4.3) clay samples (Table 4.2, Figs. 4.12 – 4.15). Muscovite, a dioctahedral (2:1) mica, is highly weathering resistant mineral, after quartz, was observed at 8.9º to 17º 2θ degrees. The method of Moore and Reynolds (1997) and Gharrabi *et al*. (1998) was useful in differentiating between illite and muscovite. The very sharp basal peak of 1st with a width of <0.10° 2θ is linked to muscovite (Figs. 4.12 – 4.15). The presence of muscovite (1 – 9 %) and traces of microcline (1 – 8 %) in almost all the air-dried samples suggested a felsic source rock that suffered incipient weathering and moderate distance of transportation (Figs. 4.12 – 4.15, Table 4.2).

The mineralogy of the solvated, ethylene glycol treated clay samples showed that the kaolinite peaks at 12.4°, 25° and 38° 2θ values, in all samples, were not affected (Figs. 4.12 – 4.15). Vermiculite also showed no shift in the 6.1 2θ peak (Figs. 4.12 – 4.15). The feldspar and muscovite peaks observed in raw and air dried samples were retained in the glycolated samples (Figs. 4.12 – 4.15).

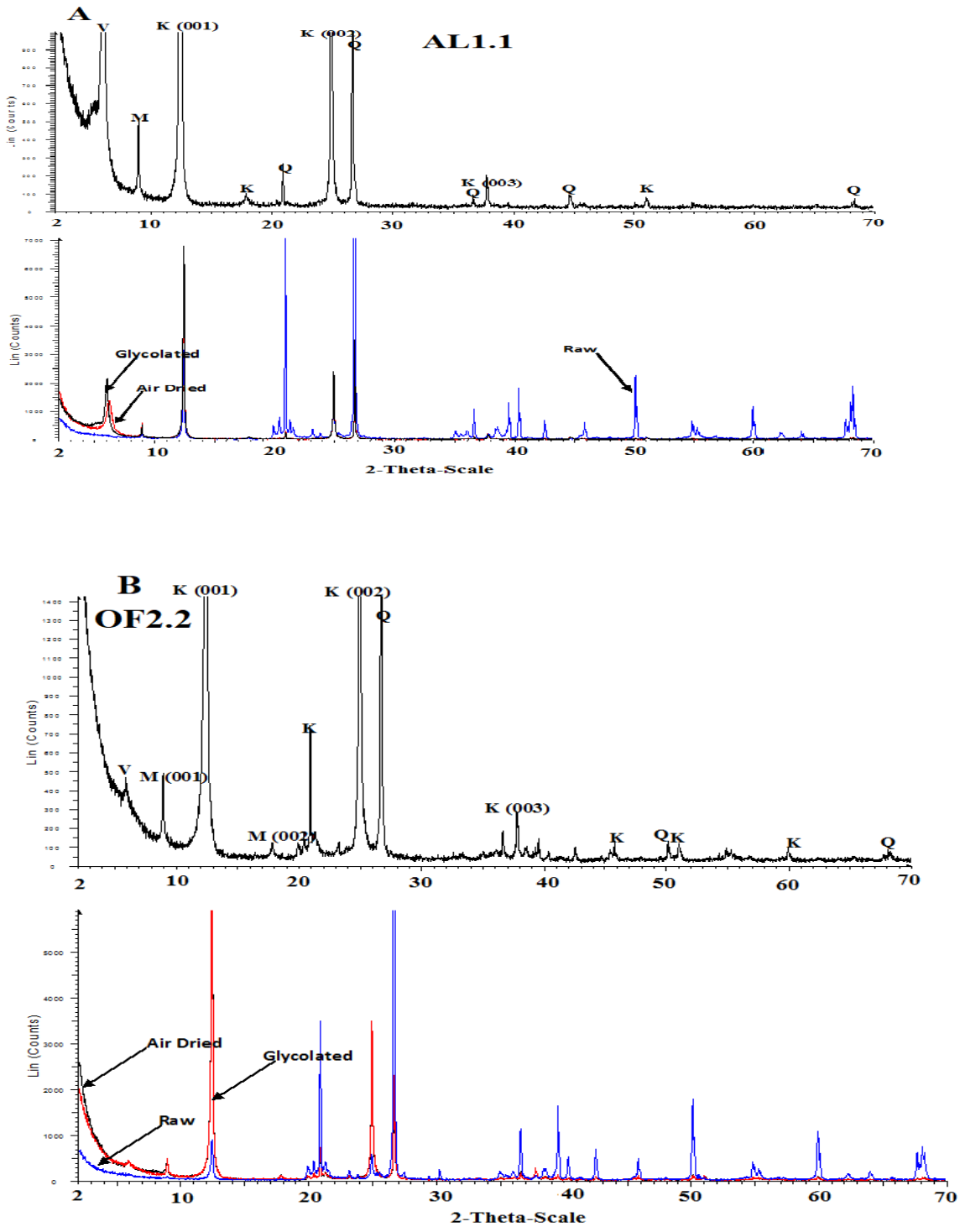

Fig. 4.12. Diffractogram of raw, air dried and glycolated clay samples from **A:** Aloji and **B:** Ofejiji of Mamu/Ajali Formation. V - Vermicullite, M - Muscovite, K - Kaolinite, Q - Quartz.

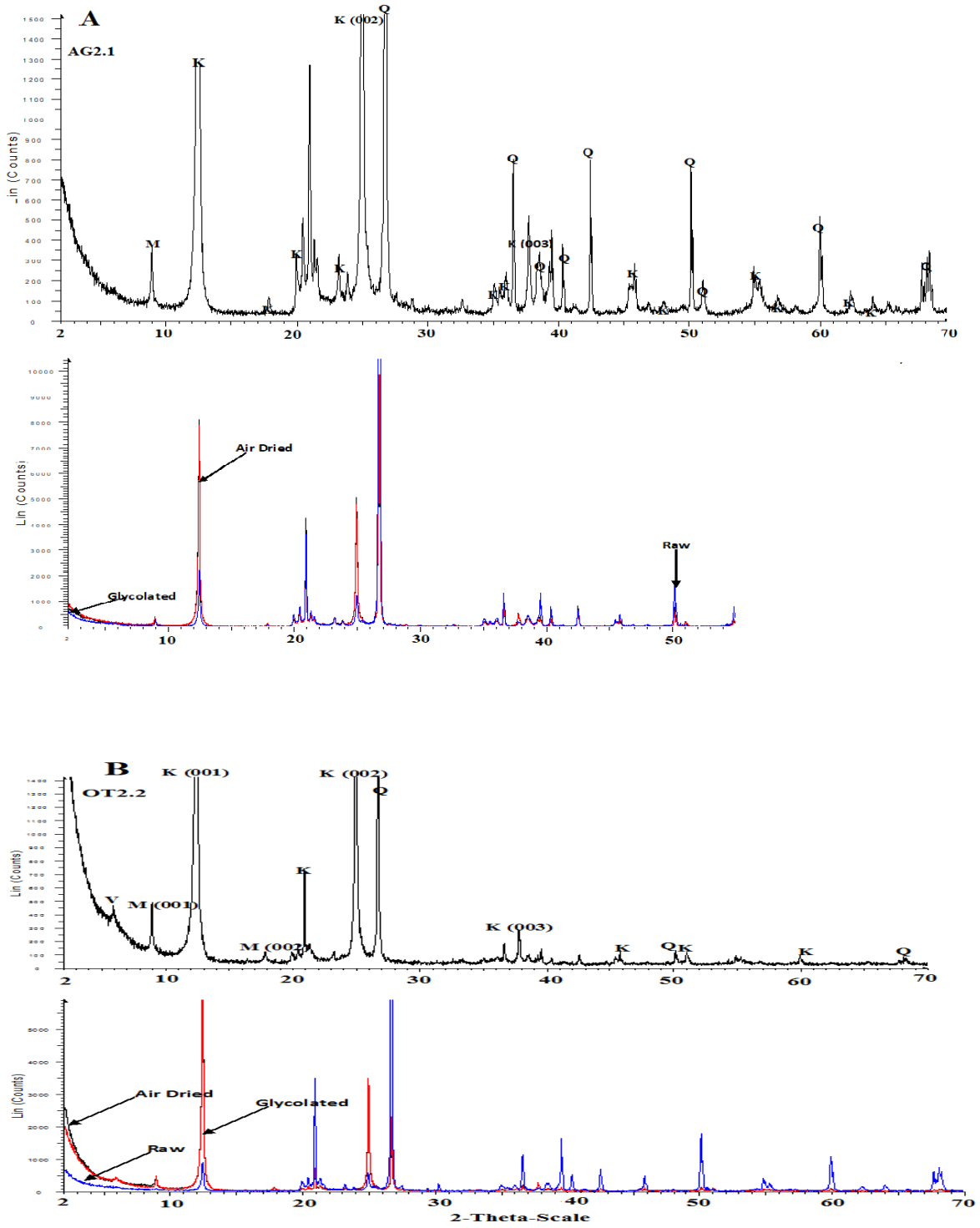

Fig. 4.13. Diffractogram of raw, air dried and glycolated clay samples from **A:** Agbenema and **B.** Oturkpa in the Mamu/Ajali Formation, Lower Benue Trough, Nigeria. V - Vermiculite, M - Muscovite, K - Kaolinite, Q - Quartz

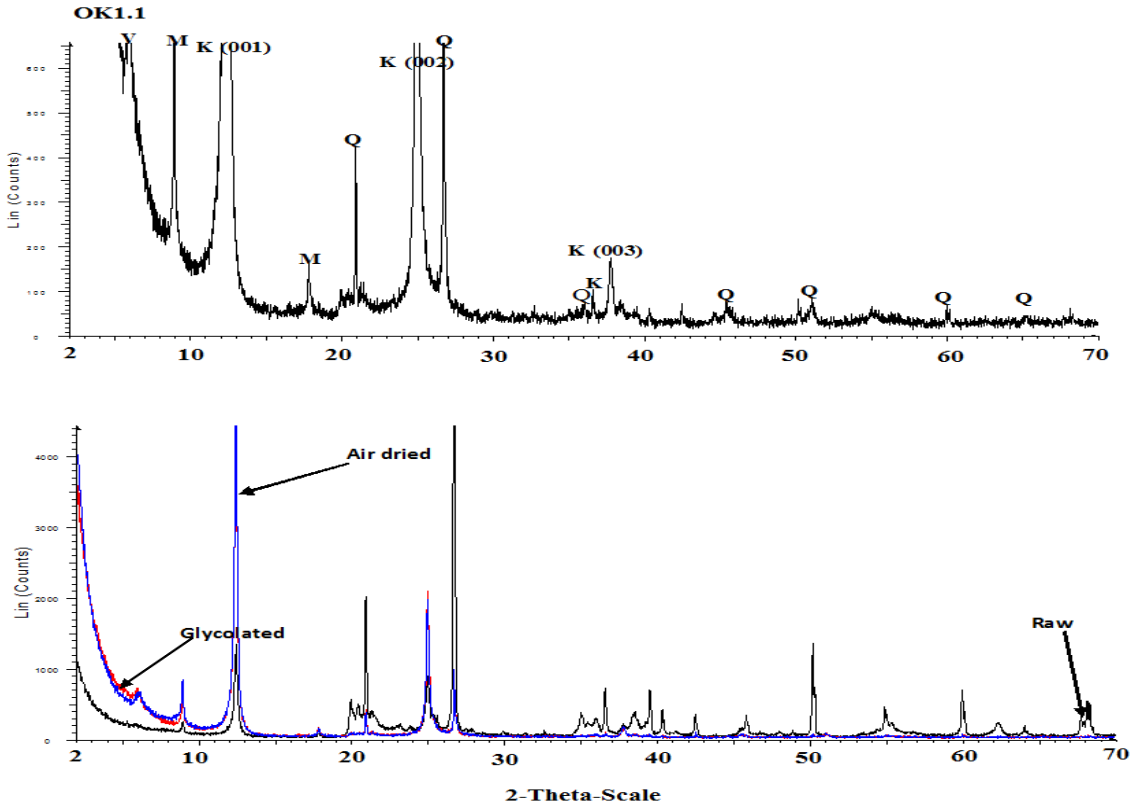

Fig. 4.14. Diffractogram of raw, air dried and glycolated clay samples from Okpokwu in the Mamu/Ajali Formation, Lower Benue Trough, Nigeria.
V - Vermiculite, M - Muscovite, K - Kaolinite, Q - Quartz

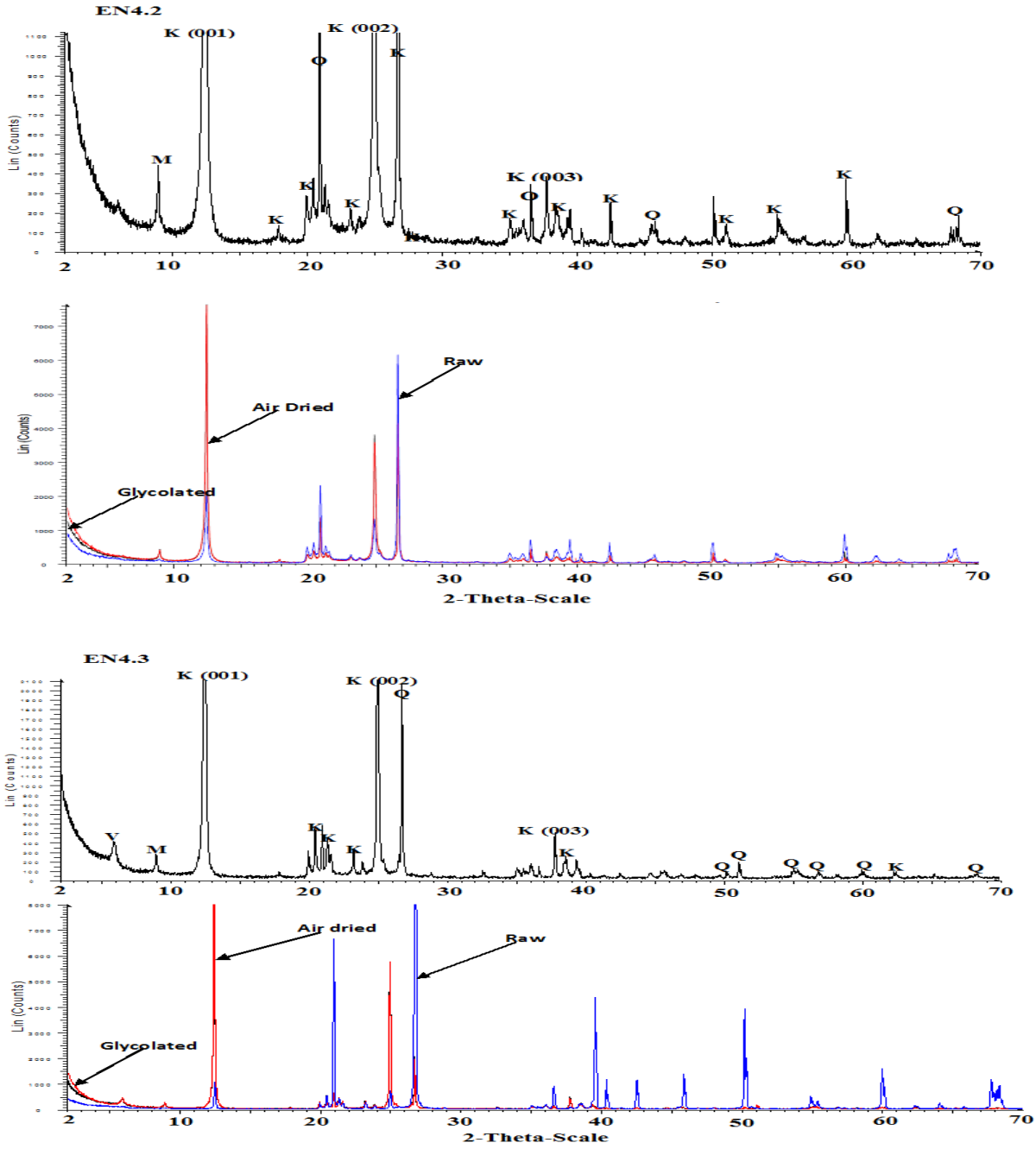

Fig. 4.15. Diffractogram of raw, air dried and glycolated clay samples from Enugu in the Enugu/Nkporo Formation, Lower Benue Trough, Nigeria.
V - Vermiculite, M - Muscovite, K - Kaolinite, Q - Quartz

Table 4.2. Mineralogical composition (vol. %) of the fine (<2μm) clay samples

Sample No→ Minerals↓	AL 1.1	AL 1.2	AL 1.3	AL 2.1	AL 2.2	AL 2.3	OF 2.1	OF 2.2	OF 2.3	AG 1.1	AG 1.2	AG 2.1	AG 2.2
Quartz	48	31	35	40	40	44	38	34	37	40	43	45	41
Microcline	2	3	8	5	2	--	2	4	2	3	2	3	2
Kaolinite	39	53	45	52	50	49	55	59	58	50	54	47	50
Vermiculite	3	1	4	--	3	4	3	1	--	--	---	---	---
Muscovite	6	9	8	3	5	3	2	1	3	7	1	5	7
Total	100	100	100	100	100	100	100	100	100	100	100	100	100

SampleNo → Elements ↓	OT 1.1	OT 1.2	OT 2.1	OT 2.2	OK 1.1	OK 1.2	OK 3.1	OK 3.2	EN 2.1	EN 2.2	EN 3.1	EN 3.3	EN 4.1	EN 4.2	EN 4.3
Quartz	30	35	32	37	27	36	35	33	30	25	21	28	20	28	17
Microcline	---	4	4	2	3	3	2	1	---	---	2	---	4	2	2
Kaolinite	65	58	60	58	69	57	62	58	63	65	73	70	73	62	79
Vermiculite	3	2	2	1	---	3	1	6	1	2	---	---	---	2	---
Muscovite	2	1	2	2	1	1	---	2	6	8	4	2	3	6	2
Total	100	100	100	100	100	100	100	100	100	100	100	100	100	100	100

Mamu/Ajali Formation clay samples:
Aloji - AL1.1, AL1.2, AL1.3, AL2.1, AL2.1 and AL2.3.

Ofejiji - OF2.1, OF2.2 and OF 2.3.

Agbenema - AG1.1, AG1.2, AG2.1 and AG2.2.

Oturkpa - OT1.1, OT1.2, OT2.1 and OT2.2.

Okpokwu - OK1.1, OK1.2, OK3.1 and OK3.2.

Enugu/Nkporo Formation clay samples:

Enugu - EN2.1, EN2.2 EN3.1, EN3.2, EN4.1, EN4.2 and EN4.3.

4.3.2 Thermal properites

The thermal properties of the Aloji, Oturkpa, Okpokwu and Enugu fine (< 2μm) clay samples were determined using differential thermal analysis (DTA) and thermogravimetric techniques (TG). The characteristic patterns are presented in Fig. 4.16 – 4.18 and the weight loss on Table 4.3. For the temperature range of 10 - 900°C, the DTA and TG curves of the clay samples were obtained.

4.3.2.1 Differential Thermal properties

Differential Thermal Analysis patterns (Fig. 4.16 – 4.18) showed structural and mineralogical features suggesting kaolinite. There were three endothermal peaks. The first peak is between 138 – 154°C, which suggests removal of adsorbed moisture and waters. The second peak observed is within the range of 408.41 to 519.67 °C indicating dehydroxylation (MacKenzie, 1957; Felhi *et al.*, 2008). An exothermic peak due to recrystallization follows the last endothermic peak at 860 to 900 °C, suggesting the formation of a new phase known as metakaolin (MacKenzie, 1957). These findings verify the prevalence of kaolinite in the clay samples in line with X-ray diffraction data.

4.3.2.2 Thermogravimetric properties

The weight loss during thermogravimetric treatment of the clay samples showed that samples from Mamu/Ajali Formation ranged between 0.76 to 1.26 mg (Table 4.3; Fig. 4.16 – 4.17) while those of Enugu/Nkporo Formation is 1.21 to 2.11 mg (Table 4.3; Fig. 4.18). The slightly higher values recorded in the Enugu/Nkporo Formation samples is due to the higher finer particles and organic matter. Weight loss for all the clay samples were recorded between 499 °C and 504 °C, probably due to large organic matter decomposition with loss in weight increasing with temperature. This is consistent with MacKenzie (1957) and Edomwonyi-Otu *et al*. (2013) assertion that kaolinites undergoes dehydroxylation at 408°C to 520°C to form metakaolin. The thermogravimetric patterns (Fig. 4.16 – 4.18, Table 4.3) of the fine (<2μm) clay sample is generally consistent with the results of the mineralogy.

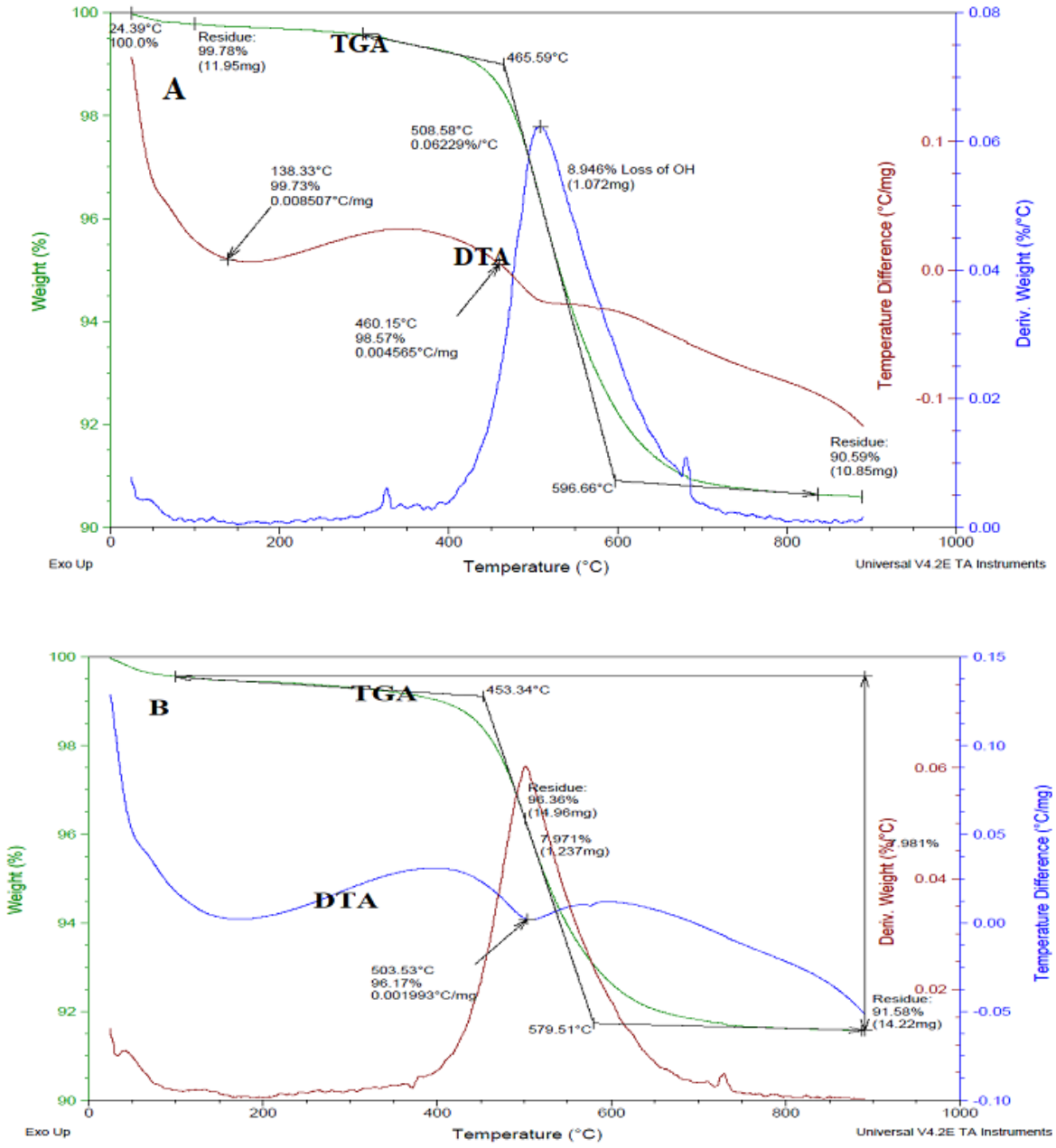

Fig. 4.16. DTA-TGA curves for fine (<2µm) clay fraction from **A**: Aloji (AL1.1) and **B**: Aloji (AL2.2), Mamu/Ajali Formation, Lower Benue Trough, Nigeria.

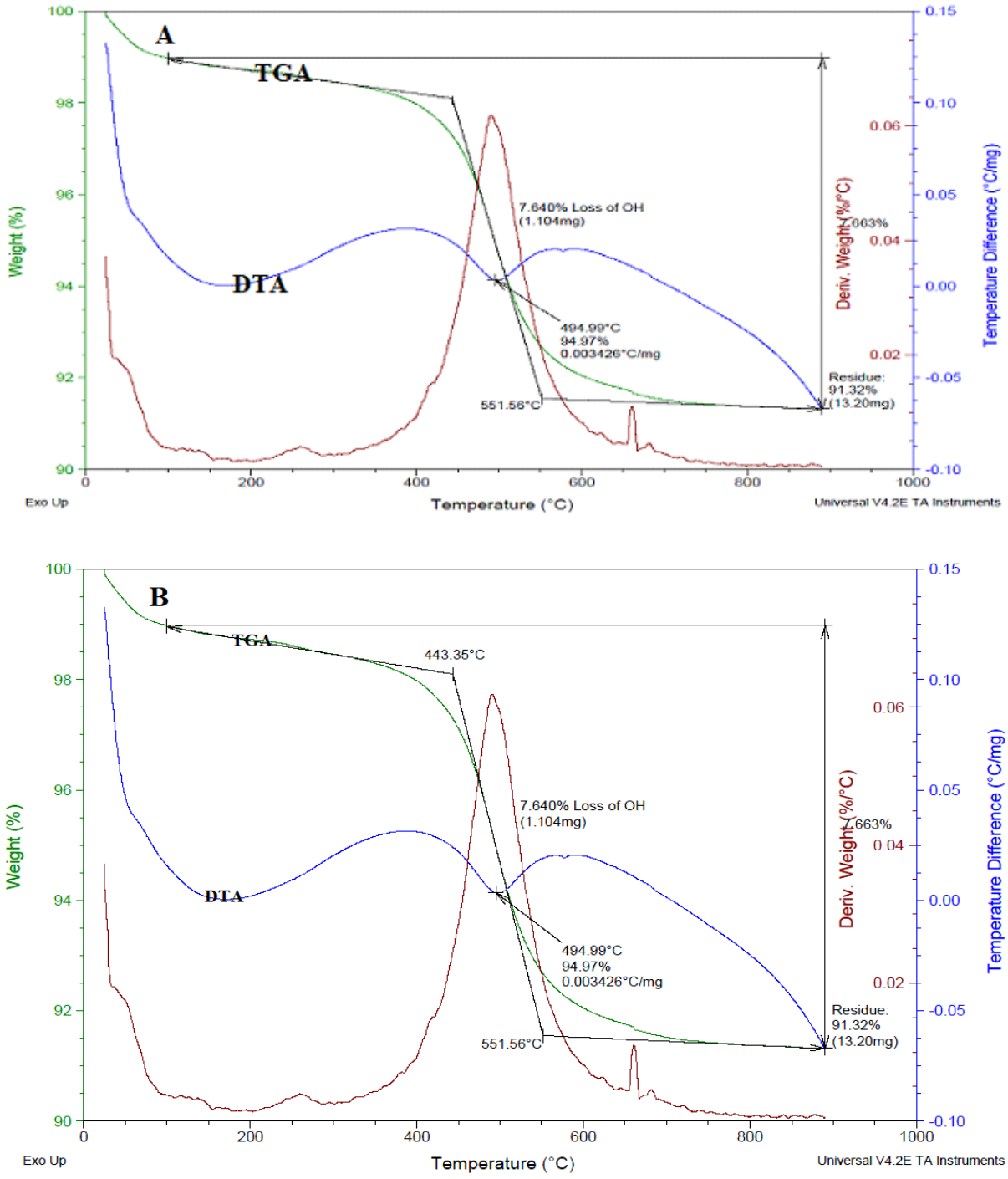

Fig. 4.17. DTA-TGA curves for fine (<2µm) clay fraction from **A**: Oturkpa (OT2.2) and **B**: Okpokwu (OK1.1), Mamu/Ajali Formation, Lower Benue Trough, Nigeria

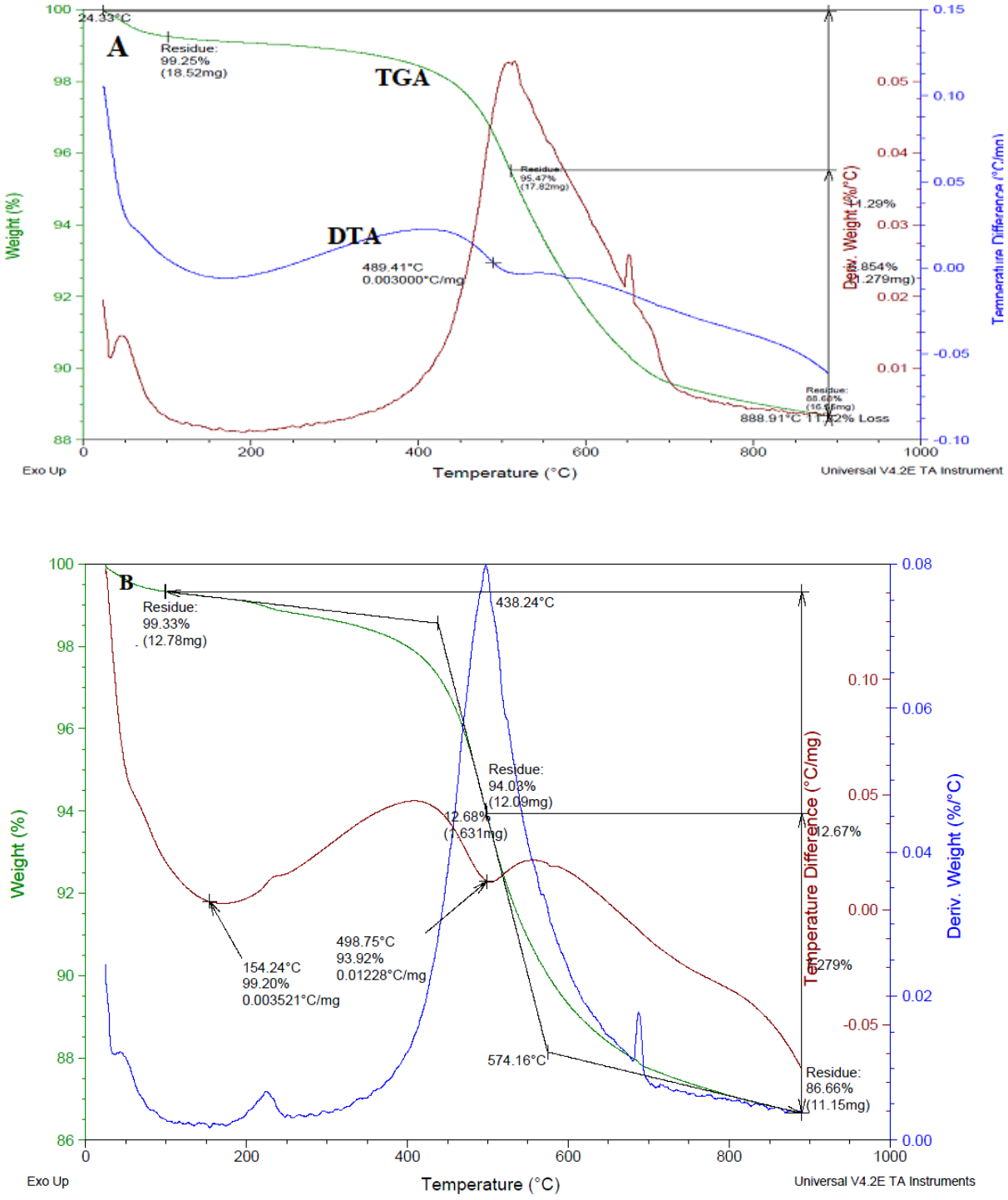

Fig. 4.18. DTA-TGA curves for fine (<2µm) clay fraction from **A:** Enugu (EN3.1) and **B:** Enugu (EN4.2) within the Lower Benue Trough, Nigeria.

Table 4.3. Weight loss (% vol.) for the investigated Ajali/Mamu and Enugu/Nkporo clay samples.

Sample No→:	AL 1.1	AL 1.2	AL 2.2	OT 2.2	OK 1.1	EN 2.1	EN 3.1	EN 4.2	EN 4.3	Mean	SD
Initial Vol. (mg)	11.98	13.36	13.01	13.45	14.46	11.57	18.66	12.86	14.63	13.78	1.97
Residue (mg)	10.85	12.60	12.10	12.27	13.20	10.25	16.55	11.15	13.42	12.49	1.75
Vol. Loss (mg)	1.13	0.76	0.91	1.18	1.26	1.32	2.11	1.71	1.21	1.29	0.38
Loss OH (wt. %)	9.41	5.68	6.94	8.10	7.66	10.35	11.29	12.67	8.17	8.92	2.09

SD = Standard deviation

Mamu/Ajali Formation clay samples:
Aloji - AL1.1, AL1.2, AL2.2; Okpokwu - OK1.1; Oturkpa - OT2.2

Enugu/Nkporo Formation clay samples:
Enugu - EN2.1 and EN3.1.

4.3.3 Fourier Transform Infrared (FTIR) Studies of the clay deposits

The < 2µm clay samples from Aloji, Okpokwu and Enugu were subjected to IR spectral studies (Balan *et al*, 2001). The FTIR bands of the clay samples obtained were compared with the typical kaolinitic spectrum proposed by Gadsen (1975).

The bands of the investigated clay samples that ranged between 3659.51 cm^{-1} and 3696.20 cm^{-1}, which is within the proposed theoretical kaolinitic bands of 3650 cm^{-1} to 3694 cm^{-1} reflects Al-O-H stretching, typical of kaolin group (Fig. 4.19 – 4.21, Table 4.4 and Appendix 2) while the bands between 3621.22 cm^{-1} and 3622.12 cm^{-1} suggest OH stretching around the distinctive 3620 cm^{-1} band (Figs. 4.19 – 4.21, Table 4.4). Spectrum between 3438.28 cm^{-1} and 3447.25 cm^{-1} reflects absorption of water (H – O – H) within the crystal layers of the clay mineral (Fig. 4.19 – 4.21, Table 4.4). Sample EN3.1 from Enugu with a spectrum band of 2925.97 cm^{-1} (Table 4.4), indicated the presence of organic matter as shown by the C – H stretching. The presence of a layer of coal sem within the Enugu/Nkporo Formation supported this inference. Bands of 1625.47 cm^{-1} to 1628.25 cm^{-1} indicated the presence of bended (H – O – H) water. Typical kaolin spectrum with Al – O – H stretching was observed within the range of 1104.00 cm^{-1} to 1110.08 cm^{-1}. Spectrum bands of 915.12 cm^{-1} to 918.10 cm^{-1}, which is close to the proposed value of 912 cm^{-1} reflects OH – $2Al^{2+}$ linkage, while the bands from 689.76 cm^{-1} to 790.41 cm^{-1} reflects abundance of quartz (Fig. 4.19 – 4.21, Table 4.4). The bands between 538.17 cm^{-1} and 542.45 cm^{-1} close to the proposed 537 cm^{-1} reveals Fe_2O_3 and Si–O–Al stretching but 457.24 to 471.11 cm^{-1} spectrum bands signify Si – O – Si bending of quartz.

The functional groups of Si-O and Al-OH are in 1000cm^{-1} and 500 cm^{-1} region. Muscovite and possibly quartz interference was observed at 1032.16 cm^{-1} in Oturkpa (OT2.2), 1034.21 in Okpokwu (OK1.1) , 1030.06 and 1033.52 in Enugu (EN3.1 and EN4.2) for the studied clay samples.

The respective bands of 915.78 – 918.17 cm^{-1} infer bending vibrations of Al-OH but 784.76 -789.78 cm^{-1} suggest Si-O-Si inter tetrahedral bridging bonds in SiO_2 for typical kaolinitic clay minerals (Table 4.4). The FTIR results corroborated the quartz-rich, kaolinitic clay results obtained from the XRD data of the clay deposits.

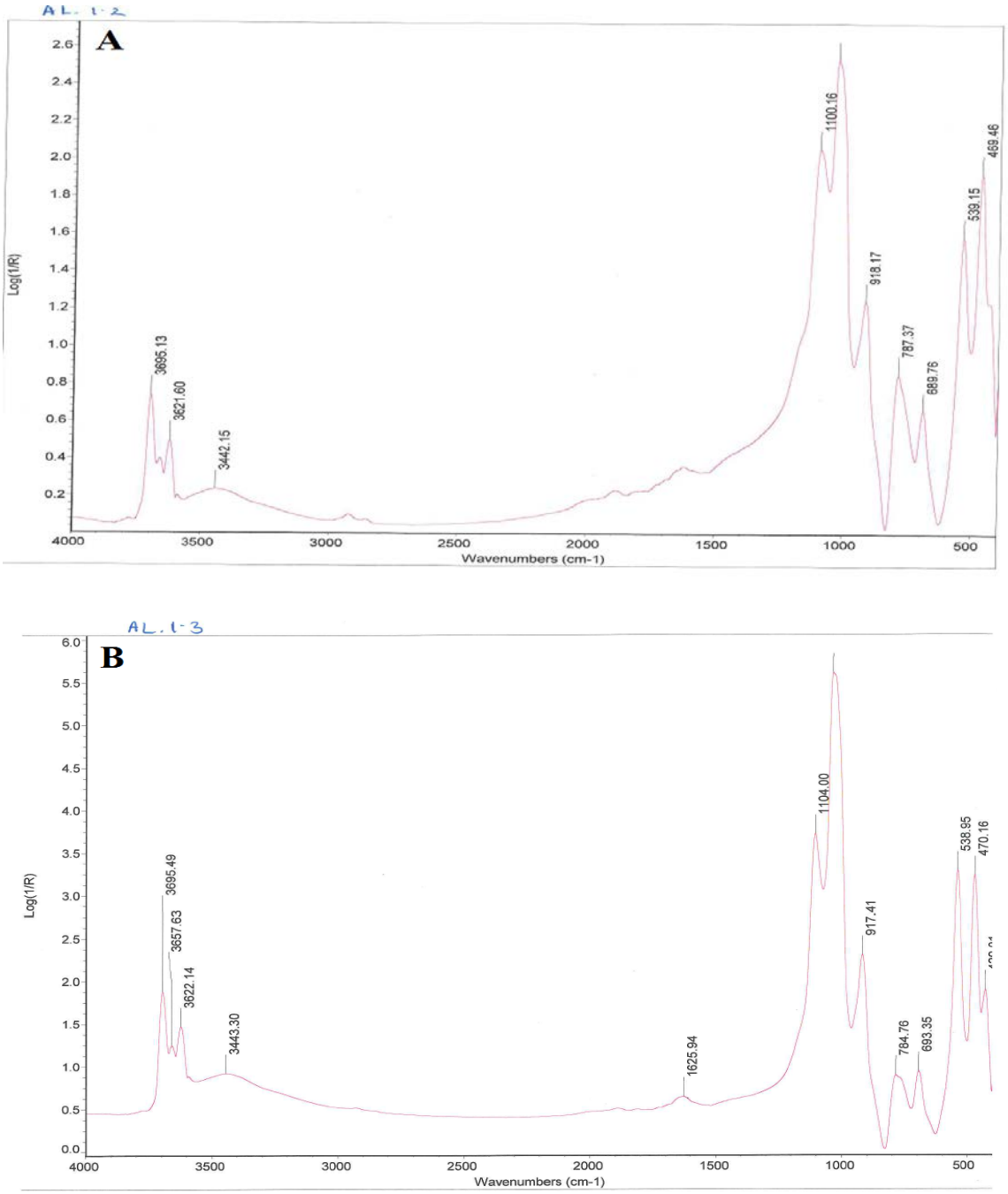

Fig. 4.19. FTIR spectra for fine (<2µm) clay sample from Aloji (**A:** Sample-AL1.2 and **B**: Sample-AL1.3) Mamu/Ajali Formation within Lower Benue Trough, Nigeria.

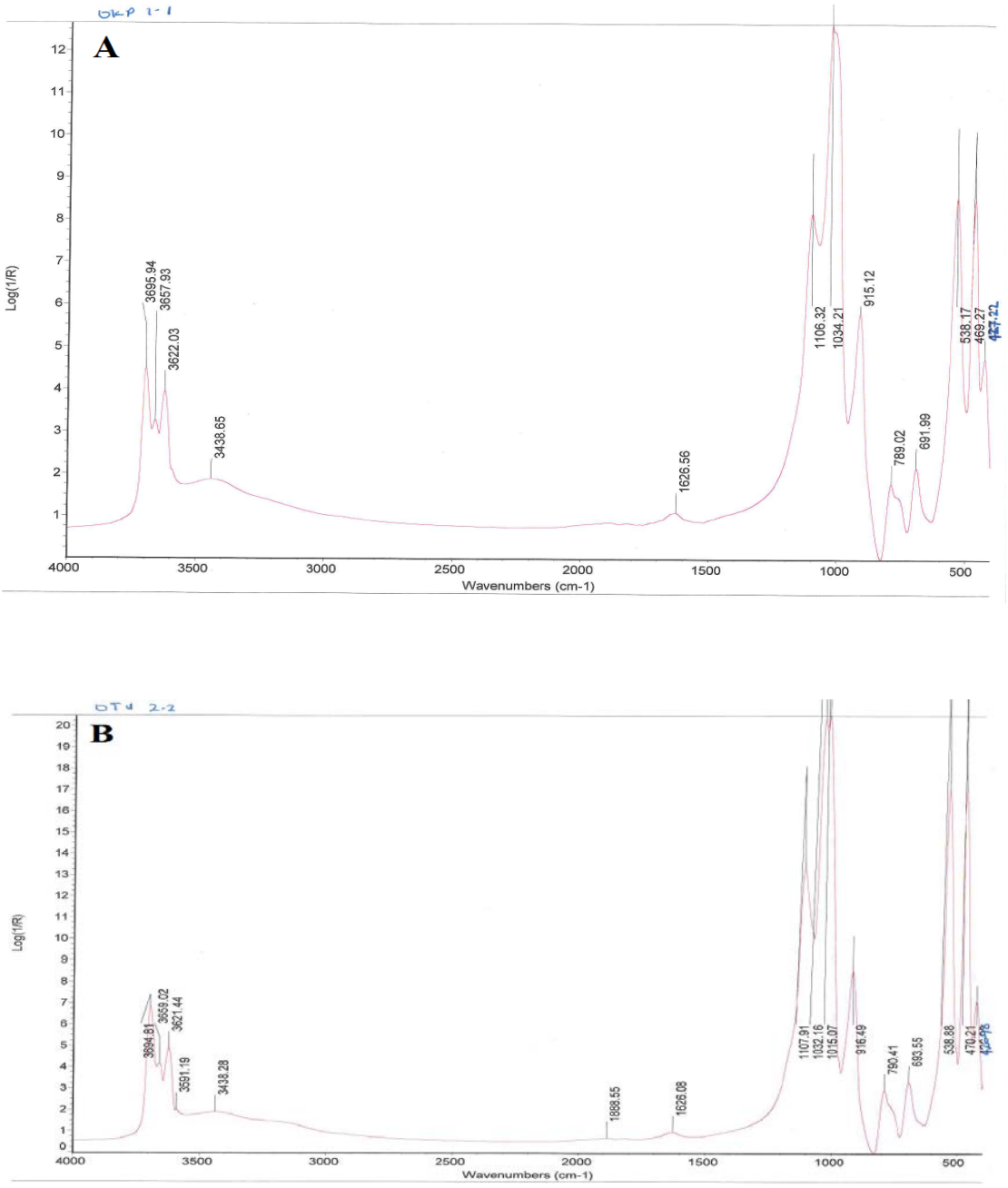

Fig. 4.20. FTIR spectra for fine (<2µm) clay sample from **A**: Okpokwu (OK1.1) and **B:**Otukpa (OTU. 2.2) Mamu/Ajali Formation within the Lower Benue Trough, Nigeria.

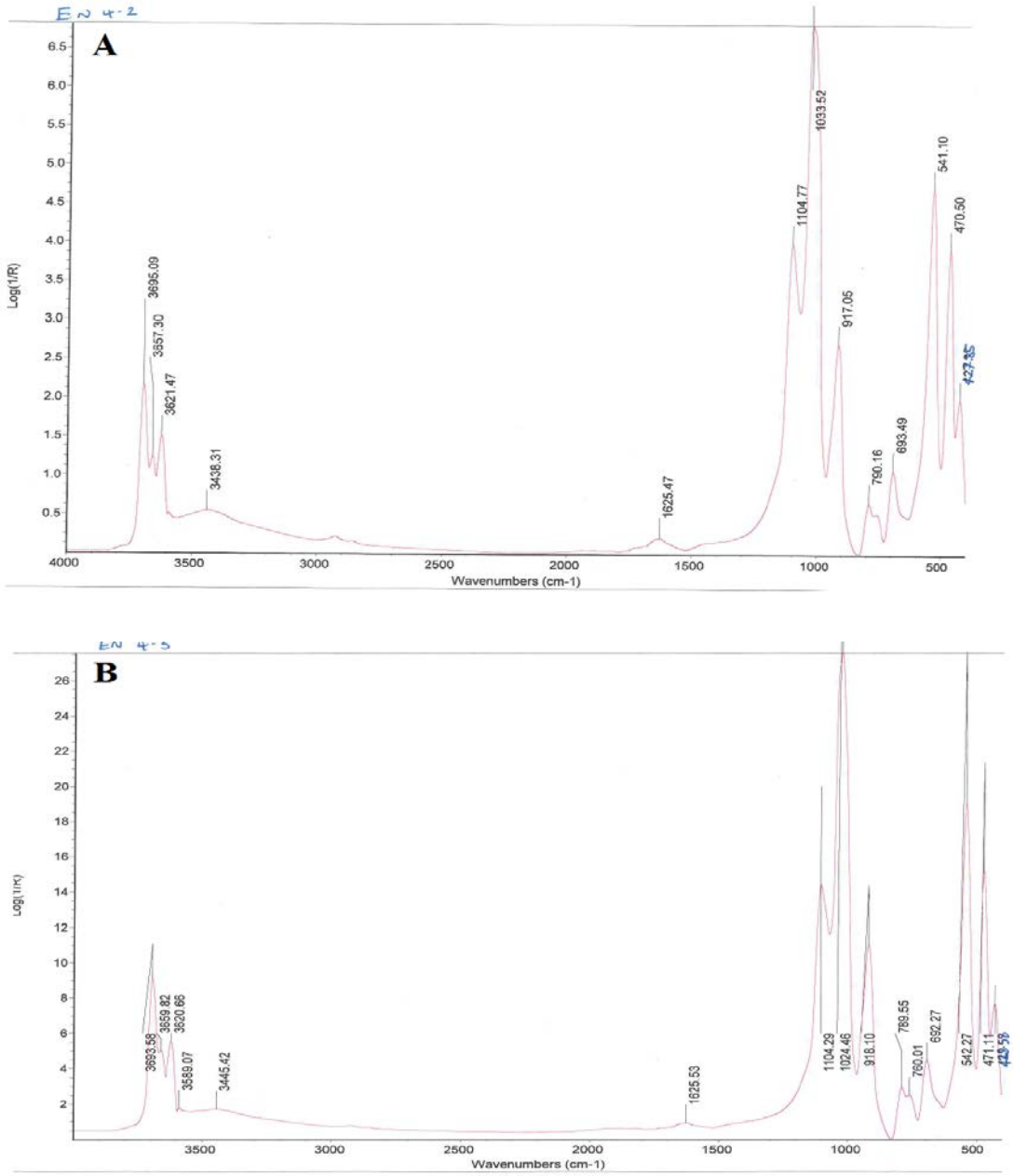

Fig. 4.21. FTIR spectra for fine (<2µm) clay samples from Enugu (**A**: Sample- EN. 4.2 and **B**: Sample-EN. 4.3), Enugu/Nkporo Formation within the Lower Benue Trough, Nigeria.

Table 4.4. Wave numbers of clay samples from the study area within the Lower Benue Trough compared to theoretical kaolin

Theoretical Kaolin	AL. 1.1	AL. 1.2	Al.1.3	OT2.2	OK.1.1	OT2.2	EN.2.1	EN.3.1	EN.4.2	EN. 4.3	Assignments
3694	3694.59	3695.13	3695.49	3694.81	3695.94	3694.81	3696.20	3694.71	3695.09	3693.58	stretching of Al--O--H
3650	3659.51	----	3657.63	3659.02	3657.93	3659.02	3656.53	3658.74	3657.30	3659.82	stretching of Al---O--H
3620	3621.70	3621.60	3622.14	3621.44	3622.03	3621.44	3621.69	3621.20	3621.47	3620.66	Stretching of OH,
				3591.19		3591.19	3593.15	3590.16		3589.07	Stretching of OH
		3442.15	3443.30	3438.28	3438.65	3438.28	3447.25	3443.04	3438.31	3445.42	water, stretching of H-O-H,
								2925.97			stretching of C-H
			1625.94	1626.08	1626.56	1626.08	1628.25	1624.73	1625.47	1625.53	bending of water , H-O-H
1114	1110.08		1104.00	1107.91	1106.32	1107.91	1110.90	1106.94	1104.77	1104.29	stretching of Al--O--H
							1071.80				Si-O quartz
1032				1032.16	1034.21	1032.16	1037.00	1030.06	1033.52		Si-O stretching, Clay minerals
1010	1001.13	110.16		1015.07		1015.07	1007.89				Si-O stretching
912	916.45	918.17	917.41	916.49	915.12	916.49	915.14	916.96	917.05	918.10	OH linked to $2Al^{3-}$
790	788.92	787.37	784.76	790.41	789.02	790.41	789.65	790.60	790.16	789.55	Si-O quartz
693		689.76	693.35	693.55	691.99	693.55	692.45	693.17	693.49	692.27	Si-O quartz
537	542.45	539.15	538.95	538.88	538.17	538.88	539.08	541.13	541.10	542.27	stretching of Fe-O, Fe_2O_3, Si-O-Al
468	457.24	469.46	470.16	470.21	469.27	470.21	468.93	470.63	470.50	471.11	Si-O-Si
430				426.98	427.22	426.98		EN.3.1	427.85	428.58	

Theoretical Kaolin values (After Gadsen (1975)

Mamu/Ajali Formation clay samples:
Aloji - AL1.1, AL1.2, AL1.3;
Oturkpa - OT2.2
Okpokwu - OK1.1;

Enugu/Nkporo Formation clay samples:
Enugu - EN2.1 and EN4.3, EN3.1, EN4.2 and EN4.3.

4.3.4 Morphology of the clay deposits

Selected clay samples from Aloji, Oturkpa in the Mamu/Ajali Formation, and Enugu in the Enugu/Nkporo Formation were subjected to SEM analysis. The micrographs provided information on the physical and geochemical processes related to the origin and the depositional setting of the clays (Giese, 1991 and Abd EL-Moghny, 2017).

The book-like morphological characterstics of some of the grains as observed under the SEM (Figs. 4.22 - 4.24), suggest a kaolinitic feature, typical of clays derived from weathering processes (Giese, 1991). The face-to-face model of platy crystals observed in all the analysed samples also supported the presene of kaolinite (Giese, 1991). In samples from Oturkpa and Enugu (Fig. 4.23 and 4.24), more swirl-like muscovite texture was noted in combination with the face-to-face arrangement of kaolinite grains and vermiculite, indicating their detrital origin (Giese, 1991; Abd EL-Moghny, 2017). Finer grains of the clay are agglomerated as they are deposited by the cementing effect of organic matter thus giving a flower - like form (Figs. 4.22b, 4.23 and 4.24). Two grain types were observed, smaller kaolinite grains of smooth edges surround bigger grains (Fig. 4.22 – 4.24).). These bimodal features indicate that the finer grains are recrystallized product while the coarser grains are of detrital origin. Such a texture in kaolinite arise due to *in situ* development of this particular mineral in a waterlaiden situation from silicate precursors (Abd EL-Moghny, 2017).

A characterised thin plates and embayed edge was observed in all the clay samples (Fig. 4.22 – 4.24), suggesting that the clay underwent relatively stronger chemical weathering (Song *et al.*, 2014).

These SEM images showed no possible effect of diagenesis when the clay minerals were formed. According to Ehrenberg *et al.* (1993), diagenetic changes are expected to be reflected in change in the kaolinitic clay morphology from aggregates of books to individual blockier crystals.

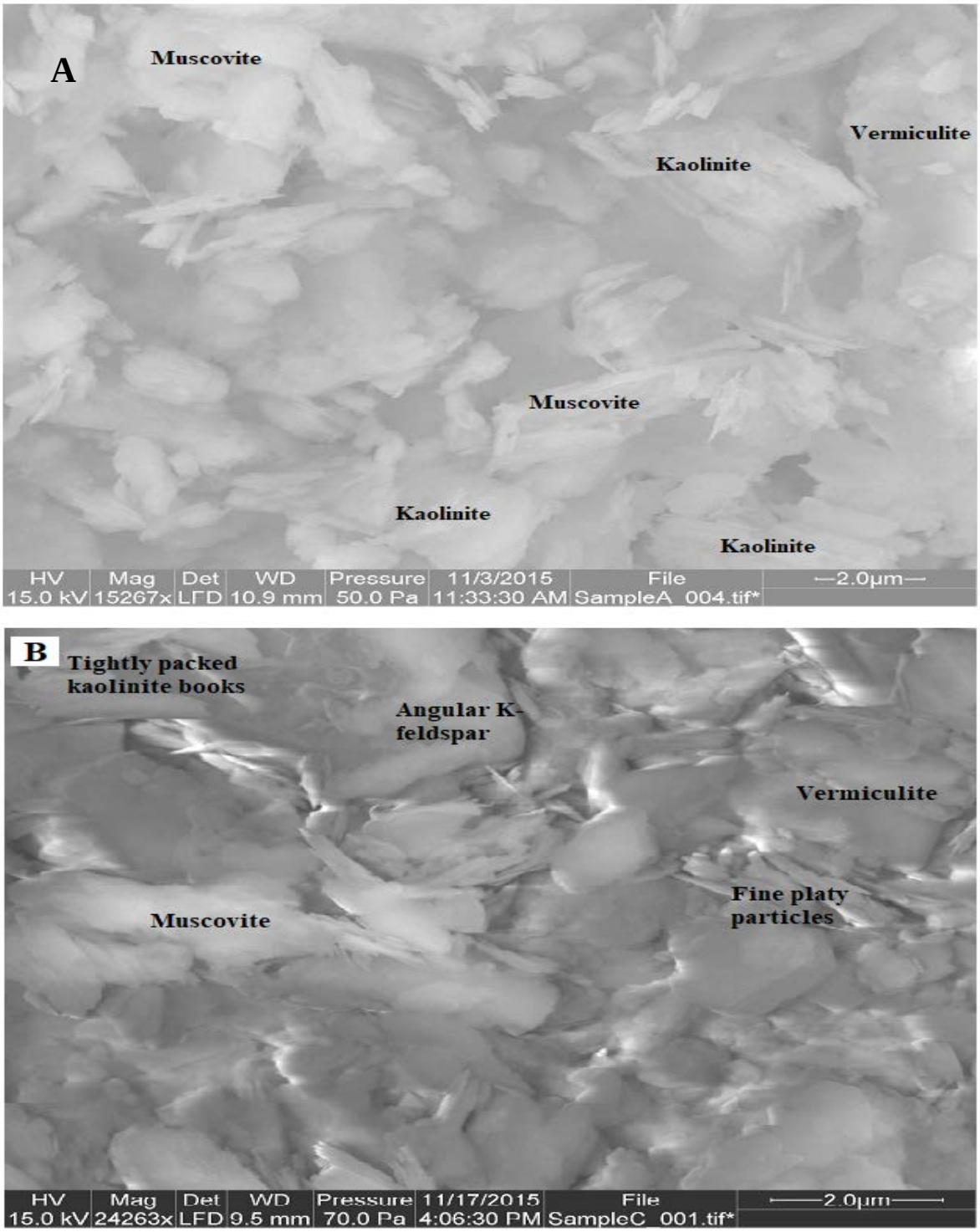

Fig. 4.22. Scanning electron micrographs of clay samples from Mamu/Ajali Formation, Lower Benue Trough, Nigeria: **A** - Aloji (AL1.1) clay sample showing book-like kaolinites having thin plates and embayed edge in association with detrital muscovite and **B** - Ofejiji (OF2.1) showing a tightly packed and fine platy particles of kaolinite in association with K-feldspar and muscovite.

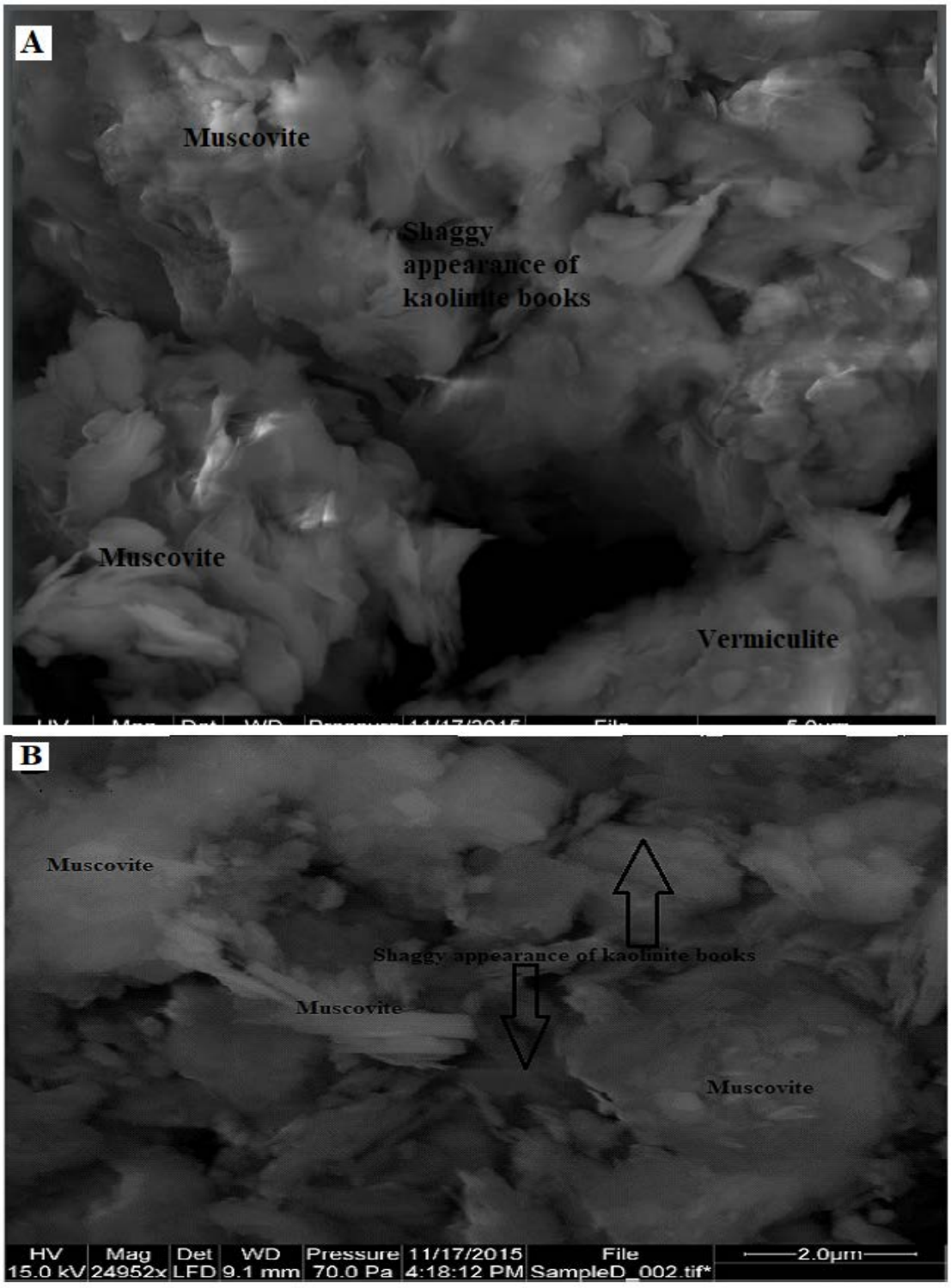

Fig. 4.23. Scanning electron micrographs of clay samples from Mamu/Ajali Formation, Lower Benue Trough, Nigeria: **A** – Agbenema (AG2.2) clay sample showing shaggy appearance of kaolinite association with detrital muscovite vermiculite and **B -** Oturkpa (OT2.2) sample showing shaggy appearance of kaolinite books with thin plates within muscovite matrix showing flower/swirl – like structures.

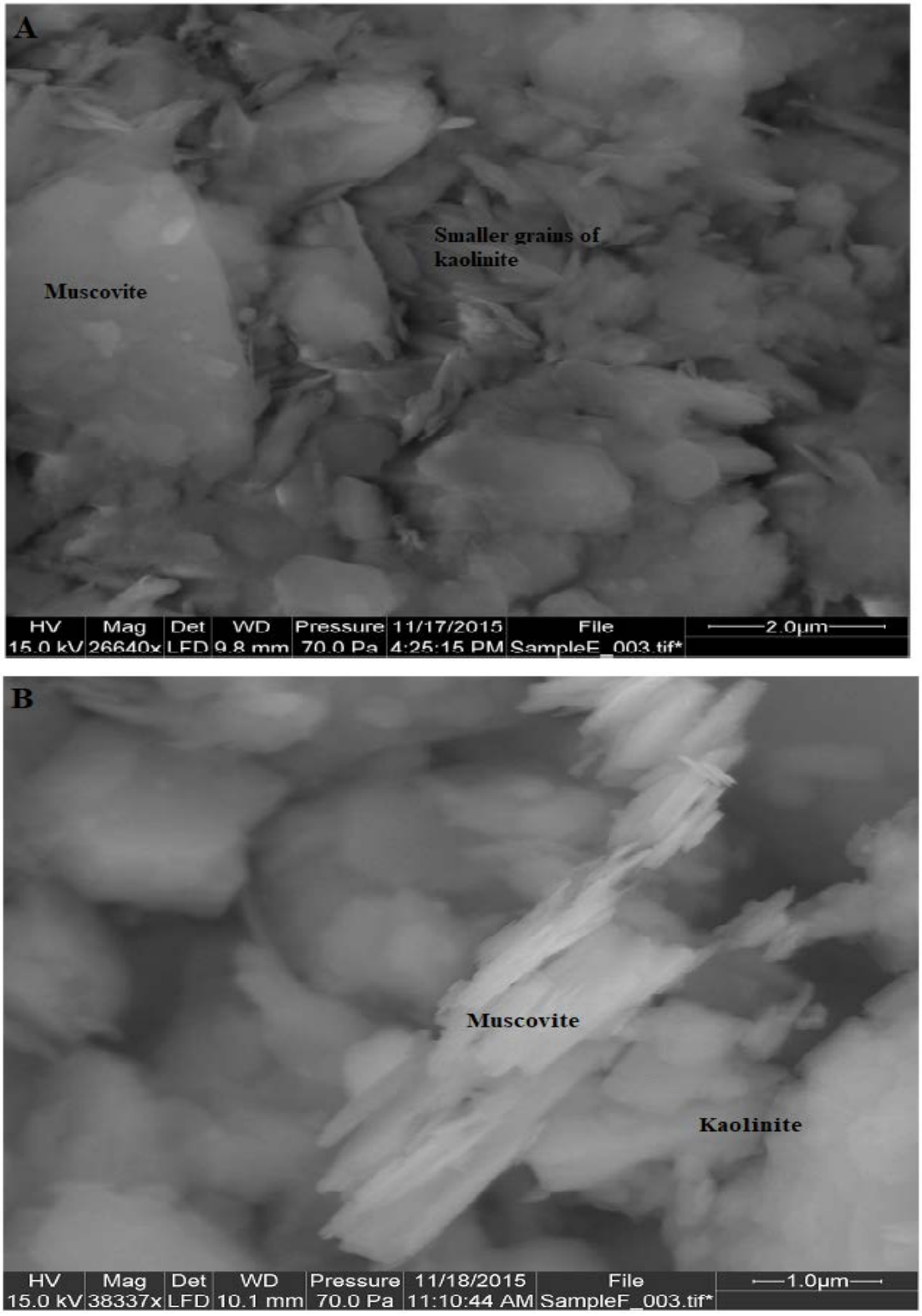

Fig. 4.24. Scanning electron micrographs of clay sample from Enugu/Nkporo Formation, Lower Benue Trough, (**C**) EN4.2 showing the smaller grains of kaolinite grains surrounding larger muscovite grains, and (**D**) EN4.3 Muscovite surrounded by grains of kaolinite.

4.3.5 Significance of the clay mineral assemblages

Rock weathering is controlled by weather, relief, source area lithology, tectonic activity and diagenetic modification (Thiry, 2000; Churchman, 2000 and Taylor and Eggleton, 2001).

The XRD, TGA/DTA, FT-IR and SEM results confirmed that the clay deposits from Aloji, Ofejiji, Udane-Biomi, Agbenema, Oturkpa, Okpokwu in the Mamu/Ajali Formation and Enugu in the Enugu/Nkporo Formation within the Lower Benue Trough are kaolinitic in nature and has not undergone diagenesis. The kaolinitic clay is derived from weathered crystalline basement rocks containing K-feldspar (microcline) and muscovite. These detrital materials were probably transported via fluvial channels and deposited during the Cretaceous at the current location within the Lower Benue Trough. The dominant clay mineral is kaolinite, which suggest hot and wet tropical climatic condition of formation for the clay deposits of Mamu/Ajali and Enugu/Nkporo Formations in the Lower Benue (Fig. 4.25). An assemblage of kaolinite + quartz describes the clay deposits studied, most especially, the deposits in Mamu/Ajali Formation, which has more quartz of 37 - 55 % compared to deposits in Enugu/Nkporo Formation of 17 – 48 %. The clay deposits were deposited under similar climatic conditions and depositional environments despite their ocurrence in different stratigraphic horizons.

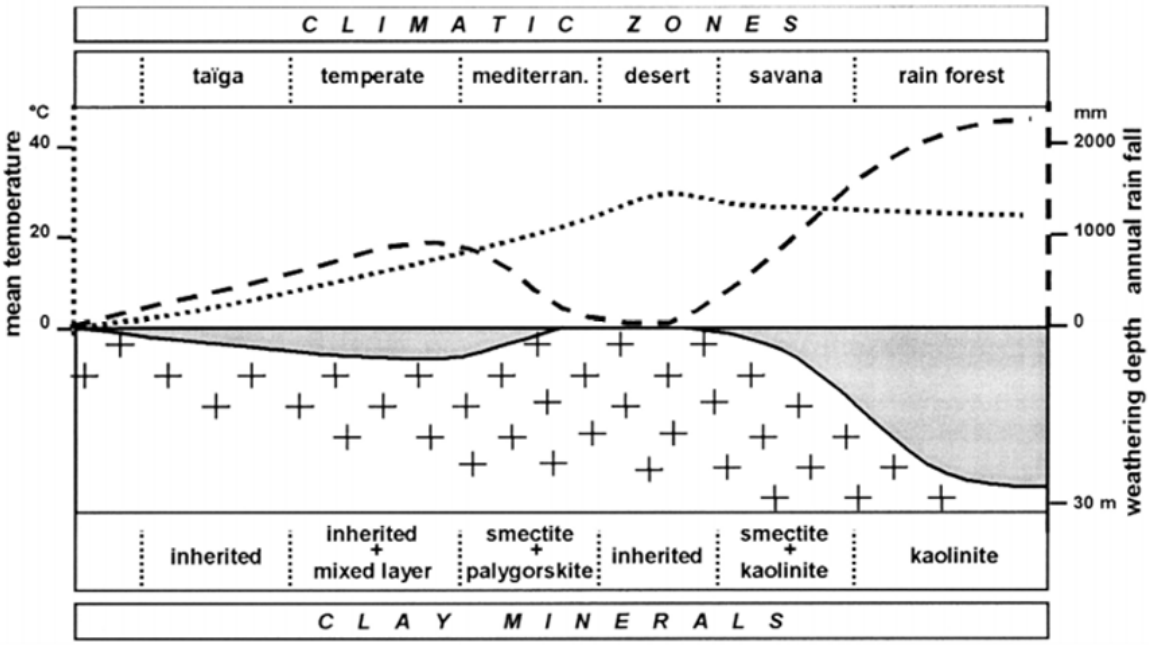

Fig. 4.25. Diagram showing the distribution of the various clay minerals relative to temperature, precipitation and climatic zones (Thiry, 2000).

4.4 Whole-rock geochemistry

Chemical compositions of both the raw and fine (<2mμ) clay samples from Aloji, Ofejiji, Agbenema, Udane-Biomi, Oturkpa, Okpokwu in the Mamu/Ajali Formation and Enugu of the Enugu/Nkporo Formation within the Lower Benue Trough is discussed below.

4.4.1 Major oxide composition of the raw clay samples

Geochemistry results for the raw clay samples are presented in Table 4.5. The SiO_2 composition varied from 69.67 to 90.28 wt% in the samples from Mamu/Ajali Formation while those of the samples from Enugu/Nkporo Formation varied from 64.61 to 69.41 wt%. The overall average of SiO_2 for both formations is 78.32 wt%. The weight percent of SiO_2 are in decreasing order from Aloji (69.67 – 88.77 wt%), Udane-Biomi (86.43 – 90.28 wt%), Ofejiji (71.39 – 84.65 wt%) and Agbenema (71.39 wt%) that vary slightly to Enugu (64.61 – 69.41 wt%) that contain the least amount of quartz (Table 4.5). This order reflect the winnowing action during transportation and deposition as sediments are moved from the northern part to the southern part, with more quartzose and coarser sediments deposited northwards and more finer, clayey sediments southwards. According to Pearsons coefficient of correlation (r) (Table 4.6), A strong negative correlation existed between SiO_2 and Al_2O_3 (r= -0.9), but positively correlated with TiO_2 (r=0.8). Therefore, SiO_2 is considered dominantly terrigenous in origin (Moosavirada *et al*., 2011).

The Al_2O_3 composition ranged between 5.90 and 19.22 wt% in the Mamu/Ajali samples while Enugu/Nkporo samples were between 15.11 and 19.21 wt%. It's is believed to be a good measure of detrital materials influx. The strong positive correlation between Al_2O_3 and TiO_2 (r=0.8) and the negative correlations between Al_2O_3 with SiO_2 and Zr (r= -0.9 and -0.2) suggested terrigenous origin. The presence of detrital K-feldspars (microcline) in the XRD supports this assertion.

Table 4.5. Major Oxide composition (wt%) of the raw clay samples

Sample No→ Oxides ↓	AL	AL1.1	AL1.2	AL1.3	AL2.1	AL2.2	AL2.3	AL2.4	AL2.5
SiO_2	83.62	69.67	82.62	75.84	82.81	87.32	85.49	88.77	87.75
TiO_2	0.98	1.63	1.00	1.41	0.90	0.79	1.08	0.85	0.85
Al_2O_3	10.05	19.22	10.53	15.24	10.32	7.34	8.73	6.65	7.24
Fe_2O_3	0.37	0.70	0.32	0.55	0.28	0.33	0.33	0.31	0.39
MnO	0.01	0.01	0.01	0.01	0.01	0.01	0.01	0.01	0.01
MgO	0.03	0.07	0.03	0.05	0.02	0.02	0.02	0.02	0.02
CaO	0.01	0.01	0.01	0.01	0.01	0.01	0.01	0.01	0.01
Na_2O	0.01	0.02	0.01	0.01	0.01	0.01	0.01	0.01	0.01
K_2O	0.10	0.33	0.14	0.22	0.07	0.04	0.07	0.04	0.04
P_2O_5	0.02	0.04	0.02	0.03	0.01	0.01	0.02	0.01	0.01
LOI	4.70	8.10	5.20	6.50	5.50	4.00	4.10	3.30	3.60
Total	99.9	99.8	99.89	99.87	99.94	99.88	99.87	99.98	99.93
SiO_2/Al_2O_3	1:8.32	1:3.62	1:7.85	1:4.98	1:8.02	1:11.90	1:9.80	1:13.35	1:12.12

Mamu/Ajali Formation samples

Aloji - AL, AL1.1, AL1.2, AL1.3,AL2.1, AL2.1, AL2.3, AL2.4, AL2.5.

Table 4.5. Cont.

Sample No→ Oxides ↓	OF2.1	OF2.2	AG2.1	UD1.1	UD1.2	UD1.3	EN4.1	EN4.2	EN4.3
SiO_2	84.65	71.39	79.99	86.53	90.28	86.43	68.56	64.61	69.41
TiO_2	0.97	1.22	1.31	1.29	0.66	1.00	2.02	1.81	1.19
Al_2O_3	6.32	12.91	9.57	7.95	5.10	7.28	17.48	19.21	15.11
Fe_2O_3	0.76	1.46	2.06	0.41	1.02	1.63	2.20	3.50	3.99
MnO	0.01	0.01	0.01	0.01	0.01	0.01	0.01	0.01	0.01
MgO	0.04	0.12	0.09	0.03	0.02	0.03	0.09	0.09	0.11
CaO	0.01	0.01	0.01	0.01	0.01	0.01	0.01	0.01	0.01
Na_2O	0.06	0.05	0.07	0.01	0.01	0.01	0.08	0.05	0.09
K_2O	1.63	1.19	1.87	0.09	0.07	0.07	0.09	1.07	0.81
P_2O_5	0.06	0.16	0.03	0.04	0.02	0.01	0.06	0.08	0.09
LOI	5.20	11.10	4.70	2.70	2.70	3.40	9.23	9.51	8.22
Total	99.71	99.62	99.71	99.07	99.9	99.88	99.83	99.95	99.99
SiO_2/Al_2O_3	1:13.39	1:5.53	1:8.36	1:10.88	1:17.70	1:11.87	1:3.92	1:3.36	1:4.59

Mamu/Ajali Formation samples:

Ofejiji - OF2.1 and OF2.2, =, = samples from.

Agbenema - AG2.1.

Udane-Biomi - Ud1.1, Ud1.2 and Ud1.3

Enugu/Nkporo Formation samples:

Enugu - EN4.1, EN4.2 and EN4.3.

Table 4.6. Correlation results for the major oxides and trace element composition for the raw clay samples from Mamu/Ajali and Enugu/Nkporo Formations.

	Al_2O_3	**Fe_2O_3**	**K_2O**	**MgO**	**Na_2O**	**SiO_2**	**TiO_2**	**Zr**
Al_2O_3	1							
Fe_2O_3	0.0182	1						
K_2O	0.0616	**0.6569**	1					
MgO	**0.5566**	**0.6674**	**0.7104**	1				
Na_2O	0.0531	**0.6716**	**0.9962**	0.727	1			
SiO_2	**-0.9248**	-0.2755	-0.3751	**-0.8106**	-0.3749	1		
TiO_2	**0.8272**	0.2463	0.3054	**0.6367**	0.2904	**-0.8178**	1	
Zr	**-0.2395**	0.2393	0.2918	0.0902	0.2834	0.1493	0.2906	1

The content of K_2O in clay samples of the Mamu/Ajali Formation ranged from 0.04 and 1.87 wt% while that of Enugu/Nkporo Formation ranged from 0.81 and 1.07 wt%. This compositional value corresponds to the results of the studied clay mineral. The low K_2O values indicated a lack of expandable clays in the clay deposits, such as montmorillonite or illite. Although insignificant, the positive correlation between K_2O and Al_2O_3, TiO_2 and Zr (r = 0.1, 0.3, and 0.3 ; Table 4.6) shows the association of aluminosilicate phases with K_2O.

The low content of CaO (<0.1 wt%) and MgO (<0.13 wt%) (Table 4.5) for all the clay samples from both formations is ascribed to the lack of marine carbonate facies (Imeokparia and Onyeobi, 2007). For both formations, the average content of MgO in the studied raw clay samples is 0.04 percent, relatively lower than the average Taylor and McLennan (1985) UCC (2.20 wt%) and PAAS (2.20 wt%) and Gromet et al. NASC (2.86 wt%) (1984). The distribution of MgO in the studied samples is mostly consistent with Fe_2O_3, this is evident from the observed high correlation coefficient between them (r = 0.67, Table 4.6), this is because these elements could be present in the same mineralogical phase, since the behaviour of Mg is only controlled by the ferromagnesian function.

The value of Fe_2O_3 in raw clay samples of Mamu/Ajali Formation ranged from 0.28 to 1.63 wt%, whereas Enugu/Nkporo Formation ranged from 2.20 to 3.99 wt% with an average of 1.27 wt%, for both Formations (Table 4.5). This average value is much lower than the UCC (5.00 wt%) and PAAS (7.22 wt%) of Taylor and McLennan (1985), and the NASC (5.56 wt%), of Gromet *et al.* (1984). The content of Fe_2O_3 can be ascribed to superficial oxidation and contamination due to the ferruginous facies capping the ridge. This is true as there is an upward increase of iron concentration in Udane-Biomi (UD1.1→UD1.2→UD1.3), Okpokwu (OK1.1→OK1.2→OK1.3) and Enugu (EN4.1→EN4.2→EN4.3) clay deposits respectively (Table 4.5), probably because of the leaching of kaolinite and quartz with simultaneous enrichment of Fe_2O_3. This is evident from the negligible positive correlation of Fe_2O_3 and Al_2O_3 (r = 0.02), TiO_2 (r = 0.23) (Table 4.6).

Titanium oxide (TiO_2) in the raw clay samples vary from 0.79 to 1.63 wt% for the Mamu/Ajali Formation clay samples and 1.19 to 2.02 wt% for the Enugu/Nkporo samples. The average TiO_2 of 1.24 % for both clay samples is slightly greater than that of average UCC (0.50 wt%) and PAAS (0.70 wt%) of Taylor and McLennan (1985), the NASC (1.00 wt%), of Gromet *et al.* (1984). The TiO_2 composition did not show any particular trend with depth at Aloji, Okpokwu and Enugu (Table 4.5) suggesting its immobile nature during weathering. The correlation of TiO_2 with Al_2O_3 (r= 0.8) and Zr (r = 0.3) (Table 4.6), reflects their terrigenous origin (Liu *et al*., 2009 and Saccà *et al*., 2011).

The raw clay samples are lower in P_2O_5 content, generally less than 0.16 wt% for all the clay samples from both formations studied; this may be due to minute accessory minerals such as apatite and monazite (Table 4.5). The alkalis (K_2O, Na_2O) as well as MgO and MnO occur at a relatiely low value, indicating their high mobility during weathering due to their elevated hydration energy (Cullers, 1988). The clay silica-alumina ratio for samples from the Mamu/Ajali ranged from 1:3.62 to 1:17.70 while the Enugu/Nkporo samples ranged from 1:3.36 to 1:4.59. The overall average for both formation is 1:8.15. These values confirms that the clay deposits from Mamu/Ajali Formation are more siliceous compared to the Enugu/Nkporo clay samples (Table 4.5). This corroborates the XRD data with quartz contents of between 39 and 69 %. The loss on ignition (LOI) for the Mamu/Ajali Formation raw clay samples varied from 2.70 to 11.00 wt% while those of Enugu/Nkporo Formation ranged from 8.22 to 9.51 wt%. The average LOI for both formations is 6.13 wt% (Table 4.5). These values indicate that the clay deposits are essentially quartz-rich kaolinite as indicated by the mineralogical data.

The general depletion of Na, K and Ca could be as a result of their high hydration energy during weathering process, resulting in their high mobility (Cullers, 1988). For the raw clay samples, the strong positive correlation between Na_2O and K_2O (r = 0.9) support such relationships (Table 4.6).

The negative correlation of SiO_2 and Fe_2O_3 (Fig. 4.26a) and the positive correlation between LOI and Al_2O_3 (Fig. 4.26b), Indicated weathering process influence through

increased silica abundance and depletion of Fe and Mg, as well as increased LOI with increased weathering and maturity of the sediment. The negative correlation observed between SiO_2 and Al_2O_3 (Fig. 4.26c) is also an indication of Al_2O_3 enrichment during weathering and deposition at the expense of SiO_2. In the presence of organic matter, the mixture of siliceous fraction and aluminous fraction could also occur. The harker diagram (Fig. 4.26d) did not show a consistent correlation trend between Fe_2O_3 and Al_2O_3 in all the samples. This is due to differential ferruginisation of the clay, which result from the gradual replacement of kaolinite by iron oxide (Liu *et al*., 2009 and Saccà *et al*., 2011).

On the Al_2O_3 - Fe_2O_3 - SiO_2 diagram of Schellmann (1986), all the sediments plot at the SiO_2 peak indicating strong kaolinitisation from a common felsic source material which began to occur at 73 % SiO_2 against the reference samples of Kutigi (Akhirevbulu, 2010), Bida (Okunlola and Idowu, 2012) and Abeokuta sedimentary clays (Elueze and Bolarinwa, 2001) which indicate moderate kaolinitisation (Fig. 4.27). The process indicates a gradual change from a SiO_2-rich to an Al_2O_3-rich composition under increasing kaolinitisation.

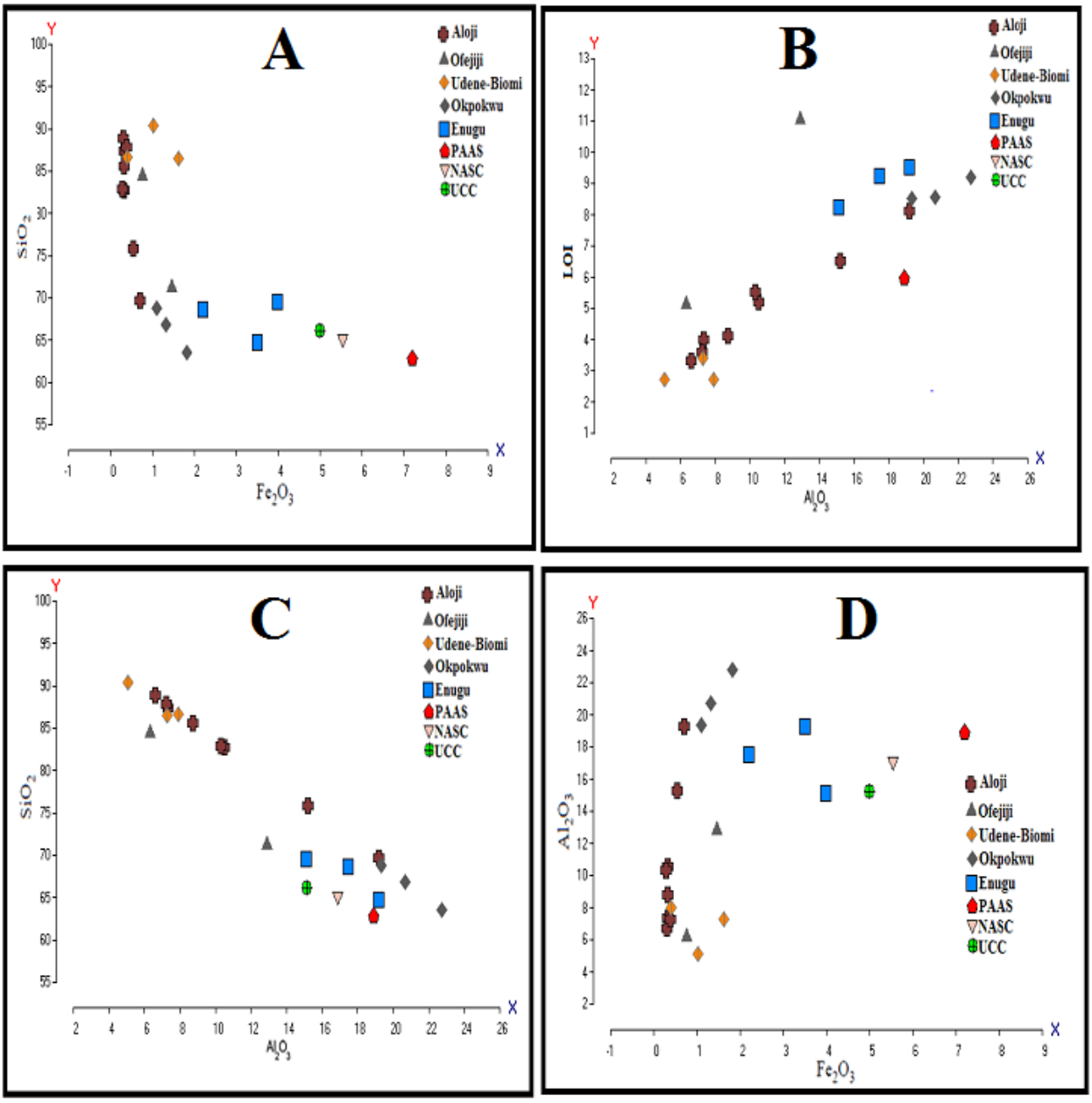

Fig. 4.26. Harker's diagram of **A**: SiO_2 vs Fe_2O_3, **B:** LOI vs Al_2O_3, **C**: SiO_2 vs Al_2O_3 and **C**: Al_2O_3 vs Fe_2O_3 of raw clay samples in the Lower Benue Trough, Nigeria.

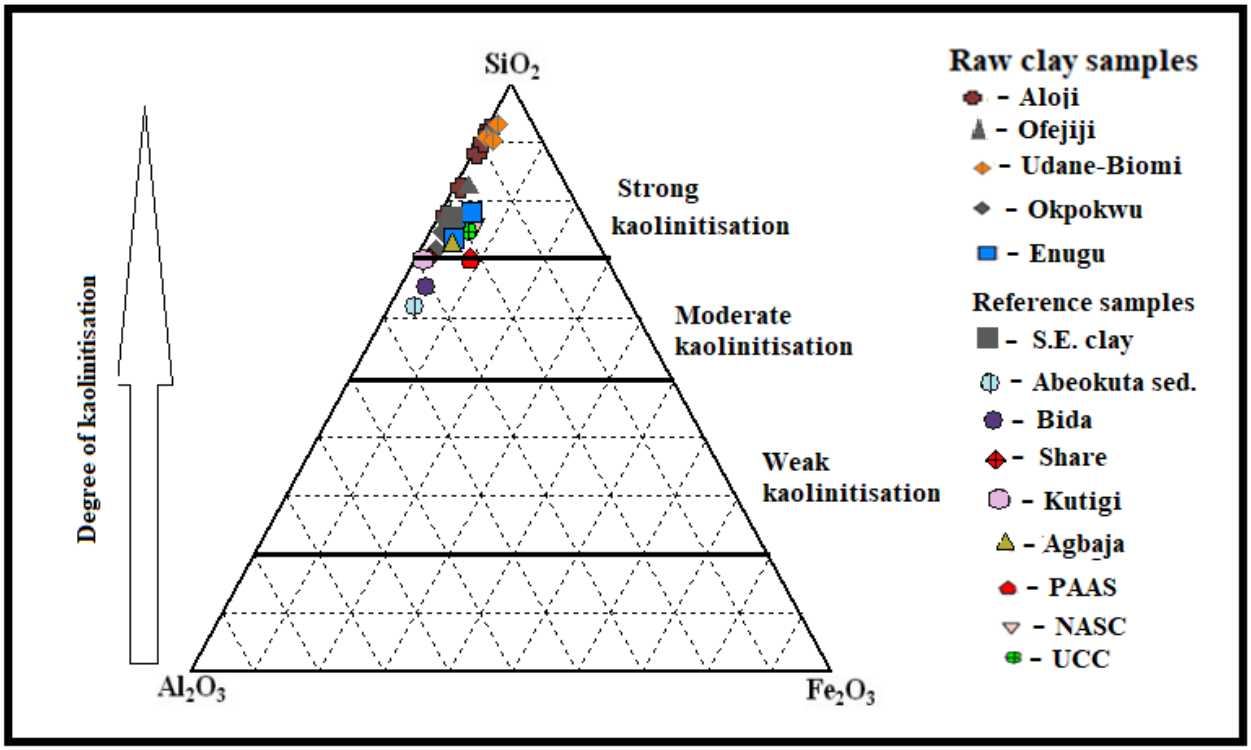

Fig. 4.27. Ternary diagram of SiO_2-Fe_2O_3-Al_2O_3 showing degree of kaolinitisation for the raw clay samples in the Mamu/Ajali and Enugu/Nkporo Formation (after Schellmann, 1986).

4.4.2 Major oxide geochemistry of fine (<2µm) clay samples

The result of the major element analyses for the fine (<2µm) clay samples of Mamu/Ajali and Enugu/Nkporo Formations in the Lower Benue Trough, Nigeria are presented in Table 4.7.

The SiO_2 composition in the fine clay fraction of the Mamu/Ajali Formation varied between 47.33 and 80.10 wt% as against 69.67 and 90.28 wt% in the raw samples while those of Enugu/Nkporo Formation fine fraction is between 54.70 and 66.45 wt% against 64.61 and 69.41 wt% in the raw clay samples. The fine fraction's overall average is 65.98 wt%. The Al_2O_3 content in the fine fraction of Mamu/Ajali Formation ranged from 12.10 to 29.64 wt% while those of Enugu/Nkporo Formation varied between 22.03 and 28.17 wt% as against 15.11 and 19.21 wt% in the raw samples. This confirms a condition of quartz-rich kaolinite mineral assemblage (Tables 4.5 and 4.7). The SiO_2 correlates negatively with Al_2O_3(r= -0.98) suggesting a terrigenous origin for both the raw clay and the fine fraction. The negative correlation of SiO_2 with TiO_2 (r= -0.47) (Table 4.8) is attributed to size sorting due to the winnowing of the sediments during transportation before deposition. Positive correlation of Al_2O_3 with TiO_2 (r=0.43 ; Table 4.8) and a strong negative correlation of Al_2O_3 with SiO_2 and Zr (r= -0.98 and -0.85 ; Table 4.8) also confirmed the terrigenous origin of the clay.

In the fine (<2µm) clay fraction, Fe_2O_3 ranged from 0.48 to 4.01 wt% in the Mamu/Ajali Formation. This value is higher than what was obtained in the raw samples (0.28 – 1.63 wt%). The Fe_2O_3 of the fine fraction from Enugu/Nkporo ranged from 0.96 to 1.94 wt%, which is much lower than the range of 2.20 to 3.99 wt% recorded in the raw clay samples (Tables 4.5 and 4.7). The relatively higher value of Fe_2O_3 obtained in the fine (<2µm) clay fraction of Mamu/Ajali could be attributed to the gradual post-depositional replacement of kaolinite by iron (Table 4.7).

Table 4.7. Oxide composition (wt%) of the fine (<2μm) clay samples.

Sample No → Oxides ↓	AL1.1	AL1.2	AL1.3	OF2.4	AG1.1	AG1.2	Ud.1.1	Ud.1.3
SiO_2	66.08	80.10	73.07	69.94	49.30	63.04	76.56	62.55
TiO_2	1.65	1.29	1.68	1.32	1.65	1.58	1.37	1.45
Al_2O_3	22.39	12.10	15.59	17.44	29.69	22.14	14.72	21.78
Fe_2O_3	0.83	0.48	1.62	2.21	3.77	2.31	0.66	4.08
MnO	0.01	0.01	0.01	0.01	0.04	0.01	0.01	0.01
MgO	0.07	0.05	0.13	0.16	0.41	0.22	0.05	0.09
CaO	0.03	0.02	0.06	0.05	0.19	0.18	0.03	0.05
Na_2O	0.03	0.02	0.08	0.10	0.07	0.11	0.02	0.03
K_2O	0.35	0.22	2.02	2.16	1.19	2.06	0.17	0.27
P_2O_5	0.05	0.05	0.03	0.05	0.08	0.05	0.11	0.06
LOI	8.30	5.50	5.50	6.30	13.3	8.00	6.00	9.40
Sum	99.87	99.84	99.77	99.78	99.78	99.75	99.75	99.81
SiO_2/Al_2O_3	1:2.95	1:6.83	1:4.69	1:4.01	1:1.66	1:2.85	1:5.20	1:2.87

Sample No → Oxides ↓	OT1.1	OT2.2	OK1.1	EN2.1	EN4.2	EN4.3
SiO_2	47.33	63.02	50.21	54.72	57.15	66.45
TiO_2	1.49	1.67	1.78	2.18	1.80	1.70
Al_2O_3	33.77	21.36	29.64	28.17	24.50	22.03
Fe_2O_3	2.41	4.01	3.92	1.94	1.73	0.96
MnO	0.01	0.01	0.01	0.01	0.01	0.01
MgO	0.24	0.14	0.46	0.28	0.10	0.04
CaO	0.16	0.08	0.22	0.11	0.02	0.02
Na_2O	0.03	0.04	0.05	0.05	0.04	0.02
K_2O	0.53	0.67	0.97	0.91	0.46	0.16
P_2O_5	0.05	0.06	0.10	0.03	0.06	0.06
LOI	13.80	8.70	12.40	11.40	14.00	8.30
Sum	99.86	99.85	99.76	99.85	99.85	99.82
SiO_2/Al_2O_3	1:1.40	1:2.95	1:1.69	1:1.94	1:2.33	1:3.02

Mamu/Ajali Formation samples:

Aloji - AL1.1, AL1.2, AL1.3, Agbeneme - AG1.1, AG1.2, UdaneBiomi - UD1.1, UD1.3.

Oturkpa - OT1.1, OT2.2, Okpokwu - OK1.1.

Enugu/Nkporo Formation samples:

Enugu - EN2.1, EN4.2, EN4.3.

Table 4.8. Correlation coefficients of major and trace element for the fine (<2μm) clay samples.

	Al_2O_3	CaO	Fe_2O_3	K_2O	MgO	Na_2O	SiO_2	TiO_2	Zr
Al_2O_3	1								
CaO	0.5415	1							
Fe_2O_3	0.3919	0.6348	1						
K_2O	-0.1282	0.4234	0.2860	1					
MgO	0.4761	**0.9188**	**0.6600**	0.4396	1				
Na_2O	-0.0745	0.461	0.3381	**0.9755**	0.4609	1			
SiO_2	**-0.9810**	**-0.623**	**-0.5381**	0.0333	**-0.5906**	-0.0334	1		
TiO_2	**0.4251**	0.2896	0.2200	0.0868	0.4337	0.0997	-0.4710	1	
Zr	-0.8533	-0.4949	-0.3286	0.1092	-0.4789	0.0449	**0.8548**	-0.4454	1

The titanium oxide (TiO_2) composition in the fine (<2µm) clay samples of Mamu/Ajali formation varied from 1.29 to 1.78 wt% as against 0.79 to 1.63 wt% in the raw samples. The Enugu/Nkporo Formation fine fraction has 1.70 to 2.18 wt% TiO_2 as against 0.81 to 1.07 wt% in the raw clay (Tables 4.5 and 4.7). Its composition is relatively higher than the raw clay samples, suggesting decomposition of acessory minerals, such as, ilmenite and rutile under intensive chemical weathering condition to produce fine (<2µm) particles within which TiO_2 is incorporated. The correlation between MgO and Fe_2O_3 is strong and positive (r = 0.66, Table 4.8), because both oxides are sourced from ferromagnesian silicates, such as, biotites and amphiboles, which though may be minor constituents of felsic igneous or metamorphic rocks.

Depletion in Na (< 0.11 wt%), K (<0.17 wt%) and Ca (<0.22 wt%) was observed in all the analyzed fine (<2µm) clay fractions (Table 4.7). This trend is similar to what was observed in the raw clay sample, thus confirming their high mobility during weathering process (Cullers, 1988). The strong positive correlation of the two oxides (Na_2O and K_2O; r = 0.9) (Table 4.8), corroborated their geochemical association. The silica - alumina ratio of the fine Mamu/Ajali Formation (<2µm) clay fraction is between 1:1.66 and 1:6.83 wt% while those of the raw clay samples are 1:3.62 to 1:17.70. The Enugu/Nkporo Formation fine samples ranged from 1:1.94 to 1:3.02 as against 1:3.36 to 4.59 in the raw clay samples. This composition is consistent with the observed XRD data. The loss on ignition (LOI) of the fine (<2µm) fraction (5.50 – 13.80 wt%) was higher than those of the raw clay samples (2.70 – 11.10 wt%) of Mamu/Ajali Formation. The same trend is reflected in the fine fractions (8.30 – 14.00 wt%) and the raw clay samples (8.22 – 9.51 wt%) of the Enugu/Nkporo Formation (Table 4.7). The high LOI value of the fine (<2µm) clay fraction is due to the high content of organic materials and water compared to the raw clay samples. The harker diagrams for the fine clay fractions (Figs. 4.28a-c) are similar to those of the raw clay samples (Fig. 4.26). The kaolinitisation trends depicted on the SiO_2 - Fe_2O_3 - Al_2O_3 diagram (Figs. 4.29a and b) is similar to that of the raw clay samples except fine fraction of Okpokwu and Enugu more enriched in Al_2O_3 .The compositional values described above suggests that both the Mamu/Ajali and the Enugu/Nkporo Formation clay samples are relatively from similar felsic parent rock.

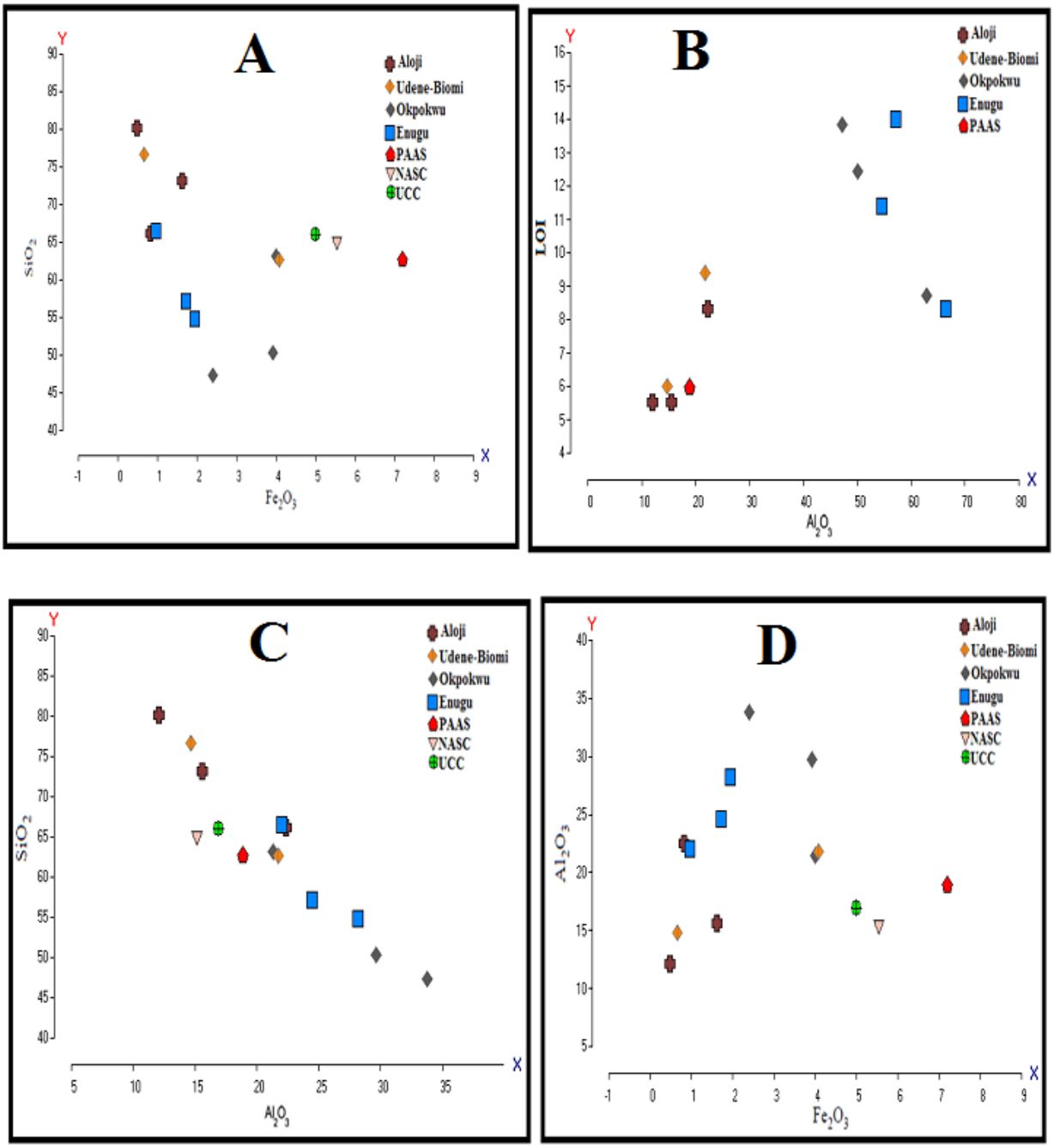

Fig. 4.28. Harker's diagram of **A**: SiO_2 vs Fe_2O_3, **B:** LOI vs AL_2O_3, **C:** SiO_2 vs Al_2O_3, **D:** Al_2O_3 vs Fe_2O_3 for the fine (<2µm) clay fractions investigated.

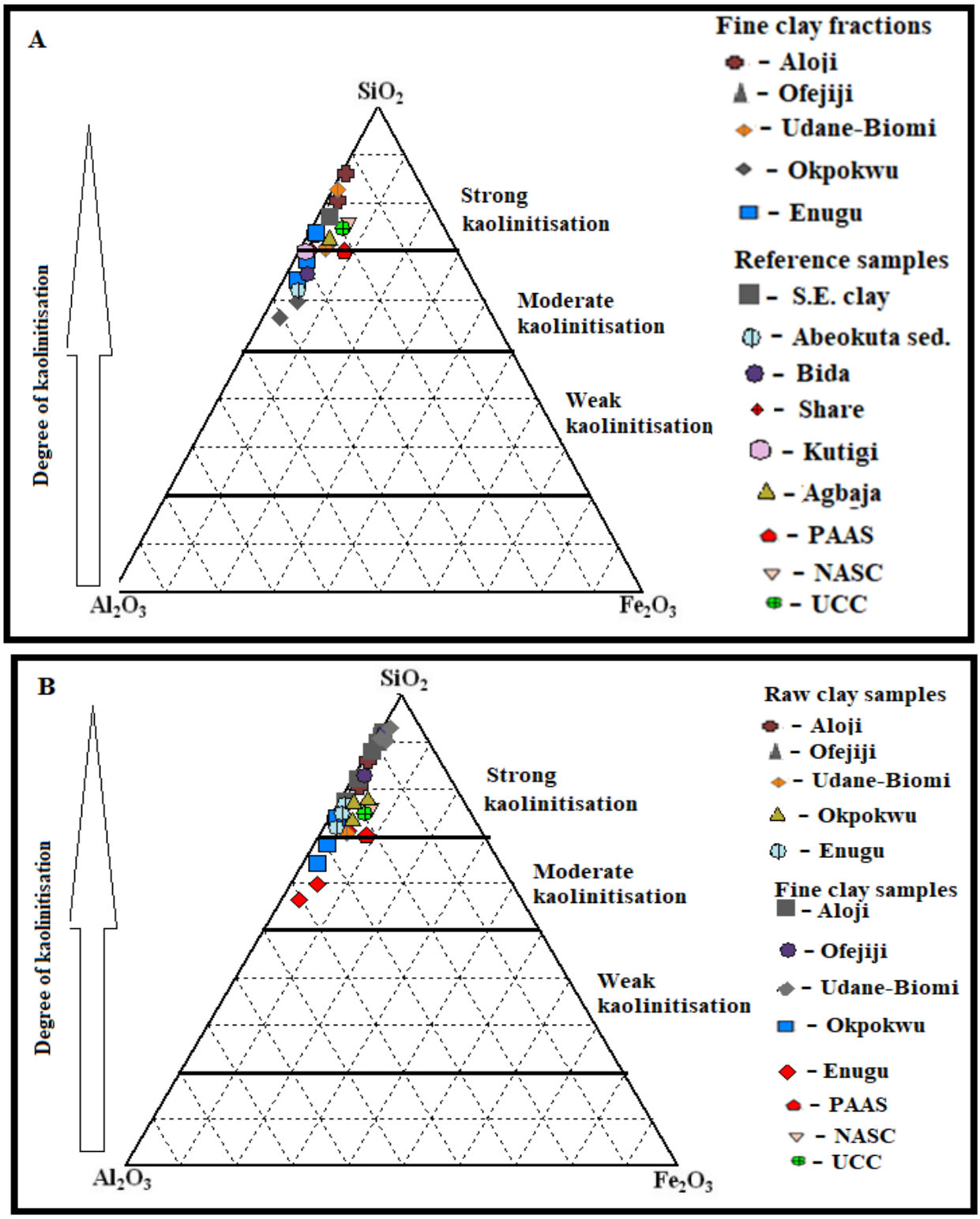

Fig.4.29. Ternary diagram of SiO_2 - Fe_2O_3 - Al_2O_3 showing degree of kaolinitisation for **A:** fine (<2µm) clay samples and **B:** Raw and fine (<2µm) clay samples investigated (after Schellmann, 1986).

4.4.3 Comparison of the major oxide composition of the clay samples

Comparison of the major oxide compositions of Aloji, Ofejiji, Udane-Biomi and Agbenema clay samples from Mamu/Ajali Formation and Enugu clay from Enugu/Nkporo Formation within the Lower Benue Trough with other well known clay deposits were carried out. It was noted that the Enugu's raw clay samples compare favourably with UCC values of Taylor and McLennan (1985) and PAAS and NASC values of Gromet *et al.* (1984), Southeasthern clay (Odoma *et al*., 2015), Abeokuta sedimentary clay (Elueze and Bolarinwa, 2001), Bida (Okunlola and Idowu, 2012), Share (Ojo *et al.*, 2011) and Agbaja (Ojo *et al.,* 2011) (Fig. 4.30). On the other hand, the fine (<2µm) clay fraction of Agbenema, Okpokwu and Enugu compare favourably with Bida, Share, Kutigi and Abeokuta (Sedimentary), Florida active kaolinite (Huber, 1985) and Average Claystone-Shale—(Pettijohn, 1957) (Fig. 4.31). The favourable comparison of the fine <2µm clay samples than the raw clay samples is primary due to its low SiO_2 content.

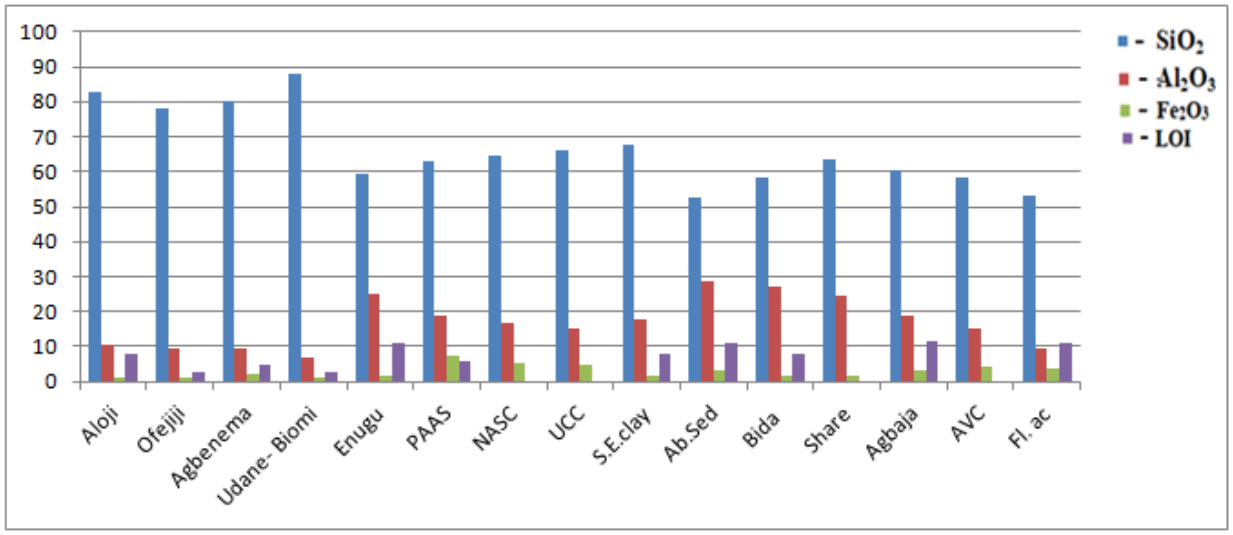

Fig: 4.30. Bar chart showing the average chemical composition of the raw clay samples studied compared with other clay. This study (Aloji to Udane-Biomi from Mamu/Ajali Formation and Enugu from Enugu/Nkporo Formation.

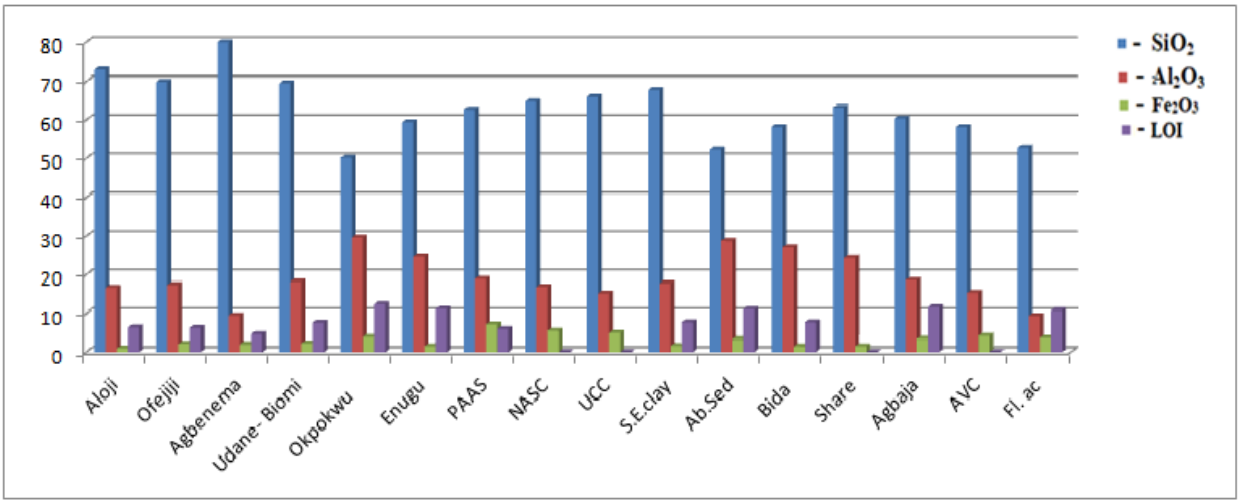

Fig. 4.31. Bar chart showing the average chemical composition of the fine (<2µm) clay samples studied compared with other clay types. This study (Aloji to Okpokwu from Mamu/Ajali Formation and Enugu from Enugu/Nkporo Formation.

4.4.4 Classification of the clay deposits

The clay deposits of the Mamu/Ajali and Enugu/Nkporo Formations in the Lower Benue Trough were classified using the ternay plot of Herron (1988) (Al_2O_3 - (K_2O+CaO+MgO) - (Fe_2O_3+MgO) (AKF)) (Fig. 4.32). The ternary plot revealed that all the investigated clay samples plot within the continental zone dominated by argillaceous and ferruginous argillite derivative of felsic igneous rock weathering to kaolinitic clay as opposed to PAAS and UCC data (Taylor and McLennan, 1985) and NASC (Gromet et al., 1984) plotting within a transition zone (Fig. 4.32). This agrees with similar research carried-out by Adeigbe and Yusuf (2013), Adeigbe and Ayoola (2014) and Odoma *et al.* (2015) on sediments from the Lower Benue Trough.

Texturally, the clay deposits were classified according to ternary plot of Shepard (1954; Fig. 4.33). The textural classification revealed sandy silt to clayey silt assemblages (Fig. 4.33). This classification corroborates the XRD data in which quartz contents decreases from Aloji >Udane-Biomi >Ofejiji and >Enugu. The abundance of quartz in the clay results in its gritty feel.

The high percentage of kaolinite obtained (Tables 4.2 and 4.3) a suggest continental type clay deposits (Parham, 1966).

The average liquid limit values for all the invesigated clay deposits were less than <100% (see appendix 2), this classified the clay as inorganic of low compressibility (Smith, 1978).

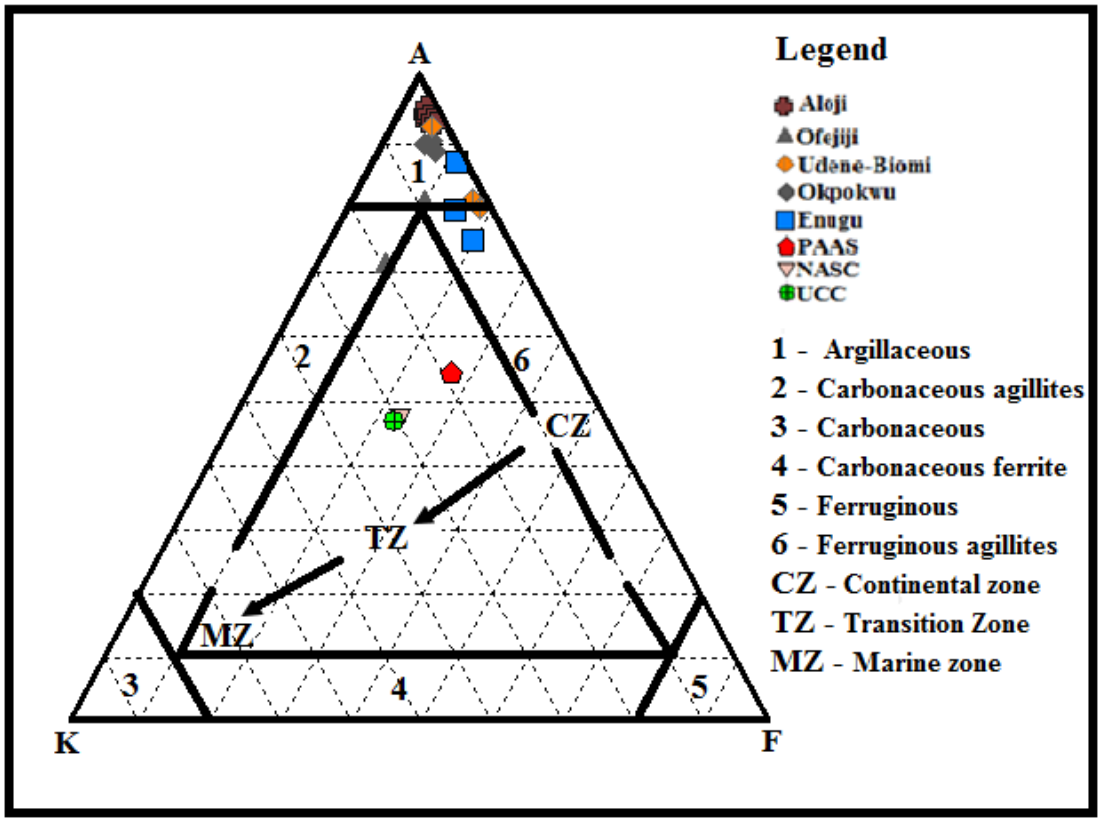

Fig. 4.32. Al_2O_3 - (K_2O+CaO+MgO) - (Fe_2O_3+MgO) (AKF) ternary diagram showing the classification of clay deposits in Mamu/Ajali and Enugu/Nkporo Formations, Lower Benue Trough (After Herron, 1988).

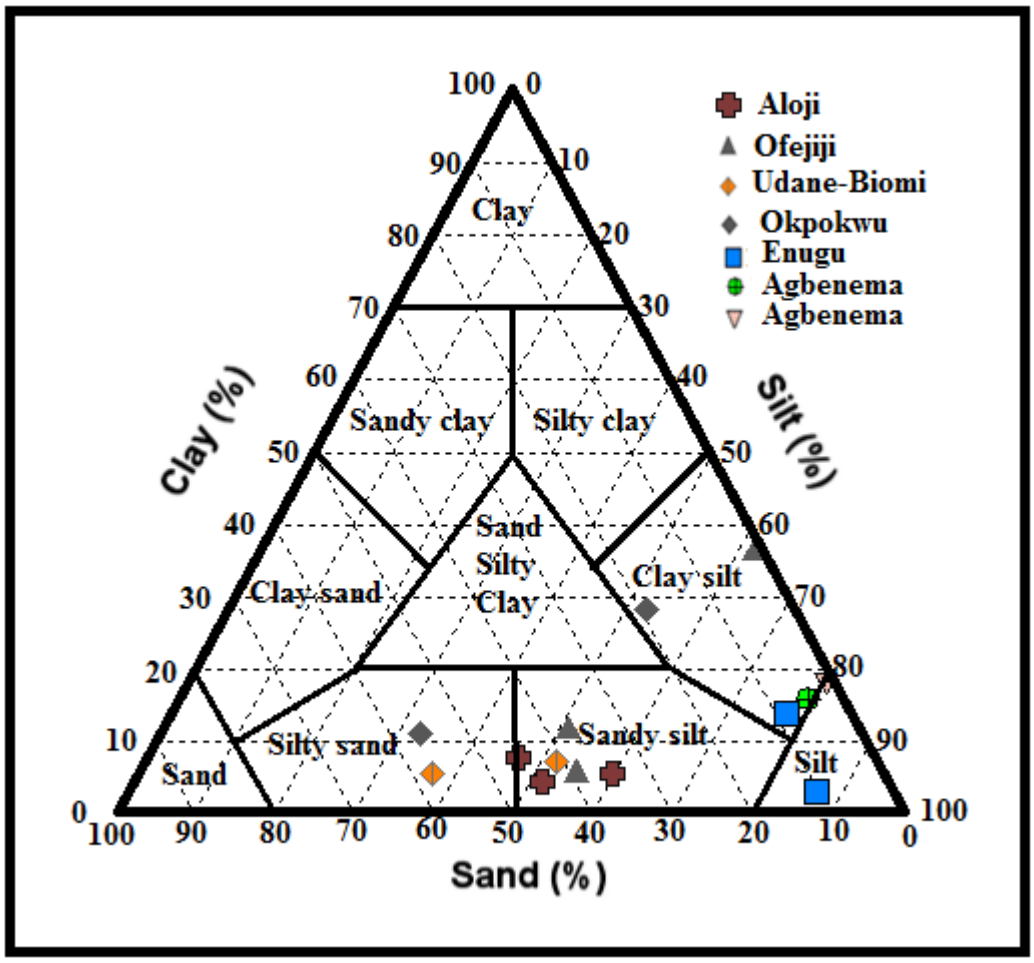

Fig. 4.33. Textural classification of the clay samples from different locations within the Lower Benue Trough, Nigeria (After Shepard, 1954).

4.4.5 Paleo-weathering indices and Maturity of the clay deposits

The Chemical Index of Alteration (CIA) and Plagioclase Index of Alteration (PIA) are the most frequently used indices for quantitative assessment of a precursor's degree of chemical weathering (Nesbitt and Young, 1982 ; Fedo et al., 1995). This provides an indication of the source region's degree of weathering. Another index that is also used is the Chemical Index of Weathering (CIW), suggested by Harnois (1988). The raw clay CIA ranged from 83.07 to 99.02 %, the PIA from 98.97 to 99.78 % and the CIW from 99.17 to 99.90 % (Tables 4.9 and 4.10) indicating intense weathering of the precursors as shown in Table 4.10. The CIA, PIA and CIW values of the fine (<2μm) clay fractions ranged (88.30 – 99.10 %), (94.31 – 99.6 %) and (98.92 – 99.34 %), respectively (Tables 4.11 and 4.12) indicating that the processing of the clay fraction did not adversely affect the result of the weathering indices but indicates a more felsic source for all the investigated clay samples (Nesbitt *et al.*, 1980; Figs. 4.34 and 4.35). The Results for raw and fine fractions are higher than the 70% recommended by McLennan (1993) and Fedo *et al.* (1995) as the minimum value for sediments derived from high chemical weathering process.

On the Al_2O_3 - ($CaO+Na_2O$) - K_2O (A-CN-K) diagrams of Nesbitt and Young (1996) and Nesbitt *et al*. (1996), all the sediments plot at the Al_2O_3 peak showing intense weathering with chemical and textural sediment maturity as highlighted in the CIA, PIA, and CIW values of the clays. (Figs. 4.34 and 4.35). The high Al_2O_3 of most of the samples could be attributed to the loss of CaO, Na_2O, and K_2O during weathering from the felsic parent rocks, as well as, during transportation of the materials in suspension and colloids. The diagrams showed clearly that the clay samples in the study area are monotonously rich in quartz-kaolinite compared to PAAS, NASC and UCC samples with higher labiles as shown in Fig. 4.34 and 4.35.

This observations support Wronkiewicz and Condie's (1987) work, which showed that Ca, Na, and Sr are easily leached during chemical weathering and that the amount lost is proportional to the degree of weathering.

Table 4.9. Weathering indices for the investigated raw clay samples.

Samples→	AL	AL1.1	AL1.2	AL1.3	AL2.1	AL2.2	AL2.3	AL2.4	AL2.5	OF 2.1	OF2.2
CIW	99.80	99.84	99.81	99.87	99.80	99.73	99.77	99.70	99.72	99.68	99.85
CIA	98.82	99.79	98.50	98.45	99.14	99.19	98.98	99.11	99.18	99.06	91.17
PIA	99.81	99.84	99.81	99.87	99.81	99.73	99.77	99.70	99.72	98.53	99.49
Th/U	5.12	4.84	4.29	4.89	6.35	5.67	5.72	5.00	5.76	3.51	3.73

Samples→	AG2.1	Ud.1.1	Ud.1.2	Ud.1.3	OK1.1	OK1.2	OK1.1.3	EN4.1	EN4.2	EN4.3
CIW	99.17	99.74	99.60	99.72	99.91	99.90	99.91	99.49	99.69	99.34
CIA	83.07	98.64	98.27	98.78	96.89	95.98	96.89	89.96	94.44	94.32
PIA	98.97	99.75	99.60	99.72	99.91	99.89	99.91	99.49	99.67	99.31
Th/U	4.70	4.83	3.15	4.26	4.05	3.83	4.05	3.97	5.35	4.18

The CIA= Chemical index of Alteration (100[Al_2O_3/ (Al_2O_3+CaO+Na_2O+K_2O)])

The PIA= Plagioclase Index of Alteration (100[(Al_2O_3-K_2O) / (Al_2O_3+CaO+Na_2O-K_2O])

The CIW=100 Chemical Index of Weathering ([Al_2O_3/ (Al_2O_3+CaO+Na_2O)])

Mamu/Ajali Fomation samples:

Aloji - AL, AL1.1, AL1.2, AL1.3, AL2.1, AL2.2, AL2.3, AL2.4, AL2.5.

Ofejiji - OF2.1, OF2.2.

Agbenema - AG2.1.

UdaneBiomi - Ud1.1, Ud1.2 and Ud1.3

Okpokwu - OK1.1, OK1.2, OK1.3.

Enugu/Nkporo Formation samples

Enugu - EN4.1, EN4.2 and EN4.3.

Table 4.10. Calculated degree of weathering for the investigated raw clay samples compared with standards.

Indices	Standard	Aloji	Ofejiji	Udane-Biomi	Okpokwu	Enugu	Agbenema
CIA Range	Intense weathering 75-100	99.11-99.79	91.17-99.06	98.27-98.78	95.98-97.46	89.96-94.44	--------
Mean	--	99.02	95.12	98.56	96.78	92.91	83.07
Median	--						
PIA Range	Intense weathering 75-100	99.70-99.87	98.53-99.49	99.60-99.75	99.89-99.91	99.31-99.67	------
Mean	--	99.78	99.01	99.69	99.90	99.49	98.97
Median	--						
CIW Range	Intense weathering 75-100	99.72-99.87	99.85-99.68	99.60-99.70	99.90-99.91	99.34-99.69	------
Mean	--	99.78	99.77	99.67	99.90	99.51	99.17
Median	--	--	--	--	--	--	--

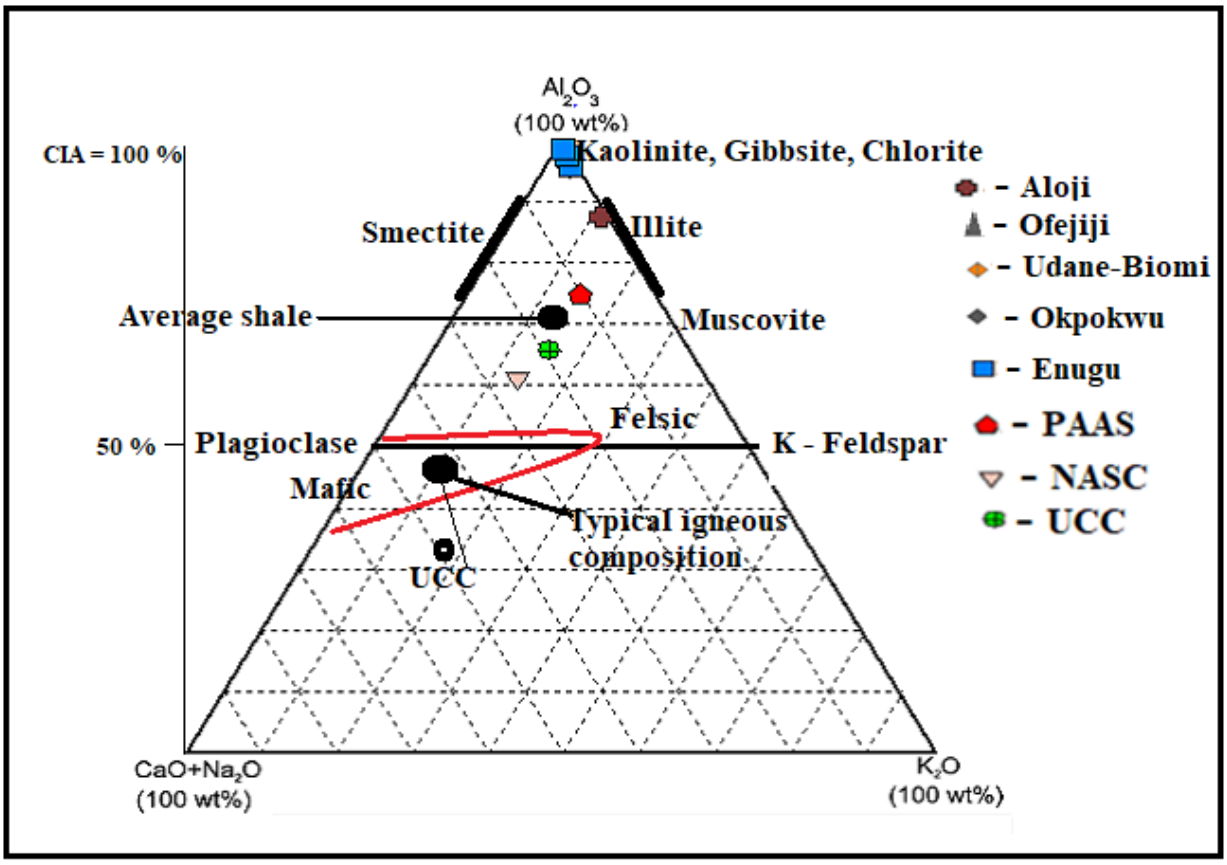

Fig. 4.34. Al_2O_3 - ($CaO+Na_2O$) - K_2O plot showing weathering trend for the raw clay samples From Mamu/Ajali and Enugu Nkporo Formations, Lower Benue Trough, Nigeria (after Nesbitt and Young, 1996; Nesbitt *et al.*, 1996).

Table 4.11. Weathering indices for the fine (<2μm) clay samples investigated.

.

Sample No →	Al.1.1	Al. 1.2	Al.1.3	OF2.4	AG1.1	AG1.2	Ud.1.1	Ud.1.3
CIW	99.73	99.18	99.11	99.15	99.13	98.71	99.66	99.63
CIA	98.85	97.42	87.83	88.30	95.34	88.77	98.53	98.42
PIA	99.82	99.17	98.98	98.71	99.10	89.52	99.66	99.63
Th/U	5.74	3.81	3.73	3.27	4.28	4.38	3.41	3.67

Sample No →	OT1.1	OT2.2	OK1.1	EN4.2	EN4.3	EN2.1
CIW	99.44	99.49	99.10	99.76	9973	99.44
CIA	97.91	96.43	96.23	99.92	99.10	96.34
PIA	99.43	99.42	99.07	99.75	99.82	99.42
Th/U	4.63	4.21	3.45	3.64	4.54	5.48

The CIA= Chemical index of Alteration (100[Al_2O_3/ (Al_2O_3+CaO+Na_2O+K_2O)])

The PIA= Plagioclase Index of Alteration (100[(Al_2O_3-K_2O) / (Al_2O_3+CaO+Na_2O-K_2O])

The CIW=100 Chemical Index of Weathering ([Al_2O_3/ (Al_2O_3+CaO+Na_2O)])

Mamu/Ajali Formation samples:

Aloji - AL1.1, AL1.2 and AL1.3.

Ofejiji – OF2.4.

Agbenema - AG1.1 and AG1.2.

Udane-Biomi - Ud1.1 and Ud1.3.

Oturkpo - OT1.1 and OT2.2.

Okpokwu - OK1.1.

Enugu/Nkporo Formation samples

Enugu - EN2.1, EN4.2, EN4.3.

Table 4.12. Calculated degree of weathering for the fine (<2μm) clay fraction investigated compared with standards.

Indices	Standard	Aloji	Agbenema	Udane-Biomi	Oturkpo	Enugu	Ofejiji	Okpokwu
CIA Range	Intense weathering 75-100	87.83-98.85	88.77-95.34	98.42-98.53	96.23-96.43	96.34-99.92	--------	-------
Mean	--	94.70	92.06	98.48	96.33	98.45	88.30	99.10
Median	--							
PIA Range	Intense weathering 75-100	98.98-99.82	89.52-99.10	99.63-99.66	99.42-99.43	99.42-99.82	------	------
Mean	--	99.32	94.31	99.65	99.43	99.66	98.71	96.23
Median	--							
CIW Range	Intense weathering 75-100	99.11-99.73	98.71-99.13	99.63-99.66	99.10-99.49	99.44-99.76	------	------
Mean	--	99.34	98.92	99.65	99.30	99.64	99.15	99.07
Median	--	--	--	--	--	--	--	

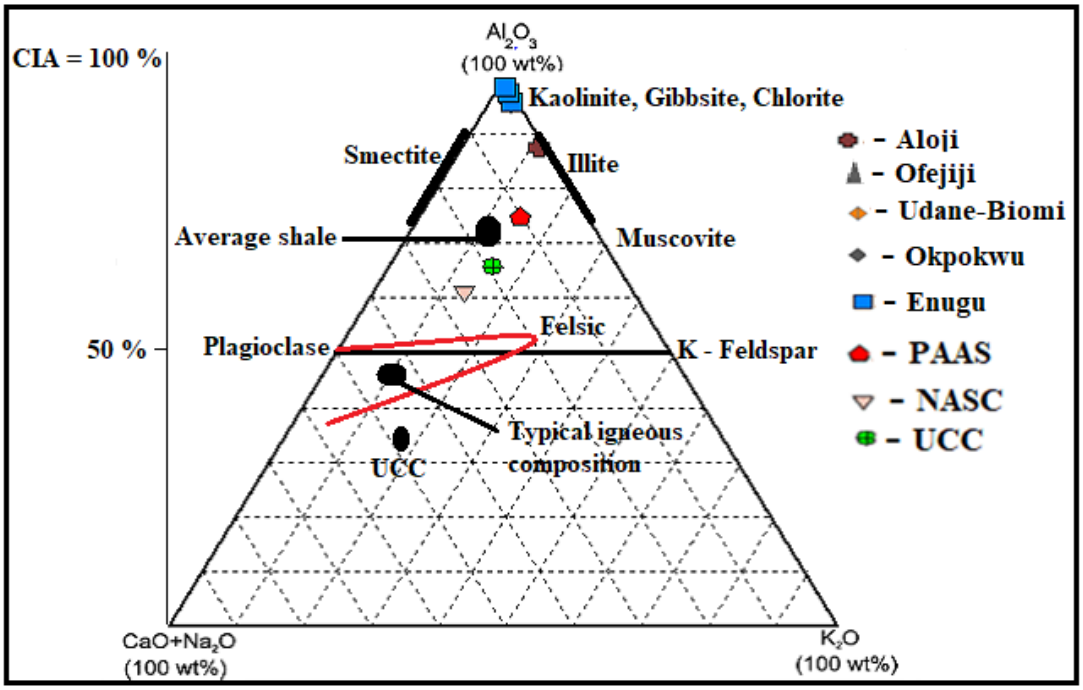

Fig. 4.35. Al_2O_3 - ($CaO+Na_2O$) - K_2O plot showing weathering trend for the fine (<2µm) clay samples from Mamu/Ajali and Enugu Nkporo Formations, Lower Benue Trough, Nigeria (after Nesbitt and Young, 1996; Nesbitt *et al*. 1996).

The plot of SiO_2 vs (Al_2O_3+K_2O+Na_2O) proposed by Suttner and Dutta, 1986 (Fig. 4.36) was used to determine the maturity of the clay deposits and the paleoclimatic condition. The results showed that the the study area's clay was generated under a semi-humid condition.

The raw clay sample Th/U ratios ranged between 3.15 and 6.35 while that of the fine fraction vary from 3.27 to 5.74 in both the Mamu/Ajali and Enugu/Nkporo Formation clays. The Th/U ratios are generally higher than 4.00 except in Ofejiji (3.51 and 3.73) and Udane-Biomi (3.15) for the raw samples (Table 4.11), and Aloji (3.41-3.81), Ofejiji (3.27), Udane-Biomi (3.67), Okpokwu (3.45) and Enugu (3.64) in the fine fractions. This indicates that the clays were generated under an intense weathering condition (McLennan *et al.,* 1993). Both Th and U during weathering are relatively immobile. The Th/U ratio is typically between 3.5 – 4.0 in most upper continental rocks. Values above 4.0 in sedimentary rocks may indicate intense weathering in the source areas or sedimentary recycling (Fig. 4.37).

4.4.6.1 Trace element geochemistry of the raw clay samples

The concentration of trace elements in the deposits of raw clay investigated from Aloji, Ofejiji, Agbenema, Udane-Biomi, Okpokwu of Mamu/Ajali Formation and Enugu of Enugu/Mamu Formation is presented in Table 4.13.

The Ni content ranged between 0.1 and 0.4 ppm in samples from the Mamu/Ajali Formation while Enugu/Nkporo Formation varied between 0.1 and 0.7 ppm (Table 4.13). Nickel indicates ultrabasic and basic source rocks when present in substantial amounts (Shapiro and Breger, 1968). Turekian (1978) claimed that, Ni is abundant in deep marine sediments (> 300 ppm) but much less in coastal sediments (<39 ppm). The low Ni content (<1) indicated that it is associated with continental materials in this present investigation. There is a weak positive correlation between Nickel with Al_2O_3 and TiO_2 (Table 4.14). This indicates terrigenous nature of the clay deposit.

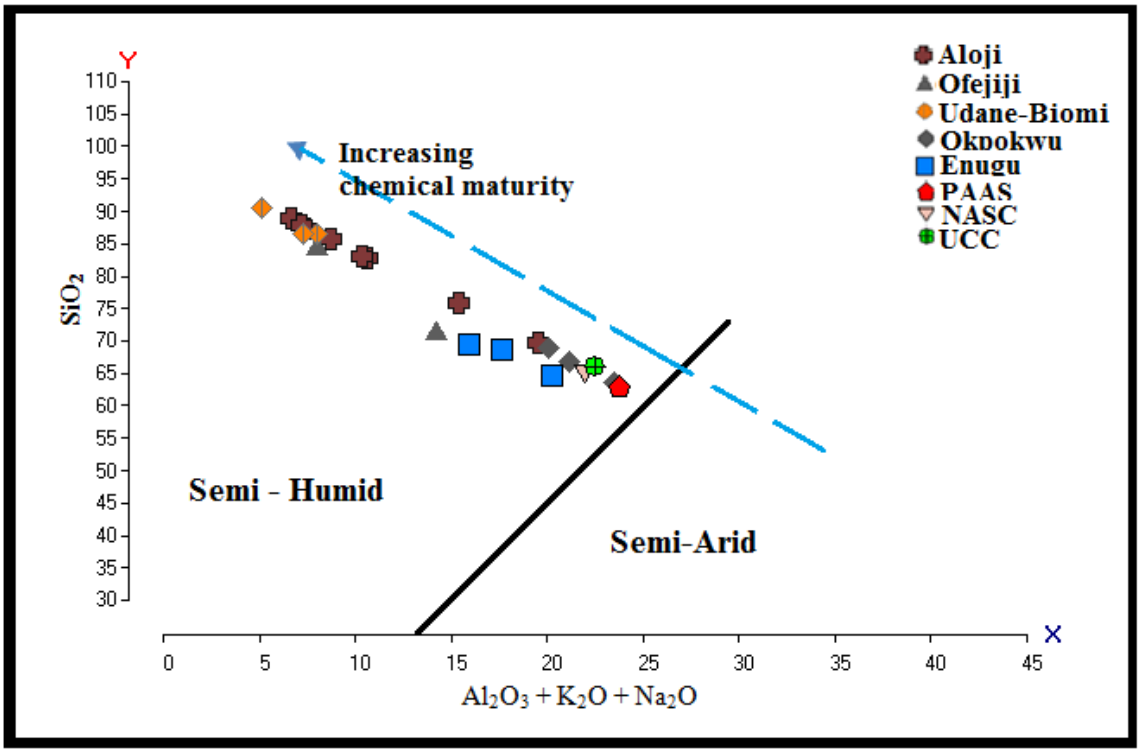

Fig. 4.36. The SiO_2 versus (Al_2O_3+K_2O+Na_2O) for clay deposits from Mamu/Ajali and Enugu/Nkporo Formation within the Lower Benue Trough showing trend of Maturity (After Suttner and Dutta, 1986).

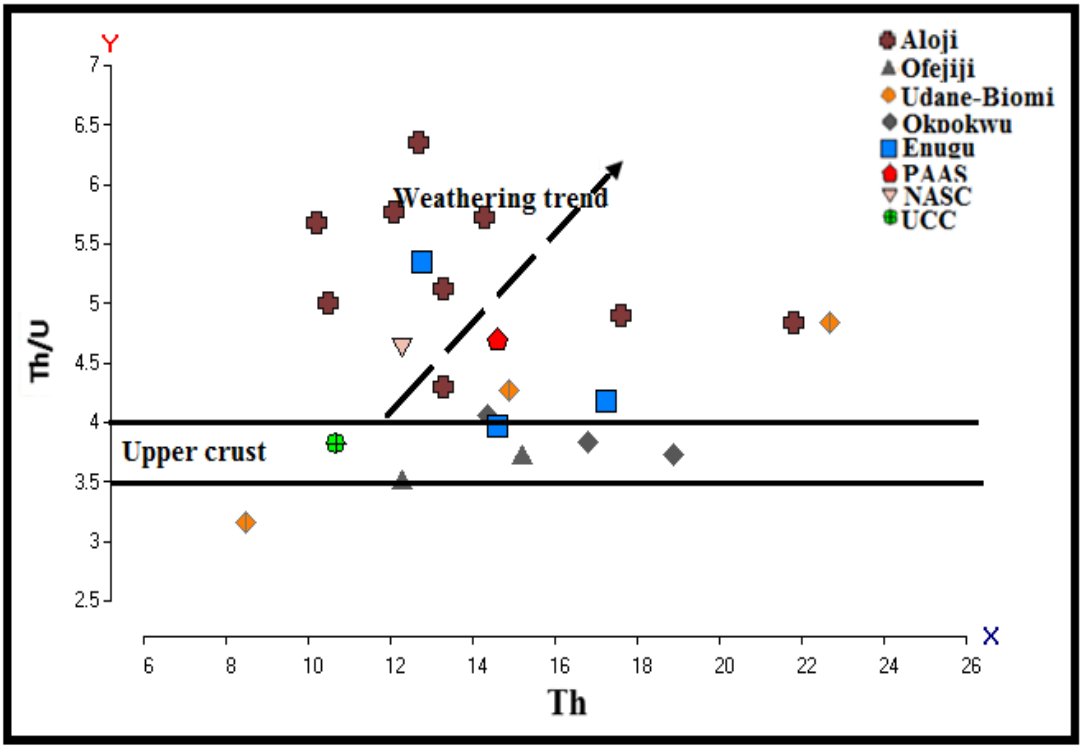

Fig. 4.37. Th/U vs Th plot for the investigated raw clay deposits. (After McLennan *et al*., 1993).

Cobalt content varied from 0.5 to 7.6 ppm in the raw clay samples of Mamu/Ajali Formation but from 1.2 to 1.8 ppm in the Enugu/Nkporo Formation. This implies that in clay minerals, cobalt is not significantly adsorbed or integrated. Cobalt is commonly concentrated in ferric oxides or ferric hydroxides in clays (Goldschmidt, 1958, Ismael, 1996).

Strontium in the raw clay samples varied from 14.9 to 235.4 ppm in the raw clay samples from Mamu/Ajali Formation as against 19.2 to 30.1 ppm in the Enugu/Nkporo raw clay samples (Table 4.13). Strontium content in the Ofejiji clay samples (116.2 and 235.4 ppm; Table 4.13) were higher compared to all other samples from Aloji, Agbenema, Udane-Biomi, Okpokwu and Enugu areas. The Ofejiji clay deposits is underlain by an organic-rich shale sequence capable of trapping Sr.

The Ba content in the Ofejiji clay samples varied from 895 to 1375 ppm while those of the other clays ranged from 48 to 197 ppm indicating incipient weathering of the Ofejiji clay. It also revealed that the transported materials are close to the source, hence the retention of it in the feldspars. Plagioclase and K-feldspar host the bulk of Sr and Ba (Liu *et al.,* 2009). Plagioclase weathers rapidly relative to K-feldspar, and in a weathering setting Sr is more mobile than Ba. According to Cullers (1988) and Liu *et al*. (2009) Ba depletion is ascribed to gradual destruction of feldspars with loss of Ba during the process of weathering and erosion. The Sr and Ba's strong positive correlation (r = 0.9; Table 4.14) showed this.

Zinc content for all the raw clay samples from both formations were generally <3.0 ppm except samples from Ofejiji (4.0 and 23 ppm; Table 4.12) of Mamu/Ajali Formation. In the raw clay samples of both formation, copper also varied from 0.1 to 12.6 ppm (Table 4.12). The average Zn and Cu values are lower than the average PAAS (50 ppm) and UCC (25 ppm) values (Taylor and McLennan, 1985), suggesting that both zinc and copper are associated with organic matter in clay minerals and not mineralization.

Table 4.13. Trace element composition (ppm) for the raw clay samples investigated.

Sample No → Elements ↓	AL	AL1.1	AL1.2	AL1.3	AL2.1	AL2.2	AL2.3	AL2.4	AL2.5	OF2.1	OF2.22
As	n.d	n.d	n.d	n.d	n.d	n.d	n.d	n.d	n.d	n.d	n.d
Ba	77.0	157.0	95.0	127.0	62.0	56.0	68.0	54.0	48.0	895.0	1375.0
Co	1.2	2.1	1.1	1.5	0.8	0.7	0.8	0.5	0.9	1.0	7.6
Cu	3.1	12.6	6.8	5.6	0.3	0.3	0.3	0.3	0.1	2.4	10.1
Ga	14.8	24.9	13.5	19.5	13.5	8.9	10.3	8.9	8.2	6.1	17.8
Hf	17.5	17.1	15.8	15.1	18.4	15.1	21.9	19.0	19.7	32.2	17.7
Nb	18.5	32.1	18.4	24.9	16.3	14.1	19.9	13.5	13.3	15.7	25.9
Ni	0.1	0.3	0.1	0.3	0.1	0.1	0.1	0.1	0.1	0.9	0.6
Mo	0.1	0.1	0.1	0.1	0.1	0.1	0.1	0.1	0.1	0.1	0.8
Pb	3.2	8.2	5.3	5.6	0.9	1.0	1.2	1.2	1.9	8.5	13.5
Rb	4.7	15.4	6.1	9.9	3.0	2.2	3.0	1.5	1.7	39.1	42.0
Sr	21.2	36.0	18.9	26.0	15.1	19.2	21.2	13.6	14.9	116.2	235.4
Th	13.3	21.8	13.3	17.6	12.7	10.2	14.3	10.5	12.1	12.3	15.3
U	2.6	4.5	3.1	3.6	2.0	1.8	2.5	2.1	2.1	3.5	4.1
V	53.0	89.0	52.0	90.0	53.0	42	45	38	38	28.0	68.0
Y	26.9.0	53.5	28.3	33.4	17.9	14.8	18.1	13.9	17.7	41.1	41.2
Zn	1.0	1.0	1.0	1.0	1.0	1.0	1.0	1.0	1.0	4.0	23.0
Zr	731.4	686.5	678.0	701.1	751.1	609.2	869.1	761.5	781.0	1245.0	819.4

Mamu/Ajali Formation samples:

Aloji - AL1.1, AL1.2, AL1.3, AL2.1, AL2.2, AL2.2, AL2.3, AL2.4 and AL2.5.

Ofejiji – OF2.1 and OF2.2

Table 4.13. Cont...

	UD1.1	UD1.2	UD1.3	OK1.1	OK1.2	OK1.3	EN4.1	EN4.2	EN4.3
As	n.d	0.6	0.7	n.d	n.d	n.d	n.d	n.d	n.d
Ba	137.0	84.0	80.0	197.0	177.0	138.0	129.0	133.0	89.7
Co	1.1	0.5	1.4	2.1	4.2	5.1	1.2	1.5	1.8
Cu	0.7	3.6	3.9	3.7	4.6	7.8	3.6	7.3	3.3
Ga	11.2	8.8	10.4	20.8	18.9	13.5	17.5	14.5	9.9
Hf	50.7	15.2	28.8	3.5	6.1	11.8	5.1	6.4	8.1
Nb	23.4	12.4	17.8	18.5	22.1	17.4	22.9	17.3	14.1
Ni	0.1	0.1	0.2	0.1	0.3	0.1	0.7	1.1	0.1
Mo	0.1	0.1	0.2	0.1	0.1	0.1	0.2	0.1	0.1
Pb	2.1	4.0	5.6	3.4	7.2	3.3	4.6	2.9	1.0
Rb	4.10	2.90	4.10	5.71	4.64	6.10	9.9	5.2	3.2
Sr	59.6	34.3	27.8	35.3	33.7	27.9	28.7	30.1	19.2
Th	22.7	8.5	14.9	14.3	16.8	18.8	14.6	12.7	17.2
U	4.7	2.7	3.5	3.5	4.3	5.0	3.6	2.3	4.1
V	47.0	39.0	55.0	72.0	86.1	57.3	88.0	55.0	42.0
Y	46.4	17.0	23.9	29.6	43.5	33.3	37.4	27.9	16.8
Zn	1.0	1.0	2.0	1.5	2.0	2.8	1.2	3.0	1.0
Zr	2180.0	651.5	1142.0	658.4	786.5	638.5	578.1	584.1	609.2

Mamu/Ajali Formation samples:
Udane-Biomi - UD1.1, UD1.2 and UD1.3.
Okpokwu - OK1.1.

Enugu/Nkporo Formation samples
Enugu – EN4.1, EN4.2, EN4.3.

Table 4.14. Correlation coefficients of major and trace elements for the raw clay samples investigated.

	Al_2O_3	Ba	Co	La	Ni	SiO_2	Sr	Th	TiO_2	V	Zr
Al_2O_3	1										
Ba	0.1276	1									
Co	**0.4260**	0.7878	1								
La	0.7666	0.4480	0.6867	1							
Ni	0.2456	0.8304	0.9706	0.5586	1						
SiO_2	-0.9248	-0.4888	-0.6799	-0.8316	-0.5317	1					
Sr	0.1460	0.9694	0.8727	0.5569	0.9093	-0.493	1				
Th	0.6302	0.1208	0.2404	0.746	0.057	-0.598	0.1778	1			
TiO_2	**0.8272**	0.2483	0.3696	0.8117	0.1821	-0.8178	0.2631	0.9207	1		
V	0.8414	-0.1651	0.6131	-0.2949	0.1468	-0.8845	-0.2291	0.7174	0.6282	1	
Zr	-0.2395	0.1778	-0.0420	0.1957	-0.0591	0.1493	0.2223	0.5785	0.2906	-0.8022	1

Zirconium dominates the trace elemental composition, it ranges from 701 to 2180 ppm in the raw clay samples of Mamu/Ajali Formation while in the Enugu/Nkporo, it ranged between 578.1 and 609.2 ppm. This substantiates its detrital nature, confirming the high quartz and silica contents in the obtained mineralogical and major oxides data. Zirconium shows a very weak positive correlation with TiO_2 (r = 0.29; Table 4.14 The very low correlation between Zr and TiO2 represents their igneous felsic origin (Hayashi *et al.*, 1997).

The presence of vanadium, 28 to 90 ppm in Mamu/Ajali raw clay samples and 42 to 88 ppm in Enugu/Nkporo Formation suggests the oxidation and weathering of felsic igneous rocks and subsequent concentration in organic matter-bearing clay (Riley and Saxby, 1983). The strong positive correlation between V and both Al_2O_3 and TiO_2 (r = 0.84 and 0.63; Table 4.14) suggest that V is frequently hosted in sediments rich in organic matter (Stow and Atkin, 1987). The low value of transitional metal Co (<1 ppm) and Ni (<8 ppm) in raw clay samples from both Mamu/Ajali and Enugu/Nkporo Formations (Table 4.12) suggest the absence of mafic components in the source (Liu *et al*., 2009).

Th content varied from 8.5 to 22.7 ppm in the raw clay samples of Mamu/Ajali Formation while Enugu/Nkporo Formation varied from 12.7 to 19.2 ppm (Table 4.12) suggesting a mixture of sand and clayey materials since sand samples are relatively enriched in Th contents than clayey samples (Abou El-Anwar and Samy, 2013). The positive correlation between Th and both of Zr and SiO_2 (r = 0.58 and 0.92; Table 4.14) further supports this.

Fig. 4.38 shows distribution of selected trace elements normalized to the average UCC values of Taylor and McLennan (1981). They show similar patterns but different abundances because of the dilution effect of quartz (Yang and Youn, 2007). This favours a weathered crystalline granitic source terrain as Zr is enriched relative to UCC, reflecting the abundance occurrence of felsic components in the source rocks area (Fig. 4.38). Sr and Ba are relatively lower than the UCC values. These elements are susceptible to mobility during weathering processes because of their high hydration energy (Cullers *et al.* 1988) (Fig. 4.26 and 4.27). Th composition in the

investigated samples is more or less similar to that in the UCC. This may be due to the effective mixing of sediment during weathering, transport and deposition (Fig.4.26 and 4.28). Th, U and Hf were also enriched.

From above observations, sediments poor in clay minerals and rich in quartz grains are defined by the smaller values except for Zr, which is ascribed to dilution by quartz and the trace element composition confirms the influence of oxidizing climatic conditions. The observed changes in trace elements is consistent with the mineralogical data.

4.4.6.2 Trace element geochemistry of the fine (<2µm) clay samples

The result of the trace elements in the fine (<2µm) clay fractions from Aloji, Ofejiji, Agbenema, Udane-Biomi, Oturkpa, Okpokwu of Mamu/Ajali Formation and Enugu of Enugu/Nkporo Formation is presented in Table 4.15.

The Sr value ranged between 29.3 and 223.3 ppm for the fine (<2µm) clay fractions from Mamu/Ajali Formation as against 13.6 to 235.4 ppm in the raw while Enugu/Nkporo varied from 37.9 to 91.6 ppm. The Ba varied from 129 to 913 ppm in the fine fraction of the Mamu/Ajali Formation as against 48 – 1375 ppm in the raw clay samples but varied from 148 to 239 ppm in the fine fraction of the Enugu/Nkporo Formation as against 89 to 133 ppm. This confirms that Sr is more mobile than Ba (Roy *et al.,* 2008), and that is evident from the weak positive correlation between Sr and Ba (r = 0.38 ; Table 4.16). In the fine clay fraction of Mamu/Ajali Formation, Zn varied between 4 and 58 ppm as against 1 to 23 ppm in the raw clay samples while in Enugu/Nkporo formation, it ranged between 3 to 48 ppm as against 1 to 3 ppm in the raw samples. This suggests an adsorption of Zn onto the clay layers. Zr was less than 900 ppm in both samples from Mamu/Ajali and Enugu/Nkporo Formations against 2180 ppm in the raw clay samples, thus corroborating the XRD data suggesting a quartz-rich kaolinite mineral assemblage.

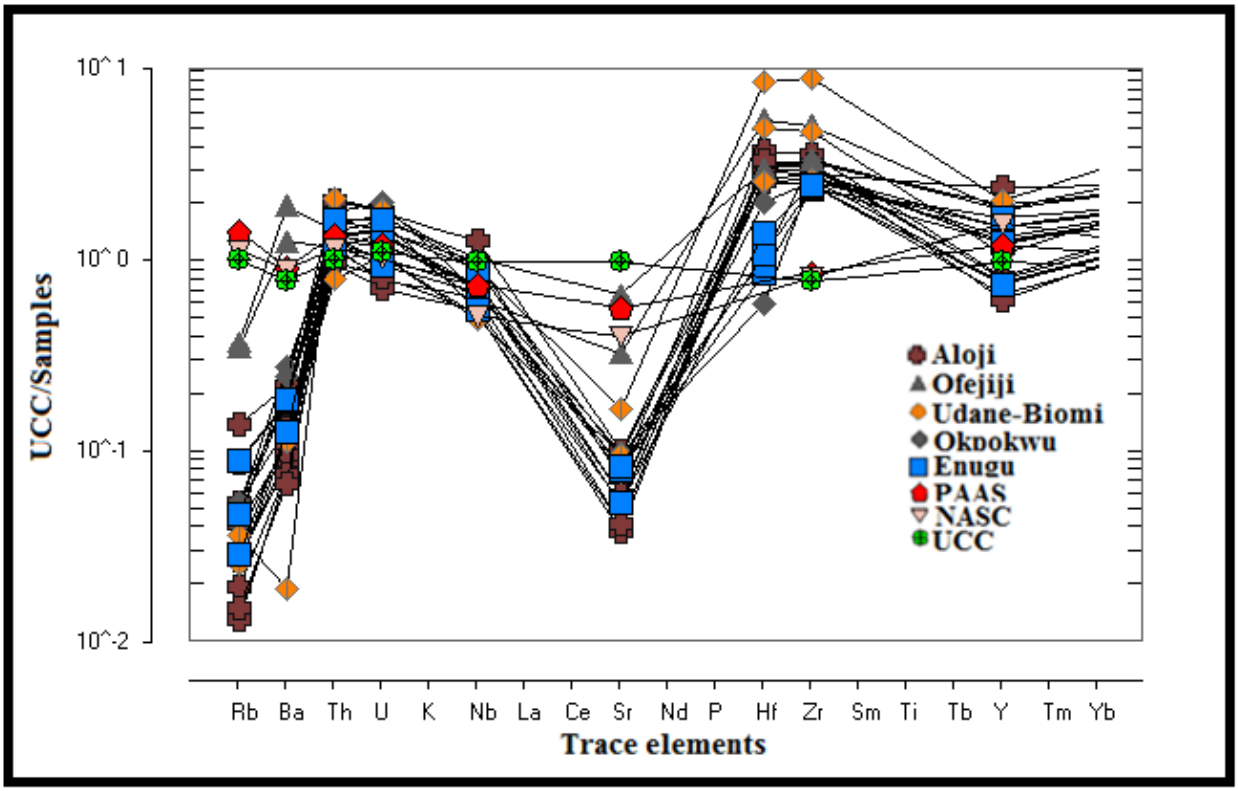

Fig. 4.38. UCC normalized trace elements of raw clay samples from Mamu/Ajali and Enugu/ Nkporo Formation, Lower Benue Trough, Nigeria (After Taylor and Mclennan, 1981).

The recorded low values of Th (16 to 27.5 ppm and 20 to 24.1 ppm; Table 4.15) in the fine clay fractions from both Mamu/Ajali and Enugu/Nkporo Formations, respectively as against the higher values (10.2 to 86.1 ppm and 12.7 to 17.2 ppm) in the raw clay samples, suggest the non-association of Th with clayey materials (Abou El-Anwar and Samy, 2013). The negative correlation between Th and both Zr and SiO_2 (r = -0.34 and -0.60 ; Table 4.16) supported this.

Vanadium composition was higher (62 to 134 ppm and 97 to 143 ppm; Table 4.16) in fine fraction of both formations compared to the raw clay samples (38 to 90 ppm and 42 to 88 ppm). These high values with the strong positive correlation of V with Al_2O_3 and TiO_2 (r = 0.8 and 0.6 ; Table 4.16) further substantiate the existence of organic matter incoperated more in the fine clay fraction (Stow and Atkin, 1987).

The raw clay samples are rich in sandy materials compared to the fine (<2µm) clay samples (Tables 4.13 and 4.15), thus, the low trace and major elements in the raw samples relative to fine (<2µm) clay samples (Tables 4.13 and 4.15) is attributed to dilution by quartz. The abundance of Zr in the samples relative to Th (Tables 4.13 and 4.15) shows their derivation from a felsic source (Feng and Kerrich, 1990).

The fractions of fine clay were normalized to the average values of Upper Continental Crust (UCC) (Taylor and McLennan, 1981) (Fig. 4.40) and similar to the raw clay samples (Fig. 4.38), Th, U, Hf and Zr were enriched but depleted Rb, Ba and Sr relative to UCC.

The composition of the clays studied suggests that they are primarily related to granitic rocks. However, the deviation recorded between the raw and fine (<2µm) samples (Tables 4.13 and 4.15) is most probably due to textural changes as well as mineralogical sorting. Thus from the above discussion we can infer that the investigated clay deposits are derived from granitic source, under considerable condition of sediment recycling.

Table 4.15. Trace element compositions (ppm) for the fine (<2μm) clay samples investigated.

Sample No → Elements ↓	AL1.1	AL1.2	AL1.3	OF2.4	AG1.1	AG1.2	UD1.1	UD1.3
As	0.80	n.d	n.d	nd	Nd	Nd	n.d	1.9
Ba	170.0	129.0	652.0	680.0	585.0	913.0	425.0	184.0
Co	3.1	2.6	2.6	3.3	13.9	4.0	4.0	13.8
Cu	43.6	19.5	12.4	23.2	60.6	36.8	30.6	38.1
Ga	24.8	14.5	17.0	19.5	37.2	24.6	18.2	27.7
Hf	8.7	18.2	20.5	16.9	8.6	14.2	22.7	17.5
Nb	30.3	22.9	30.1	23.1	32.3	29.0	23.2	26.0
Ni	87.0	29.0	40.0	95.0	181.0	72.0	122.3	160.5
Mo	1.3	0.7	1.0	2.7	2.4	2.0	3.5	2.3
Pb	7.5	8.9	8.4	9.3	14.8	10.6	4.6	11.0
Rb	14.0	8.3	56.0	62.3	56.1	62.5	7.9	12.7
Sr	37.1	29.3	79.8	94.9	90.6	95.4	223.3	75.1
Th	20.1	16.0	19.0	14.7	24.8	17.5	18.4	27.5
U	3.5	4.2	5.1	4.5	5.8	4.0	5.4	7.5
V	107.0	62.0	69.0	73.0	129.0	106.0	63.0	121.0
Zn	16.0	4.0	4.0	11.0	58.0	18.0	16.0	18.0
Zr	301.7	675.7	762.0	604.6	287.0	482.7	863.6	624.8

Mamu/Ajali Formation samples:
Aloji – AL1.1, AL1.2 and AL1.3.
Ofejiji – OF2.4.
Agbenema – AG1.1 and AG1.2.
Udane-Biomi - UD1.1, UD1.2 and UD1.3.

Table 4.15. Cont...

Sample No → Elements ↓	OT1.1	OT2.2	OK1.1	EN2.1	EN4.2	EN4.3
As	nd	1.7	nd	nd	0.6	nd
Ba	233.0	322.0	347.0	239.0	204.0	148.0
Co	4.5	3.5	9.2	8.2	3.5	2.1
Cu	34.4	24.3	30.6	29.7	14.1	60.6
Ga	38.7	26.2	35.0	33.4	30.8	21.3
Hf	5.5	12.3	8.2	9.6	8.1	17.2
Nb	26.6	28.3	34.9	35.9	31.5	27.2
Ni	49.0	80.0	71.0	78.0	78.0	186.0
Mo	0.4	1.6	0.4	1.0	1.1	3.2
Pb	18.8	14.3	30.6	29.7	16.8	7.8
Rb	32.4	26.7	58.9	31.3	21.6	6.7
Sr	60.7	72.7	125.0	37.9	85.0	91.6
Th	23.6	18.1	20.7	24.1	20.0	21.8
U	5.1	4.30	6.0	4.4	5.5	4.8
V	133.0	119.0	134.0	143.0	143.0	97.0
Zn	8.0	14.0	16.0	48.0	3.0	26.0
Zr	183.2	406.7	283.9	337.0	299.3	624.8

Mamu/Ajali samples:

Oturkpa - OT1.1 and OT2.2

Okpokwu - OK1.1.

Enugu/Nkporo Formation samples:
Enugu – EN2.1, EN4.2, EN4.3.

Table 4.16. Correlation coefficients of major and trace elements for the fine (<2μm) clay samples investigated.

	Al_2O_3	Ba	Co	La	Ni	SiO_2	Sr	Th	TiO_2	V	Zr
Al_2O_3	1										
Ba	-0.1874	1									
Co	0.6898	0.1056	1								
La	-0.3039	-0.3298	-0.3775	1							
Ni	-0.0356	0.0927	0.1779	0.4142	1						
SiO_2	-0.9785	0.0923	-0.7291	0.3141	-0.0175	1					
Sr	-0.1512	0.3889	0.0793	0.3863	0.3958	0.1105	1				
Th	0.5741	-0.2865	0.467	0.1022	0.4964	-0.6016	-0.0857	1			
TiO_2	0.4251	-0.0646	0.3576	-0.1251	0.0386	-0.4717	-0.1684	0.418	1		
V	0.8414	-0.1651	0.6131	-0.2949	0.1468	-0.8845	-0.2291	0.7174	0.6282	1	
Zr	-0.8533	0.2361	-0.548	0.402	0.2293	0.8548	0.4129	-0.3452	-0.4454	-0.8022	1

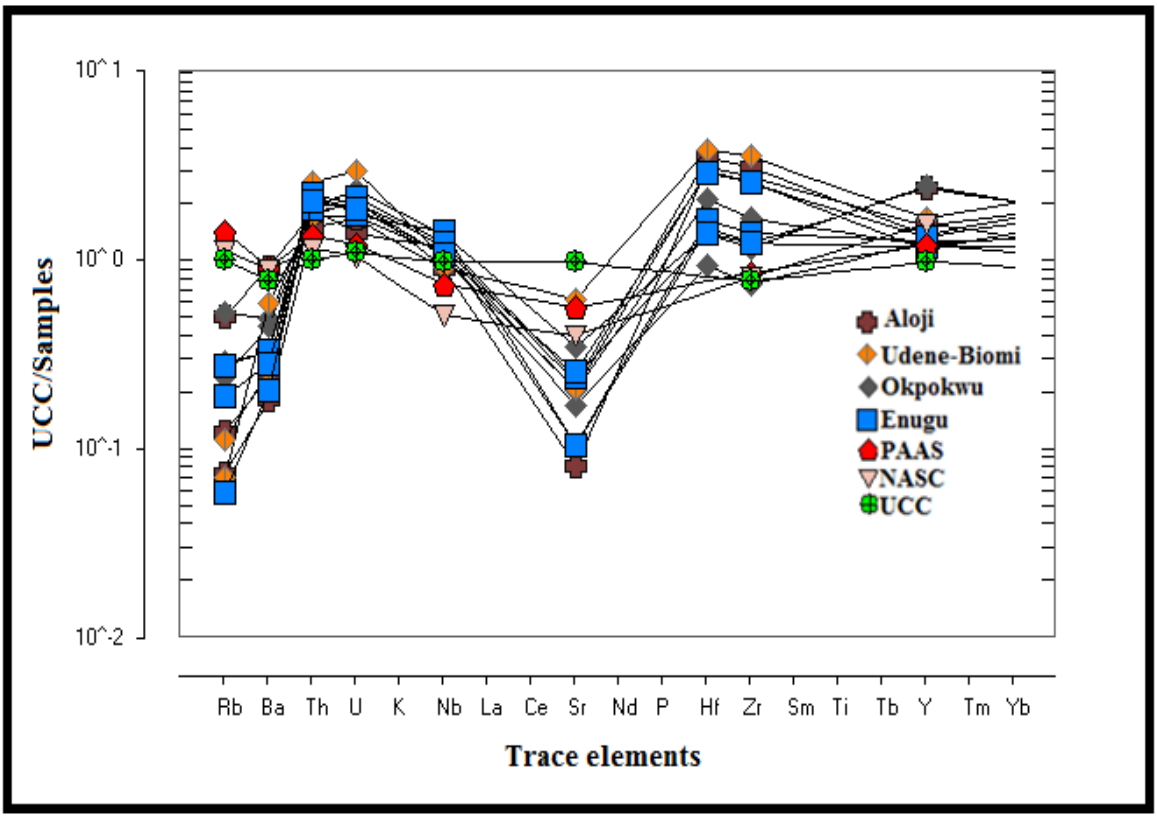

Fig. 4.39. UCC normalized of trace elements of the fine (<2μm) clay samples from the from Lower Benue Trough, Nigeria (After Taylor and Mclennan (1981).

4.4.7 Rare earth element geochemistry of both raw and fine (<2µm) clay fractions

Results for the rare earth elements for the raw and fine (<2µm) clay samples from Aloji, Agbenema, Udane-Biomi, Okpokwu of Mamu/Ajali Formation and Enugu from Enugu/Nkporo Formation within the Lower Benue Trough, Nigeria is summarized in Tables 4.17 and 4.18.

The raw clay and the fine (<2µm) samples had a characteristic negative Eu-anomalies with the raw clay samples varying from 0.55 to 1.10 for the Mamu/Ajali Formation samples and 0.33 to 0.58 in Enugu/Nkporo Formation while the fine (<2µm) samples ranged from 0.45 to 0.71 and 0.68 to 0.73 in Mamu/Ajali and Enugu/Nkporo Formations respectively. The chondrite-normalized La/Yb and Gd/Yb varied between 5.79 to 25.96 and 0.16 to 2.02 in the raw clay samples from the Mamu/Ajali Formation and 17.43 to 21.19 and 1.42 to 3.34 in the Enugu/Nkporo while the the fine (<2µm) samples in the Mamu/Ajali and Enugu Formations were from 9.51 to 30.10 and 1.20 to 2.18 and 9.05 to 20.99 and 1.38 to 2.18. Both samples are LREE enriched (Tables 4.17 and 4.18) with an almost flat HREE patterns (Figs. 4.40 and 4.42). For the studied clay samples, these features reveal granitic origin (McLennan *et al.*, 1993), in sedimentary rocks, anomaly of Eu is frequently deduced as inherited from igneous source rocks (McLennan and Taylor, 1991, Awwiller, 1994). The high value of ∑REE (242.87 to 611.16 and 268.78 to 403.71) recorded in the fine (<2µm) clay fractions as against the lower value of ∑REE (114.33 to 473.69 and 192.84 to 349.46) in the raw clay samples for both Mamu/Ajali and Enugu/Nkporo Formation confirm the effect of reduced dilution of the quartz as evident from the XRD data. Compared to the raw clay samples, the abundance of REE in the (< 2µm) clay fractions justifies an important study carried out by Cullers *et al.* (1987) on the effect of sedimentary categorization based on concentrations of REE whereby REEs are mostly represented in the fine (< 2µm) clay size samples relative to the raw clay samples.

Table 4.17. Rare earth element distribution for the raw clay samples investigated.

Sample No → Element ↓	AL	AL1.1	AL1.2	AL1.3	AL2.1	AL2.2	AL2.3	AL2.4	AL2.5	OF2.1	OF2.2
Ce	71.3	139.6	76.9	105.3	54.7	59.9	68.3	41.7	44.7	68.2	155.7
Eu	0.9	2.5	1.2	1.5	0.6	0.5	0.7	0.4	0.4	0.9	2.3
Gd	4.5	11.3	5.7	6.8	3.3	2.9	3.4	2.1	2.3	4.9	10.1
La	37.7	84.7	43.8	58	29.7	31.7	36.9	22.1	24.3	36.1	84.0
Nd	30.7	66.7	37.7	41.6	22.5	22.1	24.7	16.2	17.7	29.8	64.0
Pr	8.0	18.2	9.6	11.9	6.0	6.4	7.4	4.3	4.7	8.11	17.0
Sm	4.6	12.1	6.7	8.2	3.5	3.4	4.0	2.4	2.7	5.7	11.1
Tb	0.7	1.6	0.8	0.9	0.4	0.3	0.4	0.3	0.3	0.84	1.3
Dy	4.4	9.4	5.2	5.2	3.0	2.5	3.0	2.2	2.5	5.41	7.3
Ho	0.9	1.7	0.9	1.2	0.6	0.5	0.6	0.5	0.6	1.18	1.3
Er	2.6	5.2	2.8	3.2	1.7	1.5	1.9	1.5	1.8	4.11	4.2
Lu	0.4	0.6	0.4	0.4	0.3	0.2	0.3	0.3	0.2	0.64	0.6
Tm	0.4	0.7	0.4	0.4	0.3	0.2	0.3	0.2	0.2	0.5	0.5
Sc	7.0	14.0	7.0	11.0	5.0	5.0	6.0	4.0	5.0	4.0	9.0
Yb	2.4	4.49	2.91	2.6	2.2	1.6	2.3	1.8	1.9	4.0	4.0
Y	26.9	53.5	28.3	33.4	17.9	14.8	18.1	13.9	17.7	41.1	41.2
∑REE	203.0	426.6	230.6	292.1	152.0	154.1	178.7	114.3	127.7	215.6	414.2
R	0.011	0.013	0.010	0.011	0.006	0.005	0.007	0.060	0.006	0.173	0.052
Eu/Eu*	0.70	0.66	0.61	0.64	0.61	0.55	0.61	0.57	0.51	0.58	0.66
$(La/Yb)_{Cn}$	10.46	12.72	10.15	14.5	8.82	12.73	10.49	10.6	8.31	6.04	13.83
$(Gd/Yb)_{Cn}$	1.01	2.04	1.59	2.05	1.17	1.43	1.17	0.95	0.98	0.98	2.02

$R= (CaO+Na_2O+K_2O)/ (Al_2O_3+LOI)$

$Eu/Eu^* = Eu_{cn}/(Sm_{cn})(Gd_{cn})^{½}$

Mamu/Ajali Formation samples:

Aloji - AL1.1, AL1.2, AL1.3, AL2.1, AL2.2, AL2.2, AL2.3, AL2.4 and AL2.5.

Ofejiji – OF2.1 and OF2.2

Table 4.17. Cont..

	AG2.1	UD1.1	Ud.1.2	UD1.3	OK1.1	OK1.2	OK1.3	EN4.1	EN4.2	EN4.3
Ce	66.6	107.9	52.5	77.6	224.5	177.1	188.9	67.9	129.5	143.5
Eu	0.7	1.43	0.53	0.58	1.11	2.07	1.53	0.9	0.98	1.2
Gd	0.9	8.3	2.3	3.2	12.0	8.3	10.5	3.9	8.9	4.1
La	38.4	67.5	29.8	30.6	98.6	83.5	56.0	33.6	67.6	71.
Nd	7.6	54	17.6	22.8	68.3	87.6	53.7	26.6	61.3	55.0
Pr	7.7	14.6	5.8	5.9	18.2	20.3	17.9	6.9	18.7	16.4
Sm	4.8	9.3	3.0	3.7	9.5	14.3	10.5	4.3	9.0	10.3
Tb	0.7	1.1	0.4	0.5	1.5	1.7	0.8	0.6	1.3	1.5
Dy	5.8	7.0	2.4	4.0	5.5	8.9	7.8	3.9	2.8	1.6
Ho	1.2	1.3	0.5	0.8	0.83	1.5	1.2	0.8	0.6	0.7
Er	3.9	4.7	1.9	2.4	3.75	4.3	4.2	2.3	1.5	1.7
Lu	0.7	0.8	0.2	0.4	0.42	0.5	0.6	0.3	0.5	0.6
Tm	0.5	0.7	0.2	0.4	0.4	0.6	0.6	0.3	0.2	0.7
Sc	7.0	8	4	6	13.0	16.0	15.0	18.0	11.0	12.0
Yb	4.4	5.3	2.2	3.17	2.5	3.8	3.98	2.3	2.1	2.3
Y	37.1	46.4	17	23.9	28.7	42.80	40.60	19.9	27.30	25.5
∑REE	188.4	338.7	140.8	186.3	489.2	473.6	414.2	0.027	343.8	349.4
R	0.009	0.010	0.011	0.008	0.023	0.029	0.018	192.8	0.039	0.039
Eu/Eu*	1.10	0.83	0.60	0.51	0.32	0.58	0.44	0.70	0.33	0.58
(La/Yb)Cn	5.79	8.48	9.09	6.51	25.96	14.79	9.49	9.05	21.19	20.62
(Gd/Yb)Cn	0.16	1.26	0.86	0.82	3.81	1.77	2.46	1.38	3.34	1.42

$R = (CaO+Na_2O+K_2O)/ (Al_2O_3+LOI)$

$Eu/Eu^* = Eu_{cn}/(Sm_{cn})(Gd_{cn})^{½}$

Mamu/Ajali Formation samples:

Agbenema – AG2.1
Udane-Biomi - UD1.1, UD1.2 and UD1.3.
Okpokwu - OK1.1, OK1.2, OK1.3

Enugu/Nkporo Formation samples

Enugu – EN4.1, EN4.2, EN4.3.

Table 4.18. Rare earth element distribution for the fine (<2μm) clay samples investigated.

Sample No → Element ↓	AL1.1	AL1.2	AL1.3	OF2.4	AG1.1	AG1.2	Ud.1.1	Ud.1.3
Ce	133.5	126.7	84.1	93.3	175	118.9	152.1	193.1
Eu	2.24	1.31	0.86	0.95	3.07	2.33	2.13	1.24
Gd	10.14	8.84	5.42	4.48	12.35	9.5	10.18	5.47
La	71.84	62.2	41.4	53	83.5	56	86	62.3
Nd	59	52.7	32.7	28	77.6	53	69.7	39.4
Pr	15.43	14.11	8.82	8.72	20.34	13.99	18.83	11.91
Sm	10.35	9.04	5.95	4.94	14.34	10.55	11.95	6.78
Tb	1.55	1.31		0.73	1.74	1.43	1.34	0.85
Dy	8.95	6.85	5.41	4.63	8.94	7.81	6.95	5.11
Ho	1.75	1.31	1.13	0.97	1.57	1.48	1.37	0.97
Er	5.01	3.73	3.59	2.78	4.34	4.15	4.03	3.04
Lu	0.63	0.5	0.6	0.49	0.56	0.6	0.61	0.54
Tm	0.69	0.5	0.52	0.46	0.61	0.6	0.56	0.49
Sc	12	11	10	9	18	13	10	14
Yb	4.35	3.45	3.69	3.02	3.84	3.97	5.37	3.15
Y	54	33.7	30.4	27.4	42.8	40.6	37.3	25.3
∑REE	391.43	337.25	234.59	242.87	468.60	337.91	418.42	373.65
R	0.013	0.015	0.102	0.120	0.008	0.034	0.012	0.013
Eu/Eu*	0.76	0.45	0.46	0.62	0.71	0.71	0.59	0.62
(La/Yb)Cn	11.13	12.16	7.57	18.83	14.38	9.51	10.8	13.33
(Gd/Yb)Cn	1.88	2.07	1.19	1.2	2.55	1.93	1.53	1.4

$R= (CaO+Na_2O+K_2O)/ (Al_2O_3+LOI)$

$Eu/Eu^* = Eu_{cn}/(Sm_{cn})(Gd_{cn})^{½}$

Mamu/Ajali Formation clay samples:

Aloji – AL1.1, AL1.2 and AL1.3.
Ofejiji – OF2.4.
Agbenema – AG1.1 and AG1.2.
Udane-Biomi - UD1.1, UD1.2 and UD1.3.

Table 4.18. Cont…

Sample No → Element ↓	OK1.1	OT1.1	OT2.2	EN2.1	EN2.1	EN4.2	EN4.3
Ce	128.5	147.4	89.8	67.9	96.3	168.7	172.4
Eu	3.9	2.0	1.1	0.9	0.95	1.9	1.6
Gd	16.0	7.9	5.4	3.9	5.4	7.3	6.4
La	189.7	81.7	53.5	33.6	53.0	84.4	80.1
Nd	117.7	58.4	35.1	26.6	38.4	58.0	52.6
Pr	33.9	16.1	10.2	6.9	19.7	17.4	15.3
Sm	19.7	10.6	6.0	4.3	6.9	9.6	8.2
Tb	2.1	1.1	0.8	0.6	0.7	1.0	0.8
Dy	11.1	6.1	4.7	3.9	3.0	5.5	5.0
Ho	1.8	1.0	0.9	0.8	0.9	1.0	0.9
Er	4.9	2.8	2.8	2.3	1.0	2.9	2.8
Lu	0.6	0.3	0.4	0.3	0.4	0.4	0.4
Tm	0.6	0.3	0.4	0.3	0.1	0.4	0.4
Sc	20.0	21.0	12.0	18.0	9.0	14.0	11.0
Yb	4.2	2.5	2.7	2.3	2.05	2.7	2.7
Y	55.9	27.8	27.1	19.9	30.40	28.2	26.3
R	0.029	0.015	0.029	0.027	268.7	0.014	0.007
∑REE	611.1	387.5	253.1	192.8	0.007	403.7	387.3
Eu/Eu*	0.68	0.69	0.61	0.70	0.49	0.73	0.68
$(La/Yb)_{Cn}$	30.1	21.27	15.7	9.05	17.43	20.99	19.92
$(Gd/Yb)_{Cn}$	3.05	2.46	1.59	1.38	2.16	2.18	1.92

$R= (CaO+Na_2O+K_2O)/ (Al_2O_3+LOI)$

$Eu/Eu^* = Eu_{cn}/(Sm_{cn})(Gd_{cn})^{½}$

Mamu/Ajali samples:

Oturkpa - OT1.1 and OT2.2

Okpokwu - OK1.1.

Enugu/Nkporo Formation samples:
Enugu – EN2.1, EN4.2, EN4.3.

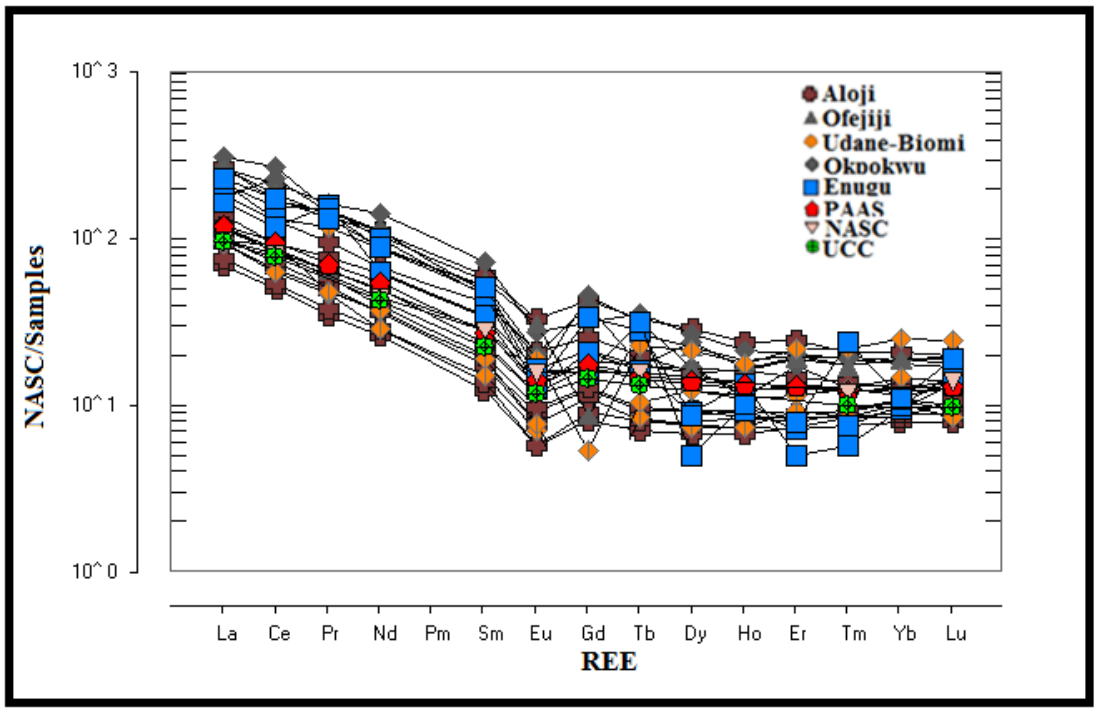

Fig. 4.40. NASC-Chondrite normalised rare elements plot for raw clay samples from Mamu/Ajali and Enugu/Nkporo Formtions, Lower Benue Trough (After Boynton, 1984).

The parameter R= ($CaO+Na_2O+K_2O$)/ (Al_2O_3+LOI) by Middelburg *et al*. (1988) was used to determine the relationship between REE compositions in the precursors and level of weathering. The R- ratios varied from 0.010 to 0.173 and 0.007 to 0.039 for the Mamu/Ajali and Enugu/Nkporo Formation clay samples correspondingly (Tables 4.17 and 4.18. This ratio that approaches zero comfirms an intensive weathering and its associated with the break down of feldsparthic materials and it's deposition to form kaolinite. The LREE composition in the clay samples suggests an enrichment of LREE with kaolinization (Figs. 4.41a and 4.43a) but the relationship between the concentration of LREE and Y in the raw and fine (<2µm) clay samples of both Mamu/Ajali and Enugu/Nkporo Formations shows a positive correlation (Figs. 4.41b and 4.43b). Such relationship confirms that LREE and Y were significantly enriched during the process of weathering and kaolinization.

Figs. 4.40 and 4.42 illustrates similar pattern in REE of the investiagted clay samples to those of NASC, PAAS and UCC. Relatively high HREEs is ascribed to heavy minerals abundance, such as zircon. This elucidation is supported by high abundances of Zr in the clay samples.

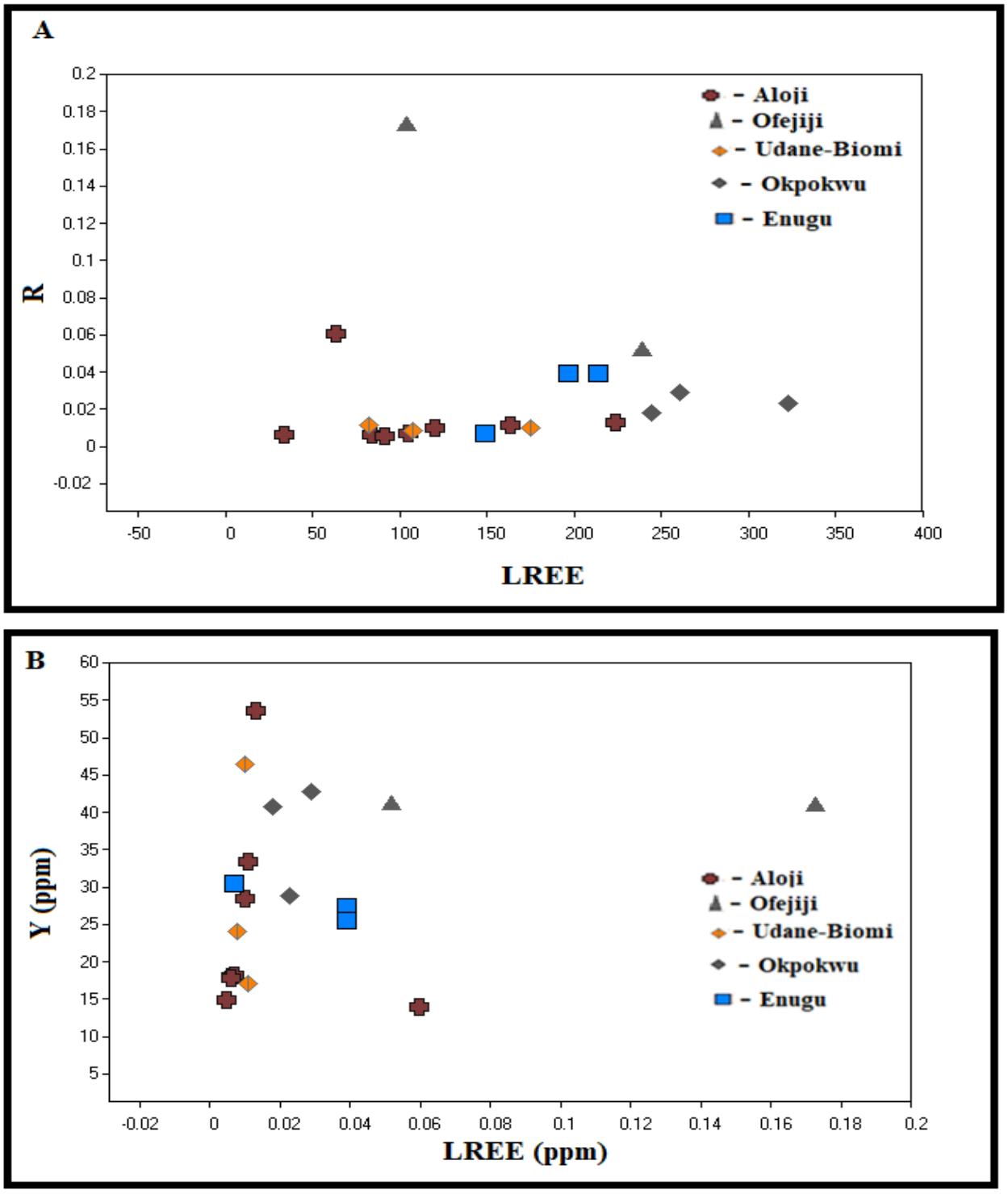

Fig. 4.41. Harker's plot showing the relationship between **A:** The ratio R, and LREE (La+Ce) and **B:** Y and LREE the raw clay samples from Mamu/Ajali and Enugu/Nkporo Formations, Lower Benue Trough, Nigeria (Middelburg *et al*., 1988).

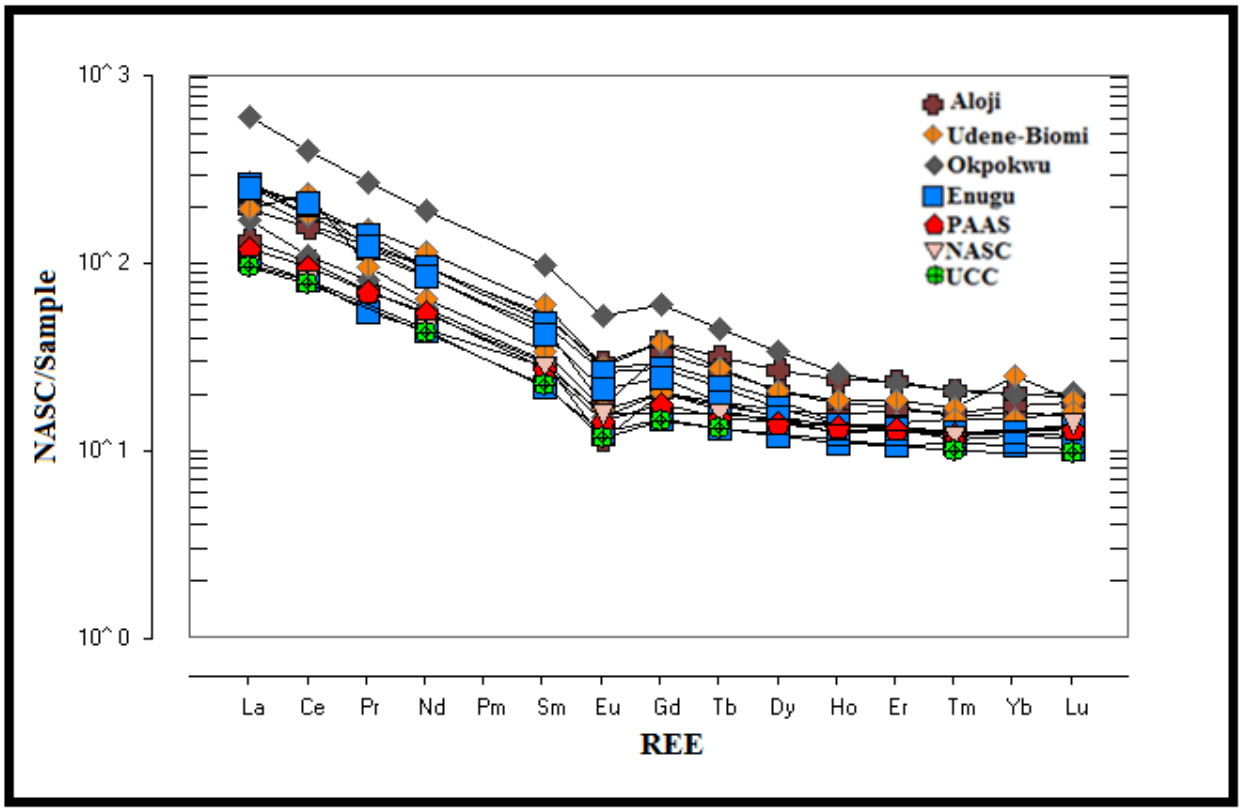

Fig. 4.42. NASC-Chondrite normalised rare elements plot for fine <2µm clay samples from Mamu/Ajali and Enugu/Nkporo Formations, Lower Benue Trough (After Boynton 1984).

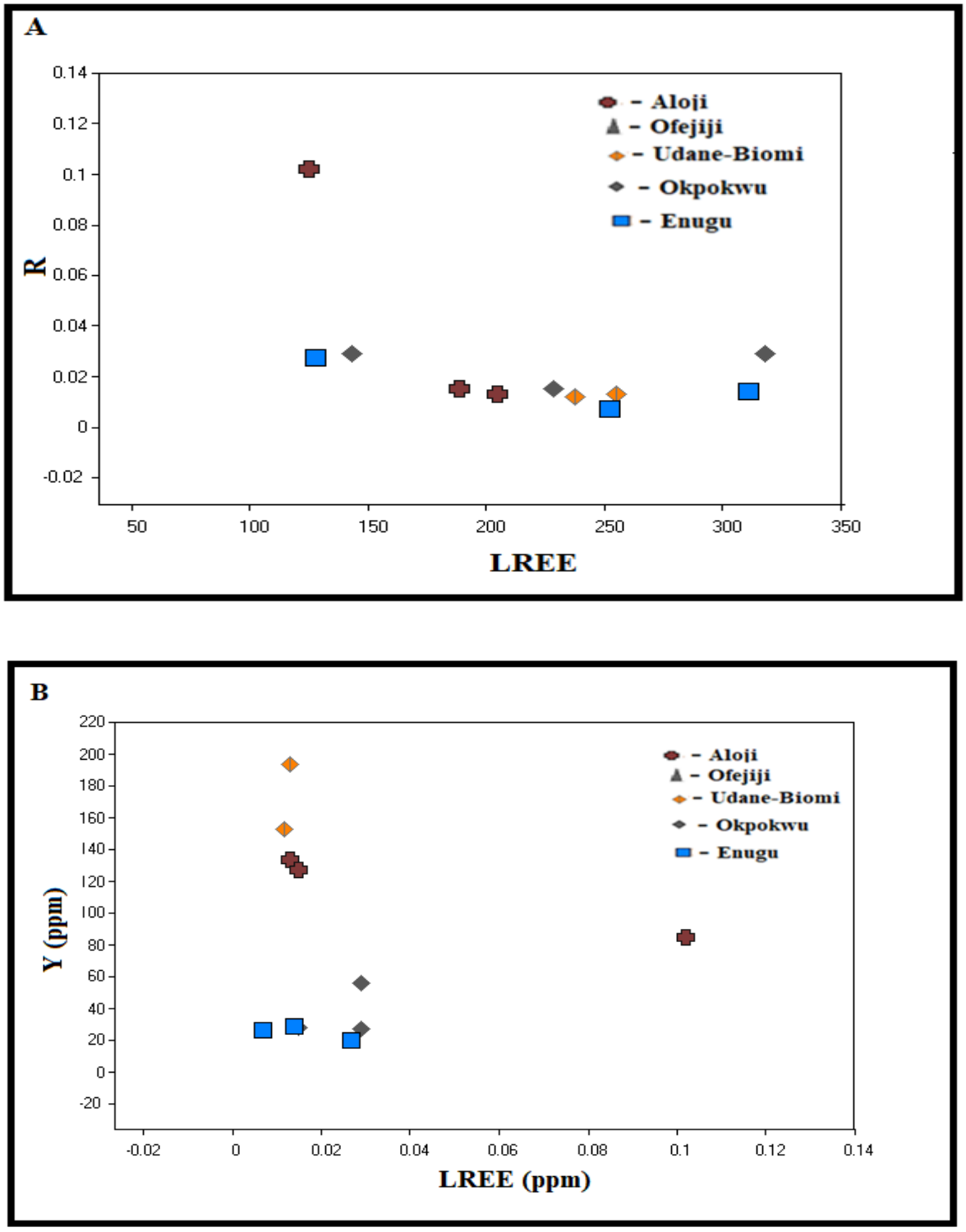

Fig. 4.43. Harker's plot showing the relationship between **A:** The ratio R, and LREE (La+Ce) and **B:** Y and LREE for the fine <2µm clay samples investigated (After Middelburg *et al*., 1988).

4.4.8 Provenance, Tectonic Setting and Depositional environment

Mineralogical maturity and geochemical signatures of clastic sediments were used to determine their origin, tectonic setting and environment of deposition (Taylor and Mclennan, 1985 and Armstrong-Altrin *et al.*, 2004).

4.4.8.1 Provenance of both raw and fine (<2µm) clay samples

Clastic rock Al_2O_3/TiO_2 ratios are used to infer rock source composition (Hayashi *et al.*, 1997), as Al_2O_3/TiO_2 ratios increase from 3 - 8 for mafic igneous rocks, from 8 - 21 for intermediate rocks and from 21 - 70 for felsic igneous rocks.

For the clay samples being studied, the ratios of Al_2O_3/TiO_2 in the raw clay samples from Mamu/Ajali ranged from 7.82 to 17.70 and 8.65 to 12.70 for Enugu/Nkporo Formations, respectively (Table 4.19) while in the fine (<2µm) clay samples, it was between 9.28 to 22.66 in the Mamu/Ajali and 12.92 to 13.61 in the Enugu/Nkporo Formations (Table 4.20). From above values, an intermediate felsic igneous source rocks with probable few quartz-rich felsic veins are suggested for the clay deposits.

In determining provenance, the composition of components (La, Th, Sc, and Co) in sediments and their respective elemental ratios (La/Sc, Th/Sc, Th/Co) may be helpful (Cullers, 1994b ; Cox *et al.*, 1995). Th/Sc ratios varied from 0.16 to 3.08 and 1.16 to 1.62 for the raw clay samples from Mamu/Ajali and Enugu/Nkporo Formations as against 1.12 to 1.96 and 1.18 to 1.96 in the fine (<2µm) clay samples Tables 4.19 and 4.20. The La/Sc ratios ranged between 3.73 and 9.30 and 5.89 and 5.99 for the raw clay samples from Mamu/Ajali and Enugu/Nkporo Formations while in the fine (<2µm) clay samples, it was from 3.89 to 9.49 and 4.45 to 9.49 but the Th/Co ratios ranged in Mamu/Ajali from 2.01 to 21.00 and 8.25 to 12.08 in Enugu/Nkporo raw clay while in the fine (<2µm) clay samples, it varied in both Mamu/Ajali and Enugu/Nkporo Formations from 1.04 to 7.25 and 1.04 to 6.67 (Tables 4.19 and 4.20). These value differences were contrasted with Taylor and Mclennan's (1985) felsic and basic rock-derived sediment (fine fraction) and (UCC) and PAAS values (Table 4.21). The values obtained suggest a dominantly felsic (granodioritic) precursor for the clay deposits.

Table 4.19. Calculated geochemical ratios for the investgated raw clay samples.

Sample No → Ratios ↓	Al	AL1.1	AL1.2	AL1.3	AL2.1	AL2.2	AL2.3	AL2.4	AL2.5	OF2.1	OF2.2
La/Sc	5.39	6.05	6.26	5.27	5.94	6.34	6.15	5.53	4.86	9.03	9.33
La/Th	2.83	3.89	3.29	3.30	2.34	3.11	2.58	2.10	2.01	2.93	5.49
Th/Sc	1.90	0.61	1.90	1.60	2.54	2.04	2.38	2.63	2.42	3.08	1.70
Th/Co	11.08	10.38	12.09	11.73	15.88	14.57	17.88	21.00	13.44	12.30	2.01
Th/U	5.12	4.84	4.29	4.89	6.35	5.67	5.72	5.00	5.76	3.51	3.73
Al_2O_3/TiO_2	10.26	11.79	10.53	10.81	11.47	9.29	9.29	7.82	8.52	13.39	5.53

Sample No → Ratios ↓	UD1.1	UD1.2	UD1.3	OK1.1	OK1.2	OK1.3	EN4.1	EN4.2	EN4.3
La/Sc	8.44	7.45	5.10	7.58	5.22	3.73	5.89	6.15	5.99
La/Th	2.97	3.51	2.05	6.86	4.96	2.96	3.63	5.29	4.16
Th/Sc	2.84	2.13	2.48	1.11	1.05	1.26	1.62	1.16	1.44
Th/Co	20.64	17.00	10.64	6.85	3.98	3.70	12.08	8.25	9.58
Th/U	4.83	3.15	4.26	4.05	3.83	3.72	3.97	5.35	4.18
Al_2O_3/TiO_2	10.88	17.70	11.87	13.02	15.99	10.89	8.65	10.61	12.70

Mamu/Ajali Formation clay samples:

Aloji – AL, AL1.1, AL1.2, AL1.3, AL2.1,AL2.2,AL2.3,AL2.4 and AL2.5.
Ofejiji – OF2.1 and OF2.2.
Udane-Biomi – UD1.1, UD1.2 and UD1.3.
Okpokwu – OK1.1, OK1.2 and OK1.3.

Enugu/Nkporo Formation clay samples:

Enugu – EN4.1, EN4.2 and EN4.3

Table 4.20. Calculated geochemical ratios for the investigated fine (<2μm) clay samples.

Sample No→ Ratios↓	AL1.1	AL1.2	AL1.3	OF2.4	AG1.1	AG1.2	UD1.1	UD1.3
La/Sc	5.98	5.65	4.14	5.89	4.64	4.31	8.60	4.45
La/Th	3.57	3.89	2.18	3.61	3.37	3.20	4.67	2.27
Th/Sc	1.67	1.45	1.90	1.63	1.38	1.35	1.84	1.96
Th/Co	6.48	6.15	7.31	2.40	1.78	4.38	6.67	4.84
Th/U	5.74	3.81	3.73	3.27	4.28	4.38	3.41	3.67
Al_2O_3/TiO_2	13.57	9.38	9.28	13.21	16.18	14.01	10.74	15.02

Sample No→ Ratios↓	OT1.1	OT2.2	OK1.1	EN2.1	EN4.2	EN4.3
La/Sc	3.89	4.46	9.49	9.49	8.60	4.45
La/Th	3.46	2.96	9.16	9.16	4.67	2.27
Th/Sc	1.12	1.51	1.18	1.18	1.84	1.96
Th/Co	5.24	5.17	1.04	1.04	6.67	4.84
Th/U	4.63	4.21	3.45	3.45	3.41	3.67
Al_2O_3/TiO_2	22.66	12.79	16.65	12.92	13.61	12.96

Mamu/Ajali Formation clay samples:

Aloji – AL1.1, AL1.2, AL1.3.
Ofejiji – OF2.4.
Udane-Biomi – UD1.1 and UD1.3.
Oturkpa – OT1.1 and OT2.2.
Okpokwu – OK1.1.

Enugu/Nkporo Formation clay samples:

Enugu – EN2.1, EN4.2 and EN4.3

Table 4.21. Range of elemental ratios for both raw and fine clay (<2µm) clay samples investigated compared to ratios for similar fractions from felsic rocks, mafic rocks, UCC and PAAS.

Ratios↓	[1]Lower Benue Trough clay samples		[2]Range of sediments		[3]UCC	[3]PAAS
	Raw	Fine	Felsic rocks	Mafic Rocks		
Th/Sc	0.61 – 3.08	1.12 – 1.96	0.84-20.50	0.05-0.22	0.79	0.90
Th/Co	2.01 – 21.00	1.04 – 7.31	0.67-19.40	0.04-10	0.63	0.63
La/Sc	3.73 – 9.33	3.89 – 9.49	2.50-16.30	0.43-0.86	2.21	2.40

UCC – Upper Continental Crust, PAAS – Post- Archean Australian average Shale.

[1]This Study, [2]Cullers (1994a and b), [3]Taylor and Mclennan (1985).

The TiO_2 vs Al_2O_3 binary plot was used by Perri (2014) to differentiate granitic from basaltic rocks. In Fig. 4.44, the binary plot of TiO_2 vs Al_2O_3 proposed a predominantly intermediate to granite rock precursors for the clay deposits. On the McLennan *et al.* (1993) Th/Sc–Zr/Sc diagram, the investigated raw and fine clay clustered around average Proterozoic granodiorite to granite, confirming a dominantly granitic source for the clay deposits (Fig. 4.45).

In Cullers ' La-Th-Sc diagram (1994a and b) (Fig. 4.46) for distinguishing between felsic and basic provenance of fine-grained sediments, the clay data falls in a predominantly felsic area. The Th - Co - Zr/10 diagram of Vital *et al.* (1999) was also used to evaluate the clay provenance. The diagram demostrates that the samples of clay studied are depleted in Co and enriched in Th. All the samples of clay studied plot within the passive margin, near the Zr/10 apex and parallel to the Th-Zr axis (Fig. 4.47).

REE patterns have shown to be a potent tool for infering sedimentary rock sources . In the raw and fine (<2µm) clay samples investigated, there are characteristic pattern of REE fractionation of distinct $La/Yb)_{cn}$ values from 6.04 to 21.19 and Gd/Yb_{cn} from 0.95 to 3.54, a negative Eu anomaly (generally <1), LREEs enriched and the HREE patterns are nearly flat and a very low tending towards negative Eu and Tm anomalies (Tables 4.17 – 4.18, Figs. 4.40 and 4.42). These characteristics indicated that the initial precursor was felsic and that the negative Eu anomaly is seen as evidence from a differentiated, granite-like source (McLennan *et al.,* 1993).

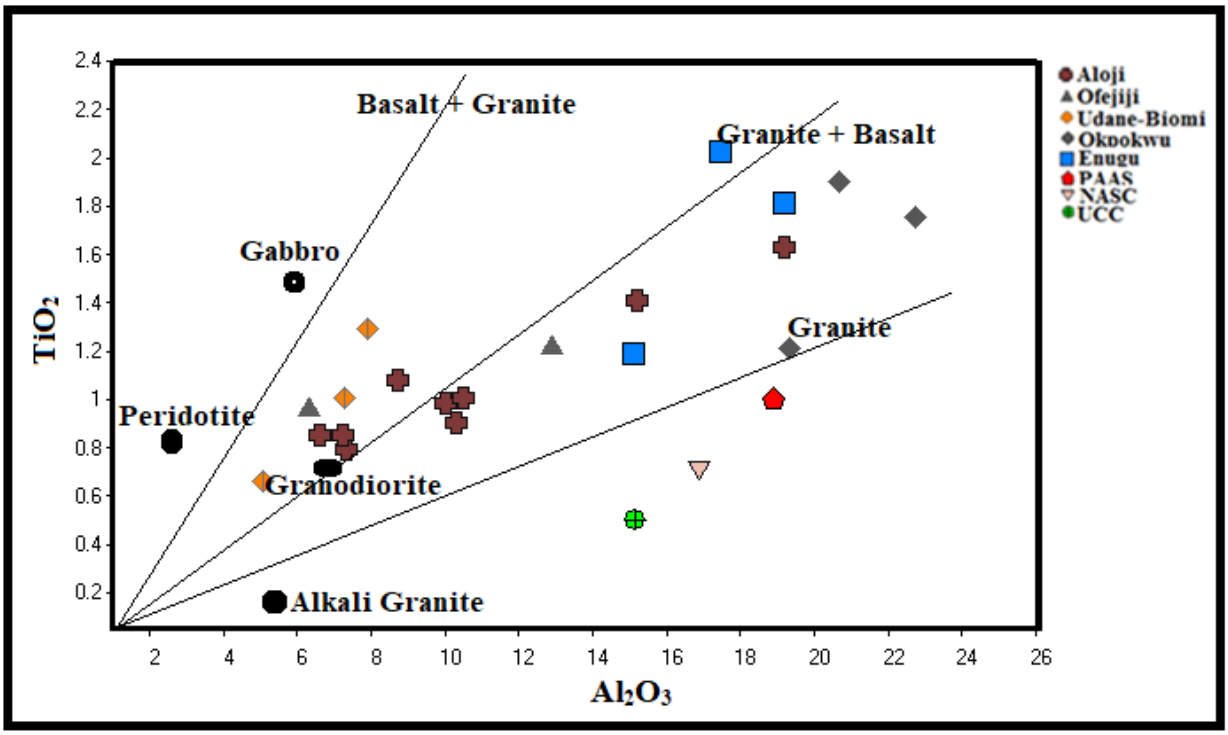

Fig. 4.44. Binary plot of TiO_2 vs Al_2O_3 for the studied raw clay samples from Mamu/Ajali and Enugu/Nkporo Formation within the Lower Benue Trough, Nigeria.
(After Perri, 2014)

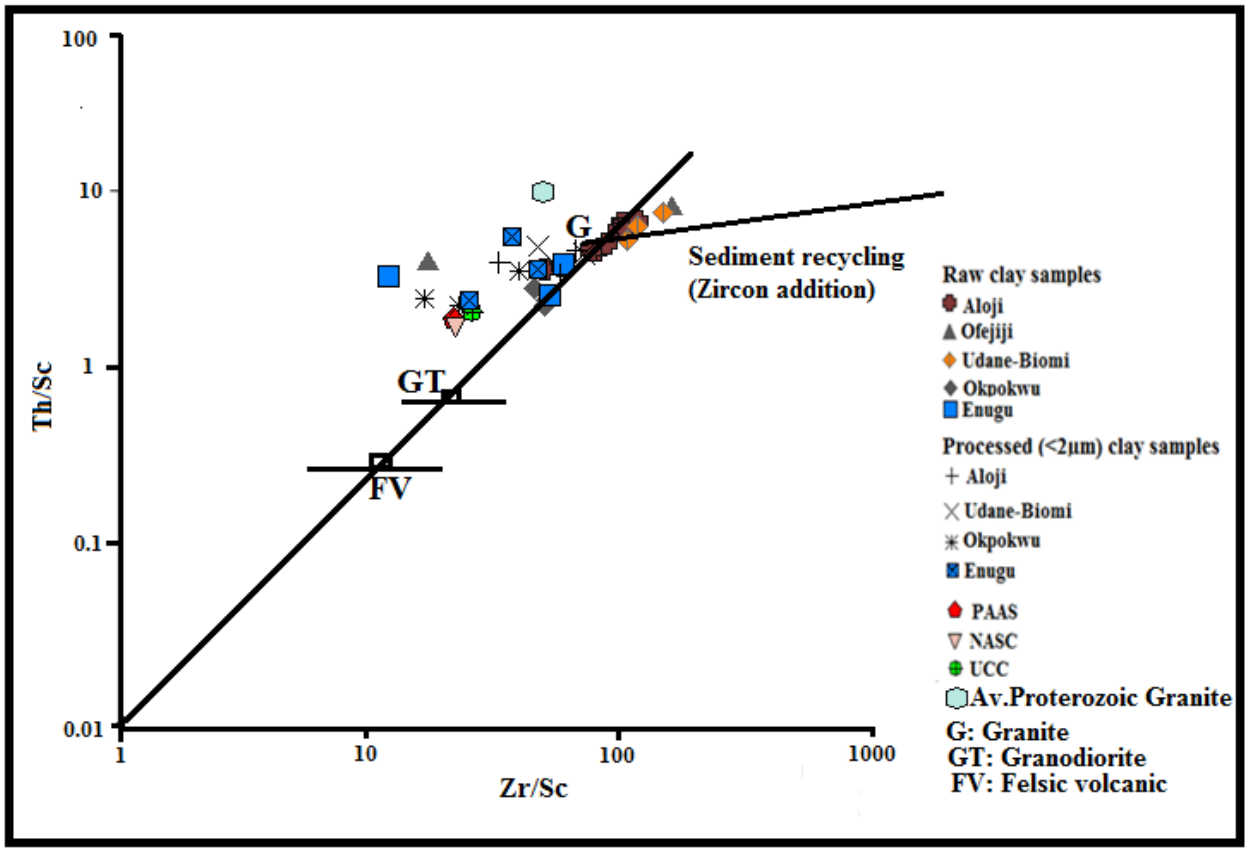

Fig. 4.45. Th/Sc–Zr/Sc diagram showing the investigated clay samples clustering around average Granite (afterMcLennan *et al.*, 1993). Granite - G, Granodiorite - GT and Felsics volcanic - FV (After Condie, 1993).

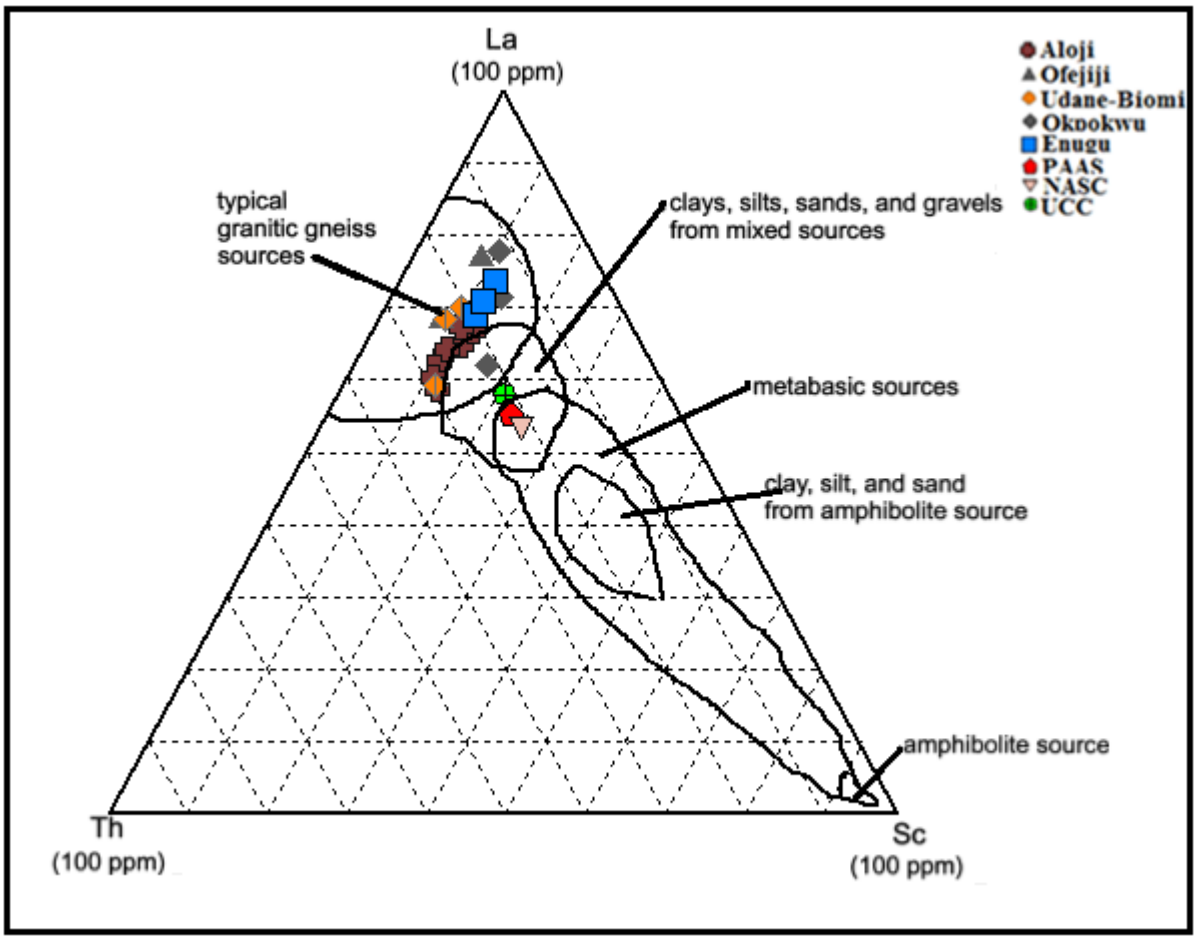

Fig. 4.46. Ternary plot of La - Th - Sc after Cullers (1994a) for the Lower Benue Trough raw claysamples.

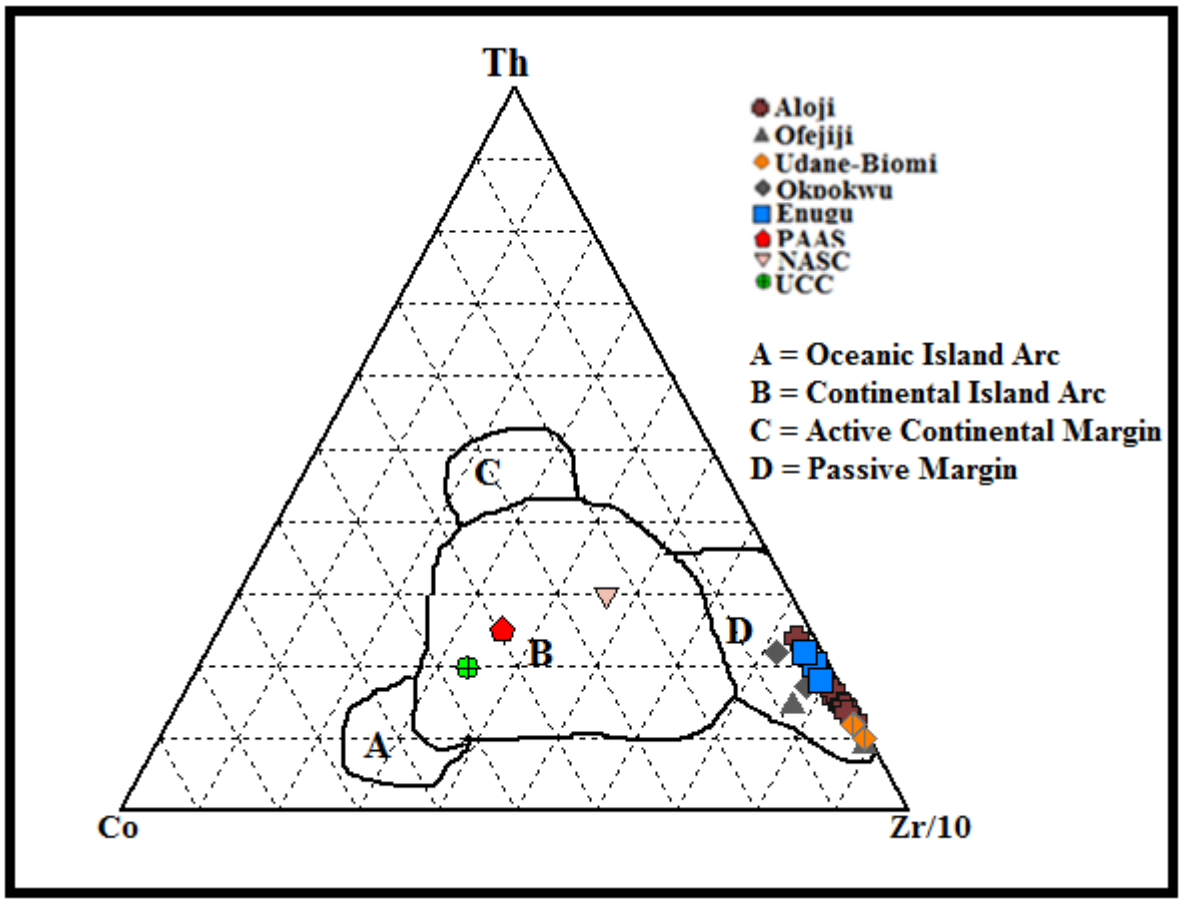

Fig. 4.47. Ternary plot of Th - Co - Zr/10 after Vital *et al.* (1999) for the investigated raw clay samples.

4.4.8.2 Tectonic settings for both raw and fine (<2µm) clay samples

The tectonic setting for the investigated clay samples from Aloji, Ofejiji, Udane-Biomi and Okpokwu of Mamu/Ajali and Enugu of Enugu/Nkporo Formations, Lower Benue Trough, was determined using the Roser and Korsch (1986) tectonic classification diagram. Plot of raw and fine (<2µm) clay samples on the binary diagram, $\log(K_2O/Na_2O)$ vs SiO_2, showed that all the samples were of Passive Margin origin (Fig. 4.48) similar to the PAAS, UCC and NASC.

The major oxide elemental analysis of the investigated clay samples from both formations of the Lower Benue Trough are quartz-rich (69.67 – 90.28 wt% for the raw and 47.33 to 80.10 wt% for the fine fraction) but depleted in Na_2O (<1 wt%), CaO (<1 wt% and TiO_2 (<3 wt%) (Tables 4.5 and 4.7) thereby justifying the assertion by Bhatia (1983) that passive-margin type clay deposits are largely quartz-rich. Bhatia and Crook's plot (1986) (Fig. 4.49) also favours the setting of Passive Margin for all the raw samples. Therefore, it implies that the deposition of the clay samples was in an intracratonic basin.

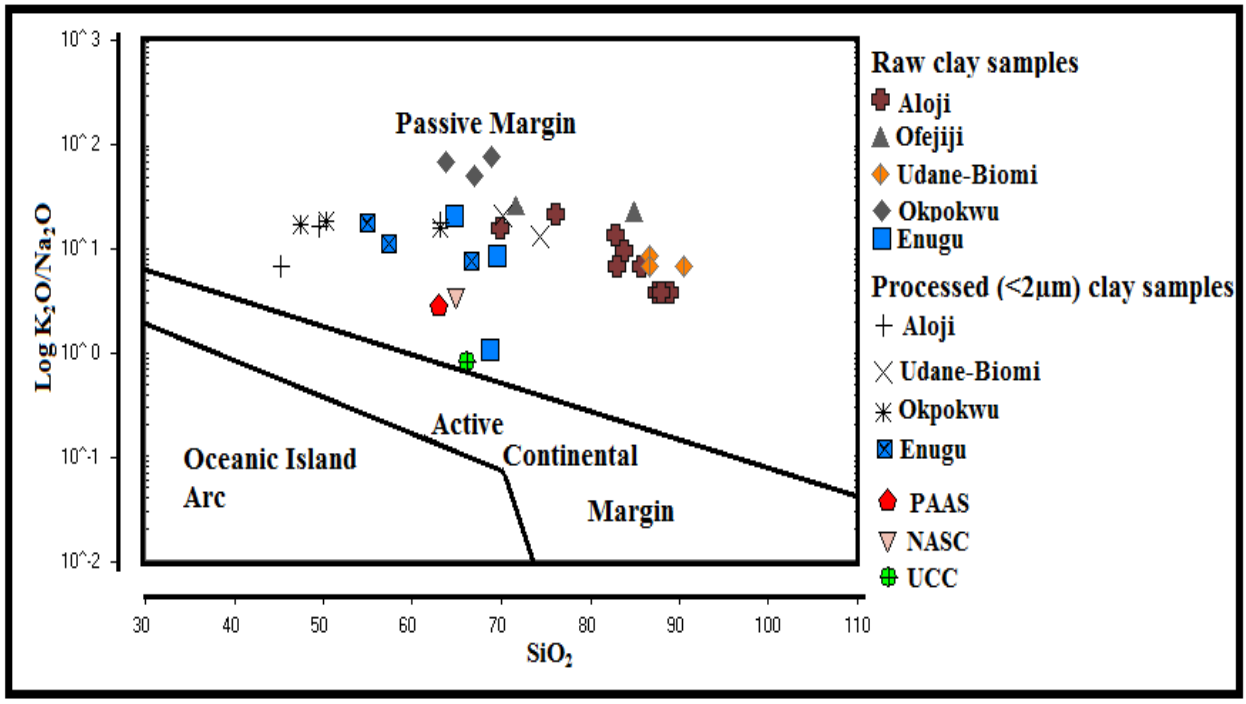

Fig.4.48. Tectonic discriminant diagram for the clay deposits in Lower Benue Trough, Nigeria. (After Roser and Korsch, 1986).

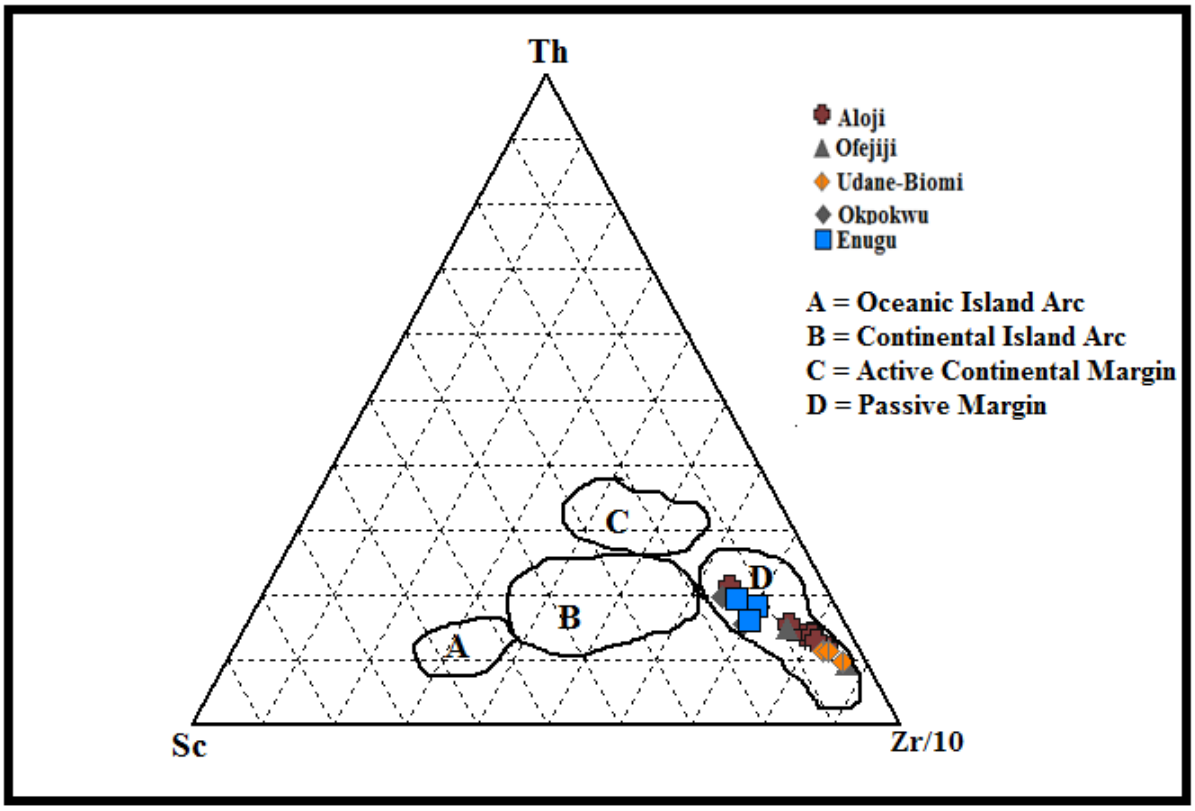

Fig. 4.49. Th-Sc-Zr/10 ternary plot (after Bhatia and Crook, 1986) for the raw clay samples.

The age of precursor for the clay deposits was inferred to be of Proterozoic age similar to PAAS and UCC (Taylor and McLennan, 1985) and NASC (Gromet *et al*., 1984). This is evident from the variations in Eu anomalies (Eu/Eu*) for these clay samples, which was generally less than 1 and $(Gd/Yb)_N$ ratios which varied between 0.95 and 3.54 for all the analysed samples from both formations (Tables 4.17 and 4.18). These recorded values, according to Taylor and McLennan (1985), Slack and Stevens (1994) and Mishra and Sen (2012) are features of upper continental crust recycled sediments and post-Archean (Proterozoic granite) rocks (Fig. 4.50). Consequently, the clay deposits within the Lower Benue Trough from both formations constitute a Proterozoic source that was directly subjected to the wearing away of basement granite and processed through sedimentary recycling.

4.4.8.3 Depositional environment for both raw and fine (<2µm) clay samples

The investigated raw clay samples from both Mamu/Ajali and Enugu/Nkporo Formations are characterized by Cu/Zn ratios <3 except Aloji (6.80 and 12.60) and (Cu+Mo)/Zn ratios <4, except Aloji (6.9 and 12.7). This suggest an oxidizing conditions for the raw clay samples of both formations (Hallberg, 1976). Also, Ni/Co ratios <5 signify oxic environments while >5 signify suboxic and anoxic environments (Jones and Manning, 1994). The U/Th ratio <1.25 reveals oxic setting, while > 1.25 reveals suboxic and anoxic conditions proposed by Nath et al. (1997). All the raw clay samples have a value of Ni/Co (<1) and U/Th (<1) indicating an oxic environments for the raw clay samples (Table 4.22). Similar values were recorded for the fine (<2µm) clay fractions from both formations (Cu/Zn <4, Cu+Mo/Zn <4, U/Th < 1) (Table 4.23), also indicating an oxic depositional environment.

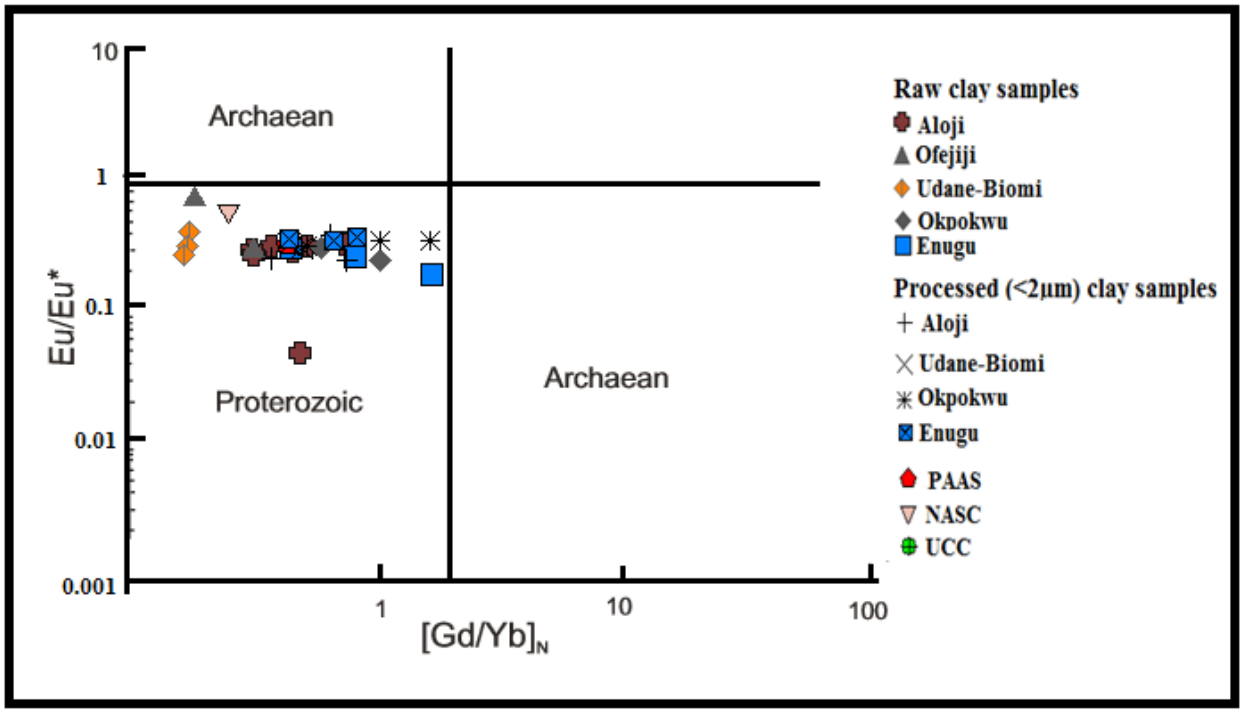

Fig 4.50. Eu/Eu * vs $[Gd/Yb]_N$ diagram illustrating the proterozoic provenance of clay samples from the Mamu / Ajali and Enugu / Nkporo Formations in the Lower Benue Trough (After Taylor and McLennan (1985) ; Slack and Stevens (1994) and Mishra and Sen (2012).

Table 4.22. Calculated oxidation parameters for the investigated raw clay samples.

.

Sample No → Ratios ↓	Al	AL1.1	AL1.2	AL1.3	AL2.1	AL2.2	AL2.3	AL2.4	AL2.5	OF2.1	OF2.2
U/Th	0.20	0.21	0.23	0.20	0.16	0.18	0.17	0.2	0.17	0.28	0.27
Cu/Zn	3.10	12.60	6.80	1.50	0.30	0.30	0.30	0.30	0.10	0.60	0.44
Cu+ Mo/Zn	3.20	12.70	6.90	1.60	0.40	0.40	0.40	0.40	0.20	0.61	0.47
Ni/Co	0.08	0.14	0.09	0.20	0.13	0.14	0.13	0.2	0.11	0.90	1.00

Sample No → Ratios ↓	UD1.1	UD1.2	UD1.3	OK1.1	OK1.2	OK1.3	EN4.1	EN4.2	EN4.3
U/Th	0.21	0.32	0.23	0.25	0.26	0.27	0.25	0.19	0.24
Cu/Zn	0.70	3.60	1.95	2.39	2.30	2.79	2.92	2.43	1.80
Cu+ Mo/Zn	0.80	3.70	2.10	3.79	2.35	2.83	3.92	3.43	1.96
Ni/Co	0.09	0.02	0.14	0.08	0.08	0.03	0.64	0.71	0.07

Table 4.23. Calculated oxidation parameters for the investigated fine (<2μm) clay samples.

Sample No→ Ratios↓	AL1.1	AL1.2	AL1.3	AG1.1	OF2.4	AG1.2	UD1.1	UD1.3
U/Th	0.17	0.26	0.27	0.23	0.31	0.23	0.29	0.27
Cu/Zn	2.73	4.88	3.10	1.04	2.11	2.04	1.91	2.12
Cu+ Mo/Zn	2.81	5.05	3.35	1.08	2.35	2.16	2.13	2.13

Sample No→ Ratios↓	OT1.1	OT2.2	OK1.1	EN4.2	EN4.3	EN2.1
U/Th	0.22	0.24	0.29	0.29	0.27	0.29
Cu/Zn	4.30	1.74	1.91	1.91	2.12	1.91
Cu+ Mo/Zn	4.35	1.85	1.94	2.13	2.13	1.94

4.5 Hydrogen and Oxygen isotope composition for the clay samples from Mamu/Ajali and Enugu/Nkporo Formations

Hydrogen (δD) and oxygen (δO^{18}) isotope compositions of clay samples from Aloji, Ofejiji, Agbenema, Udane-Biomi, Oturkpa of Mamu/Ajali and Enugu of Enugu/Nkporo Formation within the Lower Benue Trough are presented in Table 4.31. The δD value ranged from -66.1 to -50.80‰ for the clay samples of Mamu/Ajali Formation but -66.4 to -57.8‰ was obtained for the Enugu/Nkporo Formation while the δO^{18} values varied between 15.8 and 21.2‰ in the clay samples of Mamu/Ajali Formation as against 15.4 to 16.7‰ in the Enugu/Nkporo samples. (Table 4.24). The high formation temperature of 54 to 91°C (Table 4.24) is distinctive of kaolinite produced under warm and moist climate (Mizota and Longstaffe, 1996). Oxygen isotope composition of sedimentary kaolinites generally ranges between + 19 and + 23 and residual kaolinite varies between + 15 and + 19. The studied clay's oxygen isotopes obviously demonstrated that they are residual material obtained from felsic rock under chemical weathering at low altitudes. They were also eroded by flow over an extremely short expanse as a deposit of colluvial (+15.4 to +19‰), and a moderately longer expanse as an alluvium deposit (+19 to +21.2‰) in the Lower Benue Trough (Murray and Janssen, 1984), where there is sediment-meteoric water interactions with enriched δD and $\delta^{18}O$. Two depositional cycles are confirmed by the variation in oxygen isotopes. The first is the near source colluvial deposit with $\delta^{18}O$ (+15.4 to +19‰) and farther source alluvial with $\delta^{18}O$ (+19 to +21.2‰). Equations 1 and 2 of Savin and Epstein (1970) were used to calculate the O and H fractionation variables between kaolinite and water and Friedman's (1964) values of $\delta^{18}O$ = -5% and δH = -30% for meteoric water in equilibrium with kaolinitic minerals was also used. The obtained values (~1 ; Table 4.24) are consistent with Savin and Epstein (1970) values. This suggests that the kaolinitic mineral was in oxygen/hydrogen isotopic equilibrium with local groundwater.

Table 4.24. Compositions of isotopes of hydrogen and oxygen with calculated formation temperature for the clay samples of Mamu/Ajali and Enugu/Nkporo.

	AL 1.1	AL 1.2	AL 1.3	AL 2.1	OF 2.2	OF 2.3	OF 2.4	AG 1.1	AG 1.2	UD 1.1	UD 1.2	UD 1.3
$\delta\ ^{18}O/^{16}O$ (‰VSMOW)	18.9	19.0	17.8	--	--	--	--	--	19.9	15.8	---	---
δ^2H (‰VSMOW)	-50.8	-57.8	-62.0	-59.7	-63.2	-57.4	-57.4	-55.8	-55.4	-60.3	-57.8	-61.7
Ox (δKao-H_2O)	1.02	1.02	1.03	--	--	--	--	--	1.03	1.02	--	--
Hy (δKao-H_2O)	0.979	0.971	0.967	0.969	0.966	0.961	0.972	0.973	0.974	0.969	0.971	0.967
Temp. of formation °C	68	68	54	-	--	--	--	--	61	91	--	--

Mamu/Ajali Formation clay samples:

Aloji – AL1.1, AL1.2, AL1.3 and AL2.1.
Ofejiji – OF2.2, OF2.3 and OF2.4.
Agbenema – AG1.1 and AG1.2.
Udane-Biomi – UD1.1, UD1.2 and UD1.3.

Table 4.24. Cont...

Sample No→	OT1.1	OT 2.2	OK1.1	EN2.1	EN3.1	EN4.2	EN 4.3
$\delta\ ^{18}O/^{16}O$ (‰VSMOW)	21.2	19.3	18.9	18.1	--	16.7	15.4
δ^2H (‰VSMOW)	-63.8	-57.8	-66.1	-59.4	-57.8	-66.4	-58.3
Ox (δKao-H_2O)	1.026	1.024	1.024	1.023	--	1.022	1.021
Hy (δKao-H_2O)	0.967	0.971	0.969	0.967	0.971	0.962	0.971
Temp. of formation °C	54	68	68	73	--	83	91

Mamu/Ajali Formation clay samples:

Oturkpa – OT1.1 and OT2.2.
Okpokwu – OK1.1.

Enugu/Nkporo Formation clay samples:

Enugu – EN2.1, EN3.1, EN4.2 and EN4.3.

$$\alpha^{ox}_{kaolinite-H_2O} = \frac{\left(\frac{O^{18}}{O^{16}}\right)_{kaolinite}}{\left(\frac{O^{18}}{O^{16}}\right)_{water}}$$

$$\alpha^{hy}_{kaolinite-H_2O} = \frac{\left(\frac{D}{H}\right)_{kaolinite}}{\left(\frac{D}{H}\right)_{water}}$$

Equation 1

Sheppard and Gilg's (1996), based on revisions of current empirical information, suggested hydrogen and oxygen stable isotope fractionation equations between clay mineral (kaolinite) and water:

$$1000 \ln {}^{18}\alpha_{kaolinite-water} = 2.76 * 10^6/T^2 - 6.75$$

$$1000 \ln {}^{D}\alpha_{kaolinite-water} = -2.2 * 10^6/T^2 - 7.7,$$

Equation 2

Where: Ox (δKao-H_2O) is oxygen fractionation factors and Hy (δKao-H_2O) and hydrogen fractionation factors between kaolinite and water respectively, and Temperature, T (Kelvin). This equation (equation 2) was useful in estimating formation temperature for these deposits.

Fig. 4.51 shows the clustered data of δD and $\delta^{18}O$ about the line proposed by Savin and Epstein (1970a and b) and Sheppard and Gilg (1996), for kaolinitic mineral suggesting the formation of kaolinite at surface temperatures with meteoric waters. Therefore, a hydrothermal origin is not supported by this data. Hydrothermal deposits are typically characterized by low $\delta^{18}O$ values (Sheppard et al. (1969)). However, the

slight deviations from the kaolinitic line by some samples indicate post-depositional modifications in the clay isotope composition, possibly due to the downward percolating interaction between earlier-formed kaolinite and meteoric water (Table 4.24; Longstaffe and Ayalon, 1990).

The disparity in δD values observed for the deposits studied (Fig. 4.51) do not reveal variations in pore-fluid compositions, but are likely influenced by processes which minimize any original variations. For some samples (Fig. 4.51), δD values implied isotopic equilibrium of hydrogen with the current forming water, similar to that obtained in the values of $\delta^{18}O$. Such a re-equilibration for H- isotopes appears to be important at <100°C (Table 4.24). H^{+-} substitute, at approximately 200°C, would be a determinant factor instead of hydroxyil (OH) replacement (Longstaffe and Ayalon, 1990).

The present isotopic facts have been contrast by means of data published in Table 4.25, which obviously show the contrast involving high $\delta^{18}O$ clay minerals that are produced at equatorial latitudes, and those produced at higher latitudes in the region of Australia (Eastern Australia - 28°38' S and 153°38'E, Queensland - 10°41'S and 142°31'E) with lower δD and $\delta^{18}O$ values.

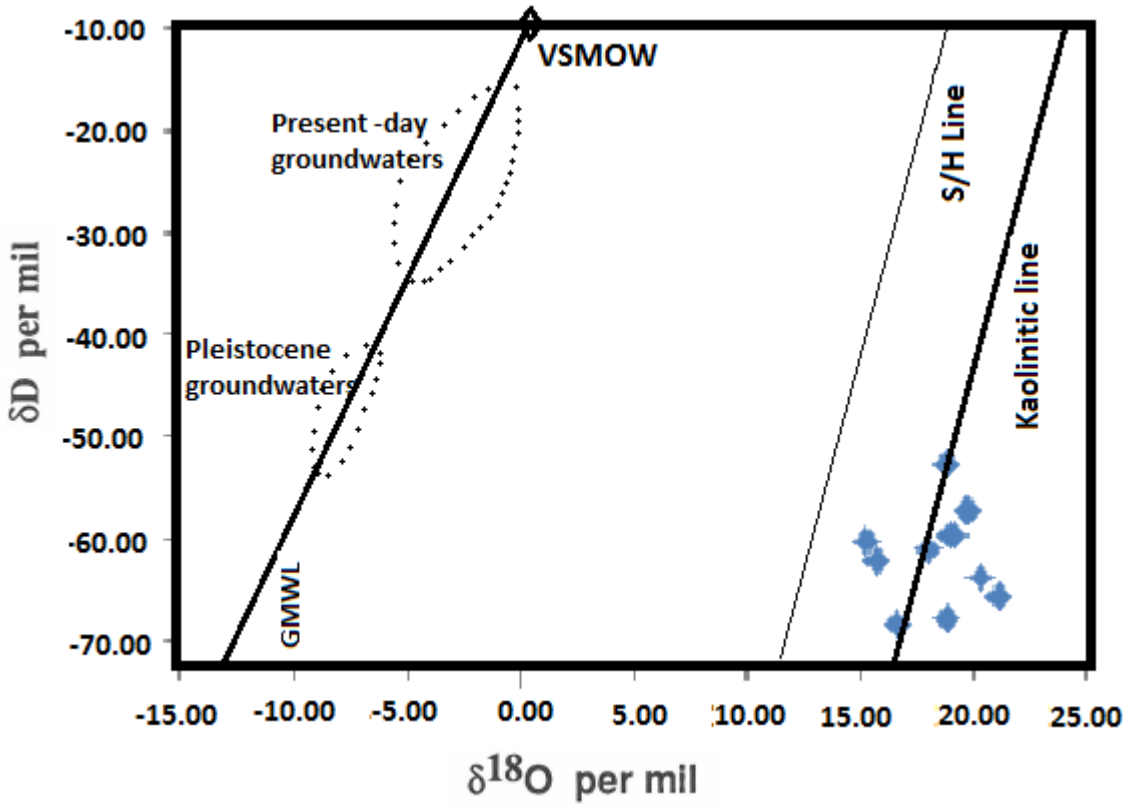

Fig. 4.51. δD and $\delta^{18}O$ isotope diagram for the investigated clay deposits describing its formation with meteoric waters at surface temperatures (Savin and Epstein, 1970a and b, Sheppard and Gilg,1996) and Sheppard *et al*., 1969).

.

Table 4.25. Average isotopic compositions of the investigated clay samples compared to other world averages.

		1	**2**	**3**	**4**	**5**	**6**
Coordinates	Latitude	6-8°N	24° 5'N	49°37'N	28°38' S	39°22'N	10°41'S
	Longitude	7-8°E	32° 53'E	11°33' E	153°38'E	141°7'E	142°31'E
$\delta\ ^{18}O/^{16}O$ (‰VSMOW)		20.36	19.44	17.8	8.03	15.33	13.68
$\delta^{2}H$ (‰VSMOW)		-62.53	-72.78	-70.10	-101.10	-71.09	-103.20

1. This study - LBT clay deposits, Nigeria
2. Egypt's Clay deposit (afterBaioumy, 2013)
3. Bavaria-Germany's Kaolinitic clay deposits (After Gilg, 2000)
4. Gunneda Basin, Eastern Australia's sample (After Bird and Chivas, 1988)
5. Japan's Sample (After Mizota and Longstaffe, 1996)
6. Queensland, Australia' Sample (After Zhou and Dobos, 1994)

4.6 Economic Potential of the clay deposits in Ajali/Mamu and Enugu/Nkporo, Lower Benue Trough

The parameters used to assess the appropriateness of clay samples from Aloji, Ofejiji, Agbenema, Udane-Biomi, Oturkpa, Okpokwu and Enugu for industrial use are physical characteristics, mineralogical and chemical composition. The physiochemical properties determined for the clays were particles size distributions, specific gravity, moisture content and plastic limit. The clay in hand specimen is generally light to brownish gray.

4.6.1 Particle size distribution

The particle size distribution of raw clay samples based on the grain diameter was determined using the British Standard (BS 1377:1990), in which, the gravel diameter is 7.62 – 4.75 mm, sand 4.75 – 0.075 mm, silt 0.075 – 0.002 mm and clay < 0.002 mm, high percentage of silt were recorded in all the samples analysed as indicated in Table 4.26; Aloji (44 – 55%), Ofejiji (42.20 – 50.10%), Agbenema (64.95 – 65.40%), Udane-Biomi (35.10 – 49.40), Okpokwu (23.60 – 25.80%) and Enugu (41.60– 52.55%). The percentage of sand was also high, Aloji (37.50 – 50.30%), Ofejiji (42.30 – 44.20%), (13.70 – 14.95%), Udane-Biomi (42.10 – 56.10%), Okpokwu (41.60 – 66.10%) and Enugu (21.40 – 26.30%) while the perentage of clay was low, Aloji (3.45 – 13.30), Ofejiji (4.90 – 24.00), Agbenema (12.45 – 14.10), Udane-Biomi (4.70 – 6.35), Okpokwu (7.60 – 13.50) and Enugu (20.50 – 29.10). Thus, indicating combinations of sandy silty and clayey silty grain size assemblages for the Ajali/Mamu and Enugu/Nkporo clay deposits (Table 4.26; Appendix 1). Percentage fines decreases from Agbenema (77.4 to 79.5%) to Enugu (70.70 – 73.00%), Ofejiji (54.15 – 66.60%), Aloji (48.8 – 51.00%), Udane-Biomi (39.80 – 55.75%) and Okpokwu (31.20 – 39.30%) (Table 4.26). The percentage of silt and sand in the analysed samples are high. This could be beneficiated with urea intercalation, which is capable of causing grain size reduction to facilitate usage in ceramic and paper manufacturing (Al-Shameri and Rong, 2009).

Table 4.26. Result of sieve analysis for the Mamu/Ajali and Enugu/Nkporo Formations' raw clay samples in the Lower Benue Trough, Nigeria.

Sample No: → Sieve size(mm)/ Mass retained(%):	AL1.1	AL1.2	AL1.3	OF1.1	OF2.3	OF2.4	OF2.5
0.600	1.00	1.60	3.85	1.00	1.00	2.55	1.40
0.425	0.90	1.05	1.55	1.80	1.80	0.60	0.90
0.250	0.70	0.90	1.20	0.20	0.20	5.90	3.80
0.150	42.60	31.45	38.65	0.50	0.50	31.65	35.10
0.075	44.30	55.20	45.35	42.20	42.20	44.30	50.10
Base pan	13.30	4.70	3.45	24.40	24.40	9.85	4.90
%Fines(0.075+base pan)	51.00	59.90	48.80	66.60	66.60	54.15	55.00

Sample No: → Sieve size(mm)/ Mass retained(%):	AG1.2	AG2.1	UD1.2	UD1.3	OK1.1	OK1.2	EN2.1	EN3.1
0.600	4.60	3.20	0.40	0.65	1.90	4.50	2.70	3.20
0.425	0.25	1.60	0.50	0.55	4.00	4.50	2.50	2.40
0.250	1.10	0.95	0.40	0.85	10.70	8.80	1.20	1.70
0.150	0.60	3.40	54.10	38.20	39.90	9.00	5.80	4.30
0.075	65.40	64.95	35.10	49.40	23.60	25.80	52.55	41.60
Base pan	14.10	12.45	4.70	6.35	7.60	13.50	20.50	29.10
%Fines(0.075+base pan)	79.50	77.40	39.80	55.75	31.20	39.30	73.00	70.70

Mamu/Ajali Formation clay samples:

Aloji – AL1.1, AL1.2 and AL1.3.
Ofejiji – OF1.1, OF2.3, OF2.4 and OF2.5.
Agbenema – AG1.2 and AG2.1.
Udane-Biomi – UD1.2 and UD1.3.
Okpokwu – OK1.1 and OK1.2.

Enugu/Nkporo Formation clay samples:

Enugu – EN2.1 and EN3.1

4.6.2 Specific gravity

Its significance is to determine the clay sample density. The average specific gravity values are as indicated; Aloji (2.17), Ofejiji (2.14), Agbenema (2.12), Udane-Biomi (2.26), Oturkpa (2.40), Okpokwu (2.38) and Enugu (2.30) (Table 4.27). The low density values (2.12 – 2.40) is a reflection of the low contents of the clay-size components. The result also showed that the clay was not suitable for construction purposes because the density is lower than the required average standard value of 2.6g/cm^3 for engineering constructions (FMWH, 1997).

4.6.3 Atterberg limits

This describes the relative ease with which it is possible to deform a clay material.

These include:

Liquid limit

This is the state at which a soil passes from plastic to the liquid. From the result obtained, the average liquid limit for Aloji (50.14%), Ofejiji (42.65%), Agbenema (33.62%), Oturkpa (48.29%), Okpokwu (43.88%), Udane-Biomi (39.09%) and Enugu (44.40) (Table 4.27). This classified the clay as inorganic, since all the values obtained are <100% and are of low compressibility (Smith, 1978).

Plastic Limit

It can be described as the moisture content at which the soil sample begins to crumble when rolled into about 3 mm diameter thin threads. The results of the plastic limits of the clay sammples are presented in Table 4.27.

Table 4.27. Results of the geotechnical tests for the Mamu/Ajali and Enugu/Nkporo Formation clay samples within the Lower Benue Trough, Nigeria.

Sample No:→	AL1.1	AL1.2	AL2.3	Al.2.4	OF2.1	OF2.2	AG2.1
Specific Gravity	2.11	2.12	2.22	2.24	2.16	2.12	2.12
Moisture Content (%)	35.80	11.11	23.69	19.52	24.65	22.33	31.55
Liquid Limit (%)	49.80	55.56	45.38	49.80	39.42	45.88	33.62
Plastic Limit (%)	25.42	19.35	23.63	21.91	28.57	21.83	18.13
Plasticity Index (%)	24.38	36.21	21.75	27.89	10.85	24.05	15.49

Sample No:→	OK1.1	OK1.2	UD1.1	UD1.2	UD1.3	EN2.1	EN3.1
Specific Gravity	2.38	2.40	2.24	2.30	2.23	2.37	2.22
Moisture Content (%)	25.44	27.64	38.89	28.25	28.25	36.66	30.92
Liquid Limit (%)	43.88	48.29	29.81	38.23	49.23	50.50	38.29
Plastic Limit (%)	18.94	17.35	14.05	20.00	20.00	18.98	18.63
Plasticity Index (%)	24.94	30.94	15.75	18.23	19.23	31.52	19.66

Mamu/Ajali Formation clay samples:

Aloji – AL1.1, AL1.2, AL2.3 and AL2.4.
Ofejiji – OF2.1 and OF2.2.
Agbenema – AG2.1.
Udane-Biomi – UD1.1, UD1.2 and UD1.3.
Okpokwu – OK1.1 and OK1.2.

Enugu/Nkporo Formation clay samples:

Enugu – EN2.1 and EN3.1

Plasticity index

The average values of plasticity indices for Aloji (25.50%), Ofejiji (17.99%), Agbenema (19.23%), Udane-Biomi (19.34%), Oturkpa (31.52%), Okpokwu (27.89%) and Enugu (17.58%) indicated a generally low to medium plasticity for the clay samples (Table 4.27). This observation was further supported by the plasticity graph of Casagrande (1948) (Fig. 4.52), on which nearly all the samples are above the A-line. Thus, the investigated clay deposits within the Lower Benue Trough can be readily moulded and meet pottery requirements though the Atterberg limits of the clay samples are lower than those of some clay deposits from Nigeria (Table 4.28).

4.6.4 Moisture Content

The average moisture content of the clays were generally high (Table 4.27). Average value for Aloji is (22.53%), Ofejiji (23.49%), Agbenema (31.55%), Udane-Biomi (31.79%), Oturkpa (27.64%), Okpokwu (25.44%) and Enugu (33.46%) (Table 4.27). According to Sidi *et al.* (2015), sand material's moisture content is between 10 and 15%, silt 15 and 30% and clay 30 and 50%. Therefore, the studied clay is silty and with the high value of moisture content, it may not be a good construction material for building because according to Stephen and Ikani (2012), materials with a moisture content of more than 16 percent are known to be flooded material and will not be good as material for construction.

4.6.5 Industrial potentials based on chemical composition

The industrial potentials in terms of chemical composition as presented in Tables 4.29 and 4.30 for both raw and fine (<2µm) clay fractions showed that the clay body in its raw state can only be used for the production of glass (Chester, 1973; Table 4.30) while in its fine (<2µm) state, samples from Agbenema, Okpokwu and Enugu can be used in ceramic (Singer and Sonja, 1971), refractory (Parker, 1967) bricks and glass (Chester, 1973). However, sizing and classification, bleaching of the clay with acids, magnetic reduction of iron oxide and other appropriates processing techniques may significantly improve the quality of the clay bodies (Elueze and Bolarinwa, 2001). Extension of the functional applications of the beneficiated clay to paints, pesticides, rubber, paper and even pharmaceuticals may be possible.

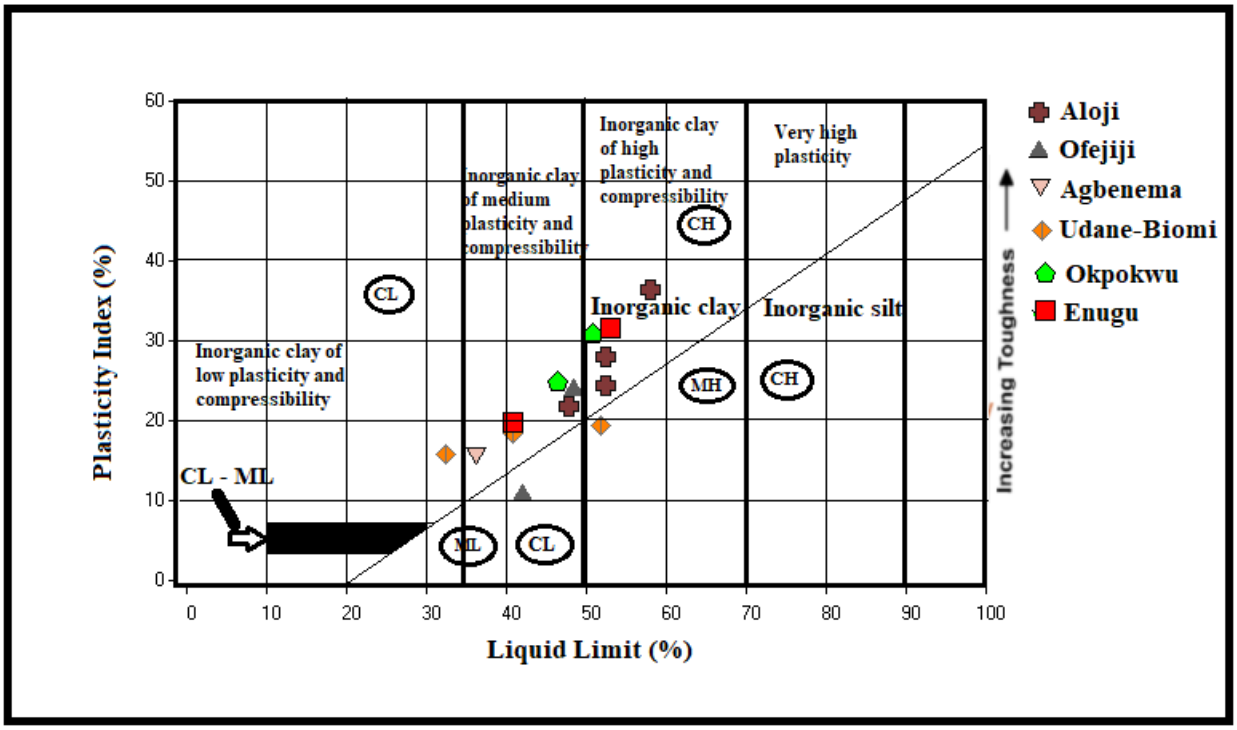

Fig. 4.52. Plasticity chart for the raw clay samples of Mamu/Ajali and Enugu/Nkporo Formations, Lower Benue Trough, Nigeria (After Casagrande, 1948). CL = low-plasticity clay, CH = high-plasticity clay, ML = low-plasticity silt, MH = high-plasticity silt.

Table 4.28. Plasticity test results of Lower Benue Trough clay samples compared with other clays and shales

	*This study	1	2	3	4	5
Liquid limit (%)	44.12	55.83	54.00	66.00	46.00	50.00
Plasticity Index (%)	22.92	31.17	26.00	36.00	78.00	24.50

*Average of 14 samples

1) Mpu Shale (Obrike *et al.,* 2012)

2) Auchi Shale (Emofurieta., 1994)

3) Gombe Shale (Emofurieta., 1994)

4) Okada Shale (Obrike *et al.,* 2007)

5) Abeokuta Sedimentary clay (Elueze and Bolarinwa, 2001)

Table 4.29. Average chemical composition of raw clay sample in the Lower Benue Trough compared with industrial specifications.

	Lower Benue Trough clay deposit					Specifications					
Oxides	1	2	3	4	5	6	7	8	9	10	11
SiO_2	82.65	78.02	87.75	66.35	67.53	48.67	67.50	51-70	47.80	44.90	80-95
Al_2O_3	10.59	9.62	6.78	20.94	17.27	9.45	26.50	25-44	37.00	32.35	12-17
Fe_2O_3	0.40	1.11	1.02	1.42	3.23	2.70	0.50-1.50	0.2-0.7	0.58	0.43	2-3
MnO	0.01	0.01	0.01	0.01	0.01	-----	-----	------	0.10	---	---
MgO	0.03	0.03	0.03	0.09	0.10	8.50	0.10-0.19	0.2-07	0.16	Trace	---
CaO	0.01	0.01	0.01	0.01	0.01	15.84	0.18-0.30	0.1-0.2	0.04	Trace	4-5
Na_2O	0.01	0.06	0.01	0.01	0.07	2.76	0.20-1.50	0.8-3.50	0.10	0.14	---
P_2O_5	0.02	0.11	0.11	0.04	0.08	---	-----	-----	----	---	---
K_2O	0.11	1.14	0.08	0.67	0.01	2.76	1.10-3.10	----	1.10	0.28	---
TiO_2	1.05	1.10	0.98	1.62	1.67	-----	--------	----	0.03	1.80	--
H_2O	4.99	9.46				3.04	12.0-12.50	-----	----	----	--

1- Aloji, 2-Ofejiji, 3-Udane-Biomi, 4- Okpokwu, 5-Enugu, 6-Paint (Payne, 1961), 7-Ceramics (Singer and Sonja 1971), 8- Refractory bricks (Parker, 1967), 9- Coating (Annon, 1972), 10- Rubber (Keller, 1964), and 11-Glass (Chester, 1973)

Table 4.30. Average chemical composition of fine clay samples in the Lower Benue Trough compared with industrial specifications

	Lower Benue Trough clay deposit						Specifications				
Oxides	1	2	3	4	5	6	7	8	9	10	11
SiO_2	73.08	69.94	69.56	66.35	59.44	56.17	48.67	67.50	51-70	47.80	80-95
Al_2O_3	16.69	17.44	18.25	29.64	24.90	25.92	9.45	26.50	25-44	37.00	12-17
Fe_2O_3	0.98	2.21	2.37	1.42	1.54	3.04	2.70	0.50-1.50	0.2-0.7	0.58	2-3
MnO	0.01	0.01	0.01	0.01	0.01	0.03	-----	-----	------	0.10	---
MgO	0.04	0.16	0.07	0.09	0.14	0.32	8.50	0.10-0.19	0.2-07	0.16	---
CaO	0.01	0.05	0.04	0.01	0.05	0.19	15.84	0.18-0.30	0.1-0.2	0.04	4-5
Na_2O	0.04	0.10	0.03	0.01	0.01	0.09	2.76	0.20-1.50	0.8-3.50	0.10	---
P_2O_5	0.04	0.05	0.09	0.04	0.08	0.07	---	-----	-----	----	---
K_2O	0.86	2.16	0.22	0.67	0.51	1.63	2.76	1.10-3.10	----	1.10	---
TiO_2	1.54	1.32	1.41	1.78	1.89	1.62	-----	--------	----	0.03	--
LOI	6.43	9.46	7.70	3.19	11.23	10.65	3.04	12.0-12.50	-----	----	--

1-Aloji, 2-Ofejiji, 3-Udane-Biomi, 4-Okpokwu, 5-Enugu, 6-Agbenema, 7-Paint (Payne, 1961), 8- Ceramics (Singer and Sonja 1971), - Refractory bricks (Parker, 1967), 10- Coating (Annon, 1972) and 11-Glass (Chester, 1973)

Thick deposits of sedimentary clay sequences were observed at Aloji, ~25 kilometres northwest of Anyigba town with thickness of about 11.5 m and Ofejij, 20 kilometres NNE of Iyale General Hospital in Kogi State, the clay deposit is about 15 m thick with intercalation of sandstone of 1.0 - 2.3 m thick. The Ofejiji clay deposit overlies a shaly layer. Agbenema clay deposit, 0.5 and 1.5 km from Iyale General Hospital, Kogi State outcrop as road cuts, which alternates with sandstone has an overall thickness of about 7.5m thick. The clay deposits under the bridge near Oyeama mine, Enugu-Onitsha and Abakaliki-Onitsha expressways in Enugu varied from 17 m to about 23 m thick with intercalation of sandstones and lamination of coal seems. Okpokwu and Oturkpo clay deposits are located along Oturkpo – Gbokolo road. The clay is yellowish brown in colour and about 5m thick with intercalation of sandstone. The thickness of the lateritised sandstone constituting the overburden is very thin. It varies in thickness from 0.3 to 1.0m. This loose overburden could be stripped easily using earth moving equipment such as a bulldozer or front-end loader. Open cast mining is considered an obvious choice due to its cost effectiveness. However, the effects on soil degradation and water pollution must be considered in the environmental impact assessment before operation.

CHAPTER FIVE

SUMMARY AND CONCLUSIONS

The Enugu/Nkporo and Mamu/Ajali Formations of the Lower Benue Trough showed from bottom to top the presence of shale with intercalation of shales overlain by clay and lateritised sandstone of Campanian-Maastrichtian age. Thick sedimentary clay sequences are exposed at Aloji, Ofejiji, Agbenema, Udane-Biomi, Oturkpa, Okpokwu towns underlain by the Mamu/Ajali Formation and Enugu underlain by the Enugu/Nkporo Formation. Thickness of the clay deposits varied from one location to the other; Aloji (8.10 -12.70m), Ofejiji (15.50m), Agbenema (7.5m), Udane-Biomi (5m), Oturkpa (5m), Okpokwu (~5m) and Enugu (17m).

Kaolinite with low subordinate vermiculite are the clay mineral phase while quartz, muscovite and microcline are the non-clay mineral phase. The book-like morphology of the kaolinite and the dominant thin plate characteristics indicated that the clay did not show any effect of possible diagenesis during its formation but underwent relatively stronger chemical weathering. The FTIR bands at 3694.59 - 3660.07 cm^{-1} indicated quartz-rich, kaolinitic clay which under thermal conditions suffered weight loss at temperature range of 499 to 504°C.

The high SiO_2 with moderate Al_2O_3, LOI, low Fe_2O_3 and K_2O compositions showed consistency with quartz-rich kaolinite mineral assemblage that lack expandable clays, such as, montmorillonite or illite. Trace and rare-earth elements concentrations were low but compare favourably with the upper continental crust, dominated by felsic rocks. Sediments poor in clay minerals and rich in quartz grains showed lowest values of most of the trace elements except for Zr. The REE was represented mostly in the samples of fine (< 2μm) clay relative to the raw clay samples.

The clay is derived from intense chemical weathering as shown by the high CIA (>90), PIA (>90) and CIW (>90) values, A-CN-K diagram and the relationship between REE compositions in the precursors and level of weathering (R~0.2) while the positive correlation between LREE and Y confirms that they were significantly enriched during the process of weathering and kaolinization. The log of (K_2O/Na_2O) vs SiO_2, La-Co-Zr/10 and Th-Sc-Zr/10 indicated a passive margin tectonic setting. Th/Sc, La/Sc and Th/Co ratios, TiO_2 vs Al_2O_3, Th/Sc–Zr/Sc, La-Th-Sc and Th - Co - Zr/10 diagrams supported with REEs data indicated a dominantly granitic gneiss provenance and the Cu/Zn, Cu+Mo/Zn, U/Th revealed an oxic depositional environment for the clay deposits while the Eu/Eu* vs $(Gd/Yb)_N$ diagram suggested a Proterozoic age for the granitic gneiss source. The oxygen and hydrogen isotope values of +15.4 to +21.2‰ and -66.4 to -50.8‰ showed a consistency with chemically weathered residual materials deposited under an oxic environmental condition at high temperature of formation (54-91°C), which suggests formation of the kaolinitic clay under a hot and humid paleoclimatic condition warmer than the current one.

Geotechnically, the clay deposits of the Ajali/Mamu and Enugu/Nkporo formations have unique characteristics. They are less plastic, non-expansive, medium to high plasticity and compressibility. Evaluation of the industrial potential of the clays based on their physical, chemical and geotechnical characteristics revealed that these clay deposits in its raw state can only be used for the production of glass and pottery making while in its fine (<2µm) state, samples from Agbenema, Okpokwu and Enugu can be used in ceramic, refractory, bricks and glass making.

The clay deposits in the Lower Benue Trough are quartz-rich kaolinitic clay mineral assemblage derived from the chemical weathering of Proterozoic felsic rocks, deposited under a warmer tropical climatic condition, in a passive margin tectonic setting. These deposits are valuable in clay-based industrial material production but would entail processing and beneficiation to alter their silica/alumina ratios if they are to meet the requirements for other industrial purposes such as rubber, paper, paint and cosmetic industries.

Contributions to knowledge are highlighted below:

- The clay deposit has not undergone diagenesis.
- The high temperature of formation (54 to 91°C) indicates that the kaolinite was formed under warm and moist climatic conditions.
- Rock-fluid interactions were at equilibrium through isotope studies.
- The clay's precursors are of Proterozoic age, evident from Eu/Eu* vs $[Gd/Yb]_N$ diagram.

REFERENCES

Abd El-Moghny, M. W. 2017. The nature, origin and distribution of kaolinite in the Lower Paleozoic Naqus Formation along Western Side of Gulf of Suez, Egypt. *Nature and Science* 15. 2: 49 – 69.

Abou El-Anwar E.A. and Samy Y.M. 2013. Clay Mineralogy and Geochemical Characterization of Some Quaternary Sediments on Giza-Fayium District, Western Nile Valley, Egypt: Relationships to Weathering and Provenance. *Journal of Applied Sciences Research* 9.8 : 4765-4780.

Acra, E. J., Etu-Efeotor J.O., Omoboriowo, A.O. 2013. Sedimentological Attributes and stratigraphic architecture of Ogwashi- Asaba Formation, Anambra Basin. *Nova Journal of Engineering and Applied Sciences* 1.1: 1-10.

Adeigbe, O.C. and Yusuf, A. J. 2013. Geochemical Fingerprints; Implication for Provenance, Tectonic and Depositional Settings of Lower Benue Trough Sequence, Southeastern Nigeria. *Journal of Environment and Earth Science* 3.10: 115-140.

Adeigbe, O. C. and Ayoola Y. J. 2014. Rare Earth Elements Fingerprints: Implication For Provenance, Tectonic And Depostional Settings Of Clastic Sediments Of Lower Benue Trough, Southeastern Nigeria. *New York Science Journal* 7.2: 11-26.

Adeleye, D.R. and Parker. 1975. Diagnostic value of clay minerals in Upper Cretaceous sediments of Southeasthern Nigeria. *Journal of West African Science Association* 20: 47-52.

Ágnes R., Béla R. and Andrea V. 2011. Palaeoenvironmental controls on the clay mineralogy of Carnian sections from the Transdanubian Range (Hungary). *Palaeogeography, Palaeoclimatology, Palaeoecology* 300: 101-112.

Agagu, O.K. 1978. Geology and Petroleum Potentials of Santonian to Maastricthian Sediments in the Anambra Basin, Eastern Nigeria. Ph.D. Thesis. Department of Geology. University of Ibadan. 261Pp.

Ajayi, C.O. 1991. Preliminary Interpretation of the Gravity Anomalies Associated with some Prominent Salt Springs in the Middle Benue Nigeria. *Journal of Mining Geology* 27.1: 87- 94.

Alege, T. S., Idakwo, S. O., Alege, E. K. And Gideon Y. B. 2014 Geology, mineralogy and geochemistry of clay occurrences within the Northern Anambra Basin, Nigeria. *British Journal of Applied Science and Technology* 4.5: 841-852.

Alege , K E., Alege, S. T., Barnabas, G.Y., Idakwo, S. O. 2015. Compositional

Characteristics and Industrial Assessment of the Cretaceous Clay Deposits within Northern Anambra Basin, Nigeria. *Journal of Environment and Earth Science* 5.6: 11-19.

Akande, S. O., Zentelli, M. and Reynolds, P. H. 1989. Fluid inclusion and stable isotope studies of Pb-Zn-fluorite-barite mineralization in the lower and middle Benue Trough, Nigeria. *Mineralium Deposita* 24: 183 – 191.

Akande, S.O., Hoffknecht, A. and Erdtmann, B.D. 1992. Environmental of Ore formation and Anchizonal Metamorphism in Pb-Zn-Ba-F Deposits of the Benue Trough, Nigeria. *Geologie en Mijnbouw* 71:131-144.

Al-Shameri, Aref. A. and Rong, Lei. Xin. 2009. Characterization and evaluation of alga of kaolin deposits of Yemen for industrial application. *American Journal of Engineering and Applied Sciences* 2.2: 292-296.

Anon, 1972. Kaolin in the UK, English China clay deposits on its lead in world paper.

Industrial Minerals 52: 9-29.

ASTM Standard D1557. 2009. Standard test methods for laboratory compaction characteristics of soil using modified effort. ASTM International West Conshohocken, PA. https://doi.org/10.1520/D1557-09.

Awwiller, D. N. 1994. Geochronology and mass transfer in Gulf Coast mudrocks (south-central Texas, USA): Rb-Sr, Sm-Nd and REE systematics. *Chemical Geology* 116: 61–84.

Baioumy, H. 2013. Hydrogen and oxygen isotopic compositions of sedimentary kaolin deposits, Egypt: Paleoclimatic implications. *Applied Geochemistry* 182-188.

Balan, E., Saitta , A. M., Mauri, F. and Calas G. 2001. First-principles modeling of the infrared spectrum of kaolinite. American Mineralogist 86: 1321–1330.

Bentabol, M., Ruiz Cruz, M.D., Huertas, F.J., Linares, J. 2006. *Clays Clay Minerals* 54: 667-677.

Bessong M. Abderrazak E.A. Hell J.V. Claude F., Ndjeng E., Ngos S., Nolla J.D., Dissombo E. Mfoumbeng M.P. and Mbang B.A.R. 2011. Diagenesis in Cretaceous Formations of Benue Trough in the Northern Part of Cameroon: Garoua Sandstone. *World Journal of Engineering and Pure and Applied Sciences* 1.3: 58-67.

Bhatia, M.R., and Crook, K.A.W., 1986. Trace Element Characteristics of Graywackes and Tectonic Setting Discrimination of Sedimentary Basins. *Contributions to mineralogy and Petrol*ogy 92: 181– 193.

Bigeleisen, J. Perlman, M.L. Prosser, H.C. 1952. Conversion of hydrogenic materials to hydrogen for isotopic analysis. *Anal. Chem.* 24, 1356-1357.

Binks, R. M. and Fairhead, J. D. 1992. A plate tectonic setting for Mesozoic rifts of

West and Central Africa. *Tectonophysics* 213: 141-151.

Bird M.I. and Chivas A.R. 1988. Stable-isotope evidence for low-temperature kaolinitic weathering and post-formational hydrogen-isotope exchange in Permian kaolinites. *Chemical Geology (Isotope Geoscience Section)* 72: 249-265.

Blatt, H. Middleton, G. and Murray, R. 1972. *Origin of sedimentary rocks*: New Jersey (Prentice Hall), 573-576.

Boynton, W.V. 1984. *Geochemistry of the rare earth elements: meteorite studies*. In: Henderson, P. (ed), Rare Earth Element Geochemistry, Elsevier, 63-114.

Burke, K.C., Dessauvagie and Whiteman, A,J. 1970. *Geological History of the Benue Valley and adjacent Areas*, In African Geology, University of Ibadan Press, 187-206.

Burke, K.C., Dessauvagie, T.F.J., and Whiteman, A,J. 1971. The opening of the Gulf of Guinea and the Geological History of the Benue Depression and Niger Delta. *Natural Physical Science* 233. 38: 51-55.

Burke, K.C., and Whiteman, T.F.J., 1973. *Uplift, Rifting and break up of Africa: Implications on Continental Drift to Earth Sciences* (Edited by Tarling, D.H. and Runcom, S.K.), 735-755.

Brindley G.W. and Brown G. 1980. *Crystal structure of clay minerals and their X-ray identification*. Mineralogical Society, London 495.

British Standards. 1990. *Methods of Testing for Soils for Civil Engineering Purposes, BS 1377*. British Standards Institution. London.

Casagrande, A. 1948. Classification and Identification of Soil. *Trans-American Society of Civil Engineer* 113 – 901.

Chester J. H. 1973. *Refractory, Production and properties*. Iron and steel institute, London, 295- 315.

Churchman G.J. 2000. *The alteration and formation of soil minerals by weathering*. In Handbook of soil science (Summer, M.E., ed.) *CRC* Press New York 1. F3-27.

Clayton R.N. and Mayeda T.K. 1963. The use of bromine pentafluoride in the extraction of oxygen from oxides and silicates for isotopic analysis. *Geochimica et Cosmochimica Acta* 27: 43- 52.

Condie, K.C., Boryta, M.D., Liu, J., and Quian, X. 1992. The origin of khondalites: geochemical evidence from the Archean to Early Proterozoic granulitic belt in the North China Craton: *Precambrian Research* 59.3-4: 207-223.

Condie, K.C. 1993. Chemical composition and evolution of the upper continental

crust: Contrasting results from surface samples and shales. *Chemical Geology* 104: 1-37

Cox, R., Lowe, D.R., Cullers, R.L., 1995. The influence of sediment recycling and basement composition on evolution of mudrock chemistry in the southwestern United States*: Geochimica et Cosmochimica Acta*, 59.14: 2919-2940.

Cox M. E., Preda M. and Brooke B. 2000. General features of the geo-setting of pumice stone for the determination of metals in sediments. *Marine Pollution Bulletin* 34.8: 637 – 644.

Cratchley C. R., and Jones G. P. 1965. An interpretation of the geology and gravity anomalies of the Benue valley, Nigeria. Overseas Geological Survey and Geophysical 1.

Cullers, R. L., Barrett, T., Carlson, R. and Robinson, B. 1987. Rare-Earth element and mineralogic changes in Holocene soil and stream sediment: a case study in the wet mountains region, Colorado, USA. *Chemical Geology* 63: 275–297.

Cullers, R. L., Basu, A. and Suttner, L. 1988. Geochemical signature of provenance in sand-size material in soils and stream sediments near the Tobacco Root batholith, Montana, USA. *Chemical Geology* 70: 335–348.

Cullers, R. L. 1994a. The chemical signature of source rocks in size fractions of Holocene stream sediment derived from metamorphic rocks in the wet mountains region, Colorado, USA. *Chemical Geology* 113: 327–343.

Cullers, R. L. 1994b. The controls on the major-and trace-element variation of shales, siltstones and sandstones of Pennsylvanian-Permian age from uplifted continental blocks in Colorado to platform sediments in Kansas, USA. *Geological Society of American Bullettin* 58: 4955–4972.

Edomwonyi-Otu L. C., Aderemi B. O., Ahmed A. S., Coville N. J., Maaza M. 2013.Influence of Thermal Treatment on Kankara Kaolinite. Opticon1826 15. 5: 1-5. DOI: http://dx.doi.org/10.5334/opt.bc

Ehrenberg, S.N., Aagaard, P., Wilson, M. J., Fraser, A.R. and Duthie, D. M.. L. 1993. Depth-dependent transformation of kaolinite to Dickite in sandstones of the Norwegian continental shelf. *Clay Minerals* 28: 325- 352.

Elueze, A. A. and Bolarinwa A. T. 2001. Appraisal of the residual and sedimentary clays in parts of Abeokuta area, southwestern Nigeria. *Journal of Mining and Geology 37*.1: 7-14.

Emofurieta, W.O., Ogundimu, T.O. and Imeokparia, E.G. 1994. Mineralogical, geochemical and economic appraisal of some clay and shale deposits in southwestern and northwestern Nigeria. *Journal of Mining and Geology* 30.2:151-159.

Etim, O. N., Louis, P. and Maurin, J. C. 1988. Interpretation of electrical soundings on the Abakaliki Lead-Zinc and barite prospects, S.E. Nigeria: Geological and genetic implications. *Journal of African Earth Sciences* 7: 743-747.

Ezepue M. C. 1984. The geologic setting of lead-zinc deposits at Ishiagu, Southeastern Nigeria. *Journal of African Earth Sciences* 2: 97-101.

Fallick, A.E., Macaulay G.I and Haszeldine R.S. 1993. Implications of linearly correlated oxygen and hydrogen isotopic compositoins fpr kaolinite and illite in the Magnus Sandstone, North Sea. Clay and clay minerals 41.2: 184 – 190.

Faure, G. and Mensing, T.M. 2005. *Isotopes: Principles and Applications*. Third Edition. Wiley and Sons, Inc., Hoboken, New Jersey Pp. 897.

Federal Ministry of Works and Housing (1997). *Nigerian General Specifications for Roads and Bridge works (NGS)*. Federal Highway Department 2.

Fedo, C.M., Nesbitt, H.W., and Young, G.M. 1995. Unraveling the effects of potassium metasomatism in sedimentary rocks and Palaesols, with implications for paleoweathering conditions and provenance.*Geology* 23: 921-924.

Felhi,M., Tlili, A., Gaied, M.E., and Montacer, M. 2008. Mineralogical study of kaolinitic clays from Sidi El Bader in the far North of Tunisia. *Applied Clay Science* 39: 208-217.

Feng, R. and Kerrich, R. 1990. Geochemistry of fine grained clastic sediments in the Archean Abitibi greenstones belt, Canada: implications for provenance and tectonic setting. *Geochimica et Cosmochimica Acta* 54: 1061–1081.

Friedman, I. 1964. The variation of the deuterium content of natural waters in the hydrological cycle. *Reviews of Geophysics* 2: 177-224.

Gadsen, J. A. 1975. "*Infrared Spectra of Minerals and Related Inorganiccompounds*," Butterworths, London.

Gaspe A., Messer P. and Young P. 1994. Clay testing. A manual on clay/non-clay measuring technique. Intermediate Technology Publications. 17Pp.

Gharrabi, M., Velde, B. and Sagon, J.P. 1998. The transformation of illite to muscovite in pelitic rocks: Constraints from X-ray diffraction. *Clays and Clay Minerals* 46: 79-88.

Giletti, B.J. 1985. The nature of oxygen transport within minerals in the presence of hydrothermal water and the role of dilusion. *Chemical Geology* 53 : 197-206.

Gilg., H.A. 2000. D/H evidence for the timing of? kaolinization in Northeast Bavaria, Germany. *Chemical Geology* 170: 5-18.

Giese R.F. 1991. Kaolin minerals: structures and stabilities. *Revised Mineralogy* 19, 29-66.

Gofiantini, 1984. Advisory group meeting on stable isotope reference samples for geochemical and hydrological investigation. *Report Director General*. IAEA, Vienna.

Goldschmidt, V.M. 1958. *Geochemistry*. Oxford University Press, UK, 491.

Grant, N.K. 1969. The Late Precambrian to Paleozoic Pan –African Orogeny of Ghana, Togo, Dahomey and Nigeria. *Geological Society of American Bullettin* 8.

Gromet, L. P., Dymek, R. F., Haskin, L. A. and Korotev, R. L. 1984. The 'North American Shale Composite': its compilation, major and trace element characteristics. *Geochimica et Cosmochimica Acta*, 48:2469–2482.

Hallberg, R.O. 1976. A geochemical method for investigation of palaeoredox conditions in sediments : *Ambio Special Report* 4:139-147.

Harnois, L. 1988. The new index, a new chemical index of weathering. *Sedimentary Geology* 55:319-322.

Hayashi, K., Fujisawa, H., Holland, H., Ohmoto, H. 1997. Geochemistry of ~1.9 Ga sedimentary rocks from northeastern Labrador, Canada: *Geochimica et Cosmochimica Acta*, 61.19: 4115-4137.

Heckroodt, R.O. and Buhmann, D. 1987. Genesis of South African residual kaolins from sedimentary rocks. Pp. 128– 134 in: *Proceedings of the International Clay Conference*, Denver, 1985. (L.G. Schultz, H. van Olphen and F.A. Mumpton, editors). The Clay Minerals Society, Bloomington, Indiana.

Herron, M.M. 1988. Geochemical Classification of Terrigenous Sands and Shales from core to log data. *Journal of sedimentary Petrology* 58: 820 – 829.

Hoefs, J. 2004. *Stable isotope geochemistry*. 5th Edition. Springer, Berlin

Huber J.M. 1985. *Kaolin Clays*. Huber Corporation (Clay Division), Georgia, U.S.A.

Idakwo, S. O., Barnabas, G. Y., Alege, S. T., Alege, K. E. 2013. Paleoclimate Reconstruction during Mamu Formations (Cretaceous) Based on Clay Mineral Distribution in Northern Anambra Basin, Nigeria. *International Journal of Science and Technology* 2.12: 879 – 885.

Ikoro, D. O., Agumanu, A.E., and Okereke C. N. 2012. Tectonic and paleoenvironmental significance of clay mineral suites in the Southern Benue Trough. *International Journal of Emerging trends in Engineering and Development* 2.2:1-10.

Imeokparia, E.G. and Onyeobi, T.U.S. 2007. Geochemical and depositional characteristics of Maastrichian shales in parts of southwestern Nigeria. *Journal of Mining and Geology* 43.2:167-174.

Ishaku, H.T. and Majid, M.R. 2010. X- Raying Rainfall Pattern and Variability in North eastern Nigeria: Impacts Access to Water Supply. Journal of Water Resource and Protection 2: 952-959.

Ismael, S.I. 1996. Mineralogical and geochemical studies of the black shales intercalated with the phosphate deposits along the Red Sea coast, Egypt. Ph.D. Thesis Ain Shams University Cairo, Egypt.

Jackson, M. L. 1979. *Soil Chemical Analysis:* An Advanced Course. 2nd edition, 11th printing. Madison, Wisconsin.

Jones, B., and Manning, D.C. 1994. Comparison of geochemical indices used for the interpretation of paleo-redox conditions in Ancient mudstones: *Chemical Geology* 111.1-4: 111-129.

Kakiuchi M. 1994. Temperature dependence of fractionation of hydrogen isotopes in aqueous sodium chloride solutions. *Journal of solution Chemistry* 23: 1073-1987.

Keller, W. D. 1964. *Kird-Othmer Encyclopedia of Chemical Technology*. New York: John Wiley and Sons Incorporation, 541-585.

Liu, Z.Z., C. Yulong, P. Colin, C. Fernando, Siringan and Q. Wua. 2009. Chemical weathering in Luzon, Philippines from clay mineralogy and major-element geochemistry of river sediments, *Applied Geochemistry*, 24: 2195-2205.

Longstaffe F.J. and Ayalon A. 1990. Hydrogen-Isotope geochemistry of diagenetic clay minerals from cretaceous sandstones, Alberta, Canada: Evidence for exchange. *Applied Geochemistry* 5: 657-668.

MacKenzie R.C. 1957. *The Differential Thermal Investigation of Clays*. Monogrph 3, Mineralogical Society, London, 456.

McLennan, S. M. and Taylor, S. R. 1991. Sedimentary rocks and crustal evolution: tectonic setting and secular trends. *Journal of Geology* 99: 1–21.

McLennan, S. M., Hemming, S., McDaniel, D. K. and Hanson, G. N. 1993. Geochemical approaches to sedimentation, provenance, and tectonics. Processes Controlling the Composition of Clastic Sediments (Johnson, M. J. and Basu, A., eds.*),Special paper, Geological Society of America* 284: 21–40.

Meunier, A. and Velde, B. 2004. *Illite*. Springer, Berlin, 286 pp

Middelburg J. J., Van der Weijden C. H. and Woittiez J. R. W. 1988. Chemical processes affecting the mobility of major, minor and trace elements during weathering of granitic rocks. Chemical Geology 68: 253–273.

Michael, E. B. 1998. *Handbook of Thermal Analysis and Calorimetry: Principles and practice*; Elsevier.

Mishra, M, and Sen, S. 2012. Provenance, tectonic setting and source area weathering of Mesoproterozoic Kaimur Group, Vindhyan Supergroup, Central India. *Geologica acta* 10.3: 283 – 293.

Mizota C. and Longstaffe F.J. 1996. Origin of cretaceous and Oligocene kaolinites from the Iwaizumi Clay deposit, Iwate, Northeastern Japan, *Clay and Clays Minerals* 44: 408-416.

Moore D.M. and Reynolds R.C. Jr. 1997. *X-ray Diffraction and the Identification and Analysis of Clay Minerals.* Oxford University Press, Oxford, 378.

Moosavirada, S.M., Janardhanab, M. R., Sethumadhava, M.S., Moghadamc, M. R. and Shankara, M. 2011. Geochemistry of lower Jurassic shales of the Shemshak Formation, Kerman Province, Central Iran: Provenance, source weathering and tetonic setting. *Chem. Erde* 71: 279 – 288.

Murray, H. H., Janssen, J. 1984. Oxygen isotopes-indicators of kaolinite genesis. In: *Proceedings of 27th International Geological Congress on Non Metallic Ores* 15: 287- 303.

Murat R.C. 1972. *Stratigraphy and paleogeography of the cretaceous and lower tertiary in Southern Nigeria.* In Dessauvagie, T.T.J. and Whiteman, A.J. (eds.) African Geology. University of Ibadan Press, Ibadan, Nigeria. 251 - 266..

Nath, B.N., Bau, M., Ramalingeswara Rao, B., Rao, Ch.M. 1997. Trace and rare earth elemental variation in Arabian Sea sediments through a transect across the oxygen minimum zone: *Geochimica et Cosmochimica Acta* 61.12: 2375-2388.

Nicholas A. R. and Neil J. T. 2013. Oxygen and hydrogen isotope compositions of paleosol phyllosilicates: Differential burial histories and determination of Middle–Late Pennsylvanian low-latitude terrestrial paleotemperatures. *Palaeogeography, Palaeoclimatology, Palaeoecology* 392: 382 – 397.

Najime, T. 2011. Depositional framework and Cretaceous stratigraphy of the Gboko Area Lower Benue Trough, Nigeria. *Journal of Mining and Geology* 47.2: 147–165.

Nesbitt, H. W. and Young, G. M. 1982. Early Proterozoic climates and plate motions inferred from major element chemistry of lutites. *Nature* 299: 715–717.

Nesbitt, H. W., Markovics, G. and Price, R. C. 1980. Chemical processes affecting alkalis and alkali earths during continental weathering. *Geochimica et Cosmochimica Acta* 44: 1659–1666.

Nesbitt, H. W. and Young, G. M. 1996. Petrogenesis of sediments in the absence of chemical weathering:effects of abrasion and sorting on bulk composition and mineralogy. *Sedimentology* 43, 341–358.

Nesbitt, H. W., Young, G. M., McLennan, S. M. and Keays, R. R. 1996. Effects of chemical weathering and sorting on the petrogenesis of siliciclastic sediments, with implications for provenance studies. *J. Geol*. 104, 525–542.

Nesse W.D. 2000. *Introduction to Mineralogy*. New York: Oxford UP

Nkwonta I.K. and Kene,P.O. 2005. *Use of Aeromagnetics in Mineral / Structural Exploration in Nigeria*. American Geophysical Union, Spring Meeting 2005, abstract #NS238 - 12.

Nwachuckwu, S.O. 1972. Tectonic Evoluion of the Southern Portion of the Benue Trough. Nigeria. *Geologcal Magazine 109. 5:* 411 – 419.

Obaje, N.G., Abaa, S.I., Najime, T., Suh, C.E. 1999. Economic geology of Nigerian coals resources—a brief review. *African Geosciences Review* 6:71–82.

Obaje, N.G. 2009. *Geology and Mineral Resources of Nigeria*. Lecture Notes in Earth Sciences. Springer-verlag, Berlin, Heildeberg, 120, 57-68.

Obrike, S.E., Osadebe, C.C. and Onyeobi, T.U.S. 2007. Mineralogical, geochemical, physical and industrial characteristics of shale from Okada area, southwestern Nigeria. *Journal* of *Mining and Geology* 43.2:109-116.

Obrike, S.E. Onyeobi, T.U.S. Anudu, G.K. and Osadebe, C.C. 2012. Compositional Characteristics and Industrial Assessment of the Asu River Group Shale in Mpu Area, Southeastern Nigeria. *Journal of Mining and Geology* 48.2: 117–126.

Odoma, A.N., Obaje, N.G.,Omada, J.I., Idakwo,S.O. and Erbacher, J. 2015. Mineralogical, chemical compositon and distribution of rare earth elements in clay-rich sediments from Southeasthern Nigeria. *Journal of African Earth Sciences* 102: 50-60.

Offodile, M.E. 1976. The Geology of the Middle Benue Nigeria. *Special Publication of Paleontological Institute University of Upsala* 4: 99. 1–166.

Ofoegbu, C.O. 1985. A Review of the Geology of the Benue Trough of Nigeria. *Journal African Earth Sciences* 3: 283 – 291.

Oha, I. A., Onuoha, K. M., Dada, S. S. 2017. Contrasting styles of lead-zinc-barium mineralization in the Lower Benue Trough, Southeastern Nigeria. *Earth Science Researh Journal* 21.1: 7 - 16.

Ojoh, K.A. 1992. The Southern part of the Benue Trough (Nigeria) Cretaceous stratigraphy, basin analysis, paleo-oceanography and geodynamic evolution in the equatorial domain of the South Atlantic. *NAPE Bull* 7:131–152.

Ojo, O. J., Adepoju, S.A., Adewole, T. M. and Abiola, A. O. 2011. Sedimentological and geochemical studies of Maastrichtian clays in Bida Basin, Nigeria: Implication for resource potential. *Centrepoint Journal (Science Edition)* 17.2: 71-88.

Okunlola, O.A. and Idowu O. 2012. The geochemistry of claystone-shale deposits from the Maastritchian Patti formation, Southern Bida basin, Nigeria. *Earth Sciences Research Journal* 16.2: 57-67.

Olade, M. A. 1975. Evolution of Nigerian Benue Trough (Aulacogen): A Tectonic Model. *Geological Magazine* 112: 575 – 583.

O'Neil, J. R. and Taylor, H.P. Jr. 1967. The oxygen isotope and cation exchange chemistry of feldspars. *American Mineralogist* 52: 1414 – 1437.

Parham W.E. 1966. Lateral variations of clay mineral assemblage in modern and ancient sediments: *In Proceedings of the International Clay Conference*, Jerusalem 1: 136 – 145.

Parker E.K. 1967. Minerals data book for Engineers and scientists. McGraw Hill Book Company, New York, 283 Pp.

Patterson, E. and Swaffield, R. 1987. Thermal analysis. In a handbook of *determinative methods in clay mineralogy*, M.J. Wilson ed., Blackie, Chapman and Hall, Newyork, 99-132

Petters, S. W. and Ekweozor, C. M. 1982. Petroleum geology of the Benue Trough and southeastern Chad Basin, Nigeria. *Geological Society of America Bulletin* 68: 1141-1149.

Pettijohn, F. J. 1975. *Sedimentary Rocks*, 3rd edn, Harper and Row, New York. 628pp.

Pettijohn, F. J., Potter, P. E., and Siever, R. 1972. Sand and sandstone*:* New York, Springer.

Perri, F. 2014. Composition, provenance and source weathering of Mesozoic sandstones from Western-Central Mediterranean Alpine Chains. *Journal African Earth Science* 91: 32-43.

Perry, C. 2006. *Library map collection.* http://www.lib.utexas.edu

Payne, H.F. 1961. *Organic coating technology*, vol. II: pigments and pigmented coatings: John Wiley and Sons, Inc. New York.

Rebelle, M. 1990. The marine transgression in the Benue Trough (N.E Nigeria) a paleogeographic interpretation of the Gongila Formation. *Journal of African Earth Sciences* 10: 643-656.

Reyment, R. A. 1965. Aspect of the geoloy of Nigeria *Univ. Ibadan Press*. Nigeria Pp. 145.

Riley, K.W. and Saxby, J.H. 1983. Association of organic matter and vanadium in oil shale from the Toolebuc Formation of the Eromanga Basin, Australia. *Chemical Geology* 37.

Roser, B.P., and Korsch, R.J. 1986. Determination of tectonic setting of sandstone. Mudstone suites using SiO_2 content and K_2O/Na_2O ratio: *Journal of Geology* 94: 635 – 650.

Roy, P.D., Caballero, M., Lozano, R. and Smykatz-Kloss, W., 2008. Geochemistry of late quaternary sediments from Tecocomulco lake, central Mexico: implication to chemical weathering and provenance. *Chem. Erde Geochem*. 68: 383–393.

Saccà C., D. Saccà P., Nucera and Fazio A.D. 2011. Composition and geochemistry of clay sediments offshore the northeastern Sicilian coast (Southeastern Tyrrhenian Sea, Italy). *Estuarine, Coastal and Shelf Science* 92: 564-572.

Savin, S.M. and Hsieh, J.C.C. 1998. The hydrogen and oxygen isotope geochemistry of pedogenic clay minerals: Principles and theoretical background. *Geoderma* 82:227-253.

Savin S.M and Epstein S. 1970a. The Oxygen and hydrogen isotope geochemistry of clay minerals. *Geochimica et Cosmochimica Acta* 34: 25-42.

Savin S.M and Epstein S. 1970b. The Oxygen and hydrogen isotope geochemistry of ocean Sediments and shales. *Geochimica et Cosmochimica Acta* 34: 43-63.

Schellmann, W. 1986. A new definitionof laterite. Geological Survey India Memo. 120: 1-7

Shapiro, L. and Breger, I.A. 1968. *Geochemistry of organic substances* by S.M. Manskaya and T.V. Drozdova. Pergamon Press, Oxford.

Shepard, F.P. 1954. Nomenclature based on sand-silt-clay ratios. Journal of Sedimentary Petrology 24: 151-158.

Sheppard, S. M. F., Neilsen, R. L., and Taylor Jr., H. P. 1969. Oxygen and hydrogen isotope ratios of clay minerals from porphyry copper deposits: *Economic Geology* 64: 755- 777.

Sheppard, S.M.F. and Gilg H.A. 1996. Stable isotope geochemistry of clay minerals. *Clay Minerals* 31:1-21.

Sidi, M.W., Thaffa, A.B. and . Garba, A.B. 2015. Geotechnical investigation of soil around Arawa-Kundulum Area of Gombe Town, North-Eastern Nigeria, Nigeria. IOSR Journal of Applied Geology and Geophysics (IOSR-JAGG) 3.1: 7-15.

Simpson, A. 1954. The Nigerian coalfield. The geology of parts of Onitsha, Owerri and Benue provinces. *Bulletin Geological Survey Nigeria* 24.8: 85.

Singer F, and Sonja S.S. 1971. *Industrial ceramics*. Chapman and Hall, London, 18-56.

Song E., Zhang K., Chen J., Wang C., Jiang G., Yin K., Hong H., Churchman J.G. 2014. Clay mineralogy and its paleoclimatic singificance of Oligocene-Miocene sediments in the Gerze Basin, Tibet. Acta Geologica Sinica 88.5: 1579-1591.

Slack, J.F. and Stevens, P.J. 1994. Clastic metasediments of the Early Proterozoic Broken Hill Group, New South Wales, Australia: geochemistry, provenance and metallogenic significance. *Geochimica et Cosmochimica Acta* 58: 3633-3652.

Smith, G. N. 1978. *Elements of soil mechanics for civil and mining engineers* (4th ed.). Crosby Lockwood Staples.

Stephen J. M. and Ikani N. A. 2012. Geotechnical investigation of soils: A case study of Gombe Town (Sheet 152NW), North Eastern Nigeria. *International Journal of Modern Engineering Research* (IJMER) 2.6: 4280-4286.

Stow, D.A. V. and Atkin, B. P. 1987. Sediment facies and geochemistry of Upper Jurassic mudrocks in the central North Sea area. - *Petroleum Geology of North West Europe* (Brooks J and Glennie K., eds.), 797-808, Graham and Trotman, London.

Suttner, L. J., and Dutta, P. K. 1986. Alluvial sandstone compositin and paleoclimate, Framework mineralogy: *Journal of Sedimentary Petrology* 56.3:329- 345.

Tan K. H. 1998. *Principle of Soil Chemistry*. Mariel Dekker Inc. U.S.A. 512 Pp.

Thiry, M. 2000. Palaeoclimatic interpretation of clay minerals in marine deposits: an outlook from the continental origin. *Earth-Science Reviews* 49: 201-221.

Taylor, G. and Eggleton, R.G. 2001. *Regolith geology and geomorphology.* John Willey and Sons. England.

Taylor S.R, McLennan S.M. 1981. The composition and evolution of the continental crust: rare earth element evidence from sedimentary rocks. *Philosophical Transactions of the Royal Society london* A 301:381–399.

Taylor, S.R., and McLennan, S. 1985. *The Continental Crust: Its Composition and Evolution:* Blackwell, Oxford.

Thomas M.F. 1994. *Geomorphology in tropics: A case study of weathering and dednudation in low latitude*. John Wiley and Sons. Chichester, England.

Turekian, K.K., 1978. Nickel. In: Wedepohl, K.H. (Ed.), *Handbook of Geochemistry*, vol. II/3. Springer, Berlin, 28-K-1–28-L-3.

Ukaegbu, V.U. and Akpabio, I.O. 2009. Geology and Stratigraphy of Middle Cretaceous Sequences Northeast of Afikpo Basin, Lower Benue Trough, Nigeria. *The Pacific Journal of Science and Technology* 10: 518-527.

Velde, B and Meunier, A. 2008. *Fundamentals of clay mineral crystal structure and physicochemical properties*. The origin of clay minerals in soils and weathered rocks, 3-73.

Vital, H., K. Stattegger and C.D. Grabe-Schonberg. 1999. Composition and trace element geochemistry of detrital clay and heavy mineral suites of the lowermost Amazon River : a provenance study. *Journal of Sedimentary Research* 69: 563- 575.

Weaver, C.E. 1985. *Development in sedimentology - Clay, Muds and Shales*. Elsevier, Amsterdam.

Wronkiewicz, D. J. and Condie, K. C. 1987. Geochemistry of Archean shales from the Witwatersrand Supergroup, South Africa: source-area weathering and provenance. *Geochimica et Cosmochimica Acta* 51: 2401–2416.

Yang, S.Y. and Youn, J.S.2007. Geochemical compositions and provenance discrimination of the central south Yellow Sea sediments. Mar. Geol. 243: 229–241.

Zhou, T. and Dobos, S. K. 1994. Stable isotope geochemistry of Kaolinite from the "White Section," Black Ridge, Clermont, Central Queensland: Implications for the age and origin of The "White Section". *Clays and Clay Minerals*. 42.3: 269-275.

Appendix 1: Result of sieve analysis for the Mamu/Ajali and Enugu/Nkporo Formations raw clay samples in the Lower Benue Trough, Nigeria.

AL 1.1

Particle size (mm)	Particle size (phi)	Mass Retained (g)	Percent Retained (%)	Cummulative Mass Retained (%)	Cummulative Mass Passing (%)
11.200	-3.49	0.00	0.00	0.00	100.00
5.600	-2.49	0.00	0.00	0.00	100.00
4.000	-2.00	0.00	0.00	0.00	100.00
2.000	-1.00	0.00	0.00	0.00	100.00
1.000	0.00	2.10	1.60	1.60	98.40
0.850	0.23	1.30	0.70	2.30	97.70
0.600	0.74	2.00	1.00	3.30	96.70
0.425	1.23	1.80	0.90	4.20	95.80
0.250	2.00	1.40	0.70	4.90	95.10
0.150	2.74	85.10	42.60	47.50	52.50
0.075	3.74	88.60	44.30	91.80	8.20
Base pan	1.00	13.30	6.70	98.50	1.50

Total = 200.00 g

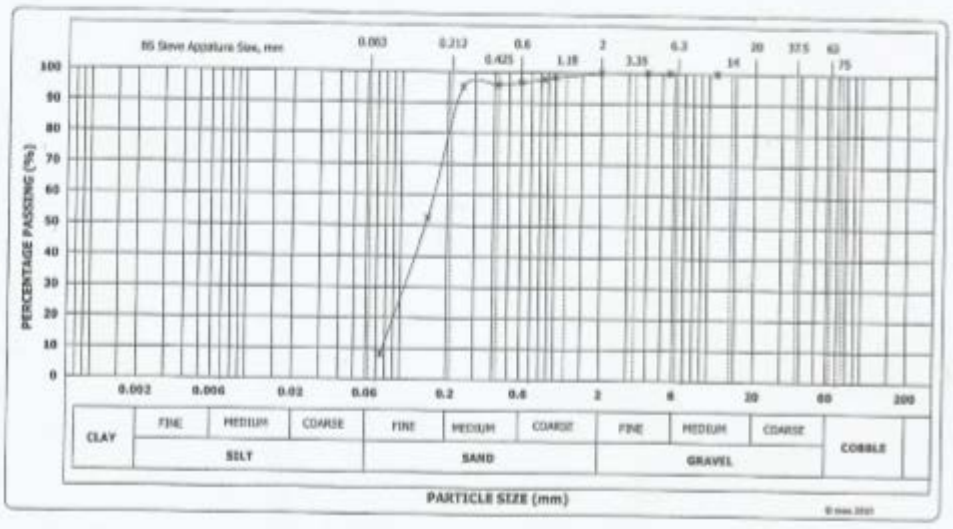

AL 1.2

Particle size (mm)	Particle size (phi)	Mass Retained (g)	Percent Retained (%)	Cummulative Mass Retained (%)	Cummulative Mass Passing (%)
4	-200	0	0	0	100
2.000	-1.00	0.30	0.15	0.15	99.85
1.000	0.00	4.10	2.05	2.20	97.80
0.850	0.23	1.00	0.50	2.70	97.30
0.600	0.74	3.20	1.60	4.30	95.70
0.425	1.23	2.10	1.05	5.35	94.65
0.250	2.00	1.80	0.90	6.25	93.75
0.150	2.74	62.90	31.45	37.70	62.30
0.075	3.74	110.40	55.20	92.90	7.10
-Base pan	1.00	9.30	4.70	99.00	1.00

Total = 200.00 g

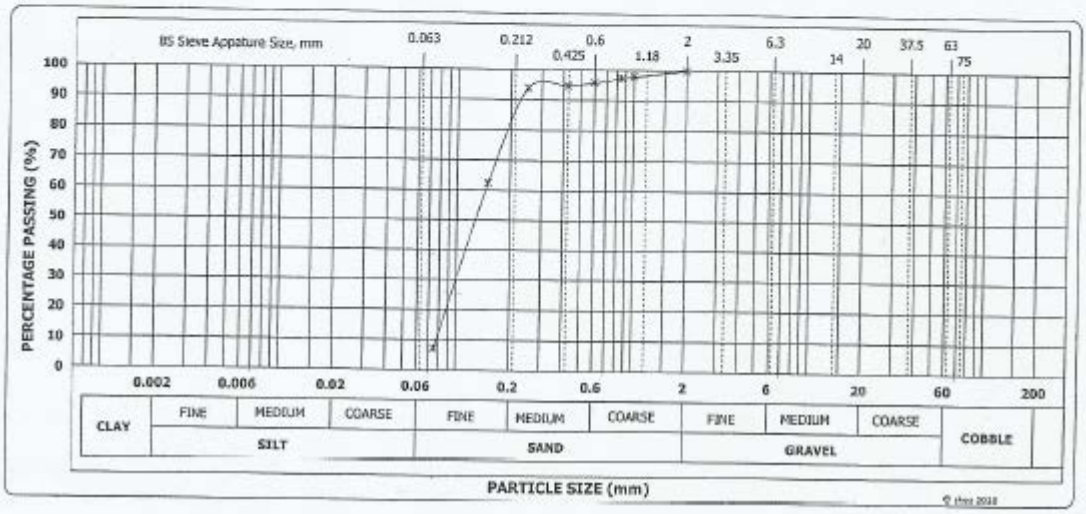

AL 2.3

Particle size (mm)	Particle size (phi)	Mass Retained (g)	Percent Retained (%)	Cummulative Mass Retained (%)	Cummulative Mass Passing (%)
4.000	-2.00	0.00	0.00	0.00	100.00
2.000	-1.00	0.00	0.00	0.00	100.00
1.000	0.00	8.10	4.05	4.05	95.95
0.850	0.23	2.00	1.00	5.05	94.95
0.600	0.74	7.70	3.85	8.90	91.10
0.425	1.23	3.10	1.55	10.45	89.55
0.250	2.00	2.40	1.20	11.65	88.35
0.150	2.74	76.30	38.65	50.30	49.70
0.075	3.74	90.70	45.35	95.65	4.35
Base pan	1.00	6.90	3.45	99.15	0.85

Total = 200.00 g

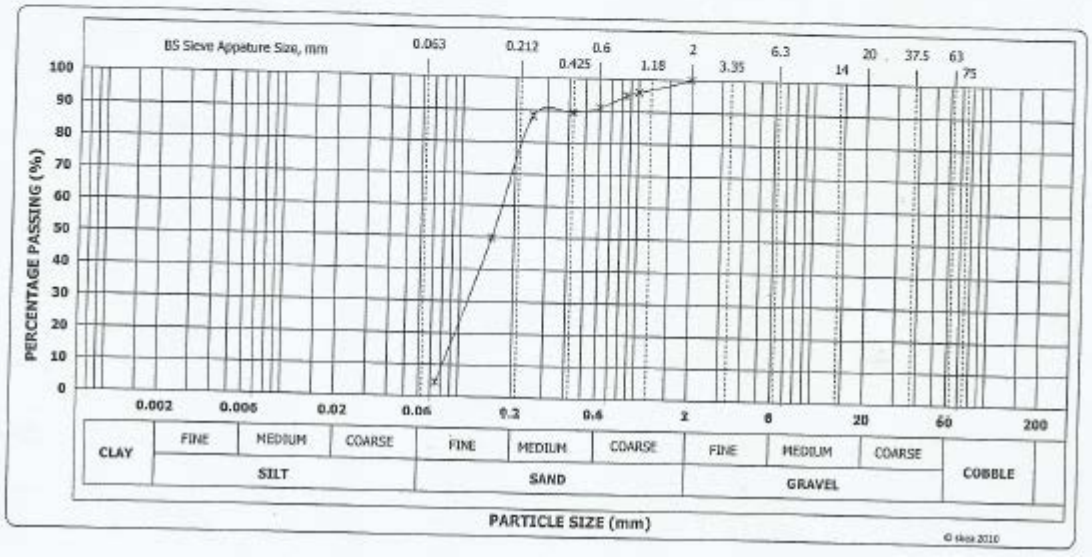

AGBENEMA 1.2

Particle size (mm)	Particle size (phi)	Mass Retained (g)	Percent Retained (%)	Cummulative Mass Retained (%)	Cummulative Mass Passing (%)
4	-2	0	0	0	100
2.000	-1.00	9.80	4.90	4.90	95.10
1.000	0.00	11.60	5.80	10.70	89.30
0.850	0.23	2.80	1.40	12.10	87.90
0.600	0.74	9.10	4.60	16.70	83.30
0.425	1.23	0.50	0.25	16.95	83.05
0.250	2.00	2.20	1.10	18.05	81.95
0.150	2.74	1.20	0.60	18.65	81.35
0.075	3.74	130.80	65.40	84.05	15.95
Base pan	1.00	28.20	14.10	98.15	1.85

Total = 200.00 g

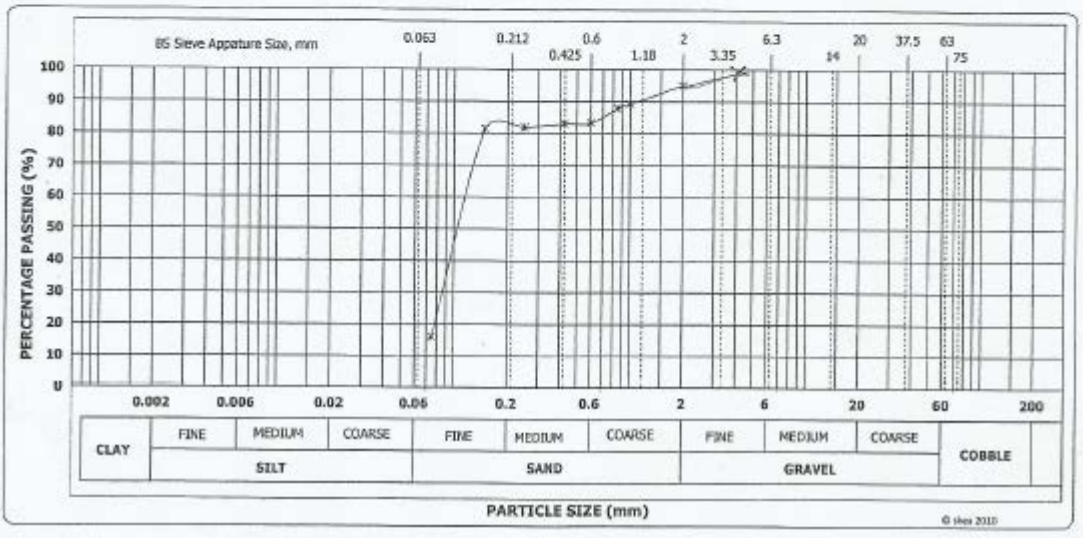

AGBENEMA 2.1

Particle size (mm)	Particle size (phi)	Mass Retained (g)	Percent Retained (%)	Cummulative Mass Retained (%)	Cummulative Mass Passing (%)
4	-2	6.9	3.45	3.45	96.55
2.000	-1.00	15.80	7.90	11.35	88.65
1.000	0.00	9.90	4.95	16.30	83.70
0.850	0.23	1.70	0.85	17.15	82.85
0.600	0.74	6.40	3.20	20.35	79.65
0.425	1.23	3.20	1.60	21.95	78.05
0.250	2.00	1.90	0.95	22.90	77.10
0.150	2.74	6.80	3.40	26.30	73.70
0.075	3.74	129.90	64.95	91.25	8.75
• Base pan	1.00	24.90	12.45	98.15	1.85

Total = 200.00 g

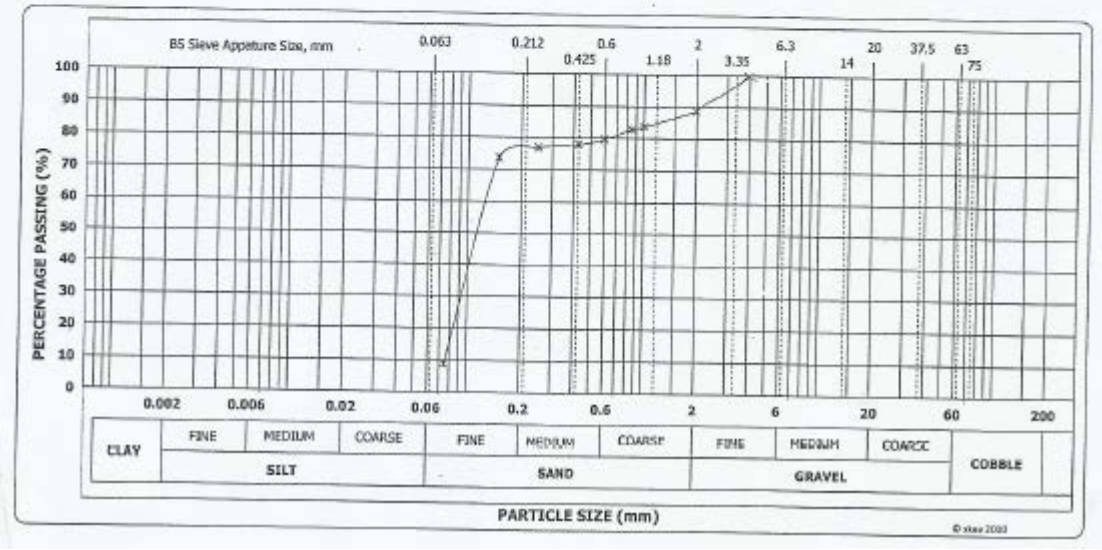

OFEFIJI 1.1

Particle size (mm)	Particle size (phi)	Mass Retained (g)	Percent Retained (%)	Cummulative Mass Retained (%)	Cummulative Mass Passing (%)
4	-2	8.2	4.1	4.1	95.9
2.000	-1.00	28.30	14.20	18.30	81.70
1.000	0.00	22.30	11.20	29.50	70.50
0.850	0.23	0.40	0.20	29.70	70.30
0.600	0.74	2.00	1.00	30.70	69.30
0.425	1.23	3.60	1.80	32.50	67.50
0.250	2.00	0.30	0.20	32.70	67.30
0.150	2.74	1.00	0.50	33.20	66.80
0.075	3.74	84.40	42.20	75.40	24.60
Base pan	1.00	48.70	24.40	99.80	0.20

Total = 200.00 g

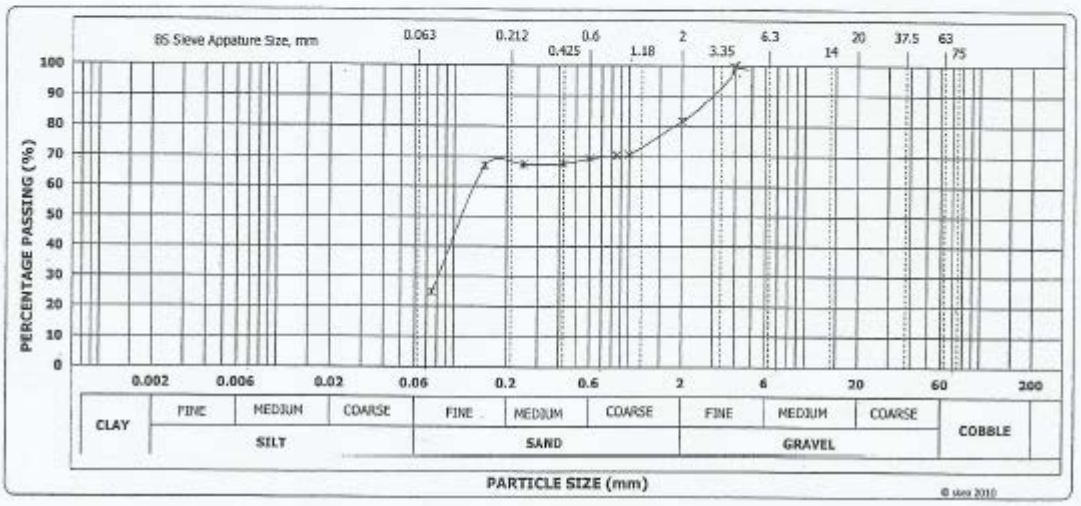

OFEFIJI 2.3

Particle size (mm)	Particle size (phi)	Mass Retained (g)	Percent Retained (%)	Cummulative Mass Retained (%)	Cummulative Mass Passing (%)
4	-2	8.2	4.1	4.1	95.9
2.000	-1.00	28.30	14.20	18.30	81.70
1.000	0.00	22.30	11.20	29.50	70.50
0.850	0.23	0.40	0.20	29.70	70.30
0.600	0.74	2.00	1.00	30.70	69.30
0.425	1.23	3.60	1.80	32.50	67.50
0.250	2.00	0.30	0.20	32.70	67.30
0.150	2.74	1.00	0.50	33.20	66.80
0.075	3.74	84.40	42.20	75.40	24.60
Base pan	1.00	48.70	24.40	99.80	0.20

Total = 200.00 g

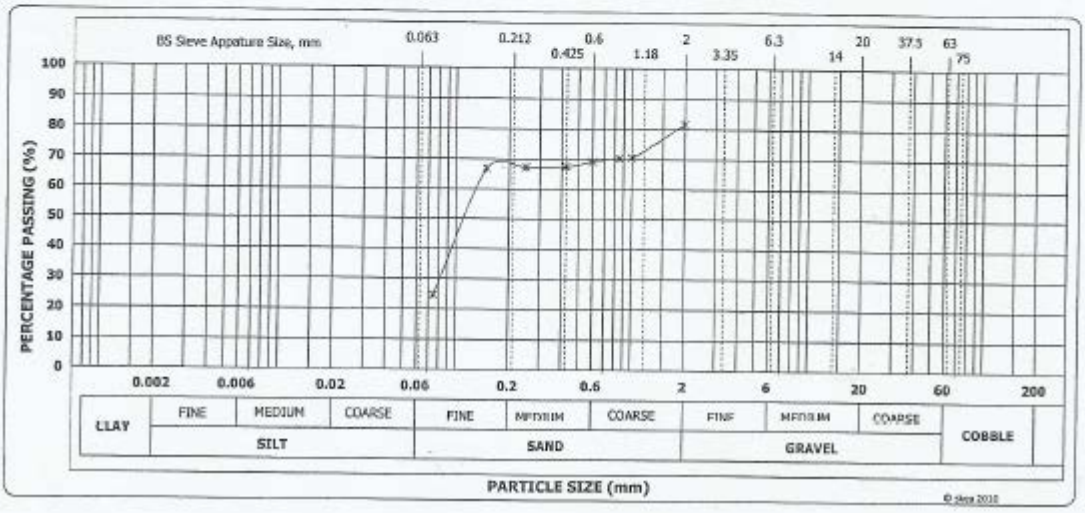

OFEFIJI 2.4

Particle size (mm)	Particle size (phi)	Mass Retained (g)	Percent Retained (%)	Cummulative Mass Retained (%)	Cummulative Mass Passing (%)
4	-2	0	0	0	100
2.000	-1.00	0.00	0.00	0.00	100.00
1.000	0.00	1.30	1.15	1.15	98.85
0.850	0.23	0.90	0.45	1.60	98.40
0.600	0.74	3.10	2.55	4.15	95.85
0.425	1.23	1.20	0.60	4.75	95.25
0.250	2.00	11.80	5.90	10.65	89.35
0.150	2.74	63.30	31.65	42.30	57.70
0.075	3.74	88.60	44.30	86.60	13.40
Base pan	1.00	19.70	9.85	97.45	2.55

Total = 200.00 g

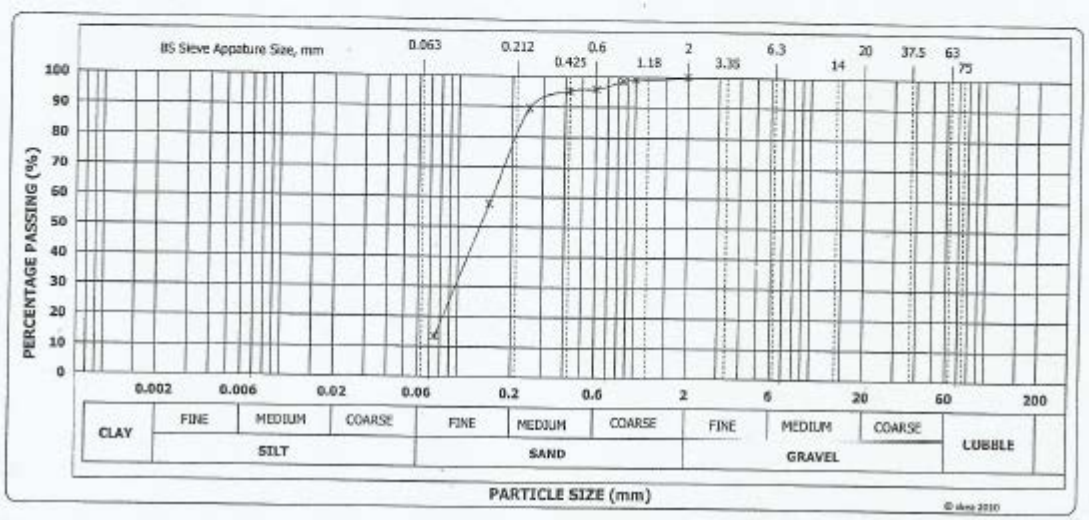

OFEFIJI 2.5

Particle size (mm)	Particle size (phi)	Mass Retained (g)	Percent Retained (%)	Cummulative Mass Retained (%)	Cummulative Mass Passing (%)
4	-2	0	0	0	100
2.000	-1.00	0.50	0.25	0.25	99.75
1.000	0.00	4.10	2.10	2.35	97.65
0.850	0.23	1.80	0.90	3.25	96.75
0.600	0.74	2.80	1.40	4.65	95.35
0.425	1.23	1.80	0.90	5.15	94.85
0.250	2.00	7.60	3.80	7.95	92.05
0.150	2.74	70.10	35.10	43.05	56.95
0.075	3.74	100.10	50.10	93.15	6.85
Base pan	1.00	9.70	4.90	98.05	1.95

Total = 200.00 g

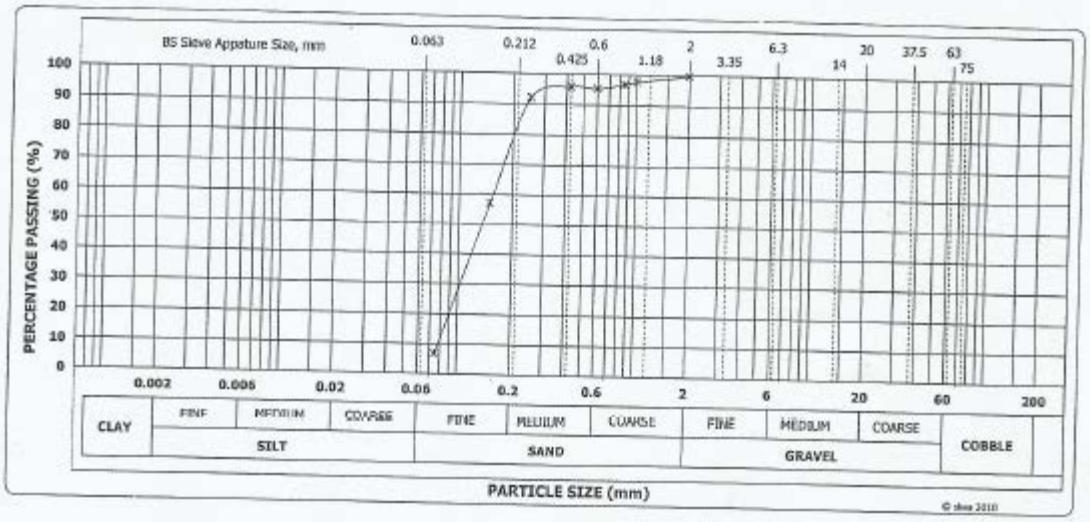

SAMPLE U.D 1.2

Particle size (mm)	Particle size (phi)	Mass Retained (g)	Percent Retained (%)	Cummulative Mass Retained (%)	Cummulative Mass Passing (%)
4	-2	1.5	0.8	0.8	99.2
2.000	-1.00	3.80	1.90	2.70	97.30
1.000	0.00	1.80	0.90	3.60	96.40
0.850	0.23	0.30	0.20	3.80	96.20
0.600	0.74	0.80	0.40	4.20	95.80
0.425	1.23	0.90	0.50	4.70	95.30
0.250	2.00	0.80	0.40	5.10	94.90
0.150	2.74	108.10	54.10	59.20	40.80
0.075	3.74	70.20	35.10	94.30	5.70
Base pan	1.00	9.30	4.70	99.00	1.00

Total - 200.00 g

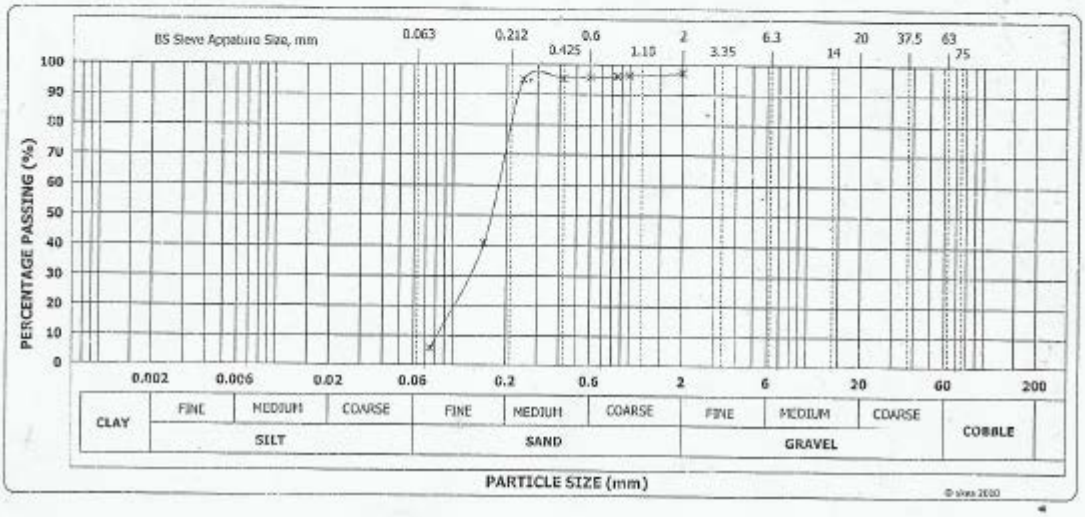

SAMPLE U.D 13

Particle size (mm)	Particle size (phi)	Mass Retained (g)	Percent Retained (%)	Cummulative Mass Retained (%)	Cummulative Mass Passing (%)
4	-2	0	0	0	100
2.000	-1.00	4.30	2.15	2.15	97.85
1.000	0.00	2.80	1.40	3.55	96.45
0.850	0.23	0.90	0.45	4.00	96.00
0.600	0.74	1.30	0.65	4.65	95.35
0.425	1.23	1.10	0.55	5.00	95.00
0.250	2.00	1.70	0.85	5.85	94.15
0.150	2.74	76.40	38.20	44.05	55.95
0.075	3.74	98.80	49.40	93.45	6.55
Base pan	1.00	12.70	6.35	99.00	1.00

Total = 200.00 g

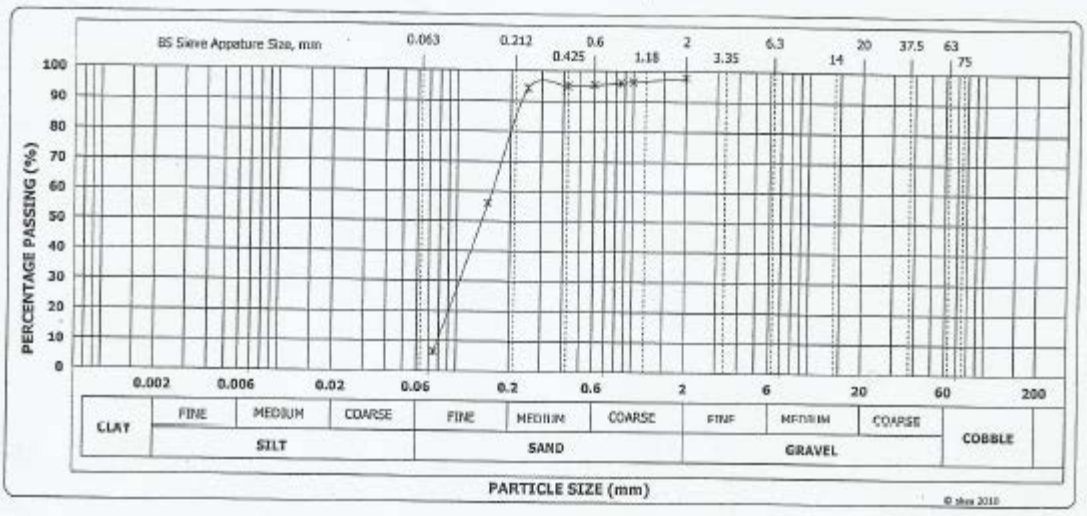

SAMPLE O T U 1.1

Particle size (mm)	Particle size (phi)	Mass Retained (g)	Percent Retained (%)	Cummulative Mass Retained (%)	Cummulative Mass Passing (%)
11.200	-3.49	0.00	0.00	0.00	100.00
5.600	-2.49	0.00	0.00	0.00	100.00
4.000	-2.00	0.00	0.00	0.00	100.00
2.000	-1.00	0.00	0.00	0.00	100.00
1.000	0.00	11.60	5.80	5.80	94.20
0.850	0.23	7.50	3.80	9.60	90.40
0.600	0.74	3.80	1.90	11.50	88.50
0.425	1.23	7.90	4.00	15.50	84.50
0.250	2.00	21.40	10.70	26.20	73.80
0.150	2.74	79.80	39.90	66.10	33.90
0.075	3.74	47.20	23.60	89.70	10.30
Base pan	1.00	15.20	7.60	97.30	2.70

Total = 200.00 g

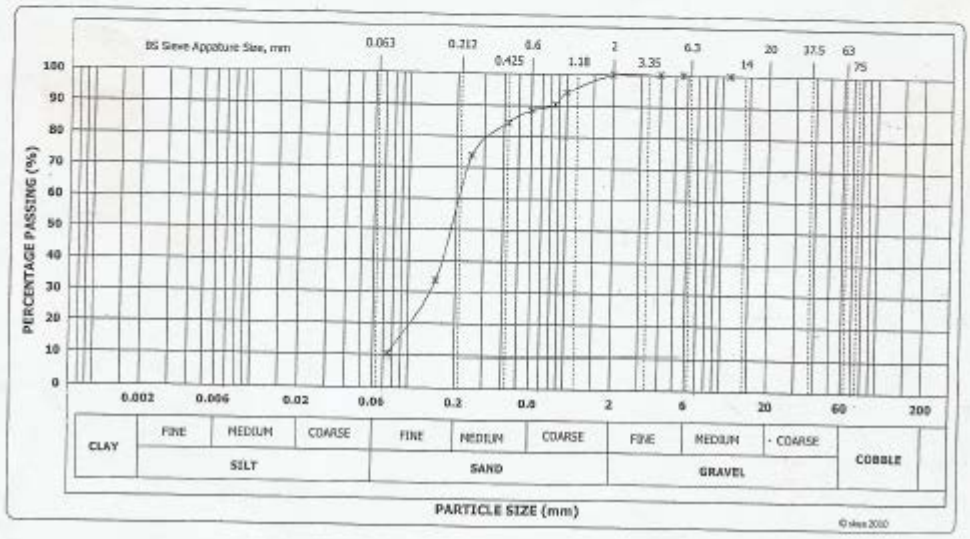

OKP 1.1

Particle size (mm)	Particle size (phi)	Mass Retained (g)	Percent Retained (%)	Cummulative Mass Retained (%)	Cummulative Mass Passing (%)
4	-2	0	0	0	100
2.000	-1.00	33.90	17.00	17.00	83.00
1.000	0.00	27.50	13.80	30.80	69.20
0.850	0.23	2.00	1.00	31.80	68.20
0.600	0.74	9.00	4.50	36.30	63.70
0.425	1.23	8.90	4.50	40.80	59.20
0.250	2.00	17.60	8.80	49.60	50.40
0.150	2.74	17.90	9.00	58.60	41.40
0.075	3.74	51.60	25.80	84.40	15.60
Base pan	1.00	26.90	13.50	96.90	3.10

Total = 200.00 g

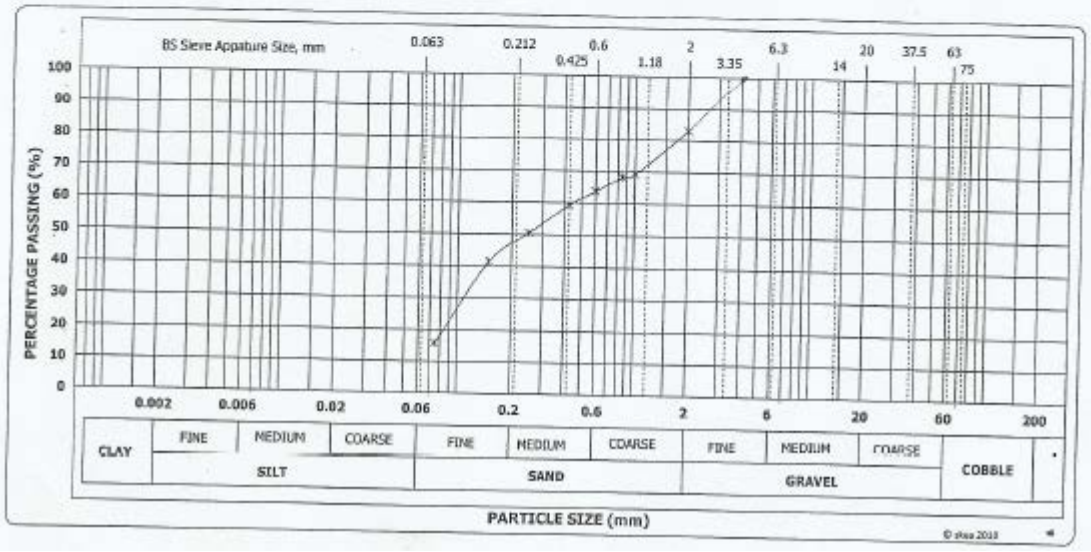

ENUGU 2.1

Particle size (mm)	Particle size (phi)	Mass Retained (g)	Percent Retained (%)	Cummulative Mass Retained (%)	Cummulative Mass Passing (%)
4.000	-2	8.7	4.35	4.35	95.65
2.000	-1.00	40.10	20.05	24.30	75.70
1.000	0.00	16.60	8.30	32.60	67.40
0.850	0.23	1.80	0.90	33.50	66.50
0.600	0.74	5.40	2.70	36.20	63.80
0.425	1.23	5.00	2.50	38.70	61.30
0.250	2.00	2.40	1.20	39.90	60.10
0.150	2.74	11.60	5.80	45.70	54.30
0.075	3.74	105.10	52.55	98.25	1.75
Base pan	1.00	3.00	1.50	99.30	0.70

Total = 200.00 g

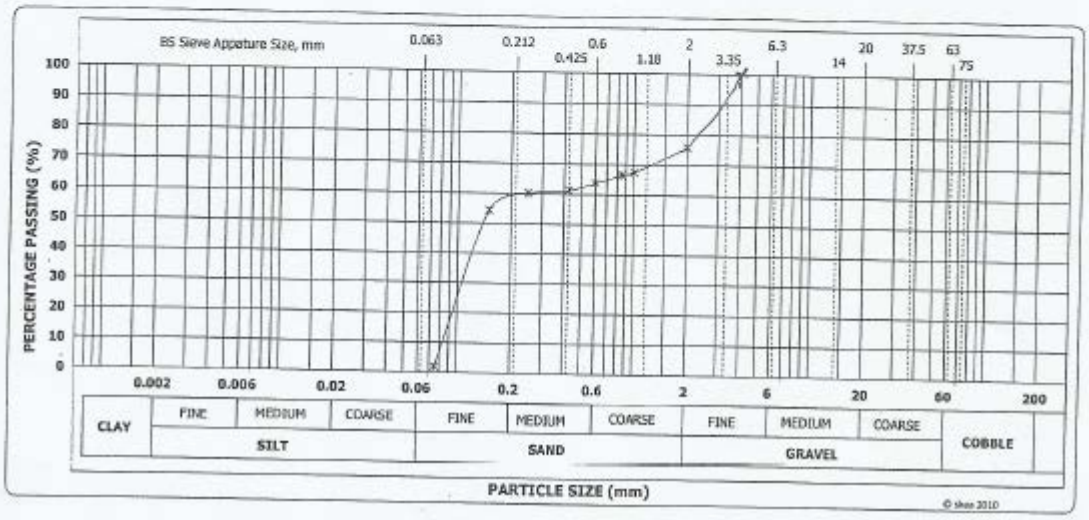

ENUGU 3.1

Particle size (mm)	Particle size (phi)	Mass Retained (g)	Percent Retained (%)	Cummulative Mass Retained (%)	Cummulative Mass Passing (%)
4	-2	19	9.5	9.5	90.5
2.000	-1.00	29.50	14.80	24.30	75.70
1.000	0.00	28.30	14.20	38.50	61.50
0.850	0.23	0.90	0.50	39.00	61.00
0.600	0.74	6.40	3.20	42.20	57.80
0.425	1.23	4.80	2.40	44.60	55.40
0.250	2.00	3.30	1.70	46.30	53.70
0.150	2.74	8.60	4.30	50.60	49.40
0.075	3.74	83.10	41.60	92.20	7.80
Base pan	1.00	14.20	7.10	99.30	0.70

Total = 200.00 g

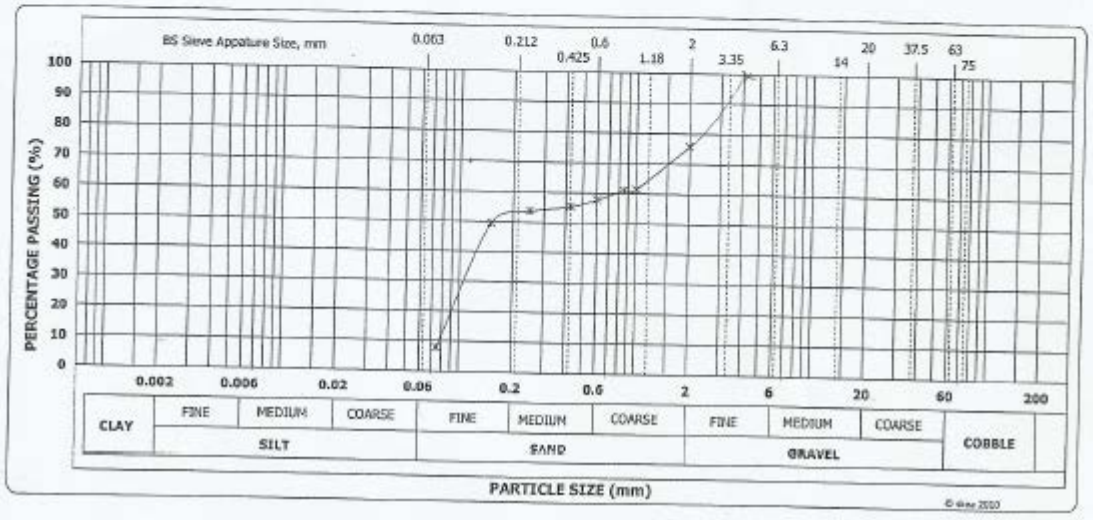

Appendix 2. DTA/TGA curves

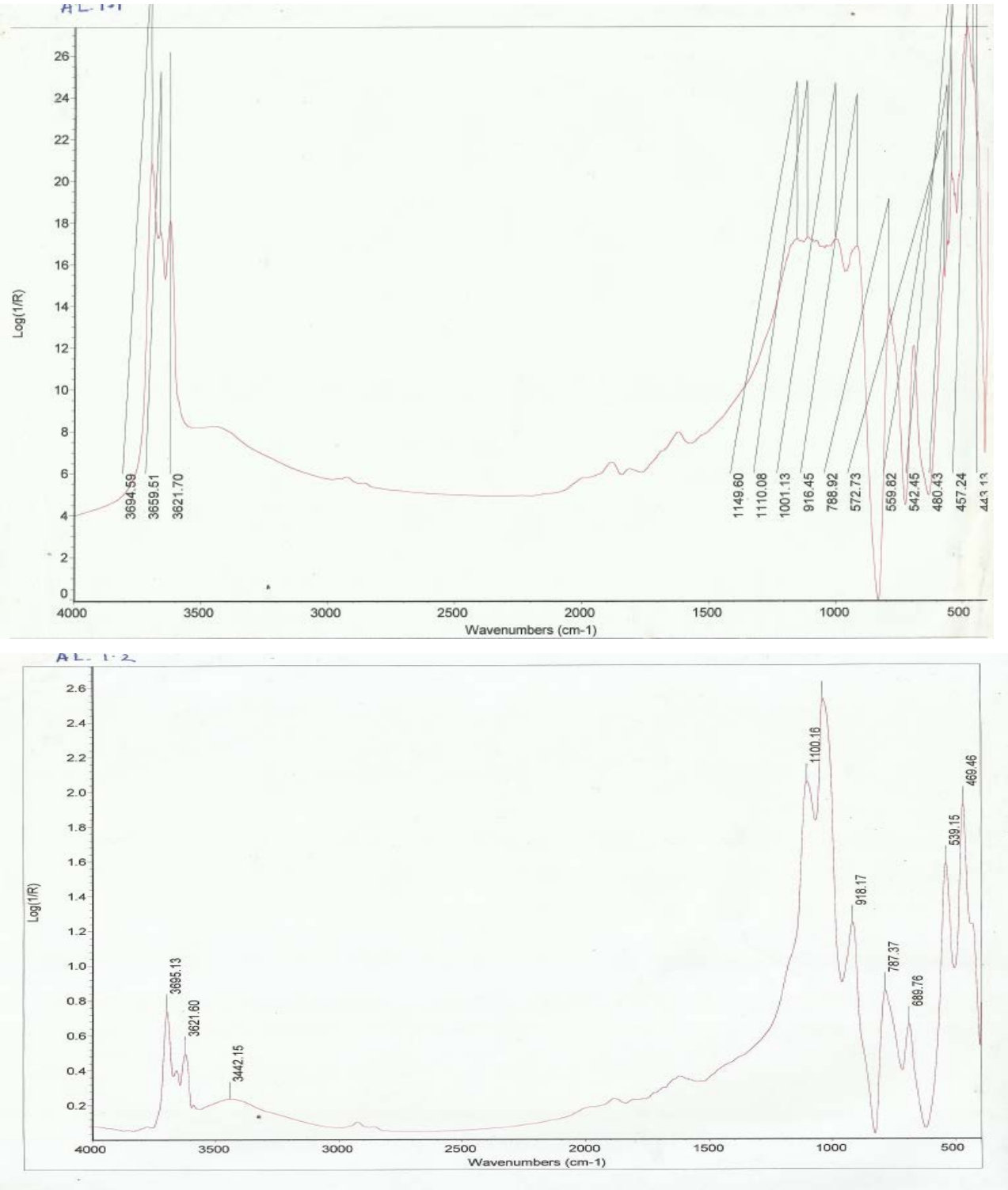

DTA-TGA curves for fine (<2µm) clay fraction from Aloji (AL1.1 and AL1.2 of Mamu/Ajali Formation, Lower Benue Trough, Nigeria.

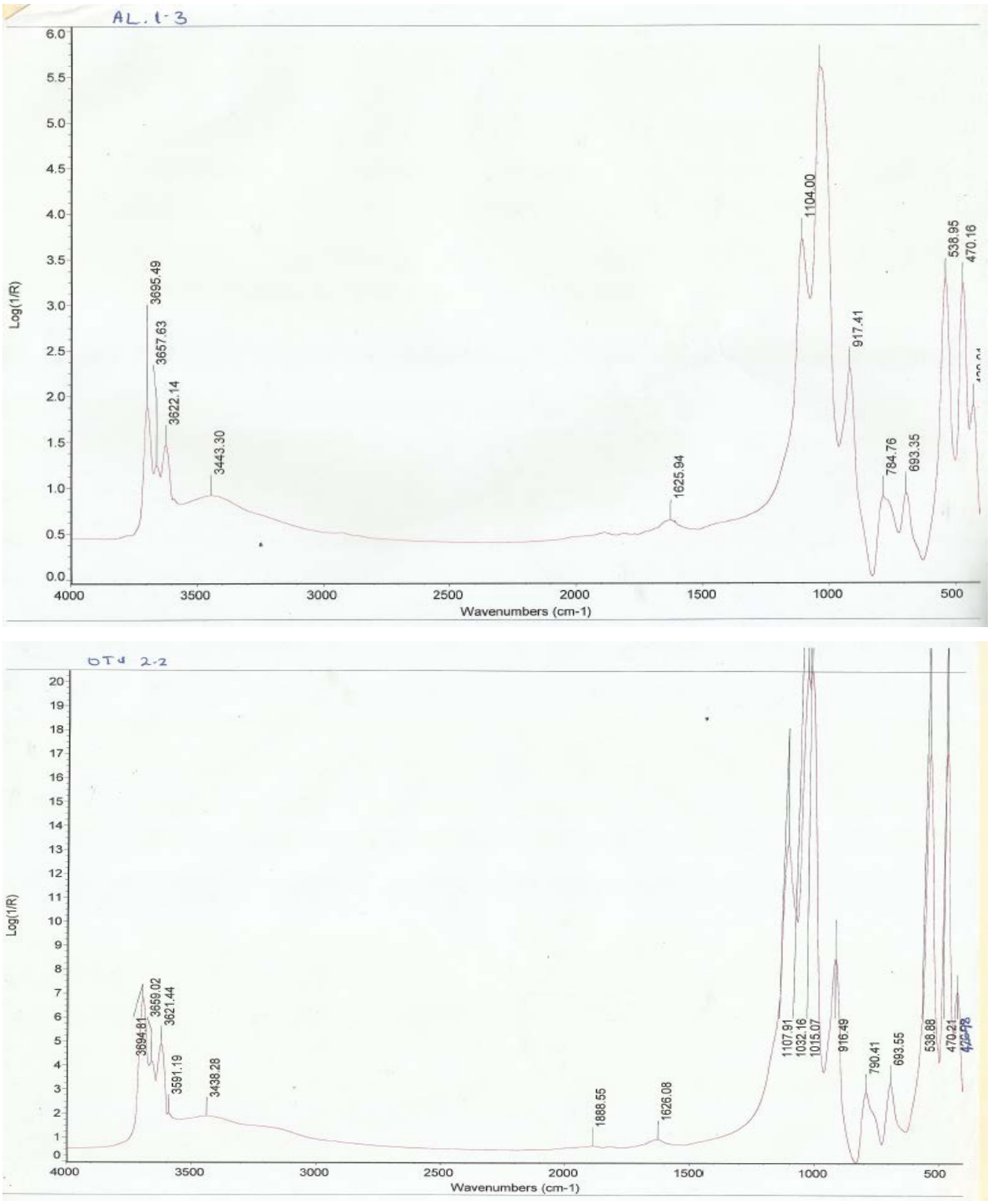

DTA-TGA curves for fine (<2µm) clay fraction from Aloji (AL1.3) and Oturkpa (OT2.2) of Mamu/Ajali Formation, Lower Benue Trough, Nigeria.

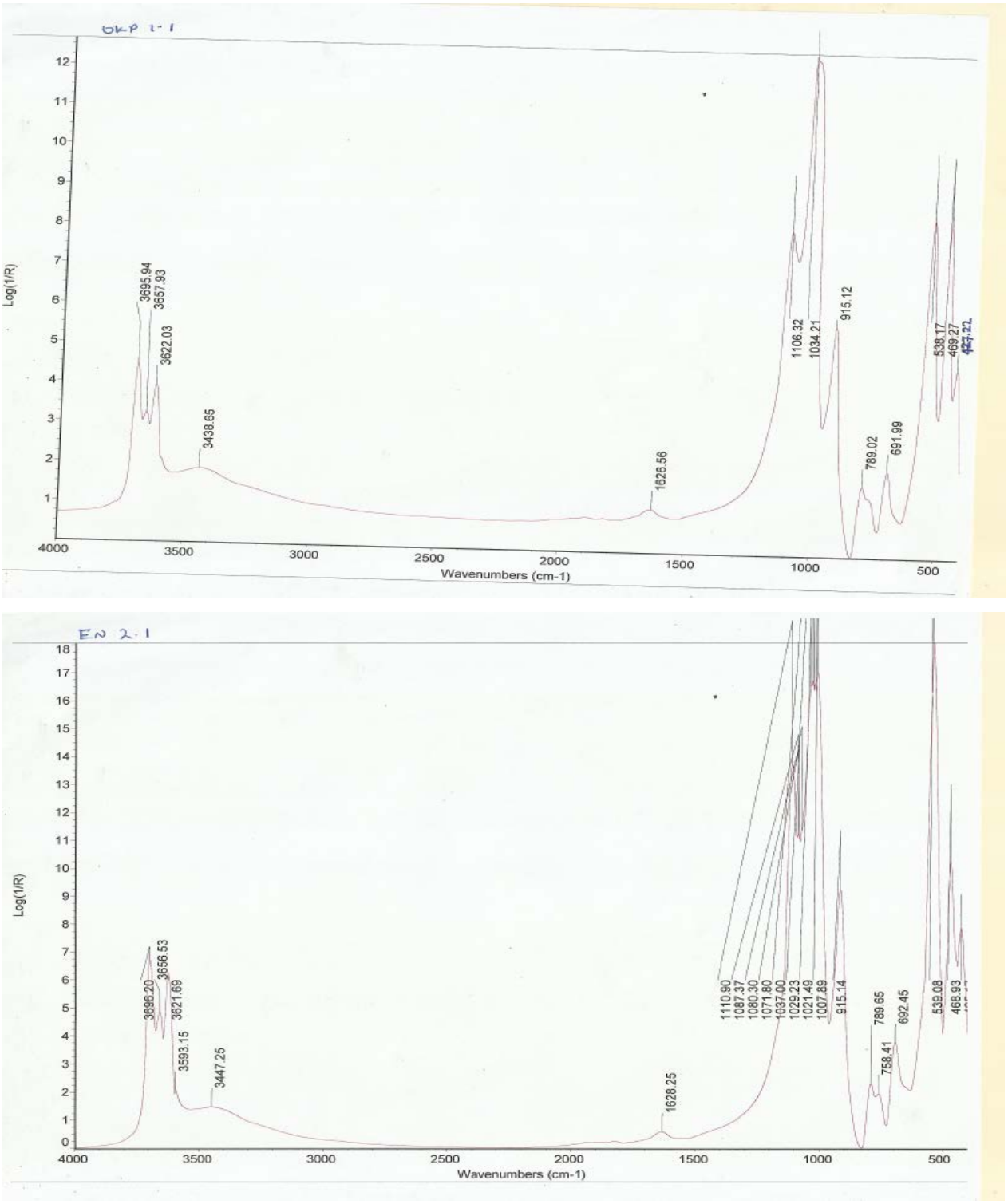

DTA-TGA curves for fine (<2µm) clay fraction from Okpokwu (OK1.1) of Mamu/Ajali Formation and Enugu (EN2.1) of Enugu/Nkporo Formation, Lower Benue Trough, Nigeria.

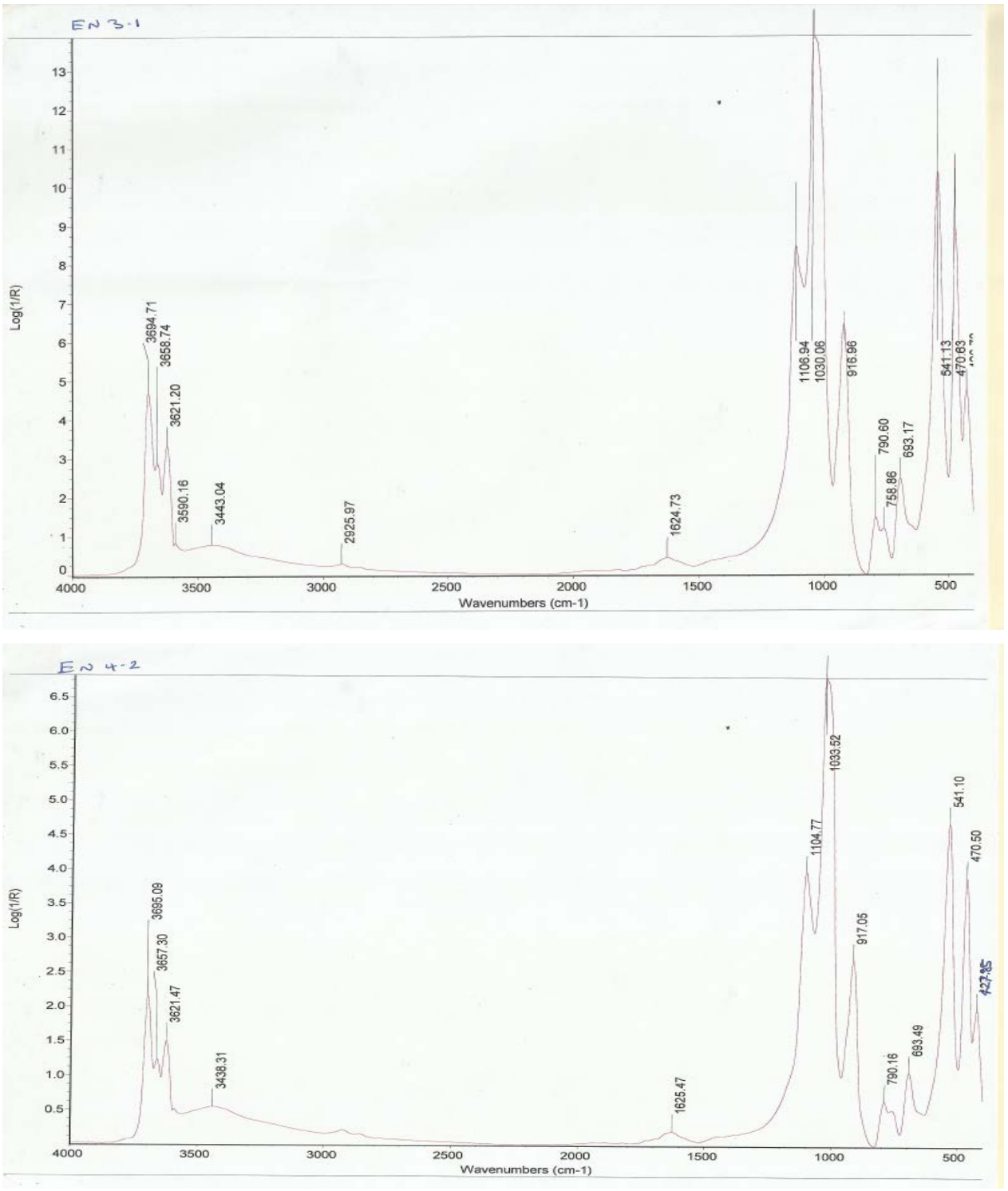

DTA-TGA curves for fine (<2µm) clay fraction from Enugu (EN3.1 and EN4.2) Enugu/Nkporo Formation, Lower Benue Trough, Nigeria.

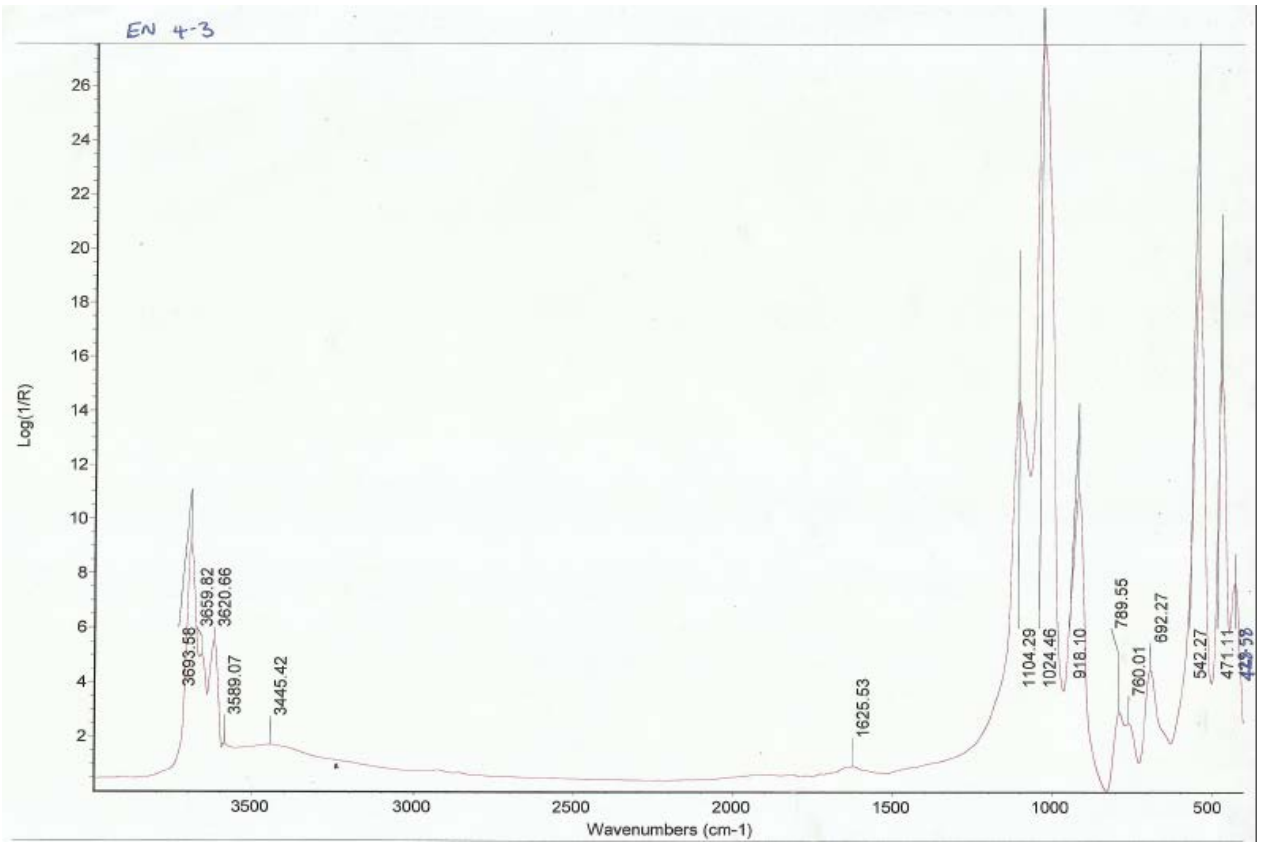

DTA-TGA curves for fine (<2µm) clay fraction from **A**: Oturkpa (OT2.2) and **B**: Okpokwu (OK1.1), Mamu/Ajali Formation, Lower Benue Trough, Nigeria.